UNIVERSITÉ D'OTTAWA UNIVERSITY OF OTTAWA

A STUDY OF FLOW AND PARTICLE HEATING IN A DROP TUBE FURNACE

by

Robert J. Flaxman, Research Assistant

William L. Hallett, Research Supervisor

Final Report for

Combustion and Carbonization Research Laboratories

CANMET

Energy, Mines and Resources Canada

DSS Contract No. 13U81-00105

File No. 01SU.23440-3-9112

A STUDY OF FLOW AND PARTICLE HEATING IN A DROP TUBE FURNACE

by

Robert J. Flaxman, Research Assistant

William L. Hallett, Research Supervisor

Final Report for

Combustion and Carbonization Research Laboratories

CANMET

Energy, Mines and Resources Canada

DSS Contract No. 1SU83-00105

File No. 03SU.23440-3-9112

224 pp

ABSTRACT

The Combustion and Carbonization Research Laboratories of CANMET/EMR has constructed a laminar flow "drop tube" furnace to study the devolatilization and combustion of pulverized coal particles. The furnace consists of a long narrow vertical ceramic tube (2m length, 0.064 m I.D.) surrounded by heating elements. The coal particles are entrained by a stoichiometric quantity of "primary" air and enter into the furnace at the top through a central tube in a burner, while a secondary stream of air enters as an annular flow surrounding the primary stream. In order that all particles experience roughly the same residence times and undergo the same heating conditions, a laminar flow throughout is required, free from any mixing or dispersion of the particles.

In order to interpret the results of experiments, it is necessary to know the velocities, temperatures and heating rates of the particles in the furnace. The design of the furnace, the relatively low velocities (Reynolds numbers less than 2000) and the very high furnace temperatures (1000 - 1700 K) makes use of measuring probes very difficult; therefore, it was decided instead to develop a mathematical model to predict rather than measure flow and particle heating in the furnace.

The present study involved two parts: a) flow visualization to determine if laminar steady flow can be obtained with the present geometry; b) development of a numerical model to examine the various parameters on particle velocities, temperatures and heating rates.

Flow visualization tests in a plexiglass scale model of the furnace showed that the original burner design led to vortex shedding and rapid dispersion of the central coal jet. An improved burner design is therefore proposed in this report, which was shown to give a laminar steady flow over a wide range of operating conditions.

The second part of the study involved the development of a numerical model of flow and heat transfer processes in the furnace. A finite difference model was developed to predict the velocity and temperature fields in the gas in the furnace under different conditions; to this was added a model for coal particle motion and heating. The parameters examined were the coal mass feed rate, the air mass flow rate, the secondary air preheat temperature and the glow bar zone temperature. This report presents velocity profiles and centre-line temperatures calculated at different axial positions along the furnace, and velocities, temperatures, residence times and heating rates for four representative particle sizes under various operating conditions.

The furnace was designed to operate in a laminar steady fashion. Based on the flow visualization and on the results of the model, operating diagrams are presented showing the limits of stability for laminar steady flow. The report concludes with recommendations for furnace operation.

EXTRAIT

Les laboratoires de recherches sur la combustion et la carbonisation de CANMET/EMR ont construit une fournaise à écoulement laminaire pour étudier la dévolatilisation et la combustion des particules de charbon pulvérisé. La fournaise est constituée d'un long tuyau vertical en céramique (2 m de longueur, 0.064 m de diamètre), encerclé d'éléments chauffants. Les particules de charbon sont injectées avec un quantité stoichiométrique d'air primaire et entrent dans le haut de la fournaise par le tuyau central du brûleur. Un écoulement d'air secondaire entre autour de l'écoulement primaire. Afin que toutes les particules obtiennent les mêmes temps de résidence et les mêmes conditions de chauffage, un écoulement parfaitement laminaire est requis pour éviter mélange ou dispersion des particules.

Afin d'interpréter les résultats des expériences dans la fournaise, il faut connaître le profile de vitesse de l'air, le profile de température et les taux de chauffage des particules. La construction de la fournaise, les basses vitesses d'écoulement (nombre de Reynolds en bas de 2000) et les températures élévées (1000-1700 K) rendent impossible l'emploi de sondes pour effectuer des mesures. Par conséquent, il fut décidé de développer un modèle numérique pour prédire l'écoulement et le taux de chauffage des particules dans la fournaise, au lieu de les mesurer.

La présente recherche comprend deux parties: a) visualization de l'écoulement, pour déterminer si un écoulement laminaire stable peut être

produit; (b) développement d'un modèle numérique pour examiner les effets de différents paramètres sur les vitesses d'écoulement, les températures et les taux de chauffage des particules.

La visualization de l'écoulement dans un modèle en plexiglas de la fournaise ont démontré que la construction originale du brûleur cause des tourbillons et un mélange rapide du jet de charbon central. La nouvelle géométrie pour le brûleur, proposée dans ce rapport, produit un écoulement laminaire et stable sous un grand éventaille de conditions.

La seconde partie de la recherche incluait le développement d'un modèle numérique de la fournaise. Un modèle de différences finies pour prédire les profiles de vitesse d'écoulement et de températures dans le gaz fut développé. Un modèle pour prédire les mouvements et le taux de chauffage des particules fut par la suite ajouté. Les paramètres examinés furent le débit massique du charbon introduit, le débit massique de l'air, la température de l'air secondaire, et la température des éléments chauffants.

Ce rapport présente les résultats obtenus pour les profiles de vitesses de l'écoulement, la température au centre de la fournaise pour différentes positions le long de l'axe, la vitesse, la température, le taux de chauffage et le temps de résidence pour quatre grosseurs représentatives de particules

de charbon sous différentes conditions d'opération.

La fournaise a été conçue pour opérer d'une façon stable et laminaire. Des diagrames d'opérations présentant les limites de stabilité de la fournaise furent développer à partir des résultats du modèle numérique et des expériences de visualization. Ce rapport se conclus avec des recommendations d'opération pour la fournaise.

NOMENCLATURE

A	constant in equation (4.3)
A	constant in equation (4.5)
B	constant in Sutherland equation
B	constant in equation (4.5)
C_D	drag coefficient of sphere
F_{PE}	view factor from particle to exit
F_{PP}	view factor from particle to primary inlet
F_{PS}	view factor from particle to secondary inlet
F_{PW}	view factor from particle to furnace wall
ID	inside diameter (m)
L	length (m)
M–S/M–P	ratio of secondary mass to primary mass
OD	outside diameter (m)
P	pressure (kPa)
P'	deviation from static pressure head
P"	pressure correction
P	node point inside control volume
Pr	Prandtl number
Q	heat transfer to furnace (W)
R	dimensionless radius
R	inside furnace tube radius (m)
R	gas constant (0.287 kJ/kg K)
Re	Reynolds number

R_g	resistance of air (K m**2/W)
R_g^*	radial position of node closest to wall (m)
R_o	outside furnace radius (m)
R_r	radiation resistance (K m**2/W)
R_w	furnace wall resistance (K m**2/W)
S	constant in Sutherland equation
Sp^ϕ	source term in numerical formulation
Su^ϕ	source term in numerical formulation
T	temperature of air (K)
T_a	temperature of gas on axis [16] (K)
T_g	temperature of gas surrounding particle (K)
T_g^*	temperature at node closest to the wall (K)
T_{gb}	glow bar temperature (K)
Tinsec	secondary inlet preheat temperature
T_o	inlet temperature (K) [16]
T_P	temperature of particle (K)
T_{P0}	temperature of particle at beginning of time increment (K)
T_w	inside furnace wall temperature (K)
T_{wo}	outside furnace wall temperature (K)
U	dimensionless velocity [15]
UP/US	ratio of primary to secondary velocity
Z	dimensionless distance [15]
Z	dimensionless distance [16]
a^ϕ	coefficient in numerical formulation
c_P	specific heat of air (kJ/kg K)

c_{PP}	specific heat of coal (kJ/kg K)
d	tube diameter (m)
d_P	particle diameter (m)
g	gravitational constant (9.806 m/s**2)
g_z	same as above in axial direction
h	convective heat transfer coefficient(W/m**2 K)
h_{PE}	radiant heat transfer coefficient (W/m**2 K) from particle to exit
h_{PP}	radiant heat transfer coefficient from particle to primary inlet (W/m**2 K)
h_{PS}	radiant heat transfer coefficient from particle to secondary inlet (W/m**2 K)
h_{PW}	radiant heat transfer coefficient from particle to furnace wall (W/m**2 K)
k_g	thermal conductivity of gas (W/m K)
k_w	thermal conductivity of furnace wall (W/m K)
m	particle mass (kg)
q_w	heat flux (W/m**2) [16]
r	radial position (m)
r_o	radius of tube (m) [15]
t	time (s)
u	axial gas velocity (m/s)
u_P	particle velocity (m/s)
u_{P0}	particle velocity at beginning of time increment (m/s)
v	radial gas velocity (m/s)
x	axial position (m)

y	radial postion (m)
Δt	time increment (s)
ΔT_{max}	maximum temperature increment (K)
Γ_ϕ	variable in equation (4.1)
Θ	dimensionless temperature [16]
ϵ	emissivity
μ	dynamic viscosity (kg m/s)
ϕ	dependent variable
ρ	density of air (kg/m**3)
ρ_{axis}	density of air on axis (kg/m**3)
ρ_0	reference density of air (kg/m**3)
ρ_P	density of coal particle (kg/m**3)
σ	Stefan-Boltzmann constant (W/m**2 T**4)
∞	infinity

CONTENTS

ABSTRACT ii

EXTRAIT iv

NOMENCLATURE vii

Chapter page

1. INTRODUCTION 1

2. LITERATURE SURVEY 5

Introduction 5
Laminar Flow Through Tubes 6
Developing Velocity – Isothermal Flow 6
Laminar Forced Convection in Tubes 7
Laminar Combined Convection in Tubes 7
Entrained Flow Reactors 8

3. FLOW VISUALIZATION 15

Introduction 15
The Experimental Apparatus 16
The Furnace Tube 16
The Burner – Original Design 16
The Gas Supply and Flow Measurement 17
The Smoke Generator 17
Experiments and Observations – Original Burner 18
Experiments and Observations – Modified Burner 18
Modifications 18
Experiments with Modified Burner 19
Conclusions from the Flow Visualization Results 20
Velocity Measurements in the Isothermal Furnace Model 21

4. THE NUMERICAL MODEL 36

Introduction 36
The Furnace Flow Field 37
The Mathematical Problem 37
The TEACH Program 37
The Formulation of the Problem 38
The Grid Pattern 41
Inlet Conditions 43
Boundary Conditions 43
Velocity Boundary Conditions 43

Temperature Boundary Condition 44
Buoyancy 46
Fluid Properties 47
Density 47
Viscosity 47
Convergence Criterion 48
Particle Motion and Heating 50
Introduction 50
Particle Motion 51
Particle Heating 52

5. NUMERICAL RESULTS 65

Test Cases 65
Developing Isothermal Pipe Flow 65
Comparison of Numerical Results for Developing Pipe Flow 65
Velocity Measurements in the Experimental Furnace 67
Fully Developed Pipe Flow Subject to Heating 68
Constant Wall Temperature 68
Constant Heat Flux 69
The Furnace Flow Field 71
Flow Field Study – Constant Glow Bar Temperature 1700 K 73
Flow Field Study – Constant Glow Bar Temperature 1400 K 74
Flow Field Study – Variable Glow Bar Temperature 75
Particle Velocity and Temperature 76
Particle Heating – Constant Glow Bar Temperature 1700 K 76
Particle Heating – Constant Glow Bar Temperature 1400 K 79
Particle Heating – Variable Glow Bar Temperature 80
Particle Heating Rates 81

6. CONCLUSIONS AND RECOMMENDATIONS 167

REFERENCES 172

Appendix page

A. PARTICLE DENSITY 175

B. VIEW FACTORS 178

C. LISTING OF THE FORTRAN COMPUTER PROGRAM 179

LIST OF TABLES

Table		page
1.	Summary of Entrained Flow Reactors	14
2.	Original Burner Design – Test Flow Rates	25
3.	Modified Burner Design – Test Flow Rates	26
4.	Governing Differential Equations	56
5.	Expressions for the Variables of the Generalized Equation	57

LIST OF FIGURES

Figure		page
1.	Cross-section of the CCRL Drop Tube Furnace	4
2.	Schematic Drawing of Experimental Apparatus	27
3.	Detail of Burner Head – Original and Modified	28
4.	Original Burner – UP/US = 1:1 – turbulent flow	29
5.	Original Burner – UP/US = 1:1 – unsteady laminar flow	30
6.	Original Burner – UP/US = 2:1 – turbulent flow	31
7.	Stability Curve for Isothermal Flow – Modified Burner	32
8.	Modified Burner – UP/US = 4:1 – turbulent flow	33
9.	Modified Burner – UP/US = 2:1 – unsteady laminar flow	34
10.	Modified Burner – UP/US = 4:1 – steady laminar flow	35
11.	Typical Control Volume for Numerical Model of Furnace	58
12.	U, V and C Cells for Numerical Model	59
13.	Flowchart of the Numerical Model	60
14.	Grid Pattern Used to Divide the Furnace into Segments	61
15.	Boundary Conditions for Furnace	62
16.	Cross-section through the Drop Tube Furnace	63
17.	Comparison of Dynamic Viscosity	64
18.	Comparison of Centre-line Velocities	85
19.	Developing Velocity Profiles in a Tube	86
20.	Comparison of Velocity Profiles at 0.010 m	87
21.	Comparison of Velocity Profiles at 0.024 m	88

22. Comparison of Velocity Profiles at 0.085 m 89
23. Comparison of Velocity Profiles at 0.250 m 90
24. Comparison of Temperature – Constant Wall Temperature 91
25. Comparison of Temperature – Constant Heat Flux 92
26. Velocity Profiles – Tgb=1700 K, Tinsec=600 K, M-S/M-P=4.0 93
27. Velocity Profiles – Tgb=1700 K, Tinsec=750 K, M-S/M-P=4.0 94
28. Velocity Profiles – Tgb=1700 K, Tinsec=900 K, M-S/M-P=4.0 95
29. Velocity Profiles – Tgb=1700 K, Tinsec=1050 K, M-S/M-P=4.0 96
30. Velocity Profiles – Tgb=1700 K, Tinsec=1200 K, M-S/M-P=4.0 97
31. Velocity Profiles – Tgb=1700 K, Tinsec=300 K, M-S/M-P=9.0 98
32. Velocity Profiles – Tgb=1700 K, Tinsec=450 K, M-S/M-P=9.0 99
33. Velocity Profiles – Tgb=1700 K, Tinsec=600 K, M-S/M-P=9.0 100
34. Velocity Profiles – Tgb=1700 K, Tinsec=750 K, M-S/M-P=9.0 101
35. Velocity Profiles – Tgb=1700 K, Tinsec=900 K, M-S/M-P=9.0 102
36. Velocity Profiles – Tgb=1700 K, Tinsec=1050 K, M-S/M-P=9.0 103
37. Velocity Profiles – Tgb=1700 K, Tinsec=1200 K, M-S/M-P=9.0 104
38. Velocity Profiles – Tgb=1400 K, Tinsec=900 K, M-S/M-P=4.0 105
39. Velocity Profiles – Tgb=1400 K, Tinsec=1050 K, M-S/M-P=4.0 106
40. Velocity Profiles – Tgb=1400 K, Tinsec=1200 K, M-S/M-P=4.0 107
41. Velocity Profiles – Tgb=1400 K, Tinsec=300 K, M-S/M-P=9.0 108
42. Velocity Profiles – Tgb=1400 K, Tinsec=450 K, M-S/M-P=9.0 109
43. Velocity Profiles – Tgb=1400 K, Tinsec=600 K, M-S/M-P=9.0 110
44. Velocity Profiles – Tgb=1400 K, Tinsec=750 K, M-S/M-P=9.0 111
45. Velocity Profiles – Tgb=1400 K, Tinsec=900 K, M-S/M-P=9.0 112
46. Velocity Profiles – Tgb=1400 K, Tinsec=1050 K, M-S/M-P=9.0 113
47. Velocity Profiles – Tgb=1400 K, Tinsec=1200 K, M-S/M-P=9.0 114
48. Velocity Profiles – Variable Zone Temp., Tinsec = 750 K 115

49. Velocity Profiles – Variable Zone Temp., Tinsec = 900 K 116

50. Velocity Profiles – Variable Zone Temp., Tinsec = 1050 K 117

51. Velocity Profiles – Variable Zone Temp., Tinsec = 1200 K 118

52. Particle Heating – Tgb=1700 K, Tinsec=600 K, M–S/M–P=4.0 119

53. Particle Heating – Tgb=1700 K, Tinsec=750 K, M–S/M–P=4.0 120

54. Particle Heating – Tgb=1700 K, Tinsec=900 K, M–S/M–P=4.0 121

55. Particle Heating – Tgb=1700 K, Tinsec=1050 K, M–S/M–P=4.0 122

56. Particle Heating – Tgb=1700 K, Tinsec=1200 K, M–S/M–P=4.0 123

57. Particle Heating – Tgb=1700 K, Tinsec=300 K, M–S/M–P=9.0 124

58. Particle Heating – Tgb=1700 K, Tinsec=450 K, M–S/M–P=9.0 125

59. Particle Heating – Tgb=1700 K, Tinsec=600 K, M–S/M–P=9.0 126

60. Particle Heating – Tgb=1700 K, Tinsec=750 K, M–S/M–P=9.0 127

61. Particle Heating – Tgb=1700 K, Tinsec=900 K, M–S/M–P=9.0 128

62. Particle Heating – Tgb=1700 K, Tinsec=1050 K, M–S/M–P=9.0 129

63. Particle Heating – Tgb=1700 K, Tinsec=1200 K, M–S/M–P=9.0 130

64. Effect of Emissivity on Particle Heating 131

65. Particle Heating, Coal = 0.5 g/min, 1700 / 750 / 4.0 132

66. Particle Heating, Coal = 0.5 g/min, 1700 / 900 / 4.0 133

67. Particle Heating, Coal = 0.5 g/min, 1700 / 1200 / 4.0 134

68. Particle Heating, Coal = 0.5 g/min, 1700 / 600 / 9.0 135

69. Particle Heating, Coal = 0.5 g/min, 1700 / 900 / 9.0 136

70. Particle Heating, Coal = 0.5 g/min, 1700 / 1200 / 9.0 137

71. Particle Heating – Tgb=1400 K, Tinsec=900 K, M–S/M–P=4.0 138

72. Particle Heating – Tgb=1400 K, Tinsec=1050 K, M–S/M–P=4.0 139

73. Particle Heating – Tgb=1400 K, Tinsec=1200 K, M–S/M–P=4.0 140

74. Particle Heating – Tgb=1400 K, Tinsec=300 K, M–S/M–P=9.0 141

75. Particle Heating – Tgb=1400 K, Tinsec=450 K, M–S/M–P=9.0 142

76. Particle Heating – Tgb=1400 K, Tinsec=600 K, M–S/M–P=9.0 143
77. Particle Heating – Tgb=1400 K, Tinsec=750 K, M–S/M–P=9.0 144
78. Particle Heating – Tgb=1400 K, Tinsec=900 K, M–S/M–P=9.0 145
79. Particle Heating – Tgb=1400 K, Tinsec=1050 K, M–S/M–P=9.0 146
80. Particle Heating – Tgb=1400 K, Tinsec=1200 K, M–S/M–P=9.0 147
81. Variable Zone Temperature, Tinsec=750 K, M–S/M–P=4.0 148
82. Variable Zone Temperature, Tinsec=900 K, M–S/M–P=4.0 149
83. Variable Zone Temperature, Tinsec=1050 K, M–S/M–P=4.0 150
84. Variable Zone Temperature, Tinsec=1200 K, M–S/M–P=4.0 151
85. Rate of Temperature Rise for a 10 μm Particle 152
86. Rate of Temperature Rise for a 30 μm Particle 153
87. Rate of Temperature Rise for a 100 μm Particle 154
88. Rate of Temperature Rise for a 300 μm Particle 155
89. Heating Rate for a 10 μm particle, 0.5 and 1.0 g/min Coal 156
90. Heating Rate for a 30 μm particle, 0.5 and 1.0 g/min Coal 157
91. Heating Rate for a 100 μm Particle, 0.5 and 1.0 g/min Coal 158
92. Heating Rate for a 300 μm particle, 0.5 and 1.0 g/min Coal 159
93. Heating Rate vs. Glow Bar Temperature for a 10 μm Particle 160
94. Heating Rate vs. Glow Bar Temperature for a 30 μm Particle 161
95. Heating Rate vs. Glow Bar Temperature for a 100 μm Particle . . . 162
96. Heating Rate vs. Glow Bar Temperature for a 300 μm Particle . . . 163
97. Residence Time vs. Preheat Temp. for a 100 μm Particle 164
98. Furnace Operating Diagram – 0.5 g/min Coal 165
99. Furnace Operating Diagram – 1.0 g/min Coal 166

Chapter 1

INTRODUCTION

The mechanism of coal combustion is extremely complex and is not fully understood, since different types of coal exhibit different combustion characteristics. Large coal-fired boilers burn coal in pulverized form in a turbulent, swirling jet; however, it is very difficult to study the combustion behaviour of coal particles in an actual furnace. In order to better understand coal combustion, it is desirable to isolate the processes undergone by the individual coal particles from the furnace flow by subjecting the particles to heating and reaction under controlled conditions. In this fashion the number of test variables can be reduced and parametric studies performed.

Energy, Mines, and Resources Canada has developed a coal testing facility that will be used to examine the combustion histories of different types of coal in pulverized form. The facility is an entrained flow reactor, also called a controlled mixing combustion history (CMCH) or "drop tube" furnace, and consists of a long, electrically heated, vertical mullite refractory tube (Figure (1)) through which a downward laminar flow of air is passed. Two streams of air are introduced into the top of the furnace through a burner; the first is a water-cooled primary flow used as a carrier gas to introduce the particles into the furnace, and the other a much larger secondary flow which constitutes the bulk of flow through the furnace. The burner is designed such that the primary flow enters the furnace through a central injector tube and the secondary flow enters the furnace through an annulus which surrounds the primary tube. The

furnace is heated by 64 – 500 W glow bars (heating elements), 32 spaced evenly along each side, and is divided into four heating zones; the power into each zone can be independently regulated to control the temperature. At the furnace exit, a water-cooled sampling probe collects the combustion products, gases, and unburned coal particles and carries them away to be analyzed. The sampling probe can be axially traversed inside the furnace, which allows the coal particles to have variable residence times.

Coal is described as being composed of four components: moisture, volatiles, "char" or fixed carbon, and ash. Volatiles are hydrocarbon components which range from light gases (eg methane, propane, etc.) to heavy oils and tars and other gases such as CO and CO_2 . The volatiles escape from the surface of the particle and mix with the surrounding air. Volatiles burn rapidly in the gas phase, while the char (largely carbon) remaining after devolatilization undergoes surface reaction and burns much more slowly. The rate at which devolatilization occurs and the quantity of volatiles are very important in determining the ignition and the stabilization behaviour of a pulverized coal flame.

The CMCH furnace is intended to subject coal particles to a wide range of temperatures and heating histories, depending on the heater temperature and the preheat temperature of the incoming air stream. The furnace simulates the heating undergone by a particle approaching a flame front in a furnace. In order to interpret the results of devolatilization experiments in this furnace, it is essential to know the particle heating histories and residence times. The velocities and temperatures within the furnace can not be measured however, owing to the fact that access to the furnace is nearly impossible, and hence the particle heating rates cannot be found experimentally. In the present work,

therefore, a finite difference scheme was developed to predict the gas velocity and temperature within the furnace under different operating conditions. Particle heating rates were also calculated, based on the furnace gas velocities and temperature. This report presents the development of the model and representative results; it also examines the flow within an isothermal model of the furnace, using flow visualization.

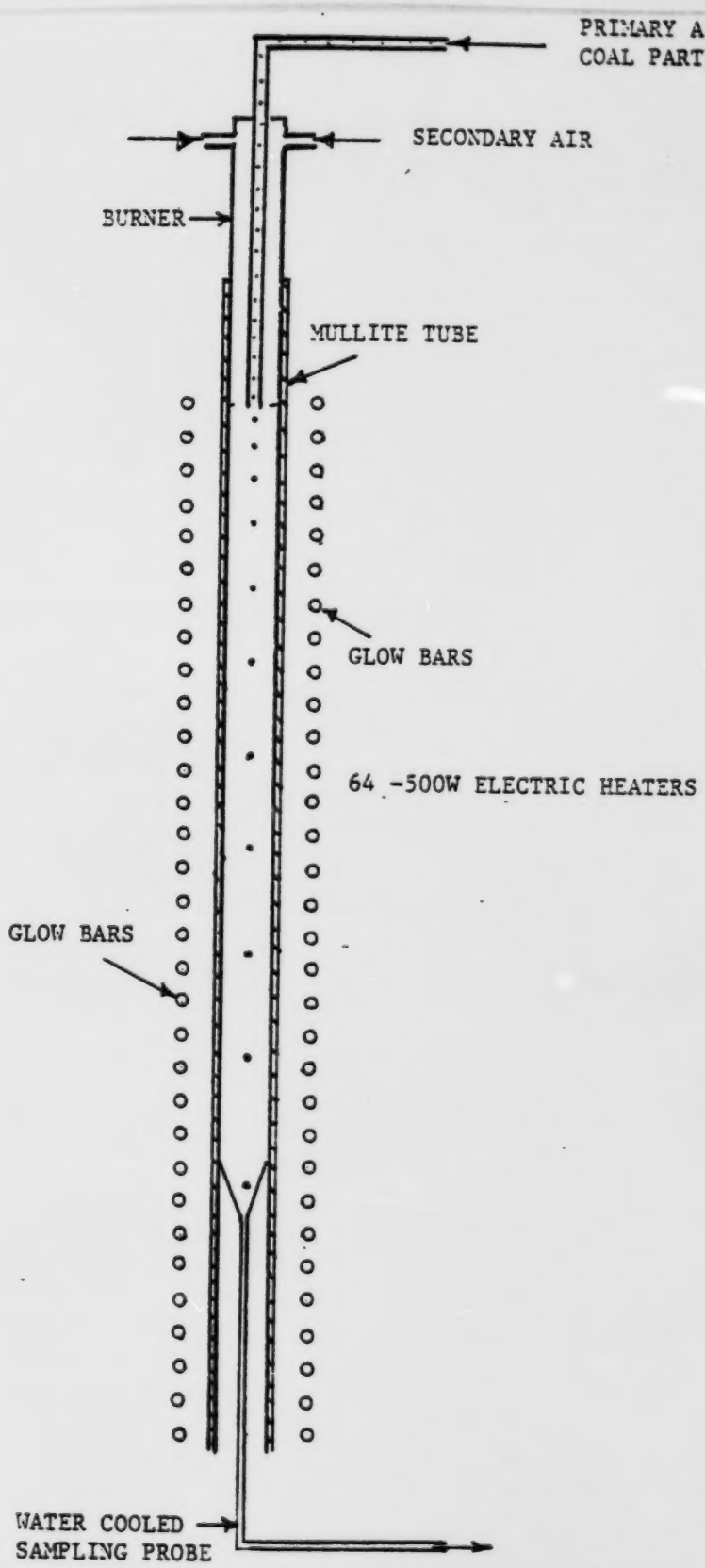

Figure 1: Cross-section of the CCRL Drop Tube Furnace

Chapter 2

LITERATURE SURVEY

2.1 INTRODUCTION

The objective of this study was to develop a numerical model to predict the temperature and heating histories of coal particles when passed through the EMR "drop tube" furnace. The physical problem is that of a downward, developing flow of gas in an externally heated circular tube, with possible buoyant effects at the hot wall. Cold particles are introduced on the axis of the flow, and are heated by convection and radiation.

A number of test cases were examined in the development of the model. The numerical model was first used to solve isothermal developing laminar pipe flow with constant properties. Subsequently, the effects of temperature, buoyancy, and variable properties were included. Once the final form of the flow regime model had been developed, the particles were introduced into the model. For the present study the particles were assumed to be inert and of low concentration; therefore, the particles were considered to have a negligible effect on the furnace flow field.

A literature review of heated laminar flow in tubes was performed to obtain solutions to which a comparison could be made in developing the model. Existing entrained flow reactors were also reviewed in order to examine their operating conditions.

2.2 LAMINAR FLOW THROUGH TUBES

2.2.1 Developing Velocity - Isothermal Flow

Laminar pipe flow has had considerable attention in the past, the main focus of which has been to determine the magnitude of the pressure drop and the length necessary to obtain fully developed flow, chiefly in connection with piping and heat exchangers. The equations to be solved are the Navier-Stokes equations of motion. Analytical difficulties arise from the non-linearity of these equations, and four methods have been used to obtain solutions: linearization , integral techniques, patched solutions (matching of boundary layer and fully developed flow solutions) [13, 33, 38] and finite element or finite difference techniques [1, 15, 18, 41]. The numerical solutions of the problem were of particular interest for the present work.

A solution of the problem using a finite difference scheme was presented by Friedman et al [15], who obtained velocity field distributions in laminar pipe flow in the range of Reynolds numbers from 0 to 500. McDonald et al [27] used finite difference methods to solve tube flow with a Reynolds number of 200 and obtained results that were in good agreement with Friedman et al. Hasan et al [18] used finite element analysis to solve for flow development in the entrance region of a tube with Reynolds numbers ranging from 0 to 40. Different inlet velocity profiles were examined and were observed to have a marked effect on the flow field in the entry region of the tube. Wagner [41] studied developing flow ahead of a piston moving at constant speed through a tube using a finite difference method for Reynolds numbers 0 to 800. In each of the numerical solutions it was discovered that if the initial velocity profile was flat, the subsequent profiles developed two maxima positioned symmetrically on either side of the axis near the wall and a local minimum

positioned on the axis of symmetry. Abarbanel et al [1] showed that these "bulges" were part of the exact solution and were not a numerical effect arising from truncation errors or from singularity at the tube wall. Friedman et al [15] found that the magnitude of the bulges decreased with increasing Reynolds numbers.

2.2.2 Laminar Forced Convection in Tubes

Most past interest in laminar forced convection has been in connection with the design of heat exchangers. The working fluids have usually been water or oil, and solutions have been presented to determine the heat transfer coefficients under various laminar flow conditions [24]. Temperature fields within the tubes were not of practical interest in these studies.

Kays [24] presented a finite difference solution for developing temperature profiles based on a Langhaar velocity distribution and a constant wall temperature. Grigull and Tratz [16] presented finite difference solutions for developing temperature profiles in fully developed laminar flow with constant properties. Three heating conditions were studied: constant wall temperature, constant heat flux, and constant temperature difference.

2.2.3 Laminar Combined Convection in Tubes

Buoyancy effects were thought to be significant in the CMCH furnace, owing to the large temperature difference between the wall and incoming flow and moderate Reynolds numbers. Free convection effects will distort the developing velocity profiles. The forced convection through the furnace is downward, while buoyancy forces act upward, producing combined convection in opposing flow. The heated tube wall causes the flow velocity near the wall to decrease, resulting in an acceleration of the flow on the tube axis.

A number of researchers [5, 9, 10, 17, 19, 30, 31] examined the effects of laminar combined convection in opposing flow with a view to determining the effect of buoyancy on the heat transfer coefficient. Scheele and Hanratty [31] studied combined convection using water in tubes and observed a sudden transition from laminar steady to laminar unsteady flow while measuring tube wall temperatures. Hanratty et al [17] experimented with combined convection in water with Reynolds numbers ranging from 100 to 2100 and observed flow instabilities on the axis by the disturbance of an axially injected dye filament. Brown and Gauvin [9] examined the effects of buoyancy on the heat transfer coefficient in air for Reynolds numbers ranging from 380 to 6900. Collins [10] incorporated buoyancy into a finite difference marching scheme and illustrated the effect of variable properties; however, for strong buoyancy effects, instability occurred in the computer treatment.

2.3 ENTRAINED FLOW REACTORS

Entrained flow reactors have been used at least since 1966 for the study of coal combustion. Many different designs exist, and each furnace has its own geometry , gas flow, and particle feed rate. Usually, a specific type of coal was tested and a combustion model was developed from the experimental results. By examining the operating conditions and heating rates obtained in past research, an insight into the present furnace can be obtained.

Field [14] examined the reaction rates of char particles in the diameter range 20 to 100 μm in a laminar flow furnace. The main flow consisted of 80 l/min of an oxygen–nitrogen–argon mixture which was preheated to 1527 C with a plasma torch. The char particles entered through an alumina feeder tube which entered through the side of the furnace. The char feed rate was 0.125

g/min, entrained in 0.2 l/min of nitrogen. Two diametrically opposed slit-windows were used to observe the burning stream of particles, and to measure wall temperatures with optical pyrometers. The transit time of the particles was 27 ms over 120 mm.

A laminar flow furnace was used by Badzioch and Hawksley [3] to study 20 μm coal particles (also 40, 60, 62 μm) with nitrogen as the primary and secondary gas. The coal particles and nitrogen carrier gas were fed into a secondary stream of hot nitrogen preheated to the furnace wall temperature. Preheating could be varied from 400 C to 1000 C. The secondary gas flow rate was 40 l/min and a zirconia flow straightener was used; the primary flow rate was varied from 1.0 to 2.1 l/min such that it matched the secondary flow velocity entering the furnace. The mixing of the cold carrier nitrogen and the hot gas stream was said to be complete 5 cm from the top. The flow was approximately parabolic henceforth, and flow velocities ranging from 1.6 m/s at 400 C to 2.9 m/s at 1000 C were obtained. A water-cooled collector was used to quench and remove particles and devolatilization products. The coal feed rate was 0.25 to 0.5 g/min, and the particles were assumed to travel at the gas velocity. The residence times were varied from 30 to 110 msec by vertical movement of the collector. The heating rates were said to be approximately 25000 to 50000 C/s, the final temperature of the particles that of the gas stream and the furnace wall.

Pulverized coal particles were burned by Baum and Street [4] in a laminar flow furnace using air as the primary and secondary flow. The secondary air flow rate was 30 l/min, preheated to approximately 917 C, while the furnace wall temperature ranged from 930 to 970 C. The coal feed rate of 2.6 to 2.7 g/min was entrained by a primary flow rate of 1 to 1.38 l/min. Visual

observations were made through a slot which ran the length of the furnace, and local gas samples were withdrawn using a water-cooled sampling probe. Exit gas samples were extracted using a water-cooled collector which could be axially traversed from the bottom. Helium tracer techniques showed that less than 1 % of the flow was recirculated.

Kobayashi et al [25] studied devolatilization of coal particles at high temperatures. Size graded particles (400-325 Tyler Mesh - 37-44 μm) were injected into a hot argon stream using a cool argon carrier gas. The secondary (main) flow was heated to the furnace wall temperature using a plasma gun, and passed through a graphite honeycomb flow straightener before entering the furnace tube. Sight holes in the furnace wall enabled the particles to be observed, showing that they travelled down the centre of the furnace. The coal feed rate was varied from 0.12 to 0.18 g/min and the cool argon carrier gas flow rate ranged from 0.015 to 0.616 l/min. The main gas flow ranged from 29.4 to 150 l/min, giving average velocities from 0.81 m/s at 1000 K to 8.65 m/s at 2100 K. The particles were quenched at the furnace exit by means of twelve small water jets in the tip of the collector. A simplified flow model based on an approximate integral method was used to predict the temperature and velocity of the coal particles.

Rapid pyrolysis of lignite in nitrogen was studied by Scaroni et al [32] in an entrained flow , isothermal furnace. A dilute stream of coal and nitrogen was injected into a preheated nitrogen stream and forced downward through a heated vertical tube. A flow straightener and careful injector design were used to limit the spreading of the coal jet. The main gas flow was preheated to the isothermal wall temperature. A variation of residence times was achieved by raising and lowering an isokinetic water-cooled collector. The mean diameter

of the coal particles varied from 41 to 201 μm. The coal feed rate for all tests was 1.0 g/min and the mean gas velocity was 1.12 m/s. Preheated gas and wall temperatures varied from 700 to 1000 C, and the ratio of secondary to primary flow ranged from 16.7 to 12.5. The primary flow rate was the minimum necessary for efficient entrainment of the particles. The coal particle heating rate was estimated to be of the order of 10000 C/s. A cold flow (isothermal) experimental model indicated that particle velocities were size dependent, and that the assumption that gas and particles have the same velocity is not always valid. Particle residence times are affected by the size and the density of the particles during devolatilization. Exact gas velocities and flow patterns were not known, and therefore an average velocity was used.

An entrained flow furnace was used by Solomon et al [36] to study high temperature rapid pyrolysis of coal. Helium or nitrogen was used for the secondary gas flow, which was preheated to the furnace temperature, and for the entrainment gas. The furnace was designed to operate at 1923 K. The particles were 325–200 graded mesh size (44–74 μm) and the coal feed rate was 2 to 3 g/min. The secondary flow was varied from 25 to 40 l/min (depending on the temperature) in order to obtain a 1 m/s velocity through the furnace. The water-cooled carrier gas flow rate was 1 l/min. The coal particles were assumed to travel at the average gas velocity and their residence times were varied from 0 to 700 ms by movement of the water-cooled injector. A water- cooled collector quenched the exiting stream. An optical port allowed Fourier Transform Infrared Spectrometer analysis of gas species and temperature.

Timothy et al [40] conducted experiments on pulverized coal using a laminar flow furnace consisting of an alumina muffle tube heated by a

surrounding graphite element. The secondary flow consisted of a mixture of oxygen and argon or helium which was independently preheated to the furnace temperature; its oxygen volume fraction was varied from 15 to 100 % . The coal was entrained by a flow of helium and injected into the hot stream such that the velocities were matched. The particle sizes were 38–45 and 90–105 μm in diameter. The furnace was operated at temperatures of 1250 and 1700 K and heating rates were estimated to be of the order 100000 K/s.

A transparent entrained flow reactor was used by Mitchell and McLean [28] to study the combustion of 90 μm coal particles employing a methane–hydrogen–oxygen–nitrogen mixture as the primary and secondary gases. The oxygen mole fraction was varied from 0 to 30 % and furnace temperatures of 1000 to 1800 K were achieved. Particles were assumed to move at the local gas velocity. A two–colour pyrometer technique was used to measure the temperature of the burning coal particles.

Jorgensen and Zuiderwyk [23] studied the combustion of single particles of sulphide minerals in a laminar flow furnace. The secondary gas flow was an air and oxygen–nitrogen mixture which was preheated 773 to 1273 K. The particles were injected into the hot stream by means of a water–cooled injector which could be raised and lowered to vary the residence time. Observation of the exiting flow showed that a majority of the particles remained on the tube axis. The furnace had two sets of viewing ports which enabled two–colour pyrometer measurements.

Typical details of the entrained flow furnaces studied can now be summarized. The particle sizes used in these laminar flow reactors have been in the range 20 to 200 μm with feed rates ranging from 0.015 to 3.0 g coal/min. The types of gas used included air, nitrogen, argon, helium, methane and

mixtures of these. The secondary gas flow rate ranged from 25 to 150 l/min, yielding velocities of 0.81 to 8.65 m/s (depending on the furnace temperature). The secondary gas flow was always preheated, and typical inlet temperatures varied from 400 to 1823 C. Particle heating rates were claimed to range from 10000 to 100000 C/s. Table 1 summarizes the operating conditions of the entrained flow reactors. The present EMR furnace falls into the range of designs studied with a coal feed rate of 0.5 to 1.0 g coal/min, inlet velocities of 0.42 to 1.67 m/s, preheat temperatures of 300 to 1200 K, and inlet Reynolds numbers of 120 to 1350. The entrained flow reactors discussed have all been laminar; however, turbulent flow reactors have also been studied [22].

TABLE 1

Summary of Entrained Flow Reactors

Author	Particle Size (μm)	Particle Feed Rate (g/min)	Primary Flow (l/min)	Primary Gas	Secondary Flow (l/min)	Secondary Gas	Average Velocity (m/s)	Secondary Preheat Temperature (C)	Furnace or (Wall) Temperature (C)	Heating Rate (C/s)
Field	20 - 100	0.125	0.2	N_2	80	O_2-N_2-Ar	*	1527	*	*
Badzioch & Hawksley	20 - 60	0.25 - 0.5	1.0 - 2.1	N_2	40	N_2	1.6 - 2.9	400 - 1000	*	25000 - 50000
Baum & Street	*	2.6 - 2.7	1.0 - 1.38	Air	30	Air	*	917	930 - 970	*
Kobayashi et al	37 - 44	0.12 - 0.18	0.015 - 0.616	Ar	29.4 - 150	Ar	0.81 - 8.65	727 - 1827	(727) - (1827)	*
Nsakala et al	58 - 180	0.5	2.0	N_2	30	N_2	1.02	*	808 (1150)	8000
Scaroni	41 - 201	1.0	**	N_2	**	N_2	1.12	700 - 1000	(700) - (1000)	10000
McLean et al	65 - 100	*	*	*	*	CH_4-H_2 - Air	1.0 - 10.0	*	827 - 1527	50000 200000
Solomon et al	44 - 74	2.0 - 3.0	1.0	He or N_2	25 - 40	He or N_2	1.0	1650	1650	*
Timothy et al	38 -105	*	*	He	*	O_2-Ar or O_2-He	*	977 - 1427	977 - 1427	100000
Mitchel & McLean	90	*	*	CH_4-H_2 -O_2-N_2	*	CH_4-H_2 -O_2-N_2	*	*	727 - 1527	*
Jorgensen & Zuiderwyk	*	*	*	*	*	O_2-N_2	*	500	*	*

* Information not provided

** Secondary/Primary Flow Ratio 16.7 - 12.5

Chapter 3

FLOW VISUALIZATION

3.1 INTRODUCTION

The CMCH furnace is a laminar flow test furnace designed to examine the heating histories of coal particles. Ideally, particles traversing the furnace should all be subjected to the same heating conditions and residence time. This can be achieved if the particles travel down the axis of the furnace with a minimum of spreading. A random dispersion of the coal particles would lead to variable particle heating rates and transit times and is therefore highly undesirable.

The furnace entrance geometry as originally designed included a thick water-cooled jacket between the primary and secondary streams. It was felt likely that a recirculating wake could form behind this jacket, which in turn could lead to flow instabilities such as vortex shedding and to particle dispersion within the furnace. In order to determine if the desired flow pattern could actually be obtained with the original geometry, a cold flow (isothermal) experimental model was constructed to match the geometry of the actual furnace (see Figure (2)). Flow visualization experiments were carried out using smoke in the primary flow as a tracer to study the effects of primary and secondary flow rates on the flow characteristics.

3.2 THE EXPERIMENTAL APPARATUS

3.2.1 The Furnace Tube

The flow visualization model was a full-size, exact scale replica of the actual CMCH furnace. The model furnace tube consisted of a 1.83 m long cast acrylic tube (76.2mm OD, 63.5mm ID). A flange was attached to the top of the furnace tube to enable the furnace to be fastened to a steel support frame. A centering ring at the bottom of the furnace allowed it to be accurately adjusted vertically. The burner slid into the top of the furnace tube and was held in place by three nylon bolts which passed through the flange. A flexible exhaust hose was attached to the bottom of the furnace tube to direct the exiting smoke into an exhaust system.

3.2.2 The Burner – Original Design

The model of the original burner consisted of three straight concentric tubes (Figure (3a)). The primary air and smoke entered through the top into the central tube (6.4 mm DIA), while the secondary air entered into the burner from the sides through two horizontally opposed tubes near the top of the outer annulus (57.1 mm OD, 38.1 mm ID). The lengths of the inlet sections were the same as those in the actual furnace, so that the exit velocity profiles would be the same. A jacket occupied the inside annulus (38.1 mm OD, 6.4 mm ID) which separated the two streams. This in the actual furnace is a water-cooled jacket to keep the coal particles cold and prevent reaction before the particles enter the furnace.

3.2.3 The Gas Supply and Flow Measurement

Air was used as the primary and secondary fluid. The air supplied to the experimental system was delivered at 100 psig to a pressure regulator, which reduced the pressure down to 60 psig. The flow was then split into two streams, a primary flow and a secondary flow; each passed through a needle valve and a rotameter which measured the volumetric flow rate of each stream. The flow rates were chosen such that the Reynolds number of the flow through the furnace model would be 2000 or less (ie laminar region). The secondary flow rotameter had a range of 12 to 120 l/min and the primary rotameter 0.2 to 4.8 l/min. Rotameter readings were corrected for temperature and barometric pressure variations. The secondary air was directed into the model, while the primary air flowed first into a smoke generator.

3.2.4 The Smoke Generator

Smoke was generated by the combustion of pipe tobacco with the primary air. The primary air was fed into an Erlenmeyer flask through a glass nipple molded onto its side. Pipe tobacco was placed inside a large glass tube (22 mm OD, 150 mm L) and ignited. A one hole stopper with a glass tube was placed onto the end of the large glass tube and this combustion tube was placed inside the flask. The primary air and smoke exited through the glass tube into a similar but smaller Erlenmeyer flask filled with crushed charcoal and fiber matting. This filtering flask was placed in an ice bath in order to cool the mixture. The cool filtered smoke then entered the furnace model through the primary inlet.

A bypass tube and a stop cock was used to control the quantity of smoke that mixed with the primary air entering the furnace model. The flow of smoke was reduced to the minimum amount necessary for visual observation.

3.3 EXPERIMENTS AND OBSERVATIONS – ORIGINAL BURNER

The original design called for identical burner exit velocities for the primary and secondary flows. The two flows were to merge together and continue down the furnace tube as a laminar steady stream.

A series of flow rates were chosen with Reynolds numbers in the laminar region and with identical secondary and primary burner exit velocities. Recirculation and flow instabilities were observed for all flow rates of practical interest. The flow became stable only at flow rates too low for practical operation of the furnace (Reynolds number less than 100). The recirculation occurred behind the jacket and the flow rapidly dispersed following the recirculation zone. The flow instabilities were observed to lead to turbulence and dispersion of the central jet for all flows of practical interest. This is highly undesirable for the function of the furnace, as it would cause the coal particles to disperse randomly.

A series of primary/secondary flow ratios were also examined and similar instabilities were observed (see Table (2)). Figures (4) to (6) show the recirculation and instabilities that were observed at the top of the furnace; the flow remained unstable until the exit.

3.4 EXPERIMENTS AND OBSERVATIONS – MODIFIED BURNER

3.4.1 Modifications

The tests showed that the original burner design could not achieve the desired flow pattern through the furnace, and it was necessary to modify the burner to obtain a laminar steady flow. To eliminate the recirculation as much as possible, the "cooling jacket" was removed (Figure (3b)) and a honey-comb flow straightener and a foam screen were fitted snugly between the primary

air tube and the furnace wall. The flow straightener is intended to produce a uniform velocity at the secondary flow outlet.

3.4.2 Experiments with Modified Burner

The addition of a flow straightener and elimination of the cooling jacket enabled the desired flow pattern to be obtained in the furnace. The smoke mixture entered the furnace and continued in a laminar steady stream until the exit; however, the flow was found to be stable only up to certain Reynolds numbers. A series of primary/secondary flow ratios were examined to determine the limit of this stability region. A primary/secondary flow ratio was chosen and was kept fixed through out the test; the resulting flow patterns were observed while both flows were reduced to the lowest possible values. A number of ratios were chosen and the procedure was repeated thereafter (see Table 3).

The flow stability curve that was obtained is shown in Figure (7). There is an apparent upper limit of stability for the furnace, marked by a transition from steady laminar flow with no noticable dispersion of the primary stream through increasingly unsteady laminar flow to fully turbulent conditions with increasing Reynolds number. The turbulent region had no discernible regular pattern and was entirely characteristic of turbulent flow (see Figure (8)). The unsteady laminar region exhibited distinguishable laminar filaments which oscillated in a regular "wiggly" pattern; the magnitude of the oscillations decreased with decreasing Reynolds number (see Figure (9)). The steady laminar region was characterized by smooth, undisturbed laminar flow with negligible dispersion of the central "coal" jet (see Figure (10)). At very low Reynolds numbers the flow was observed to break down at some point in the furnace

tube. Since the flow in general can be expected to become more stable as the Reynolds number decreases, the breakdown observed here is evidently caused by an external disturbance, and is not an intrinsic feature of the flow. The point of break down was found to roughly correspond to the position of the lamp used to illuminate the smoke particles; it is probable that radiation from the hot lamp was absorbed by the smoke particles inducing a buoyancy effect which resulted in a breakdown of the flow. These points are noted in the lower left of Figure 7.

3.5 CONCLUSIONS FROM THE FLOW VISUALIZATION RESULTS

Past designs of actual entrained flow reactors have had success in obtaining a laminar flow through the furnace tube; observation ports in the sides of these furnaces have verified this claim [4, 25, 28, 36]. The stream of coal particles was observed to travel down the centre of the furnace tube while the furnace was running at its operating temperature.

However, the present cold flow experimental model showed that flow in the EMR furnace with the original burner design was unstable for almost all flow rates and was therefore unsatisfactory for the purpose of controlled mixing and controlled heating.

The results of the flow visualization tests using the experimental model yielded two conclusions to be drawn about the EMR furnace.

1. The EMR burner as originally designed must be modified in order to achieve the desired flow pattern in the furnace. A flow straightener should be used to obtain a uniform secondary velocity profile at the inlet to the furnace.

2. The primary and secondary flow rates must be adjusted such that the inlet velocity ratio and secondary Reynolds number fall within the range of stability in Figure 7.

These conclusions can strictly speaking only be applied to the real furnace under isothermal conditions; temperature differences and buoyancy effects in the furnace under non-isothermal conditions would change the limits shown in Figure 7. Owing to the inaccessibility of the interior of the EMR furnace, conclusions about dispersion in it could only be made from residence time distribution measurements.

3.6 VELOCITY MEASUREMENTS IN THE ISOTHERMAL FURNACE MODEL

The experimental portion of the work was used as an aid in the development of a numerical model for the furnace. The flow visualization experiments had given a range for laminar steady flow; as a further step in the development of the model, a series of velocity measurements were made in the plexiglass furnace model to compare to the predictions of the numerical model. The velocity measurements were made using a pitot tube and a differential pressure transducer. The probe was a simple total head pressure tube made of 0.13 cm diameter stainless steel tubing bent at a right angle; the static pressure was measured with wall taps. A series of five 1.28 cm diameter ports for probe insertion spaced approximately 30.5 cm apart were located through the side of the furnace tube. Opposite each of these ports a 0.2 cm static pressure tap was installed through the tube wall. Since the velocities through the tube were very low (0.5 m/s maximum), the highest possible velocities for both the primary and the secondary flows were used; however, the velocity ratio and the secondary Reynolds number were chosen

such that they were within the range of the stability diagram (Figure (7)). The velocity ratio was chosen as 1:1 and the secondary Reynolds number as 1660; this gave a high velocity (0.5 m/s) and was well within the range of the stability diagram.

In developing a numerical model, the flow field area is divided up into cells forming a grid pattern. The governing differential equations are then solved on this grid (The formulation of the numerical model is discussed in detail in the following chapter). The predicted velocities from the numerical model were stored at the grid point nodes corresponding to the U velocity cells. The pitot tube was used to measure at the same location as the grid nodes, so that a direct axial velocity comparison could be made. Four representative axial positions were chosen to measure the axial velocities; these positions were 0.01, 0.024, 0.085, and 0.25 m measured vertically downward from the burner mouth. The radial positions were chosen at the radial grid points and the probe was positioned radially using a horizontally traversing slider with a vernier scale. Axial movement of the pitot probe and slide were provided by means of a vertical track.

The probe was aligned on the model by the following procedure. The centre of the model tube was located by using a plumb line. A small plug with a centred hole was inserted into the top of the primary tube of the burner (the air hose was disconnected). A plumb line was extended down through the burner and into the furnace tube. The line exited the furnace tube at the bottom, passing through a small centred hole in a centering disk. A weight was suspended from the plumb line to ensure that it was taut. The tube was adjusted by means of the three adjusting screws until it was vertical, as indicated by the plumb line. The pitot tube was traversed into one of the

holes and aligned so that it would touch the centred plumb line. The distance from the inside wall of the furnace tube to the plumb line was measured using the scale on the traversing slide. The distance from the plumb line to the far inside wall of the tube was also measured to ensure that the plumb line was at the tube centre. The measured diameter of the tube was found to be 6.30 cm, whereas the diameter used in the numerical model was 6.36 cm. This difference would result in a 2 % difference between calculated and measured velocities.

The primary flow rate was set at 0.96 l/min and the secondary flow rate set at 92 l/min. Both the primary and secondary rotameters had an accuracy of ± 2 % of full scale (full scale = 2.2 l/min for primary; 120 l/min for secondary). Smoke was used initially in the primary flow to ensure that the two flow rates would give a steady laminar flow; the measurements were made in the absence of smoke.

The pressure transducer used was a MKS Baratron Type 220B; the error of the pressure transducer was estimated using manufacture's data. The pressure readings were recorded with a strip chart recorder and a digital voltmeter (time constant = 10 sec). A certain amount of noise and pressure oscillation was associated with the measurements. The source of the noise was found to be from small vibrations in the support structure (caused by the overhead ventilation system) and in the tubing connecting the pitot tube to the transducer. These oscillations were damped by minimizing the diameter of the connecting tubing (0.16 cm). The noise and pressure oscillations that were evident with the chart recorder were approximately ± 0.0266 Pa. The highest pressure measured was 0.4459 Pa and the lowest measured was 0.0133 Pa; therefore, the noise and oscillations represented a fluctuation of 6 % of the

highest recorded pressure and a fluctuation of 200 % of the lowest recorded pressure. Compared with these fluctuations, the error of the pressure transducer itself was small. Pressures at all the radial grid point locations were measured at each of the four selected axial positions; the results are presented in Chapter 5 together with numerical predictions for the same flow.

TABLE 2

Original Burner Design – Test Flow Rates

Sec. Flow	US	Prim. Flow	UP	UP/US	Re-sec	Remarks
l/min	m/s	l/min	m/s			
120.0	1.399	2.70	1.397	1.00	1700	-turbulent after 8 cm
60.0	0.700	1.35	0.700	1.00	851	-turbulent
30.0	0.350	0.66	0.342	0.98	425	-unsteady laminar
105.0	1.224	4.80	2.487	2.03	1487	-turbulent dispersion
53.4	0.623	2.40	1.243	2.00	757	-unsteady laminar
26.7	0.311	1.20	0.622	2.00	378	-unsteady laminar
13.4	0.156	0.60	0.311	1.99	190	-unsteady laminar
53.4	0.623	4.80	2.487	3.99	757	-rapid dispersion
26.7	0.311	2.40	1.243	4.00	378	-turbulent
20.0	0.233	1.80	0.933	4.00	283	-unsteady laminar
13.4	0.156	1.20	0.622	3.99	190	-unsteady/turbulent
26.7	0.311	4.80	2.487	8.00	378	-turbulent
13.4	0.156	2.40	1.243	7.97	190	-turbulent after 30 cm
10.0	0.117	1.80	0.933	7.97	142	-unsteady laminar

TABLE 3

Modified Burner Design – Test Flow Rates

Sec. Flow	Vs	Prim. Flow	Vp	Vp/Vs	Re-sec	Remarks
l/min	m/s	l/min	m/s			
96.0	0.525	1.00	0.518	0.99	1700	-laminar
20.0	0.109	0.20	0.104	0.95	354	-first disturbance
10.0	0.055	0.10	0.052	0.95	177	-breakdown at tube bottom
119.0	0.651	1.50	0.777	1.19	2107	-unsteady laminar
110.0	0.602	1.38	0.715	1.19	1948	-unsteady laminar
100.0	0.547	1.25	0.648	1.18	1771	-unsteady laminar
90.0	0.492	1.13	0.585	1.19	1594	-nearly steady
80.0	0.438	1.00	0.518	1.18	1417	-steady laminar
119.0	0.651	1.87	0.969	1.49	2107	-fully turbulent
96.0	0.525	1.50	0.777	1.48	1700	-turbulent, more regular
83.0	0.454	1.30	0.674	1.48	1470	-turbulent, regular
70.0	0.383	1.09	0.565	1.48	1240	-nearly steady
60.0	0.328	0.94	0.487	1.48	1063	-steady laminar
96.0	0.525	2.00	1.036	1.97	1700	-turbulent
72.0	0.394	1.40	0.725	1.84	1275	-unsteady laminar
63.0	0.345	1.20	0.622	1.80	1116	-unsteady laminar
48.0	0.262	1.00	0.518	1.98	850	-steady laminar
5.0	0.027	0.10	0.052	1.93	89	-breakdown at bottom
70.4	0.385	2.20	1.140	2.96	1247	-fully turbulent
64.0	0.350	2.00	1.036	2.96	1133	-turbulent-regular
60.0	0.328	1.88	0.974	2.97	1063	-unsteady laminar
50.0	0.273	1.56	0.808	2.96	885	-nearly steady
53.0	0.290	2.20	1.140	3.93	940	-fully turbulent
52.8	0.289	2.20	1.140	3.94	936	-turbulent
51.0	0.279	2.10	1.088	3.90	904	-periodic laminar
48.0	0.262	2.00	1.036	3.95	849	-unsteady laminar
46.0	0.252	1.90	0.984	3.90	817	-nearly laminar
9.0	0.049	1.40	0.207	4.22	159	-remained laminar
42.2	0.231	2.20	1.140	4.94	749	-unsteady laminar
38.0	0.208	2.00	1.036	4.98	674	-nearly laminar
34.6	0.189	1.80	0.933	4.94	612	-steady laminar
35.2	0.192	2.20	1.140	5.94	622	-laminar/turbulent bursts
32.0	0.175	2.00	1.036	5.92	567	-laminar/unsteady bursts
26.5	0.145	2.20	1.140	7.86	470	-laminar

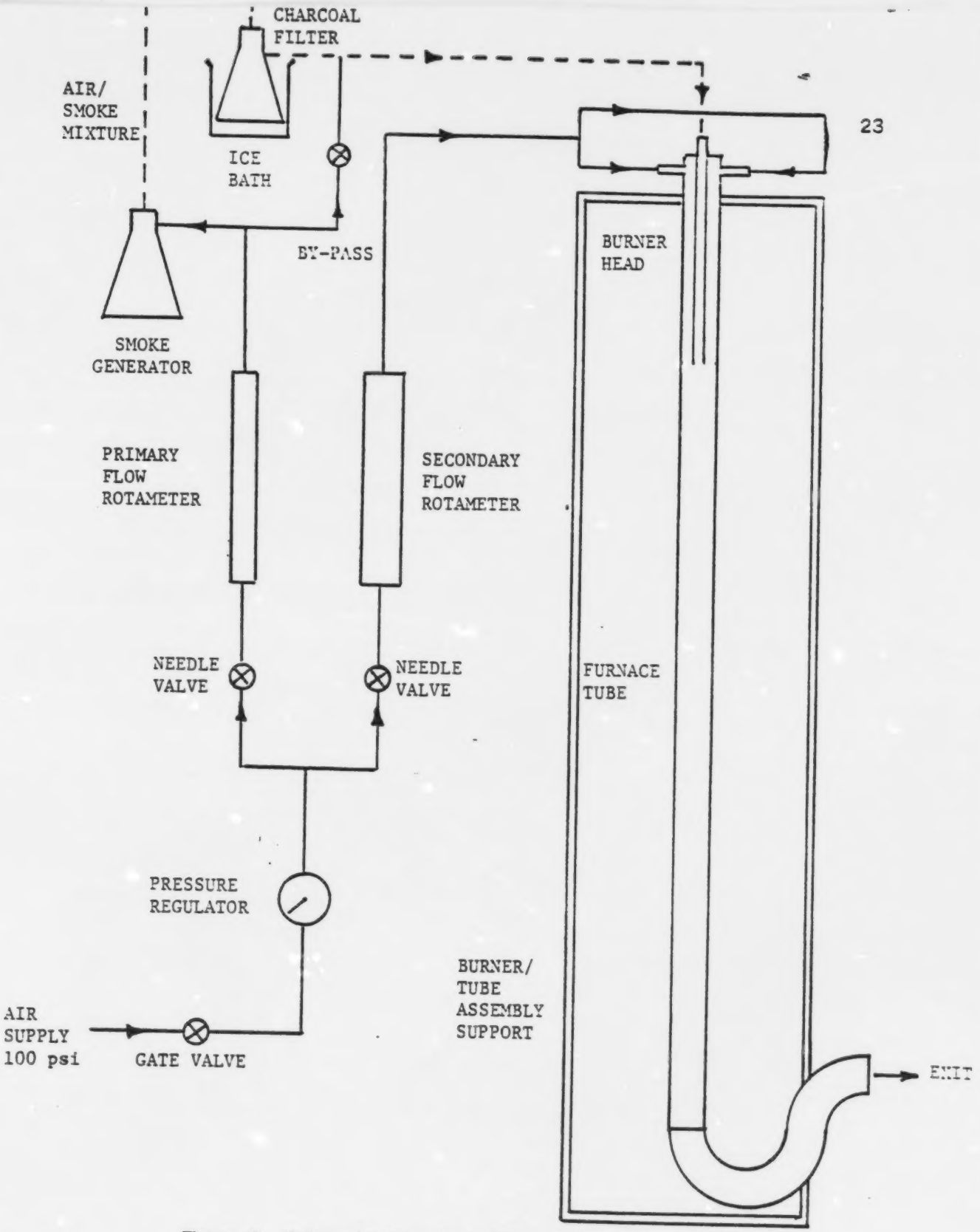

Figure 2: Schematic Drawing of Experimental Apparatus

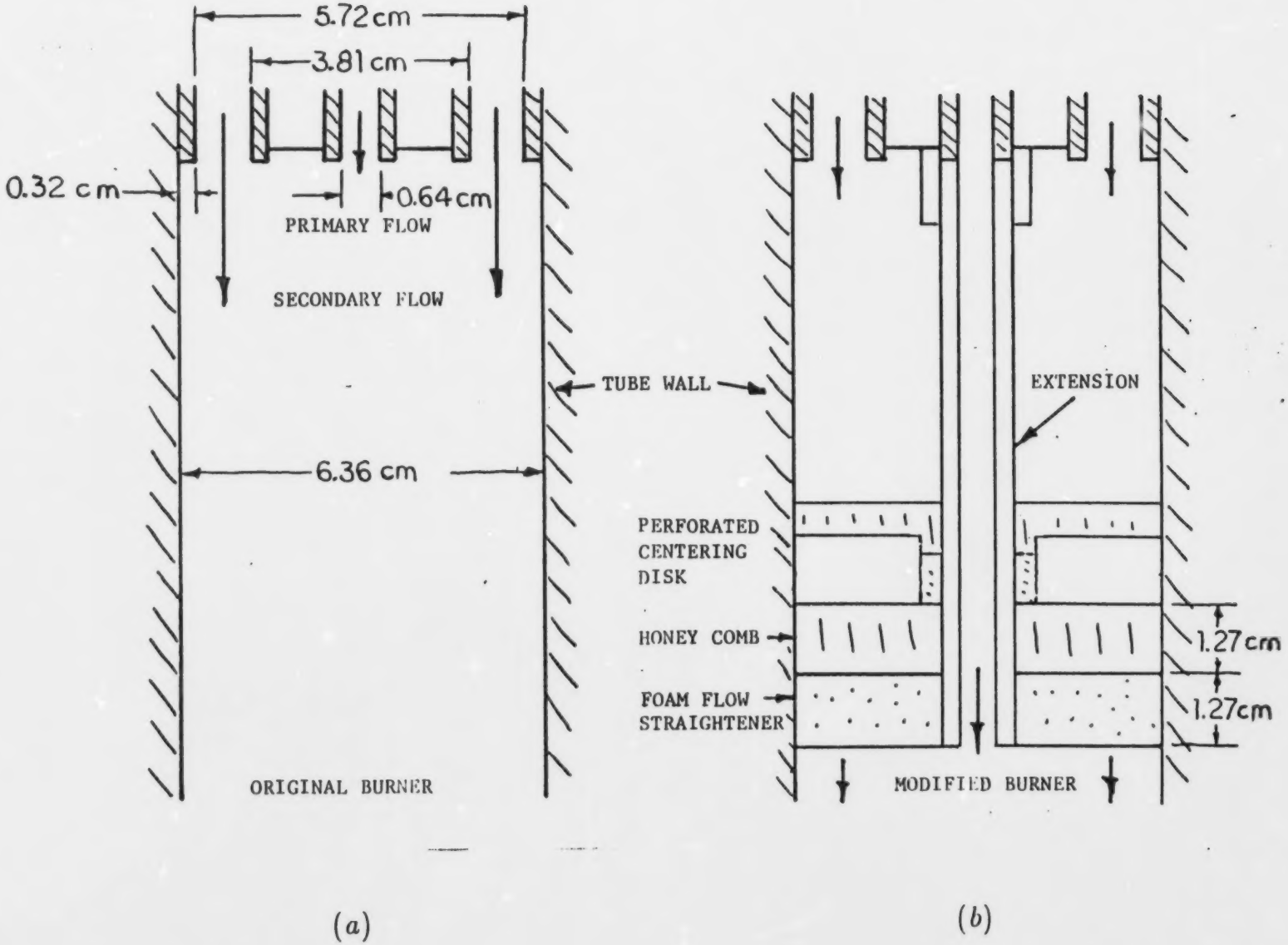

Figure 3: Detail of Burner Head - Original and Modified

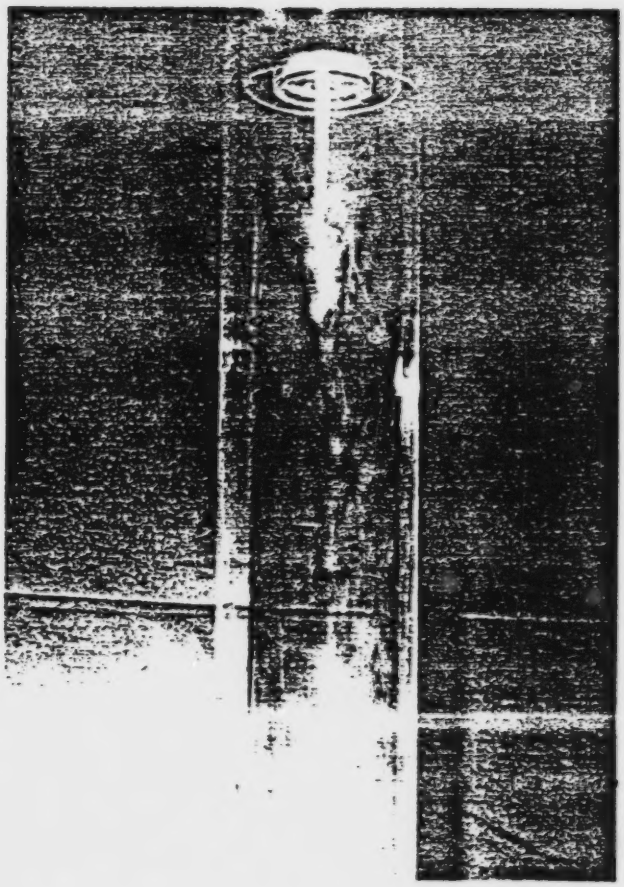

Primary Inlet Reynolds number 234
Secondary Inlet Reynolds number 850
Furnace Tube Reynolds number 1310

Figure 4: Original Burner – UP/US = 1:1 – turbulent flow (UP/US = Primary Inlet Velocity/Secondary Inlet Velocity)

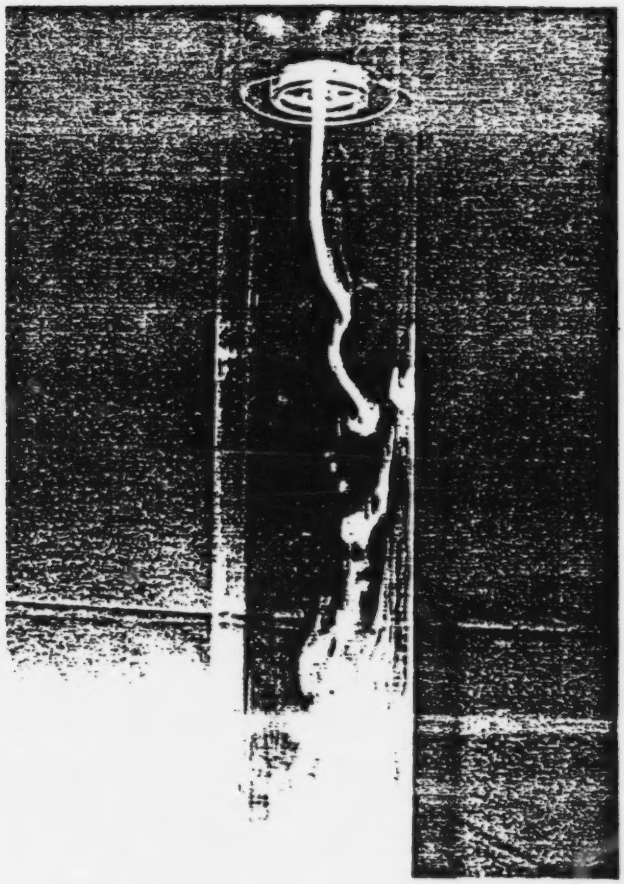

Primary Inlet Reynolds number	142
Secondary Inlet Reynolds number	427
Furnace Tube Reynolds number	656

Figure 5: **Original Burner – UP/US = 1:1 – unsteady laminar flow (UP/US = Primary Inlet Velocity/Secondary Inlet Velocity)**

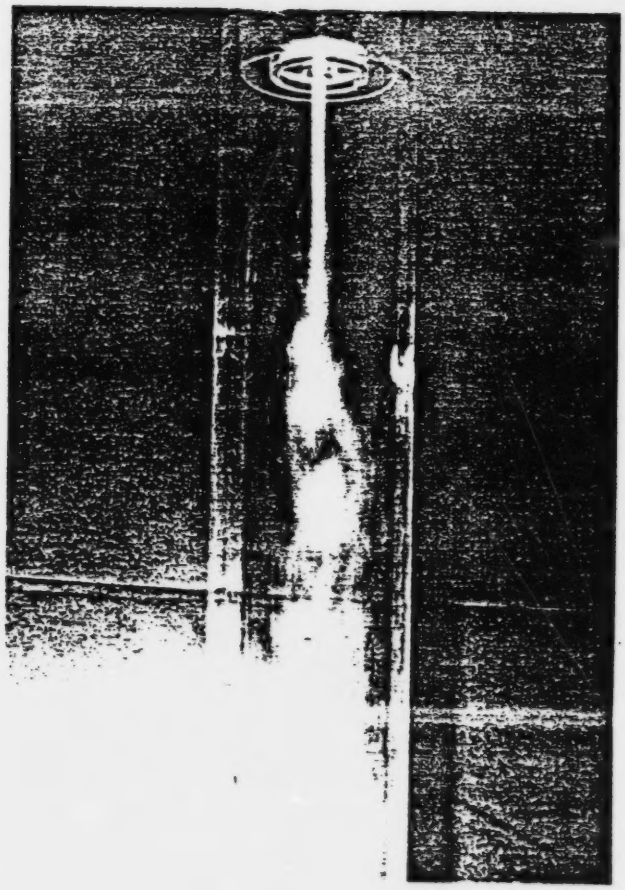

Primary Inlet Reynolds number 947
Secondary Inlet Reynolds number 1447
Furnace Tube Reynolds number 2257

Figure 6: Original Burner – UP/US = 2:1 – turbulent flow (UP/US = Primary Inlet Velocity/Secondary Inlet Velocity)

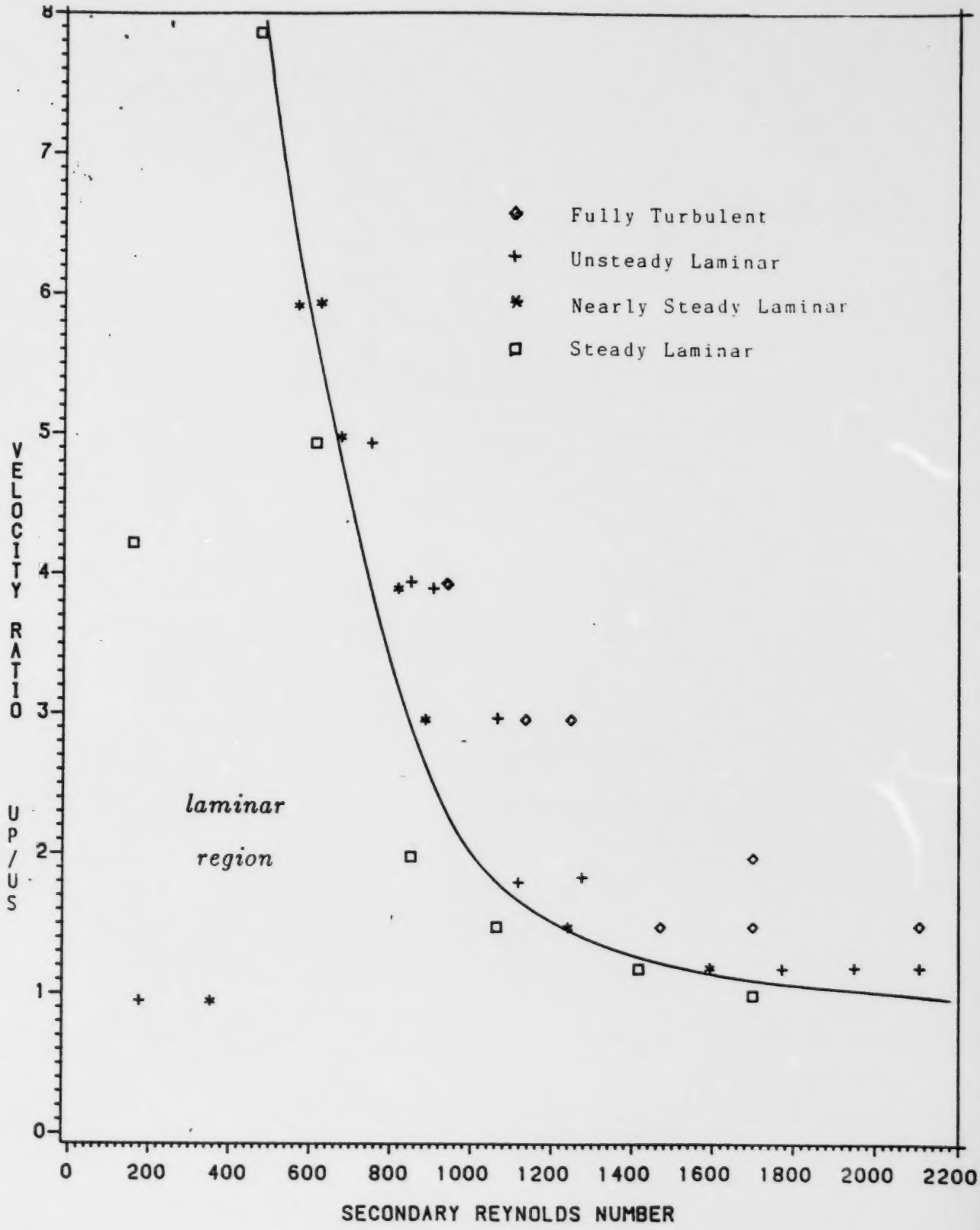

Figure 7: **Stability Curve for Isothermal Flow – Modified Burner**

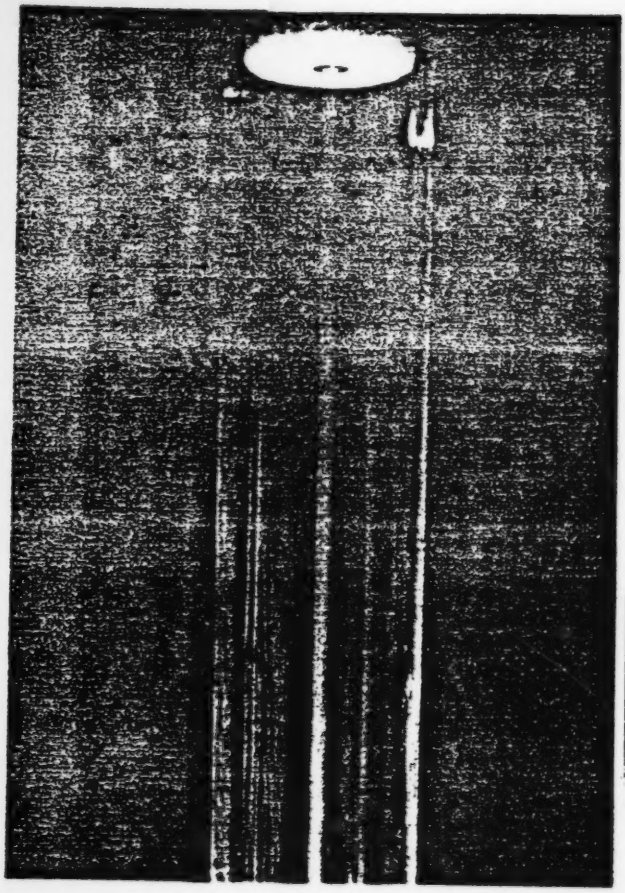

← TOP

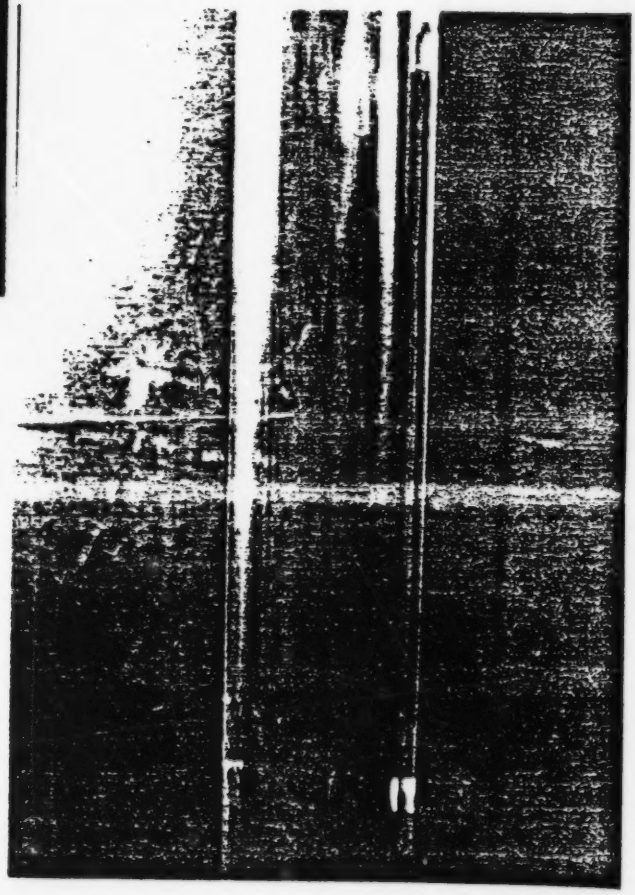

BOTTOM →

Primary Inlet Reynolds number 466
Secondary Inlet Reynolds number 940
Furnace Tube Reynolds number 1180

Figure 8: Modified Burner – UP/US = 4:1 – turbulent flow (UP/US = Primary Inlet Velocity/Secondary Inlet Velocity)

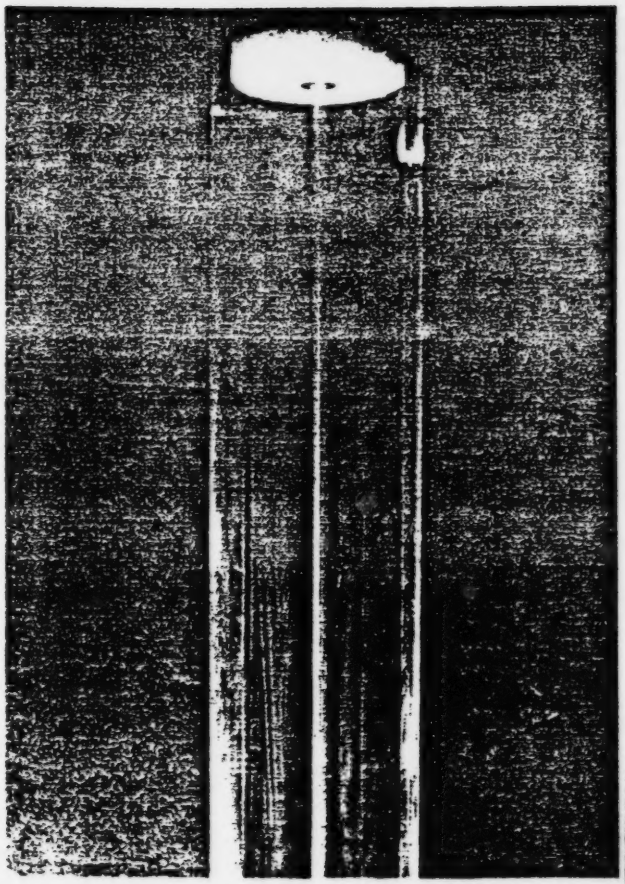

← TOP

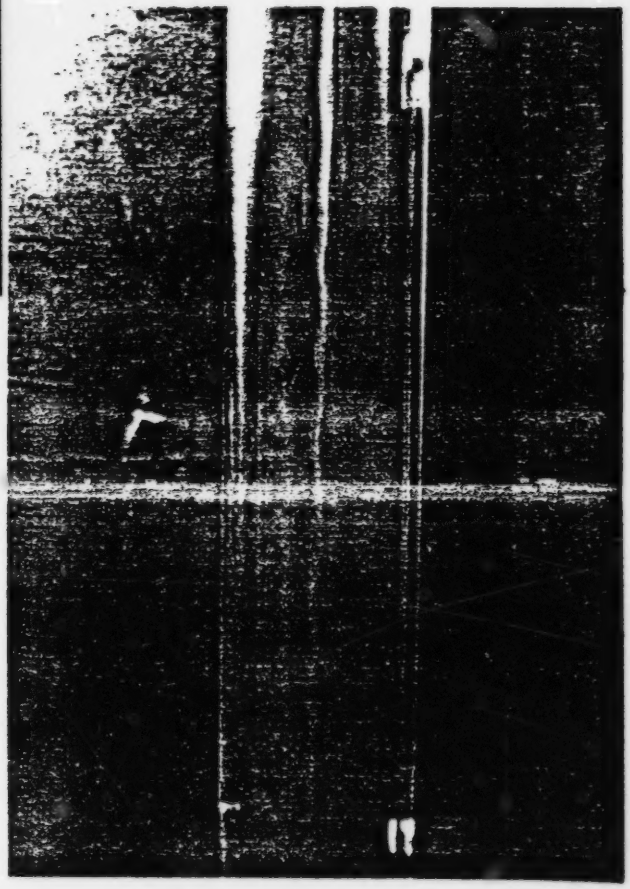

BOTTOM →

Primary Inlet Reynolds number 250
Secondary Inlet Reynolds number 1120
Furnace Tube Reynlods number 1370

Figure 9: **Modified Burner – UP/US = 2:1 – unsteady laminar flow (UP/US = Primary Inlet Velocity/Secondary Inlet Velocity)**

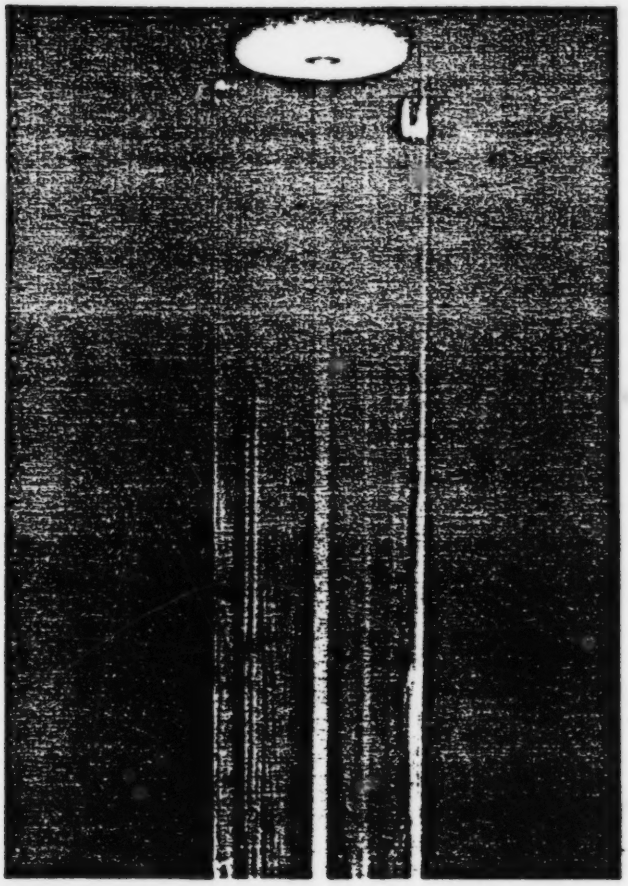

← TOP

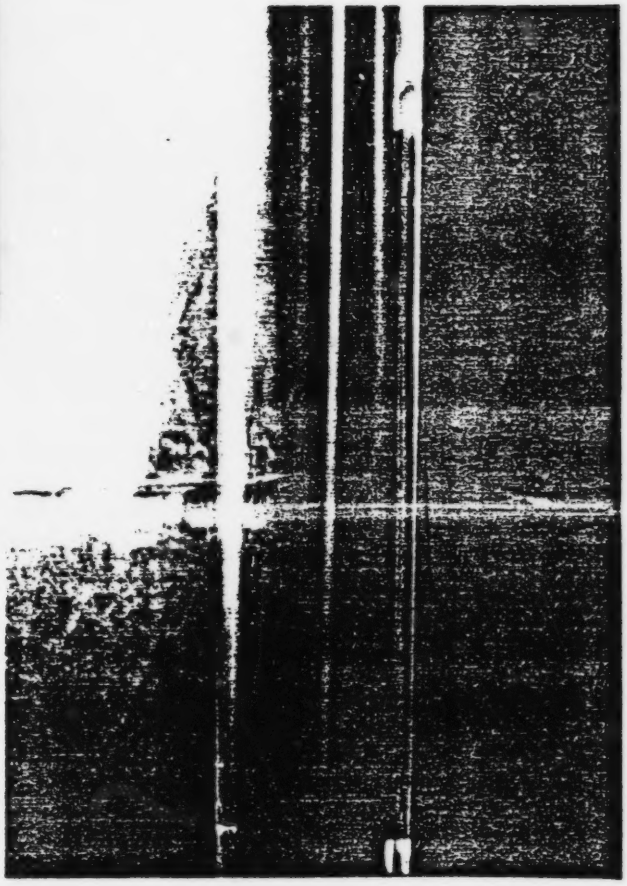

BOTTOM →

Primary Inlet Reynolds number	210
Secondary Inlet Reynolds number	425
Furnace Tube Reynolds number	535

Figure 10: **Modified Burner – UP/US = 4:1 – steady laminar flow (UP/US = Primary Inlet Velocity/Secondary Inlet Velocity)**

Chapter 4

THE NUMERICAL MODEL

4.1 INTRODUCTION

A numerical model which gives flow field patterns and particle heating rates was developed for the CMCH coal testing facility; it is to be used in a parametric study to determine the various particle heating rates that could be achieved with the furnace. Input data are the inlet flow velocities and temperatures and the heating element temperatures of each of the four heating zones. The model incorporates variable properties and the buoyancy effects which result from the large temperature difference between the downward flow and the furnace wall. The coal particles are treated as inert (ie no chemical reaction) for this study; a combustion model is to be the subject of future research. The small concentration of particles was considered to contribute very little to the overall energy and momentum balances; the effects of the particles on the gas flow were therefore ignored, allowing the gas flow and particle heating problems to be decoupled (see Appendix A). The numerical scheme was required to resolve a laminar flow downwards through a vertical tube furnace with four independent heating zones and subsequently solve particle heating and transit times through the same furnace.

4.2 THE FURNACE FLOW FIELD

4.2.1 The Mathematical Problem

The problem to be solved is a parabolic, 2-D axisymmetric, non-isothermal, steady laminar flow. The equations involved are those of momentum, energy and continuity. The reduced forms of the differential equations necessary to solve this problem are shown in Table 4 . It was assumed that viscous dissipation and compressibility effects were negligible in the energy equation, and specific heats and Prandtl number were assumed constant over the temperature range of interest. The differential equations are all interlinked with each other and with the inlet and boundary conditions. These interactions add to the complexity of the problem, and a successful numerical scheme must be able to conform to all these interactions.

4.2.2 The TEACH Program

The numerical scheme that was chosen for the solution was the 1974 Imperial College TEACH (Teaching Elliptic Axisymmetric Characteristics Heuristically) finite difference program. The TEACH computer code is based on a primitive pressure - velocity approach, solving for pressure and velocity as primary variables. TEACH is a widely used, standard computer code that has been used for a number of fluid dynamic and heat transfer problems [2, 26, 29]. TEACH puts the governing differential equations into finite difference form by integration over a control volume. The solution combines each of the equations of energy, momentum and continuity with the boundary and inlet conditions and solves them simultaneously using an iterative procedure. The program consists of a main routine which calls a series of subroutines to solve for the dependent variables. A TDMA (Tri-Diagonal Matrix Algorithm) is used to

solve the flow field equations and the equations are solved iteratively until a convergence criterion is met.

4.2.3 The Formulation of the Problem

The equations of momentum, energy and continuity are similar and contain terms for both convection and diffusion of momentum, energy and mass as well as source terms. The governing differential equations in Table 4 can all be put into the following convenient form:

$$\frac{1}{r}\left[\frac{\partial}{\partial x}(\rho u r\phi) + \frac{\partial}{\partial r}(\rho v r\phi) - \frac{\partial}{\partial x}(r\Gamma_\phi \frac{\partial \phi}{\partial x}) - \frac{\partial}{\partial r}(r\Gamma_\phi \frac{\partial \phi}{\partial r})\right] = Su^\phi + Sp^\phi \phi \qquad (4.1)$$

The values for ϕ , Γ_ϕ , Su^ϕ and Sp^ϕ for each equation are shown in Table 5 . These are the equations necessary to solve the furnace flow field. The unknown variables are the axial and radial velocities, the pressure and the temperature.

The flow field area is divided into small control volumes which form a grid pattern. The control volumes need not be uniform, and can have varying sizes. Figure 11 shows a typical control volume, through which momentum, energy and mass are transported by convection and diffusion, while generation and dissipation of momentum within the cell also takes place. Conservation of these quantities is necessary for each cell. Values of variables are stored at the node points within the cell, except for the axial and radial velocity, which are stored at points on the control volume boundaries. The nodes are placed such that the control volume boundaries lie exactly halfway between adjacent nodes. This type of formulation results in a staggered grid, as discussed by Patankar [29].

As a result of the staggered grid, two further control volumes arise for the axial and radial velocities ("U" and "V" cells – the cell first shown in Figure 11 is referred to as a "C" cell). These are shown in Figure 12. For each control volume there is a centre point P and its four neighbouring points N,S,W,and E, as illustrated in Figure (11). By integrating over the appropriate control volume, a quantity at the centre of the control volume can be expressed in terms of the neighbouring grid point values. Details of the integration can be found in [2, 26, 29]. The result is an equation of the form:

$$a_P^{\phi}\phi_P = \sum_j a_j^{\phi}\phi j + Su^{\phi}$$

where $$a_P^{\phi} = \sum_j a_j^{\phi} - Sp^{\phi}$$

for each cell, where ϕ can represent any variable, and the coefficients " a^{ϕ} " represent the influence of each neighbour cell on P.

This formulation is applied to each cell control volume in the grid domain. The cells in the grid are adjacent to each other; therefore, the east face of one cell is the west face of the cell immediately to the right, and so forth. Similarly, the south face of one cell is the north face of the cell beneath it. Expressions for each cell are obtained in this fashion.

For each control volume there will be a diffusive and a convective flux into and out of the cell. A "hybrid" scheme is used to calculate these, which employs different expressions for the total flux, depending on whether one flux dominates or the two are of the same order of magnitude. Defining the Peclet number as the ratio of convective to diffusive transport of the variable ϕ , the hybrid scheme uses as a criterion a Peclet number equal to 2 to determine the dominating flux. If the Peclet number is greater than 2, the upstream

convective flux dominates (ie the flux through the west cell face), and an upwind difference formulation is used, in which the value of ϕ at point W is assumed convected into cell P, and diffusion is neglected. If the Peclet number is less than -2, the downstream convective flux dominates (ie flux through east cell face), leading to a similar formulation involving point E. If the Peclet number lies between -2 and 2 (convection and diffusion of the same order of magnitude), diffusion is included, and a central difference formulation is used for convection, in which the value of ϕ at the cell boundary (determined by linear interpolation) is convected into the cell. All the cells in the grid domain are treated in the same manner. The hybrid scheme is said to be a good approximation to an exact one-dimensional solution. The exact solution is not recommended because it contains exponentials, which are expensive to compute, and because it is not exact for two or three dimensions (Patankar [29]).

The U and V cells (representing the axial and radial equations of motion) contain pressure gradient terms not present in the C cell. In order to solve the U and V equations, the pressure field must be known. An estimate of the pressure field P^* is used as a trial, and subsequent estimates of velocity fields U^* and V^* are made based on this pressure field. A pressure correction is then made, which forces the velocity field to obey the continuity equation by applying the correction to U^* and V^* to give U and V. The corrected pressures are then used as the new trial values, and so on till convergence is achieved.

The finite difference equations are coupled with the inlet and boundary conditions, all of which must be solved simultaneously. The coefficients and source terms are functions of the variables, and the velocities are strongly dependent on the pressure. The equations are solved by a cyclic repetition of the following steps:

1. Estimate all of the dependent variables
2. Solve the axial and radial momentum equations and obtain estimates for the U and V velocity fields
3. Solve for the pressure correction field P'
4. Calculate the true pressure field and correct the U and V velocity fields
5. Calculate the temperature field T
6. Calculate the density and viscosity
7. Treat the values obtained as better estimates of each field. Return to 2. and repeat the procedure until convergence

A flow chart of the procedure is shown in Figure 13. A listing of the computer program is included at the end of this report in Appendix C.

4.2.4 The Grid Pattern

The grid pattern for a particular problem is determined from the geometry, the type of flow and the boundary and inlet conditions. The number of grid points and the spacing between them is important in obtaining an accurate solution. The CMCH furnace was considered to be a heated pipe with developing temperature and velocity profiles, and four wall heating zones whose temperatures could be varied independently.

The furnace can be represented by a series of annular segments, which are the control volumes over which the differential equations are integrated. Since the furnace is axisymmetric, only one half of the furnace need be examined. Developing velocity and temperature profiles in a tube approach their final form asymptotically. The profiles change quite rapidly in the initial region of the tube, and the changes become less as the flow approaches its final fully

developed state. To correspond to this, a grid spacing was chosen such that there were many points in the region of large gradients and fewer points as the gradients became smaller; the resulting scheme gave a grid spacing which increased approximately exponentially with distance along the furnace. Similarly, the grid lines were spaced more closely in the radial direction at the tube wall and the burner inlet because of the large gradients expected there.

A series of tests were performed to determine the number and spacing of points that were necessary for accuracy, taking into account the points discussed above and the requirement that the boundaries of the four heating zones correspond with the cell boundaries. To aid in this decision, the program was used to solve a number of simple test cases for which solutions were available from the literature. The test cases were as follows:

1. Iso-thermal developing pipe flow
2. Fully developed pipe flow subject to heating at constant wall temperature
3. As in 2. but heating with constant heat flux

These are discussed in detail in Section 5.1. The number of points and their spacing in the furnace tube was consequently modified so that they would conform to published results.

The grid pattern that was chosen for this problem consisted of 28 nodal points in the axial direction and 20 nodal points in the radial direction. The grid is shown in Figure 14.

4.2.5 Inlet Conditions

The flow was introduced into the furnace through the burner mouth. It consisted of a primary and secondary stream of air. The primary flow was assumed to have had sufficient length to attain a fully developed parabolic profile before entering the furnace, while the secondary flow velocity was assumed uniform. The results of the flow visualization experiments showed that a modification to the burner was necessary in order to obtain a stable flow; hence, the modified burner geometry was used for all calculations.

The primary flow was assumed kept at a constant temperature by means of the water-cooled jacket, while the secondary flow was assumed preheated to a specified inlet temperature.

4.2.6 Boundary Conditions

The physical boundaries for this problem were the furnace wall, the burner and the water-cooled injector. The grid cells which lie along these boundaries have to be modified to incorporate the known boundary values. Each cell is a small control volume over which the differential equations are integrated. If a cell face falls on a boundary, the known boundary value is used for that face, and any fluxes (heat) associated with the boundary are introduced via a source term (Equation 4.1). The boundary value incorporated into the source term remains fixed throughout each iteration. The remaining faces of the boundary cell and subsequently all cells throughout the flow field adjust with each iteration to incorporate the boundary value.

4.2.6.1 Velocity Boundary Conditions

The boundary conditions for the axial and radial velocity fields are shown in Figure (15). The boundaries specified are the furnace wall, the tube axis and the water-cooled section of the burner. The outlet represents no physical boundary, therefore no boundary conditions are imposed. The only requirement at the outlet boundary is the overall conservation of mass. At each iteration, the total mass leaving the furnace is subtracted from the total mass entering the furnace. The difference is evenly divided and added to the control volumes on the outlet boundary, and the flow field equations are solved using this mass correction.

4.2.6.2 Temperature Boundary Condition

There are two wall surfaces which need to have a temperature boundary condition specified: the face of the water-cooled jacket of the burner, and the furnace tube wall. The temperature of the water-cooled jacket is considered to remain constant at the cooling water temperature, while the temperature of the furnace wall is unknown and must be solved for.

The furnace tube is heated by 64 - 500 W glow bars (heating elements). These are spaced evenly down the length of the tube, 32 on each side. The furnace tube is completely surrounded by refractory material in which the glow bars are embedded. The furnace is separated into four independent heating zones and the temperature of each zone is measured using a thermocouple. The refractory surface and glow bars surrounding the tube were treated as a uniformly radiating black surface at the measured average zone temperature. Figure 16 shows a cross section through the furnace tube. The radiation from the refractory brick to the outside wall of the furnace tube is given by:

$$\dot{Q} = 2\pi R_o L \sigma \epsilon (T_{gb}^4 - T_{wo}^4)$$

or $$\dot{Q} = 2\pi R_o L \sigma \epsilon (T_{gb} - T_{wo})(T_{gb} + T_{wo})(T_{gb}^2 + T_{wo}^2)$$

where ϵ = 0.90 furnace tube (Bolz and Tuve [8])

Heat conduction through the mullite furnace tube is given by:

$$\frac{\dot{Q}}{2\pi RL} = \frac{k_w(T_{wo} - T_w)}{Rln(R_o/R)}$$

where k_w = 2.076 W/m K (Bolz and Tuve [8])

Heat conduction from the inner tube wall to the flowing gas is given by:

$$\frac{Q}{2\pi RL} = k_g\left(\frac{\partial T}{\partial r}\right)_w \qquad \text{where} \qquad \left(\frac{\partial T}{\partial r}\right)_w = \frac{T_w - T_g^*}{R - R_g^*}$$

The overall expression for the heat transfer from the glow bars (heating elements) to the gas inside the tube is then:

$$\frac{Q}{2\pi RL} = \frac{T_{gb} - T_g^*}{R_w + R_g + R_r}$$

where

$$R_w = \frac{Rln(R_o/R)}{k_w}$$

$$R_g = \frac{R - R_g^*}{k_g}$$

$$R_r = \frac{R}{R_o}\frac{1}{\sigma\epsilon(T_{gb} + T_{wo})(T_{gb}^2 + T_{wo}^2)}$$

This expression is used as the boundary condition for the furnace wall temperature. The four zone temperatures can be changed independently.

4.2.7 Buoyancy

Buoyancy forces become significant in this problem because of the large temperature differences between the furnace wall and the incoming fluid, leading to large density differences within the furnace.

Consider the following terms in the U momentum equation:

$$\ldots = -\frac{\partial P}{\partial x} + \rho g_x$$

This will appear as a source term in the axial momentum equation. In order to avoid instability in a numerical solution, it is desirable to make sources as small as possible. In this case, this can be done by choosing a arbitrary reference density ρ_0 ,leading to:

$$\ldots = -\frac{\partial P'}{\partial x} + g_x(\rho - \rho_0)$$

where $$P' = P - \int \rho_0 g_x dx$$

Since this integral is only a function of x and not of y:

$$\frac{\partial P}{\partial y} = \frac{\partial P'}{\partial y}$$

the radial velocity field is not affected. The reference density was chosen as ρ_{axis} since:

$$\frac{\partial}{\partial y}(\rho_{axis}) = 0$$

The pressure calculated now becomes the "pressure head" at the centre of the flow. By using this formulation for the reference density, the number of iterations necessary for convergence is reduced because of less round-off error and less instability. The disadvantage is that the pressure now is calculated as P' rather than the actual pressure P; however, P is not required for any further purpose (Spalding [37]).

4.2.8 Fluid Properties

4.2.8.1 Density

Air is considered to be an ideal gas, therefore the density is calculated using the ideal gas law:

$$\rho = P/RT$$

where P = pressure
R = gas constant
T = temperature

The temperature is calculated from the solution of the energy equation; hence,the density must be updated with each iteration.

4.2.8.2 Viscosity

The variation of viscosity with temperature was accounted for by using the Sutherland equation:

$$\mu = \frac{BT^{\frac{3}{2}}}{(T+S)}$$

where B = 1.5 E-6
S = 130.0
T = temperature

The constants B and S were determined by fitting the equation to values in tables (Holman [20]). Figure (17) compares actual air viscosities to those predicted by the Sutherland equation. As with the density, the local viscosity must be updated each iteration.

4.2.9 Convergence Criterion

The respective differential equations (Equation 4.1) are integrated over each corresponding control volume (ie C, U, or V cell) in the grid domain. If these equations are not satisfied, there will be a remaining or residual momentum, mass or energy source in the control volume, which can be either positive or negative. There will be axial momentum residuals for the U cells, radial momentum residuals for the V cells, and mass and energy residuals for the C cells. The absolute values of the residuals for each control volume are totalled over the grid domain for each of the four residual quantities and made non–dimensional by means of the corresponding inlet values (ie inlet momentum, mass and energy fluxes).

$$\text{Inlet momentum flux} = 2\pi \int_0^{r_o} \rho u^2 r\,dr$$

$$\text{Inlet mass flux} = 2\pi \int_0^{r_o} \rho u r\,dr$$

$$\frac{\text{Inlet energy flux}}{c_P} = 2\pi \int_0^{r_o} u T r\,dr$$

where u = inlet velocity

r = radial postion

T = temperature

ρ = density

c_P = specific heat

With each iteration and subsequent adjustments of the flow field, each of the four residuals will be reduced (or increased). If the solution is converging, then the residual terms will tend to zero (conversely, if the solution is diverging, then the terms will tend to infinity). If the residual terms are small enough that further adjustments of the flow field are negligible then the solution can be said to be converged. In this case, the criterion used for convergence was that all four dimensionless residuals be less than 1%. Tests showed that a more stringent criterion did not significantly change the solution. It should be noted that, since there are 560 points in the grid, this represents a residual source of less than 0.002% for each cell on the average. The criterion is made more stringent by the fact that the residuals are calculated before the pressure correction is applied to obtain the final, correct velocity field. The execution of the program will stop if any of the following criteria are met:

1. The solution has converged.
2. The solution has diverged.
3. The maximum number of iterations has been reached.

To aid in the convergence and avoid oscillations, the solution uses an under-relaxation factor (URF) which reduces the magnitude of the flow field changes after each iteration. The formulation for under-relaxation is as follows:

$$\phi_P^{n+1} = (URF)\tilde{\phi}_P^{n+1} + (1 - URF)\phi_P^n$$

where $\tilde{\phi}_P^{n+1}$ represents the newly calculated value of ϕ_P at the (n+1)th iteration. A fraction (URF) of the new calculated value of ϕ_P at the (n+1)th iteration is taken and the remaining fraction is taken as the previously calculated value at the (n)th iteration. This is done for each value in the domain, thus reducing the magnitude of the changes of ϕ_P between successive

iterations; the resulting field is used for calculations in the other subroutines. The effect of the under-relaxation factor is substantial, and oscillating or diverging solutions can result if URF is not chosen correctly. The URF must be chosen to suit each problem. Four URF are used in this problem:

axial velocity URFU = 0.5

radial velocity URFV = 0.5

pressure URFP = 0.2

temperature URFT = 0.8

4.3 PARTICLE MOTION AND HEATING

4.3.1 Introduction

Once the flow and temperature field has been solved for, the flow and heating of the particles can be introduced. In order to simplify the problem, a number of assumptions were made in the development of this model:

1. The volumetric concentration of particles is small enough such that individual particles are not affected by neighbouring ones (see Appendix A).
2. The addition of particles to the furnace does not affect the momentum, energy or continuity balances in the gas significantly.
3. The particles are treated as grey spheres exchanging heat by radiation and convection with the gas and the furnace wall and are considered small enough and of sufficiently low concentration not to cause any effect on the radiant exchange between surfaces. By the same token, scattering of radiation by particles ("cloud effects") is neglected.
4. The particles do not react chemically

5. The particles follow a straight line down the centre line and are not dispersed radially.
6. The temperature is assumed uniform within each particle, ie internal temperature gradients due to heating are neglected.

4.3.2 Particle Motion

The coal particles were considered spherical in shape; therefore, the forces experienced by the particle are those of gravity and drag. The acceleration of the particle is given by:

$$\frac{\partial u_P}{\partial t} = g - \frac{3}{4}\frac{C_D \rho}{\rho_P d_P}(u_P - u)|u_P - u|$$

where

$$C_D = \frac{24}{Re}(1 + 0.15Re^{0.687}) \qquad (4.2)$$

(Smoot [35])

$$Re = \frac{\rho|u_P - u|d_P}{\mu}$$

For small Re, the expression inside the brackets on the right of Equation (4.2) will be small; therefore, it can be linearized as:

$$\frac{du_P}{dt} = g - A(u_P - u) \qquad (4.3)$$

where

$$A = \frac{18\mu}{\rho d_P^2}(1 + 0.15Re_0^{0.687})$$

The solution uses an explicit marching scheme, following the particle along the axis of the tube in discrete time steps Δt and calculating each new velocity based on the local air velocities and previous particle velocities. Equation (4.3) is an exact differential equation and could be solved directly if A were constant; however, the gas velocity and the Reynolds number are constantly changing. If a small enough time step is chosen, then u and Re can be assumed constant throughout the time step Δt (Smoot [35]), and Equation (4.3) integrated to give:

$$u_P = u - \frac{1}{A}\left[\left(g - A(u_{P0} - u)\right)e^{-A\Delta t} - g\right]$$

where u_P = the velocity at the end of the time step

u_{P0} = the velocity from the previous time step

Properties of the gas are evaluated at the film temperature, which is the arithmetic mean of the particle temperature and the surrounding gas temperature.

4.3.3 Particle Heating

The heating of a particle is based on the net energy received by the particle as it travels through the furnace. The particle receives or loses energy by radiation from/to the surrounding surfaces and loses or gains energy by convection to/from the surrounding gas. The furnace was separated into four radiating surfaces: the furnace wall, the primary inlet and water-cooled jacket, the secondary inlet, and the water-cooled collector. The temperature of the furnace wall is not constant, but varies along the furnace length. To simplify

the problem, the model uses a "long furnace" approximation, which assumes that the effective radiating temperature of the wall is the temperature of the wall section radially opposite the particle (Hottel and Sarofim [21]). The temperature of the other radiating surfaces was assumed constant, and the appropriate view factor was used in determining the radiant balance. Since the particle is small, the radiant exchange between it and the other particles was considered negligible.

The expression for particle heat transfer is given as follows:

$$mc_{PP}\frac{dT}{dt} = A_P q_{net} \qquad (4.4)$$

where $$m = \rho_P \frac{\pi}{6} d_P^3$$

$$A_P = \pi d_P^2$$

$$q_{net} = [q_{rad} - q_{conv}]$$

c_{PP} coal = 1.3 kJ/kg K (Bolz and Tuve [8])

therefore, rearranging;

$$\frac{dT}{dt} = \frac{6}{\rho_P c_{PP} d_P}[q_{rad} - q_{conv}]$$

where $$q_{conv} = h(T_P - T_g)$$

$$h = \left[2.0 + (0.4Re^{1/2} + 0.06Re^{2/3})(Pr^{0.4})\left(\frac{\mu}{\mu_P}\right)^{1/4}\right]\frac{\mu c_P}{Prd_P}$$ (Holman [20])

and

$$q_{rad} = h_{PP}(T_1 - T_P) + h_{PS}(T_S - T_P) + h_{PE}(T_E - T_P) + h_{PW}(T_W - T_P)$$

$$h_{PP} = \sigma\epsilon F_{PP}(T_1 + T_P)(T_1^2 + T_P^2)$$
$$h_{PS} = \sigma\epsilon F_{PS}(T_S + T_P)(T_S^2 + T_P^2)$$
$$h_{PE} = \sigma\epsilon F_{PE}(T_E + T_P)(T_E^2 + T_P^2)$$
$$h_{PW} = \sigma\epsilon F_{PW}(T_W + T_P)(T_E^2 + T_P^2)$$

ϵ coal = 0.8 (Hottel and Sarofim [21])

F_{PP} , F_{PS}, F_{PE}, F_{PW} are the view factors and can be found in Appendix (B).

The expression for particle heating can be written as:

$$\frac{dT_P}{dt} = -AT_P + B \qquad (4.5)$$

where $$A = \frac{6}{\rho_P c_{PP} d_P}[h_{PP} + h_{PS} + h_{PE} + h_{PW} + h]$$

$$B = \frac{6}{\rho_P c_{PP} d_P}[h_{PP}T_1 + h_{PS}T_S + h_{PE}T_E + h_{PW}T_W + hT_g]$$

As with the particle velocity, the wall temperature and the gas temperature are changing axially along the furnace tube. To be able to integrate this equation, these values are assumed constant over the time step Δt. By integrating Equation (4.5) over Δt the expression leads to:

$$T_P = \frac{1}{A}[B + AT_{P0}e^{-A\Delta t}] \qquad (4.6)$$

The value of Δt must be selected such that the assumptions of constant u, T, Re are valid. By choosing a time step such that $T_{P0} - T_P$ is less than ΔT_{max}, where ΔT_{max} is an arbitrarily chosen constant which would give a fixed increase in temperature between points, (chosen as 5 K), Equation (4.4) becomes:

$$\Delta t \approx \frac{\rho_P c_P d_P \Delta T_{max}}{6(q_{rad0} - q_{conv0})}$$

where q_{rad0} , q_{conv0} are from the previous time step

By selecting Δt in this manner, Δt would be small initially where the heating was very rapid, and would become progressively larger downstream where the temperature increase becomes less. An upper limit for the time step was chosen (5 ms) in order to ensure the validity of the assumption that the gas velocity was constant over the time step.

The particle velocity and temperature model was added onto the main furnace flow program as a subroutine. Once the furnace flow field had been calculated, the particle model subroutine was called to calculate particle velocities and temperatures.

TABLE 4

Governing Differential Equations

EQUATION OF CONTINUITY

$$\frac{1}{r}\left[\frac{\partial}{\partial x}(\rho u r) + \frac{\partial}{\partial r}(\rho v r)\right] = 0$$

EQUATION OF MOTION

axial direction

$$\frac{1}{r}\left[\frac{\partial}{\partial x}(\rho u^2 r) + \frac{\partial}{\partial r}(\rho u v r) - \frac{\partial}{\partial x}(r\mu\frac{\partial u}{\partial x}) - \frac{\partial}{\partial r}(r\mu\frac{\partial u}{\partial r})\right]$$
$$= -\frac{\partial P}{\partial x} + \frac{\partial}{\partial x}(\mu\frac{\partial u}{\partial x}) + \frac{1}{r}\frac{\partial}{\partial r}(r\mu\frac{\partial v}{\partial x}) - \frac{2}{3}\frac{\partial}{\partial x}(\frac{\mu}{r}\frac{\partial}{\partial r}(rv) + \mu\frac{\partial u}{\partial x}) + \rho g_x$$

radial direction

$$\frac{1}{r}\left[\frac{\partial}{\partial x}(\rho u v r) + \frac{\partial}{\partial r}(\rho v^2 r) - \frac{\partial}{\partial x}(r\mu\frac{\partial v}{\partial x}) - \frac{\partial}{\partial r}(r\mu\frac{\partial v}{\partial r})\right]$$
$$= -\frac{\partial P}{\partial r} - \frac{2\mu v}{r^2} + \frac{\partial}{\partial x}(\mu\frac{\partial u}{\partial r}) + \frac{1}{r}\frac{\partial}{\partial r}(r\mu\frac{\partial v}{\partial r}) - \frac{2}{3}\frac{\partial}{\partial r}(\frac{\mu}{r}\frac{\partial}{\partial r}(rv) + \mu\frac{\partial u}{\partial x})$$

EQUATION OF ENERGY

$$\frac{1}{r}\left[\frac{\partial}{\partial x}(\rho u T r) + \frac{\partial}{\partial r}(\rho v T r) - \frac{\partial}{\partial x}(r\frac{k}{c_P}\frac{\partial T}{\partial x}) - \frac{\partial}{\partial r}(r\frac{k}{c_P}\frac{\partial T}{\partial r})\right] = 0$$

TABLE 5

Expressions for the Variables of the Generalized Equation

ϕ	Γ_ϕ	Sp^ϕ	Su^ϕ
1	0	0	0
u	μ	0	$\frac{\partial}{\partial x}(\mu\frac{\partial u}{\partial x}) + \frac{1}{r}\frac{\partial}{\partial r}(r\mu\frac{\partial v}{\partial x}) - \frac{\partial P}{\partial x} + \rho g_x$
v	μ	$-\frac{2\mu}{r^2}$	$\frac{\partial}{\partial x}(\mu\frac{\partial u}{\partial r}) + \frac{1}{r}\frac{\partial}{\partial r}(r\mu\frac{\partial v}{\partial r}) - \frac{\partial P}{\partial r}$
T	$\frac{k}{c_P}$	0	0

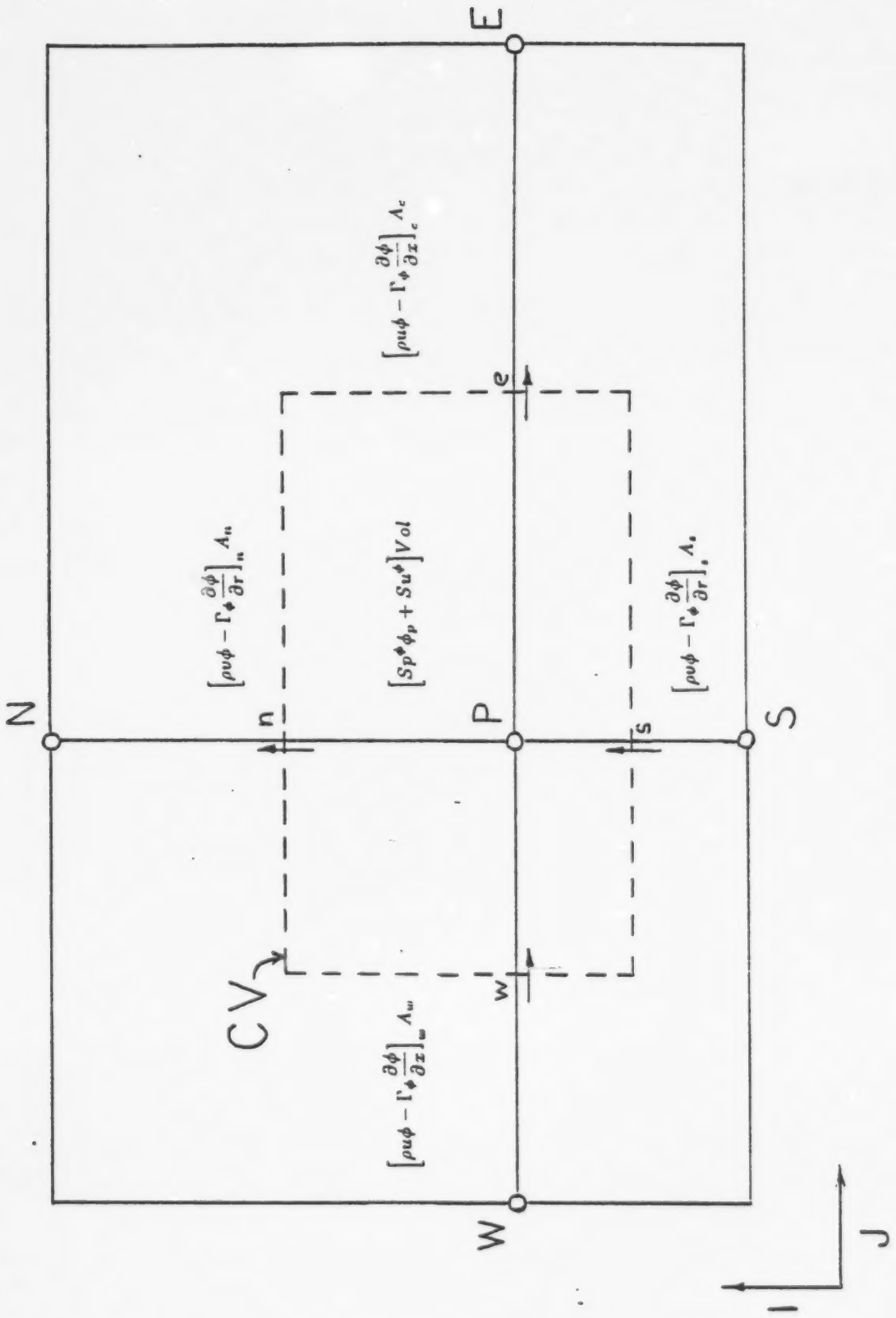

Figure 11: Typical Control Volume for Numerical Model of Furnace

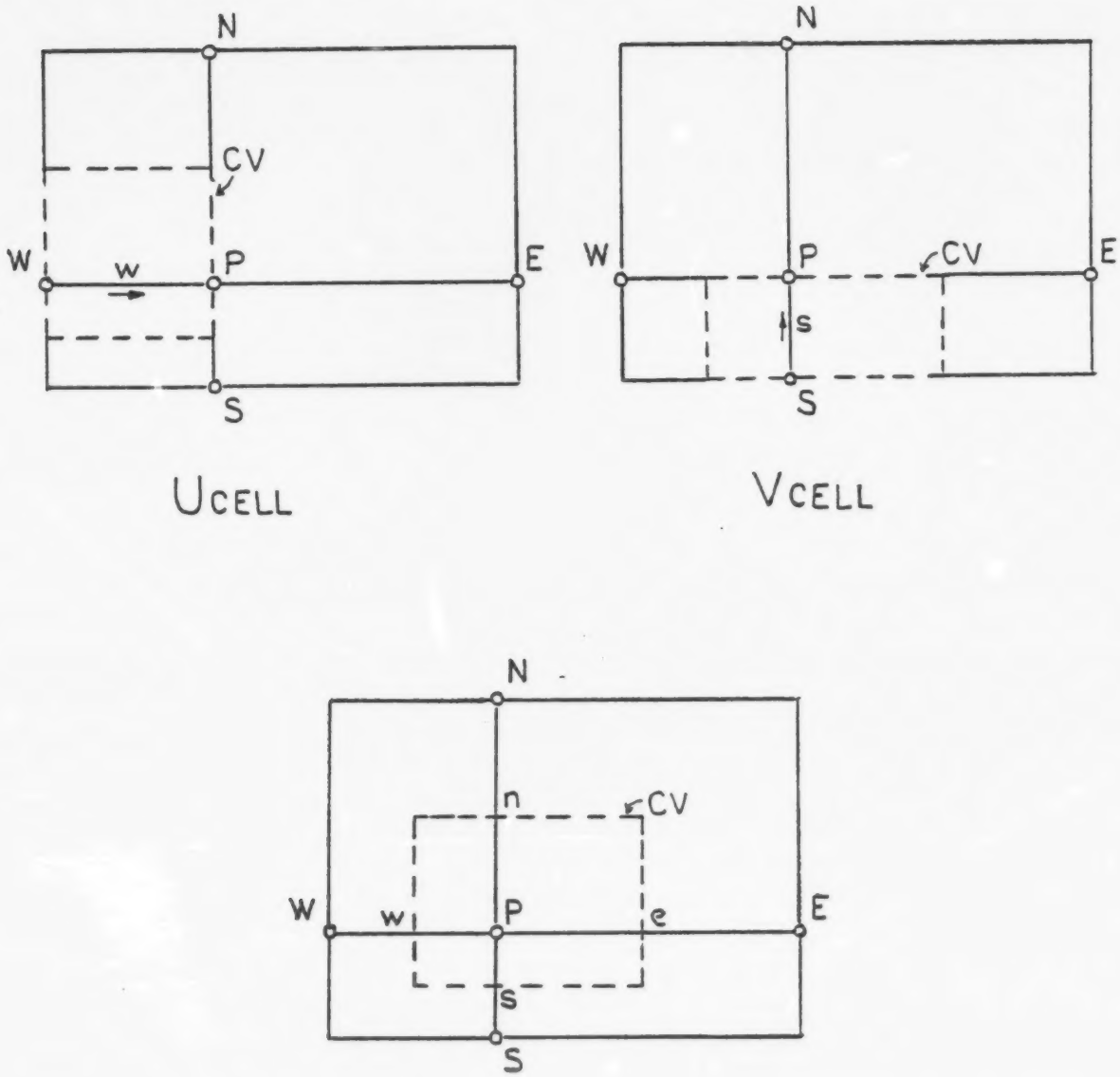

Figure 12: U, V and C Cells for Numerical Model

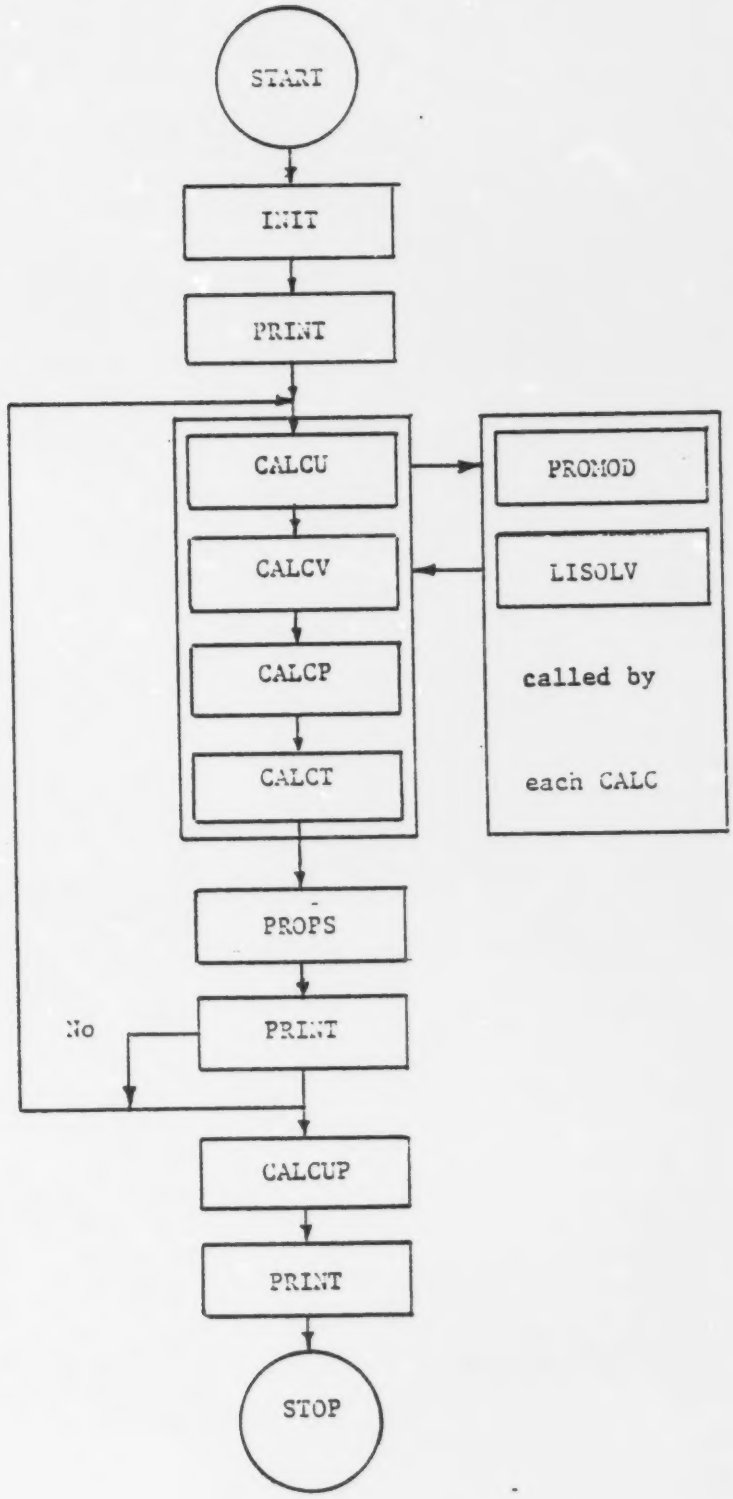

Figure 13: Flowchart of the Numerical Model

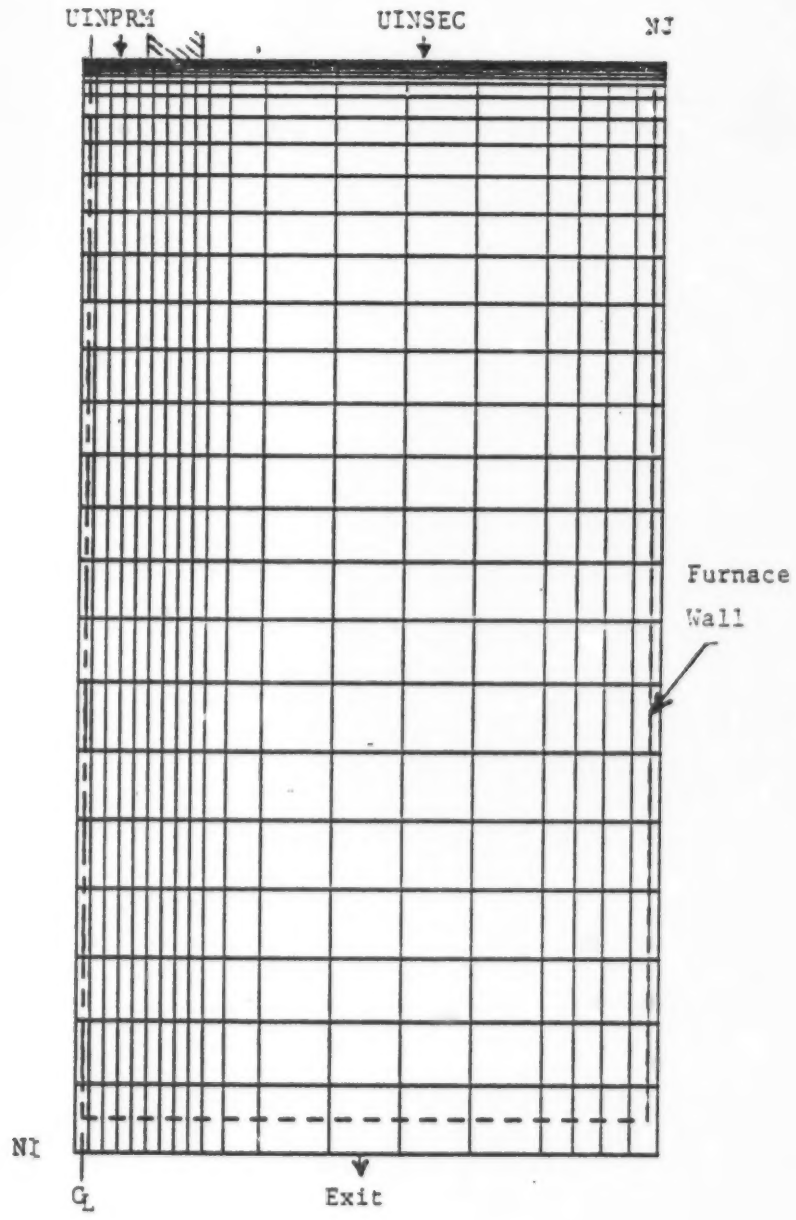

Figure 14: Grid Pattern Used to Divide the Furnace into Segments

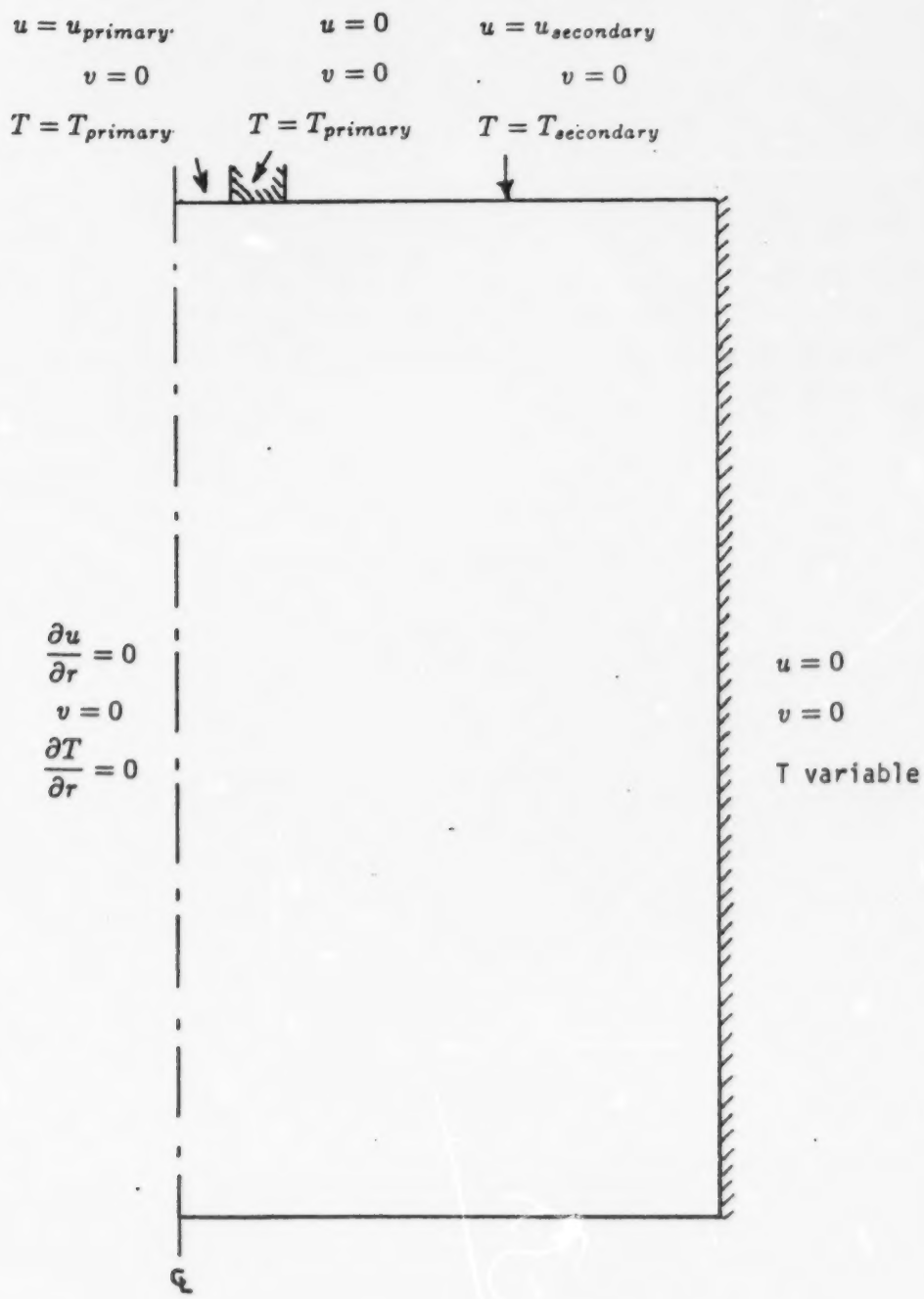

Figure 15: Boundary Conditions for Furnace

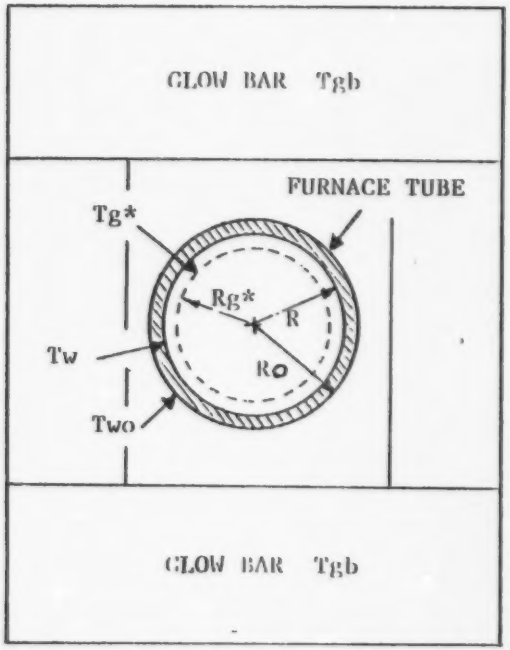

Figure 16: Cross-section through the Drop Tube Furnace Showing Temperature Boundary Conditions

GLOW BARS TO OUTSIDE WALL

$$\dot{q} = \frac{\sigma\varepsilon(Tgb - Two)(Tgb + Two)(Tgb^2 + Two^2)}{R/Ro}$$

OUTSIDE WALL TO INSIDE WALL

$$\dot{q} = \frac{kw(Two - Tw)}{R\ln(Ro/R)}$$

INSIDE WALL TO GAS

$$\dot{q} = kg\left(\frac{\partial T}{\partial r}\right)_w \qquad \text{where} \quad \left(\frac{\partial T}{\partial r}\right)_w = \frac{Tw - Tg*}{R - Rg*}$$

HEAT FLUX FROM GLOW BARS TO GAS

$$\dot{q} = \frac{Tgb - Tg*}{Rr + Rw + Rg}$$

where $Rr = R/(Ro\sigma\varepsilon(Tgb + Two)(Tgb^2 + Two^2))$

$Rw = R\ln(Ro/R)/kw$

$Rg = (R - Rg*)/kg$

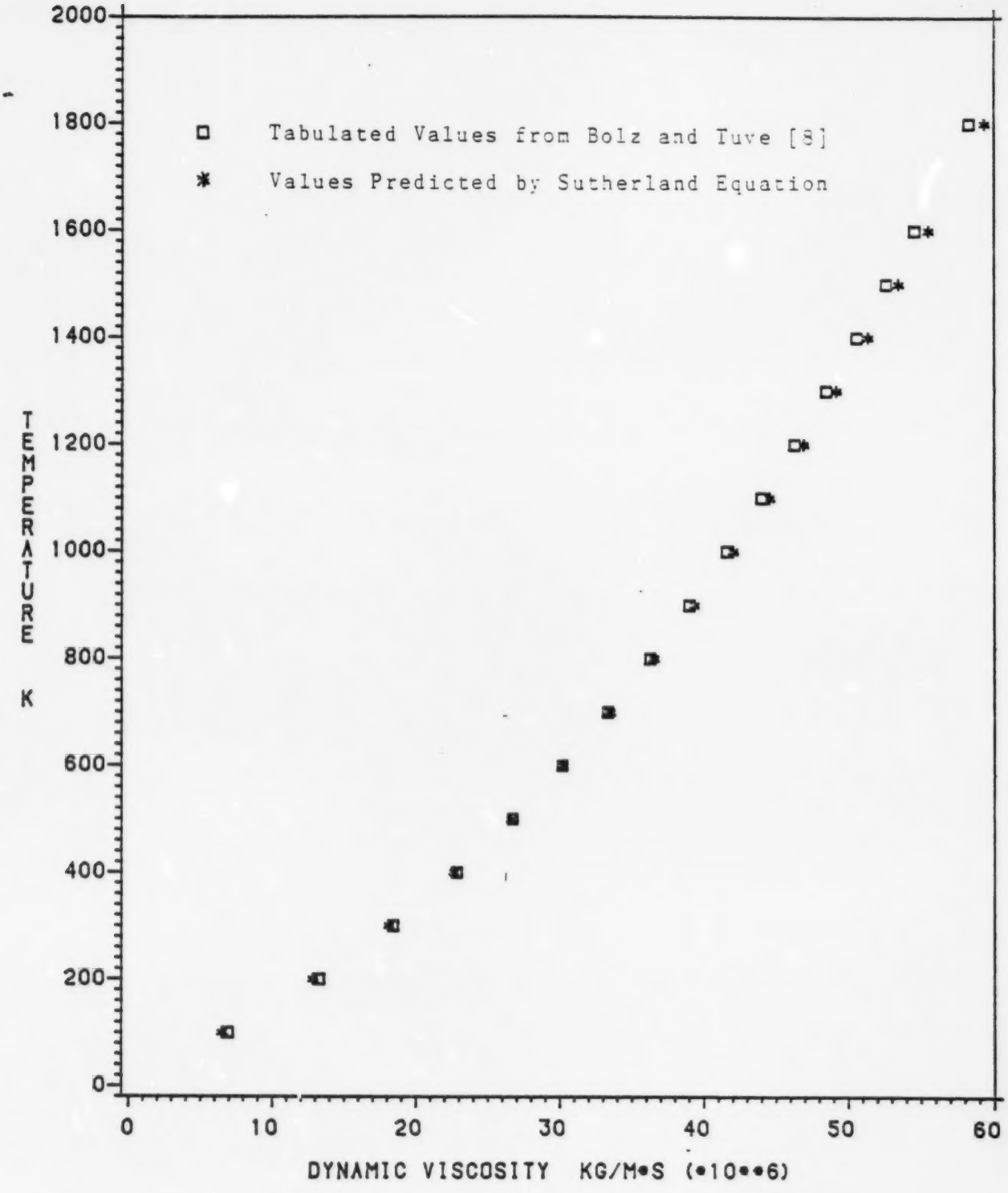

Figure 17: Comparison of Dynamic Viscosity Using Tabulated and Predicted Values

Chapter 5

NUMERICAL RESULTS

5.1 TEST CASES

To verify the program, a series of test cases were run: isothermal,developing pipe flow; fully developed pipe flow with constant wall temperature; and fully developed pipe flow with constant heat flux. Comparisons were also made with the velocity measurements in the isothermal furnace model described in Chapter 3.

5.1.1 Developing Isothermal Pipe Flow

The program was tested to see if it would predict accurate results for the velocity profiles. The program was compared to other numerical solutions under the same flow conditions for developing pipe flow. The program was also used to predict velocity profiles in the experimental model and actual measurements in the experimental model were taken to verify the predictions.

5.1.1.1 Comparison of Numerical Results for Developing Pipe Flow

The program was used to solve isothermal developing pipe flow and the results compared to published data. The grid spacing and the geometry were similar to the furnace tube dimensions: 28 nodes in the axial direction (with variable spacing as discussed in section 4.2.4), 20 in the radial direction; 2 m length, 0.032 m inside radius. An inlet air flow at 800 K was introduced into the tube with a 0.795 m/s uniform velocity. These conditions resulted in a

Reynolds number of 500, roughly in the range expected in the drop tube furnace. The program solved the axial and radial momentum equations and obtained a converged solution after 168 iterations. The calculated velocities and the distances were made dimensionless by the following expressions:

$$U = \frac{u}{u_o}$$ where u = velocity at point (x,r)
u_o = inlet velocity (average)

$$R = \frac{r}{r_o}$$ where r = radius
r_o = radius of tube

$$Z = \frac{200x}{r_o Re}$$ where x = axial distance from inlet
r_o = radius of tube
Re = Reynolds number

The arrangement of the grid results in axial velocities being solved for near rather than on the centre-line; this radial position was very close to the axis (r/r_o = 0.05). Figure 18 shows the developing velocities at r/r_o = 0.05 that were obtained from the present work and compares them to the published results of Friedman et al [15]. A very close agreement is observed between the values. The work performed by Friedman et al compares well with that of several other authors [1, 13, 27], and hence the velocity predictions of the present work were considered satisfactory. The solution of the momentum equations using a numerical scheme resulted in the initial velocity profiles developing a "bump" near the wall (see Figure 19), as noted by several researchers [1, 15, 18, 27, 33] in developing pipe and channel flow. This "bump" arises because the reduction of velocity in the boundary layer at the wall forces the velocity to increase outside the boundary layer. This increase

does not immediately spread over the whole profile, because the rate of spread is limited by laminar momentum diffusion, hence a velocity maximum arises. This phenomenon has not been observed experimentally because it is nearly impossible to produce a truly uniform inlet velocity (no inlet boundary layer).

5.1.1.2 Velocity Measurements in the Experimental Furnace

The actual velocity profiles in the experimental model used for flow visualization were measured using a pitot tube and a differential pressure transducer. Four axial positions corresponding to grid point nodes were chosen to measure the axial velocities. All of the radial positions corresponding to radial grid point nodes were measured; the resulting velocity profiles are shown in Figures 20 to 23. The measured velocity profiles are in very good agreement with the predicted velocity profiles at the position furthest downstream from the furnace tube inlet; the measurements close to the furnace tube inlet have some what more scatter. The high velocities of the primary flow are predicted very accurately; however, the lower velocities have greater error associated with them and are less accurate.

Several designs and combinations of flow straighteners were examined before a satisfactory one was found. The adequacy of a flow straightener (or combination of straighteners) was determined by inserting it in place in the model and measuring the resulting velocity profile. The main difficulty here was in sealing the foam used as a straightener to the tube walls; if this was not done properly, some air would bypass the straightener, producing a local velocity peak. The chosen flow straightener yielded the most uniform velocity profile; however, a certain amount of scatter is apparent at the axial positions closest to the inlet.

The scatter illustrates the error associated with taking measurements at such low velocities (the error involved with taking measurements in the model at such low velocities has been discussed in section 3.6) and the difficulties in obtaining an "ideal" flow straightener with a perfectly uniform velocity profile. In view of the fairly large error associated with the experimental measurements, the agreement between the calculated and measured velocities is considered satisfactory.

5.1.2 Fully Developed Pipe Flow Subject to Heating

The program was used to solve developing temperature profiles in fully developed pipe flow with constant properties. This was carried out with the same geometry and grid spacing as the developing pipe flow discussed in the previous section (5.1.1).

5.1.2.1 Constant Wall Temperature

The velocity profile to be studied in the tube was a fully developed parabolic flow with an average velocity of 0.250 m/s. The air properties were evaluated at the inlet temperature which was at 300 K and the tube wall temperature was fixed at 1500 K. This resulted in an inlet Reynolds number of 950 and a Prandtl number of 0.700. The program was used to solve the energy equation only and a converged solution was reached after 2 iterations. The temperatures and distances were made dimensionless by the following expressions:

$$Z = \frac{1000x}{dRePr}$$

where x = axial distance from inlet

d = diameter of tube

Re = Reynolds number

Pr = Prandtl number

$$R = \frac{r}{r_o}$$

where r = radial position

r_o = radius of tube

$$\Theta = \frac{T - T_w}{T_o - T_w}$$

where T = temperature at point (x,r)

T_o = inlet temperature

T_w = wall temperature at (x,ro)

Two radial positions were examined: one position close to the axis (r/r_o = 0.05), and the other close to the wall (r/r_o = 0.9). The values obtained are compared to the finite difference solutions obtained by Grigull and Tratz [16] and are shown in Figure 24. There is very good agreement between the results and it can be concluded that the program can predict the temperatures accurately.

5.1.2.2 Constant Heat Flux

In a similar test, a fully developed constant property parabolic flow through a tube was subjected to constant heat flux heating. The tube had the same geometry and grid spacing as in the constant wall temperature tests. The average velocity was 0.25 m/s and the properties were evaluated at the inlet temperature of 300 K; this gave a Reynolds number of 950. The heat flux into the tube was 1093 W/m**2 and the Prandtl number was 0.708. The program was used to solve the energy equation only and the solution converged after 2 iterations. The resulting temperatures and the distances were made dimensionless by the following expression:

$$Z = \frac{1000x}{dRePr}$$

see section 5.1.2.1

$$R = \frac{r}{r_o}$$ see section 5.1.2.1

$$\Theta = \frac{T_w - T}{(T_w - T_a)_\infty}$$ where T_w = wall temperature at (x,ro)

T = temperature at (x,r)

$$(T_w - T_a)_\infty = \frac{3q_w d}{k}$$ where q_w = heat flux

d = diameter of tube

k = thermal conductivity

As the distance x approaches infinity, the temperature profile becomes fully developed. The difference between the wall and the centre-line temperature is constant and can be expressed in terms of the diameter, the heat flux and the thermal conductivity [16], and this expression was used to non-dimensionalize the temperature. Two radial positions were examined: one position is very close to the centre-line (r/r_0 = 0.05), the other very close to the tube wall (r/r_0 = 0.90). The results are shown in Figure 25 and compared to the solutions obtained by Grigull and Tratz. There is very good agreement with the published results and it can be concluded that the program can accurately predict the temperatures with constant heat flux.

5.2 THE FURNACE FLOW FIELD

As satisfactory results had been obtained for the different test cases of pipe flow, the boundary conditions were now changed to conform to the actual furnace geometry. Since flow visualization experiments showed that the original burner configuration was unsuitable, all calculations here were performed with the modified burner proposed in Section 3.4. The primary flow of air was chosen as 10.0 g/min, corresponding to a roughly stoichiometric air quantity for a coal feed rate of 1.0 g/min (specified); this resulted in a 4.4 m/s average primary air velocity entering the furnace. The effect of reducing the coal feed rate to 0.5 g/min was also examined; the primary flow of stoichiometric air was then 5.0 g/min, resulting in a 2.2 m/s average primary air velocity entering the furnace. The primary tube in the burner was assumed to be long enough to allow the primary flow to achieve a fully developed parabolic profile. The flow visualization experiments led to the conclusion that the flow through the furnace would be stable if the secondary flow velocity profile entering the furnace was uniform and the flow fell within the range of the stability diagram. Two air numbers (total air mass / stoichiometric air mass) were chosen: 5:1 and 10:1, giving secondary to primary air mass flow ratios of 4:1 and 9:1 (400 % and 900 % excess air respectively). The temperature of the primary flow entering the furnace was assumed to be 300 K.

The program was used to solve the flow field in the furnace using this data. Since the coal particles were assumed to travel along the axis of the furnace, the centre-line flow velocities and temperatures were of the most interest. For a 300 K inlet, the calculated temperature values at the axis of the furnace were low compared to a typical combustion temperature for coal (900 - 1100 C); thus it was felt that the secondary air flow would need a certain degree of preheating.

A study of the effect of varying certain parameters was conducted as follows:

1. Stoichiometric primary air flow rate based on a coal feed rate of 1.0 and 0.5 g/min.
2. Secondary flow temperature at 300 (no preheating) and with preheating to 450, 600, 750, 900, 1050 and 1200 K before entering the furnace.
3. Air number equal to 5 and 10 (secondary mass/primary mass ratio equal to 4 and 9)
4. Variation in temperature of the surrounding glow bars (heating elements).
   a) Heating zones at 1250, 1400, 1550 and 1700 K; all four zone temperatures equal.
   b) Unequal zone temperatures, individual zones varied 750 to 1700 K.

Because flow recirculation induced by buoyancy was deemed to increase dispersion of the primary coal stream, one aim of this study was to determine under which conditions such recirculation could be avoided. It was felt that the effects of buoyancy which could lead to recirculation would be stronger at lower preheat temperatures; therefore, the secondary air preheat temperature was reduced in steps of 150 K from 1200 K down to the temperature where recirculation was first noted. As soon as recirculation was apparent, calculations were halted, because lowering the preheat temperature further would only enhance recirculation. The minimum preheat temperature was 300 K. The velocity profiles under different conditions are illustrated in Figures 26 to 47. In order to make the illustrations more clear, only a selected number of

axial positions were chosen to show the developing profiles along the furnace tube length. The axial positions are at 0.010, 0.052, 0.250, 0.595, 1.000, 1.500, and 2.000 m measured from the furnace tube inlet plane.

5.2.1 Flow Field Study – Constant Glow Bar Temperature 1700 K

For the first set of tests, the inlet mass flow of the secondary air was specified as 40.0 g/min. A coal feed rate of 1.0 g/min was chosen, therefore the primary air mass flow was fixed at 10 g/min, and the mass secondary/mass primary (ie M–S/M–P) was equal to 4.0. The resulting axial velocity profiles are illustrated in Figures 26 to 30. As the preheat temperature increases, the centre–line velocity decreases. The buoyancy forces are greater at the lower preheat temperature because of the greater temperature differences between the wall and the incoming flow. Since the momentum forces and the buoyant forces oppose each other, a deceleration of the flow at the wall is observed, and this in turn causes an acceleration of the flow in the tube centre. The minimum preheat temperature required to avoid flow reversal was found to be close to 600 K; below this point flow reversal near the wall results. The velocity of the flow reversal is small compared to the final centre–line velocity (0.1%), and the furnace could probably be operated with a secondary preheat temperature of 600 K without a significant increase in dispersion of the primary jet. Even without flow reversal, buoyancy is seen to result in a much thicker wall boundary layer than is found in isothermal, developing flow.

For the second set of tests, the inlet mass flow of the secondary air was specified as 90.0 g/min (ie M–S/M–P = 9.0). The results are shown in Figures 31 to 37. The larger inlet mass (momentum) flux reduces the effect of

buoyancy and lowers the shear stress between the secondary and primary flow, both of which result in higher velocities on the tube axis. There is no recirculation apparent for any of the preheat temperatures with a 90.0 g/min flow rate. For both secondary flows, the velocities near the axis change little with secondary inlet temperature; this suggests that particle transit times will not be strongly affected by preheating.

The effect of reducing the coal feed rate was also examined. The feed rate of coal was reduced to 0.5 g/min which gave a 5.0 g/min primary air flow rate. The corresponding secondary air flow rate was 20.0 g/min for a M–S/M–P = 4.0 and 45.0 g/min for a M–S/M–P = 9.0. The buoyancy forces were more apparent because of the lower momentum associated with the lower mass flow, especially at M–S/M–P = 4.0. For M–S/M–P = 4.0, recirculation was first noted at a preheat of 900 K; for M–S/M–P = 9.0, recirculation was first noted at 450 K. The velocity profiles obtained with a 0.5 g/min coal feed rate were very similar to those obtained with a 1.0 g/min coal feed rate and therefore are not illustrated.

5.2.2 Flow Field Study – Constant Glow Bar Temperature 1400 K

The same set of secondary air flow rates and preheat temperatures used with a 1.0 g/min coal feed rate were examined at a lower glow bar temperature. The results with the lower glow bar temperature and 40.0 g/min (M–S/M–P = 4.0) air flow are shown in Figures 38 to 40; those with a 90.0 g/min (M–S/M–P = 9.0) air flow are shown in Figures 41 to 47. If the velocity profiles with a 1400 K glow bar temperature are compared to the velocity profiles with a 1700 K glow bar temperature using the same inlet conditions, very little difference is apparent. The effect of buoyancy is seen to be slightly

stronger at the lower glow bar temperature, if results at 1700 K are compared to results for the same inlet conditions at 1400 K. One might expect that an increase in the glow bar temperature would result in a greater distortion near the furnace wall, but the reverse was observed. The glow bars heat the incoming gas, which decreases in density and accelerates to conserve mass. Momentum increases with the square of the velocity while buoyancy increases with the difference in temperatures; thus the momentum forces increase somewhat more rapidly than the buoyancy forces as the temperature is increased. The momentum of the gas flow is greater at the higher glow bar temperature, thus the effects of buoyancy are reduced. This effect is small, but can be seen most clearly by comparing results for M-S/M-P = 9.0 with Tinsec = 300 K at the two glow bar temperatures. A reversal of the flow near the wall was noted with 90.0 g/min at 300 K but it was small compared to the final centre line velocity (0.1%). This reversal resulted from the relatively low flow velocities and large buoyant forces. The buoyancy effect at 1400 K is particularly strong for the 90.0 g/min flow rate with a low preheat temperature (see Figure 41). These conditions represent the lowest momentum forces and the greatest buoyancy forces.

5.2.3 Flow Field Study - Variable Glow Bar Temperature

Each set of conditions has associated with it a corresponding particle heating curve (discussed in the next section). It was noted that for certain flow conditions using a 0.5 g/min coal feed rate, particles could be maintained at a nearly constant temperature after the initial heating. Operating the furnace under isothermal conditions would be most useful for the study of particle heating. These heating conditions are discussed in detail in Section 5.3.3.

Figures (48) to (51) show the effect of the variable zone temperature on the velocity profiles. The chosen conditions result in the flow being rapidly heated in the initial zone; since the heat must penetrate the surrounding secondary flow, the effects of this heating on the centre-line temperature are not felt until the next zone. The velocities are low because of the smaller mass flow and the lower temperatures; the effects of buoyancy are notably stronger at the lower glow bar temperatures.

5.3 PARTICLE VELOCITY AND TEMPERATURE

Four different sizes of particles that were considered representative of the size to be tested in the furnace were examined: these were 10, 30, 100, and 300 μm particles. The temperature increase and furnace residence times of these particles were examined under each of the flow conditions studied in the previous section. A series of heating curves were obtained and are shown in Figures 52 to 78. Particle heating rates were examined in preheated flows up until the onset of recirculation was noted; therefore, particle heating rates for some of the flows at lower preheat temperatures are not given.

5.3.1 Particle Heating - Constant Glow Bar Temperature 1700 K

The four sizes of coal particles were introduced into the furnace flow with a 40.0 g/min secondary mass flow rate (M-S/M-P = 4.0) at preheat temperatures of 600 to 1200 K (see Figures 52 to 56). The five curves represent the gas centre-line temperature and the four particle temperatures. Before the centre-line gas can increase in temperature, the heat from the furnace walls must penetrate the surrounding secondary flow; therefore, preheating the secondary flow will allow the temperature of the central primary

stream to increase more rapidly. As the particles enter the furnace, the initial particle heating is dependent on the particle size. The 10 μm particle has the largest initial temperature increase while the 300 μm particle has the smallest initial temperature increase. This pattern of heating for the different particles remains the same for each preheat temperature. The 10 μm particle then heats very quickly because of small thermal inertia, and follows the centre-line temperature closely. The 10 μm particle also has the largest convective heat transfer coefficient because of its small diameter, and most of the heat it receives by radiation is convected to the surrounding cooler gas. As the preheat temperature is increased, the 10 μm particle approaches the centre-line gas temperature more closely. The 30 and 100 μm particles follow a similar pattern for each preheat temperature. The convective heat transfer coefficient becomes less as the diameter becomes greater; therefore, radiation from the furnace walls becomes relatively more important, and the final temperature of these particles rises with increasing particle size. The 300 μm particle has the lowest initial heating rate; because of its large mass, it requires a large quantity of heat to heat up, and spends most of its time undergoing transient heating. With a preheat temperature of 750 K, the temperature of the 300 μm particle actually falls below the surrounding gas temperature; the particle is then heated by both radiation and convection. By the end of the furnace, the particle temperature has increased to a temperature close to that of the 100 μm particle. Higher preheat temperatures yield similar results.

The same size particles were introduced into a 90.0 g/min secondary air mass flow (M-S/M-P = 9.0) with preheating from 300 to 1200 K. The results are shown in Figures 57 to 63. Much lower particle temperatures were achieved because of the higher secondary mass flow rates. With the 90.0

g/min mass flow, the preheating of the secondary flow does not have a strong effect on the heating history; radiant heating is the main factor responsible for particle heating. At gas preheat temperatures of 900 K and higher, the temperature of the 300 μm particle falls below the gas centre-line temperature, hence receiving energy by both radiation and convection.

The emissivity of the coal particles in these calculations was assumed to be 0.8. The effect of changing the emissivity of the particle was examined. Figure (64) shows the effect of varying the emissivity of a 100 μm particle from 0.6 to 1.0. The particle heating curves were obtained with a secondary mass flow of 90.0 g/min (M-S/M-P = 9.0) at a 1200 K preheat temperature and a glow bar temperature of 1700 K. Choosing an arbitrary distance of 0.5 m along the length of the furnace, the effect of increasing the emissivity of the 100 μm particle by 0.1 is seen to be a temperature rise of roughly 40 K. The increases in temperature associated with each rise of 0.1 in emissivity for a 10, 30 ,and 300 μm particle were approximately 4, 10, and 25 K, respectively.

The effect of changing the mass feed rate of coal was also examined. The heating of the four particles was studied with a 20.0 g/min (M-S/M-P = 4.0) secondary mass flow rate with preheating from 1200 down to 750 K (750 K was the point at which buoyancy was observed). The maximum temperature of the particles was approximately 200 to 300 K higher than for the same conditions at a 1.0 g/min coal feed rate (compare Figures (53, 54, 56) with Figures (65, 66, 67)). With the lower coal feed rate the four different particle heating curves become closer together. The heat transfer coefficient increases with the temperature, therefore the particles are more sensitive to convective heat losses.

The smaller coal feed rate was also studied using a 45.0 g/min secondary air flow rate (M-S/M-P = 9.0) with a preheating from 1200 down to 600 K. The temperature of the particles at different points along the furnace was approximately 200 to 300 K higher than those obtained with 1.0 g/min at the same conditions. The mass of air flow through the furnace is proportionately less at the lower coal feed rate, therefore the gas velocity is less, allowing the gas more time in the furnace to heat up. The effect of reducing the coal feed rate with M-S/M-P = 9.0 is illustrated by comparing Figures(68, 69, 70) to Figures(59, 61, 63).

5.3.2 Particle Heating - Constant Glow Bar Temperature 1400 K

The four particles were introduced into the flow field obtained at a 40.0 g/min secondary air flow with a preheat of 900 to 1200 K (see Figures 71 to 73). The 10, 30 and 100 μm particles follow the gas centre-line temperatures very closely; however, the 300 μm particle spends almost all its time (except for a small initial distance) below the furnace gas temperature being heated by radiation and convection. In contrast to the results with a 1700 K glow bar temperature, the 300 μm particle reaches the lowest final temperature of all the particles. The 100 μm particle also exhibits a different behaviour than the results at 1700 K glow bar temperature; its temperature falls below that of the 30 μm particle in the initial region of the furnace (0.5 m). An increase in the preheating from 900 to 1200 results in the temperature of the 100 μm particle falling below the gas centre-line temperature; however, this particle eventually reaches the highest particle temperature. The radiation produced by the furnace walls is much less but the convective heat transfer coefficient essentially remains the same, therefore the particles remain closer to the gas temperature.

The four particles were subjected to a 90.0 g/min secondary air mass flow rate with preheating from 300 to 1200 K (see Figures 74 to 80). The 10 and 30 μm particles have curves similar to those of the other test conditions. The thermal inertia of the 100 and 300 μm particles is more noticeable at the 1400 K glow bar temperature. Much lower particle temperatures are achieved at the 1400 K glow bar temperature. These results indicate the considerable reduction in radiation heat transfer to the particles at the lower glow bar temperature.

5.3.3 Particle Heating - Variable Glow Bar Temperature

The furnace is divided into four independently controlled heating zones and a series of varied zone temperatures were studied to see their effect on particle heating. Ideally, the particles should undergo rapid heating in the initial region of the furnace and then experience isothermal conditions along the remaining length. Various combinations of heating zone temperatures and secondary preheat temperatures were tried to see if these conditions could be achieved. The results showed that isothermal conditions were best obtained by keeping the second, third, and fourth zones (from the top) at the same temperature as the preheated secondary flow entering the furnace, while the temperature of the first zone was set to:

Zone 1 Temp. = (Sec. Preheat Temp. / 1200) * 1700 K

Use of a higher Zone 1 temperature than this resulted in an "overshoot" in the coal particle temperature. The velocity profiles reported earlier suggest that, owing to buoyancy effects, the lowest (Zone 1 Temp./Sec. Preheat Temp.) feasible is (1063 K / 750 K) (see Figure (48)).

The resulting particle heating curves are shown in Figures (81) to (84). For each curve there is rapid heating in the initial zone of the furnace where the glow bar temperature is highest, followed by a constant particle temperature (for the 10, 30, 100 μm particles) throughout the remaining zones of the furnace.

The 10, 30, and 100 μm particles have approximately the same temperature as the gas for all the flow conditions, a further advantage of this mode of operation; the low gas velocities allow the gas to heat up quickly and the lower glow bar temperatures decreases the rate of temperature rise of the particles after the initial heating. The 300 μm particle experiences transient heating for all the flow conditions studied owing to its large thermal inertia, and its temperature remains well below the temperatures of the other three particles.

5.3.4 Particle Heating Rates

One of the objectives of this study was to find the particle heating rates under various flow and preheat conditions. The resulting heating rates for 10, 30, 100 and 300 μm particles taken from the results discussed previously (with all four zone temperatures equal) are shown in Figures 85 to 92. The heating rates were calculated by taking the temperature achieved by the particle after travelling 0.25 m in the furnace and dividing by the time taken to travel that distance. A distance of 0.25 metres was chosen because it represents a point of continual and relatively linear temperature rise for all particle sizes. In all the particle heating curves, the 1700 K glow bar temperature gives a greater heating rate than the 1400 K glow bar temperature at the same preheat temperature. This is expected owing to the greater energy received by

radiation. All the heating rates increase with preheat temperature, and the rate of this increase is dependent on the particle size. The heating rate of the 10 μm particle is affected most by the preheat temperature because of the large convective transfer coefficient for small particles; the 300 μm particle is affected the least, owing to the greater thermal inertia of larger particle diameters.

Calculations with other particle sizes besides those reported here showed that particles of about 100 μm in diameter experience the highest heating rates. With small particles, the heating rate increases with diameter because the heat loss by convection to the gas decreases, while for large particles, the thermal inertia causes the trend to be reversed. The result is a maximum near 100 μm.

For all the particle sizes examined, the mass flow rate of the secondary flow (ie the stoichiometry of the furnace) has a very small effect. Both mass flow rates give very similar particle heating rates (see Figures 85 to 88). As particle size increases, the difference in heating rates between the two glow bar temperatures becomes greater. This is true for the 10, 30 and 100 μm particles; however, owing to the large thermal inertia of the 300 μm particle, the heating rate is somewhat less than for the 100 μm particle.

The results for a coal feed rate of 0.5 g/min are shown in Figures (89) to (92). The smaller mass flow gave lower heating rates for the 30 and 100 μm particles: the temperature of the particles was found to be greater with the smaller mass flow; however, the gas velocity is much less and the transit time is longer, resulting in lower heating rates. For the 10 μm particle a higher heating rate was observed for the 0.5 g/min coal feed rate, conflicting with the results at larger particle diameters. This is because the 10 μm particle is very sensitive to changes in the gas temperature (large heat transfer coefficient) and

the temperature rise of the gas in the initial 0.25 m for a 0.5 g/min coal feed rate is very large. The effect of coal feed rate can be considered negligible for the 300 μm particle (see Figure (92).

The effect of glow bar temperature for each of the four particle sizes is illustrated in Figures (93) to (96). The coal feed rate was 1.0 g/min with M–S/M–P = 9.0 at a preheat of 600 K and of 1200 K. A rise in the glow bar temperature has a significant effect on the particle heating rates; the 100 μm particle has the largest increase in particle heating rate.

Figure (97) illustrates the effect of secondary air preheating on the residence time of a 100 μm particle. Increasing the preheat temperature results in a longer residence time for all flow rates because the centre–line velocity rises less (see Figures 26 to 47). The mass flow rate of the secondary air has a significant effect on the residence time. The larger mass flow rate has a high initial velocity and is accelerated further in the furnace tube. The smaller mass flow has a lower inlet velocity and is accelerated less in the furnace tube, thus the residence time is longer for the lower mass flow. Varying the glow bar temperature has a slight effect on the residence time. The higher glow bar temperature heats the flow to a higher temperature, which leads to higher velocities and slightly shorter residence times.

Heating rates for the variable zone temperature cases are not reported here; they will be identical to heating rates for glow bar temperatures equal to the first zone (Zone 1) of the variable zone temperatures.

The results of the experimental work and the numerical simulation can now be summarized. Using the stability diagram found from the results of the flow visualization tests (Figure (7)) and the results from the numerical work, a furnace operating diagram can be constructed. Figures (98) and (99)

illustrate the operating diagrams for a 1.0 and a 0.5 g/min coal feed rate. The non-dimensional axes of Figures (98) and (99) are the primary to secondary velocity ratio and the secondary inlet Reynolds number. Moving from the left to the right of Figure (98), the flow undergoes a transition from laminar steady to laminar unsteady to turbulent. The curve on the marks the line of transition from laminar to turbulent flow (the transition boundary was obtained with the modified burner). Also illustrated in Figure (98) are lines of constant mass flow (air number) and lines of constant preheat temperature. There is no upper limit for secondary preheat temperature; however, the expense of preheating the secondary air would be a restriction. In the upper left region of Figures (98) and (99), there is shown a small circle (or square) on the lines of constant number (mass flow). These are the points at which buoyancy-induced recirculation was first observed with the numerical model (note that this limit was observed with equal glow bar temperatures in all zones).

The stable operating region is then bounded by three limits: transition to turbulence limit, secondary preheat limit, and buoyancy induced recirculation limit. Comparing the two operating diagrams (Figures (98) and (99)), a larger stability range is found with the lower coal feed rate. The region bounded by the three limits is larger with the 0.5 g/min coal feed rate. The lower coal feed rate allows a lower secondary preheat temperature and a larger air number to be used.

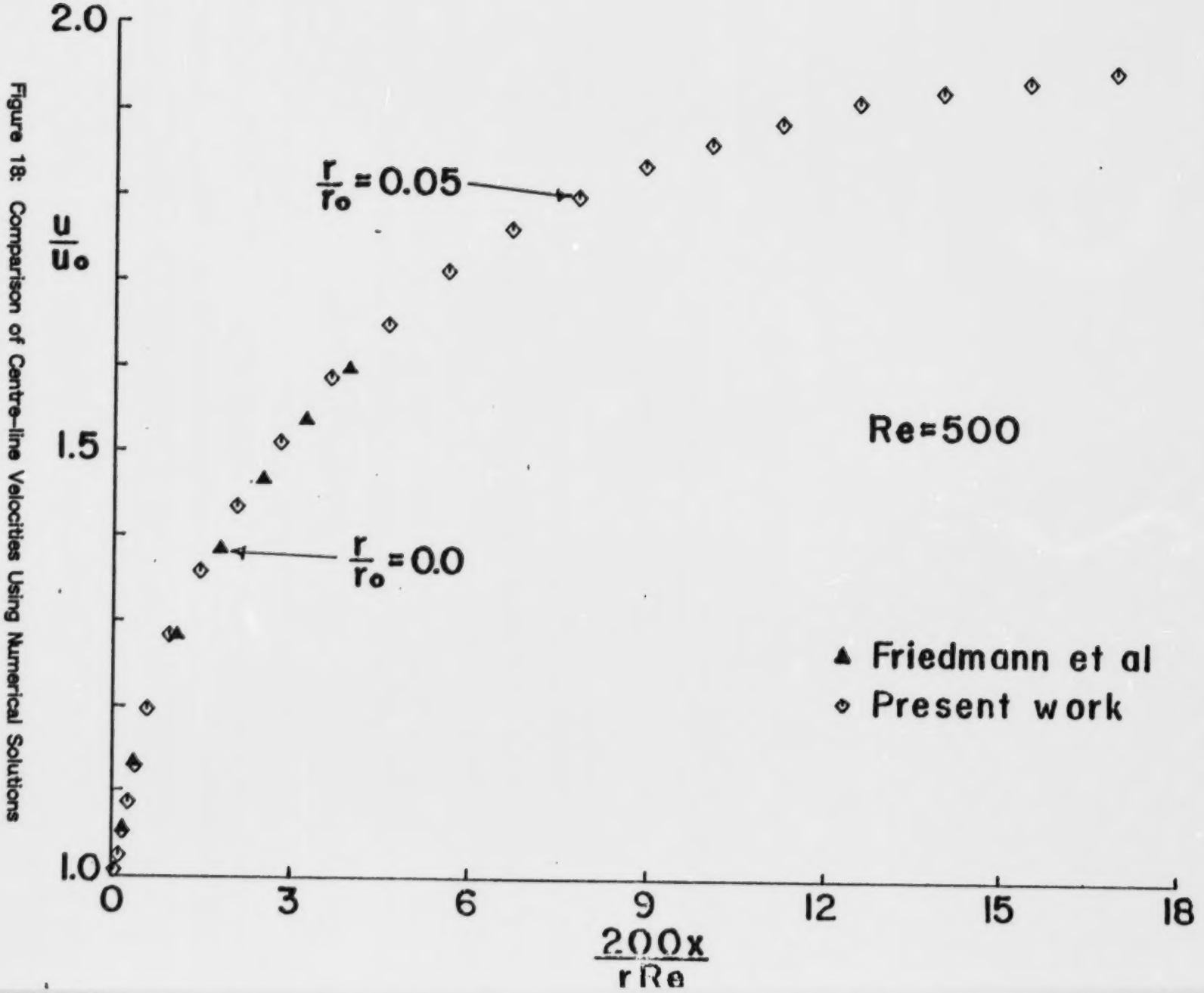

Figure 18: Comparison of Centre-line Velocities Using Numerical Solutions

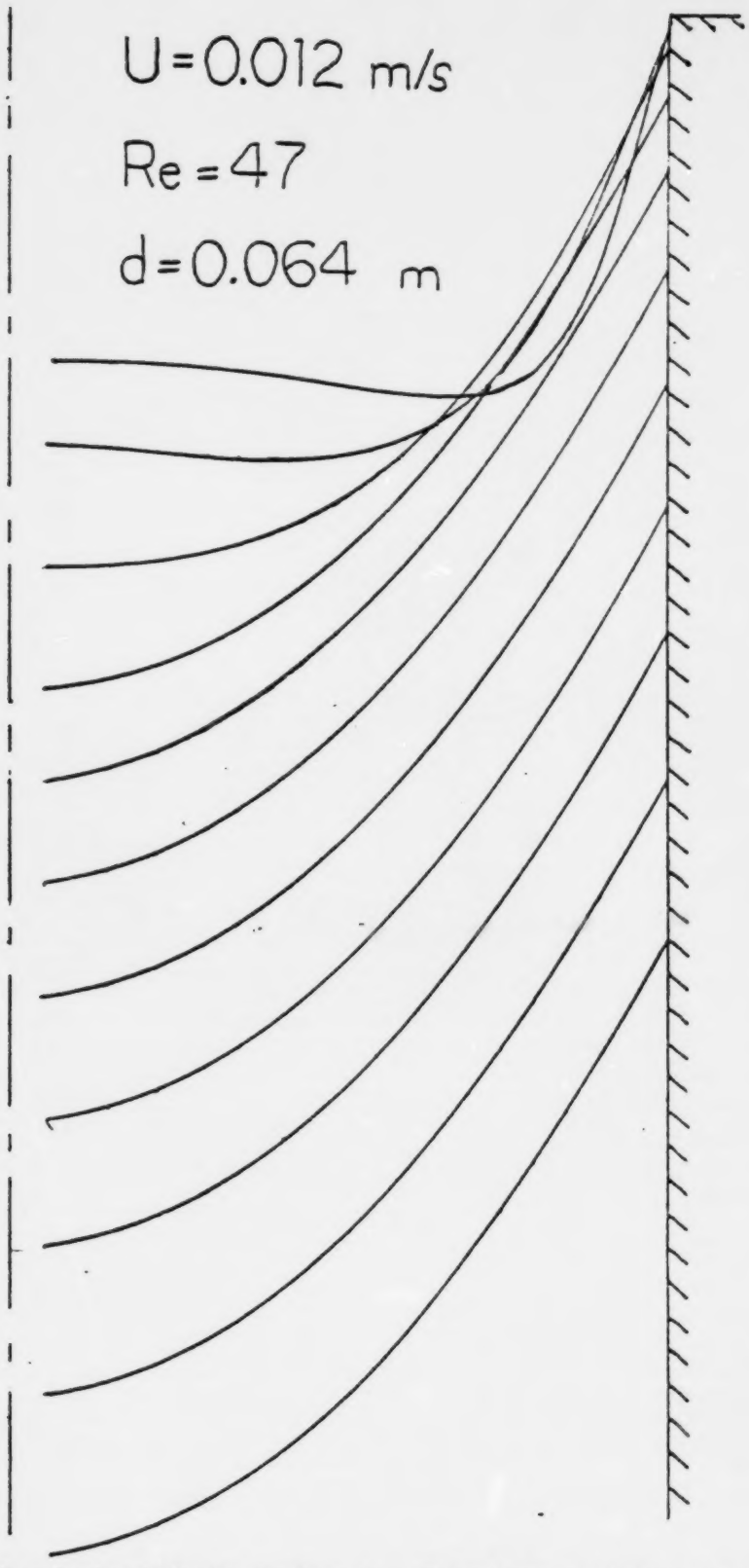

Figure 19: Developing Velocity Profiles in a Tube from a Uniform to Parabolic Velocity Profile

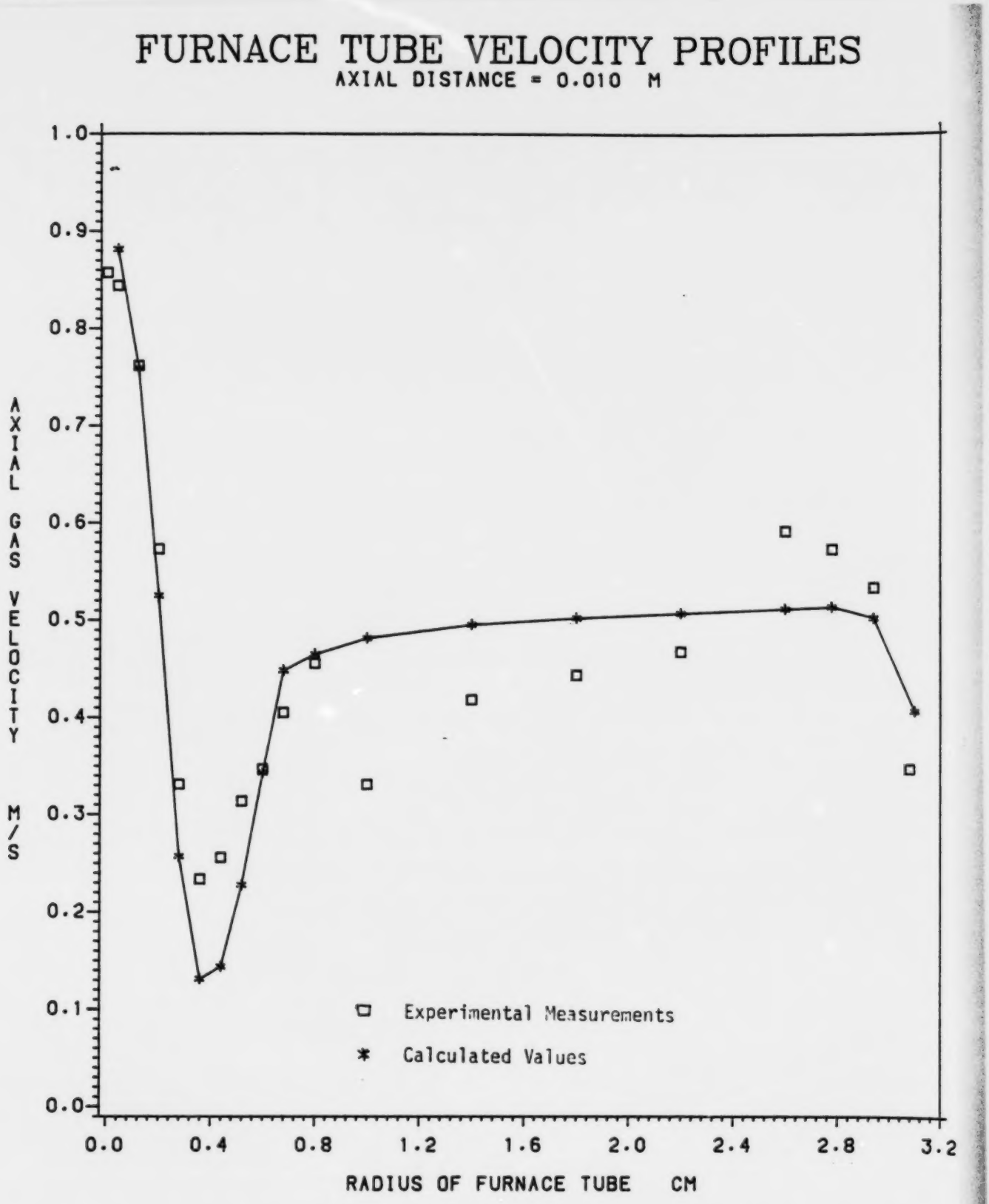

Figure 20: Comparison of Velocity Profiles at 0.010 m Showing Experimental Measurements and Calculated Values

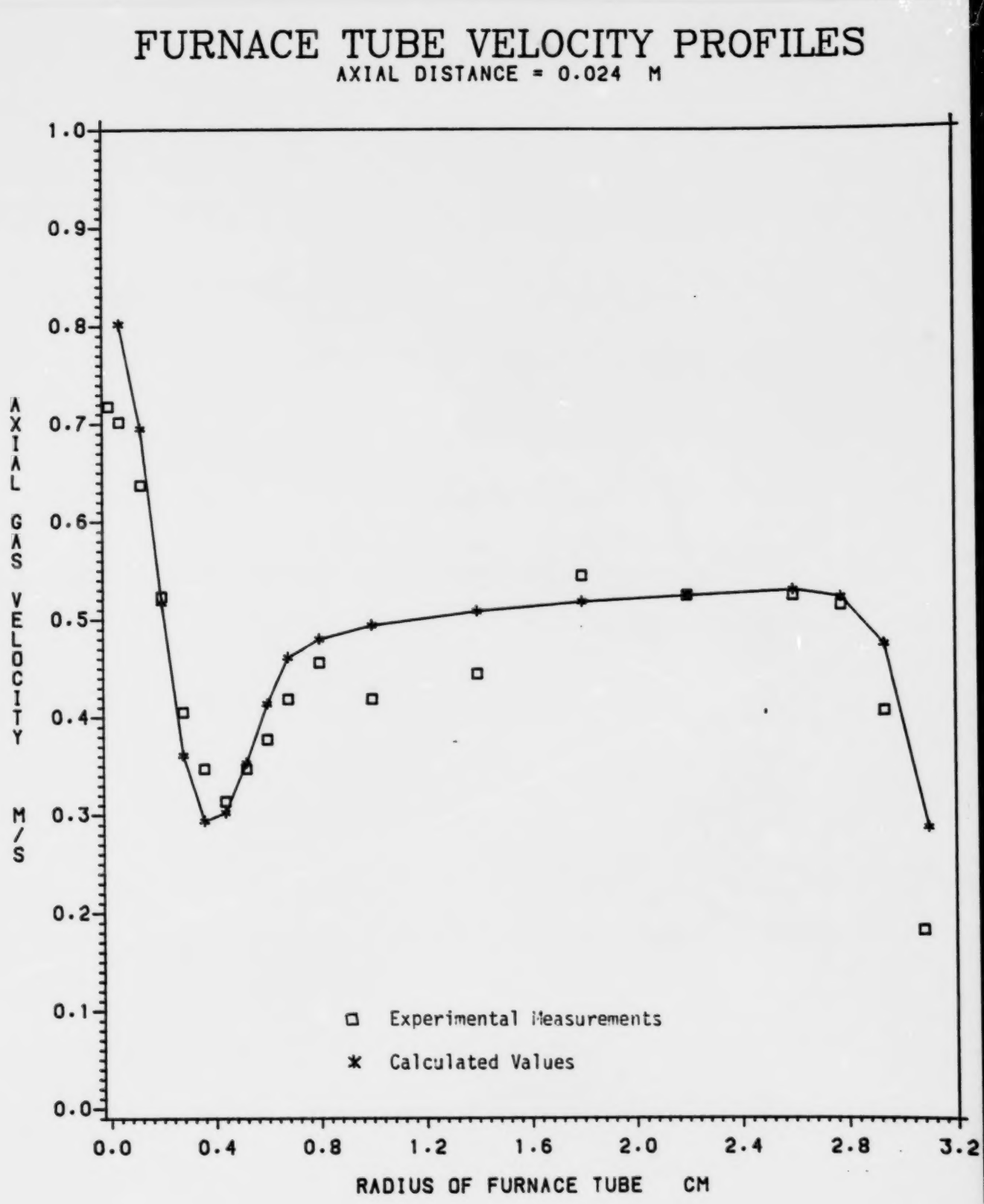

Figure 21: Comparison of Velocity Profiles at 0.024 m Showing Experimental Measurements and Calculated Values

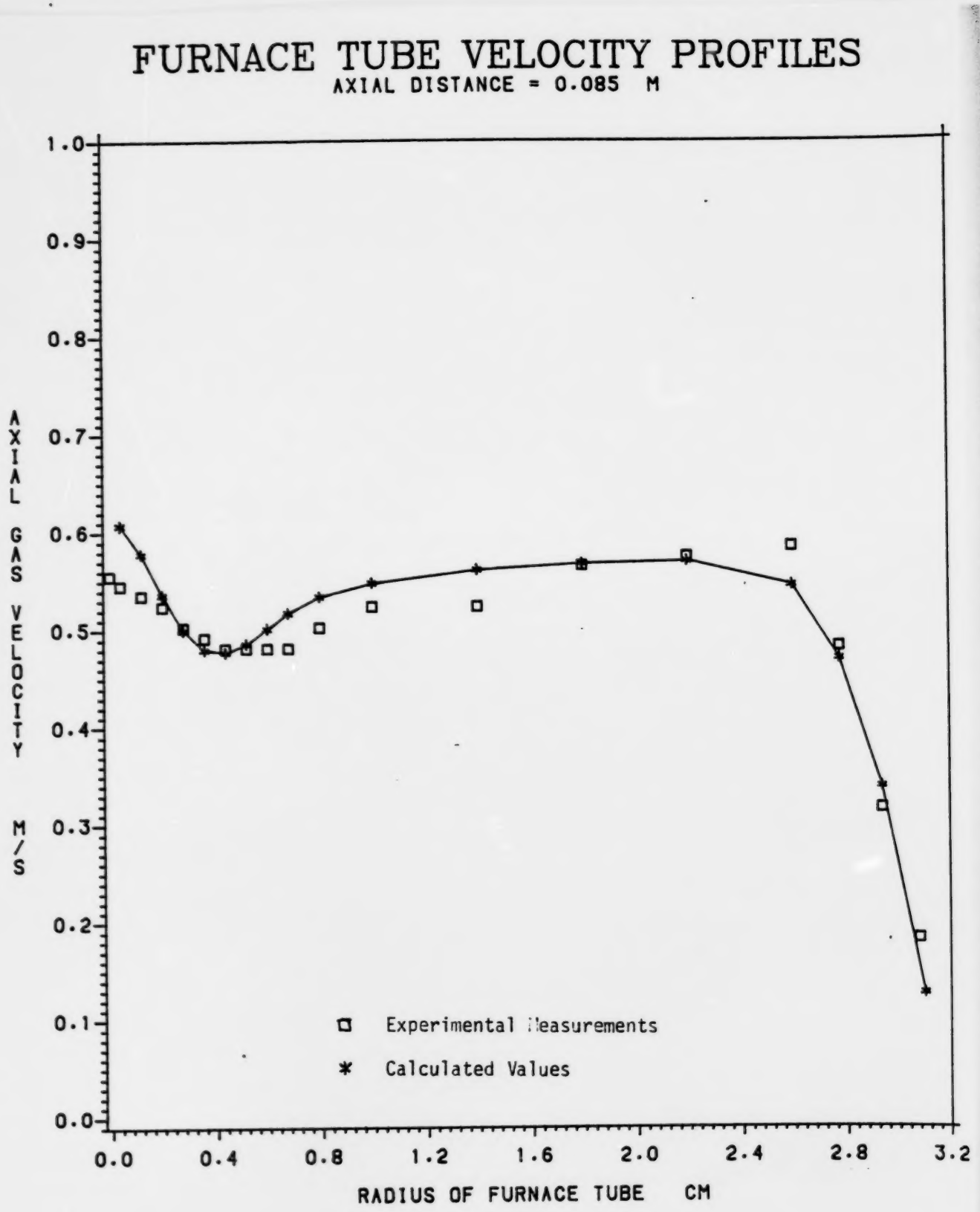

Figure 22: Comparison of Velocity Profiles at 0.085 m Showing Experimental Measurements and Calculated Values

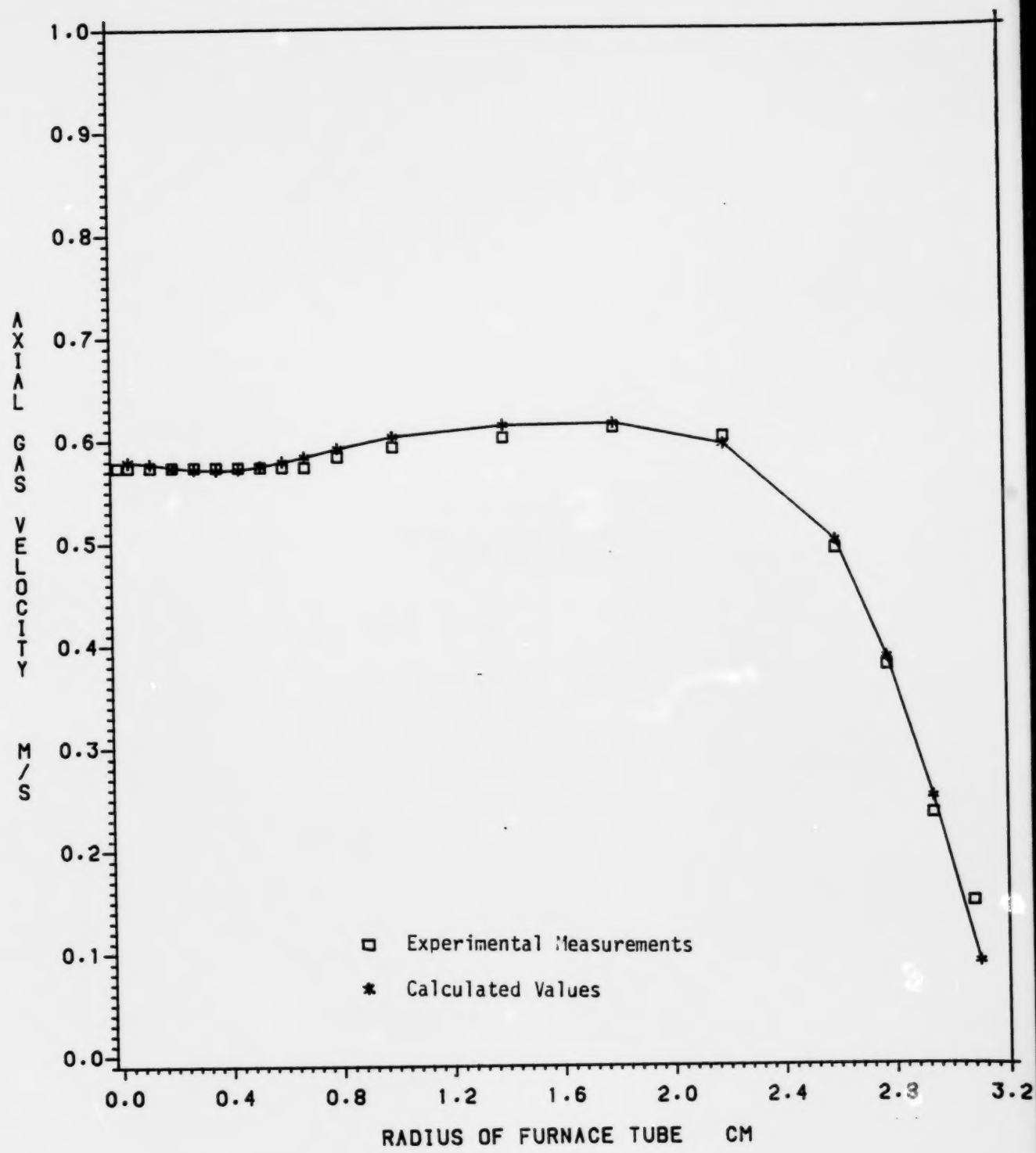

Figure 23: Comparison of Velocity Profiles at 0.250 m Showing Experimental Measurements and Calculated Values

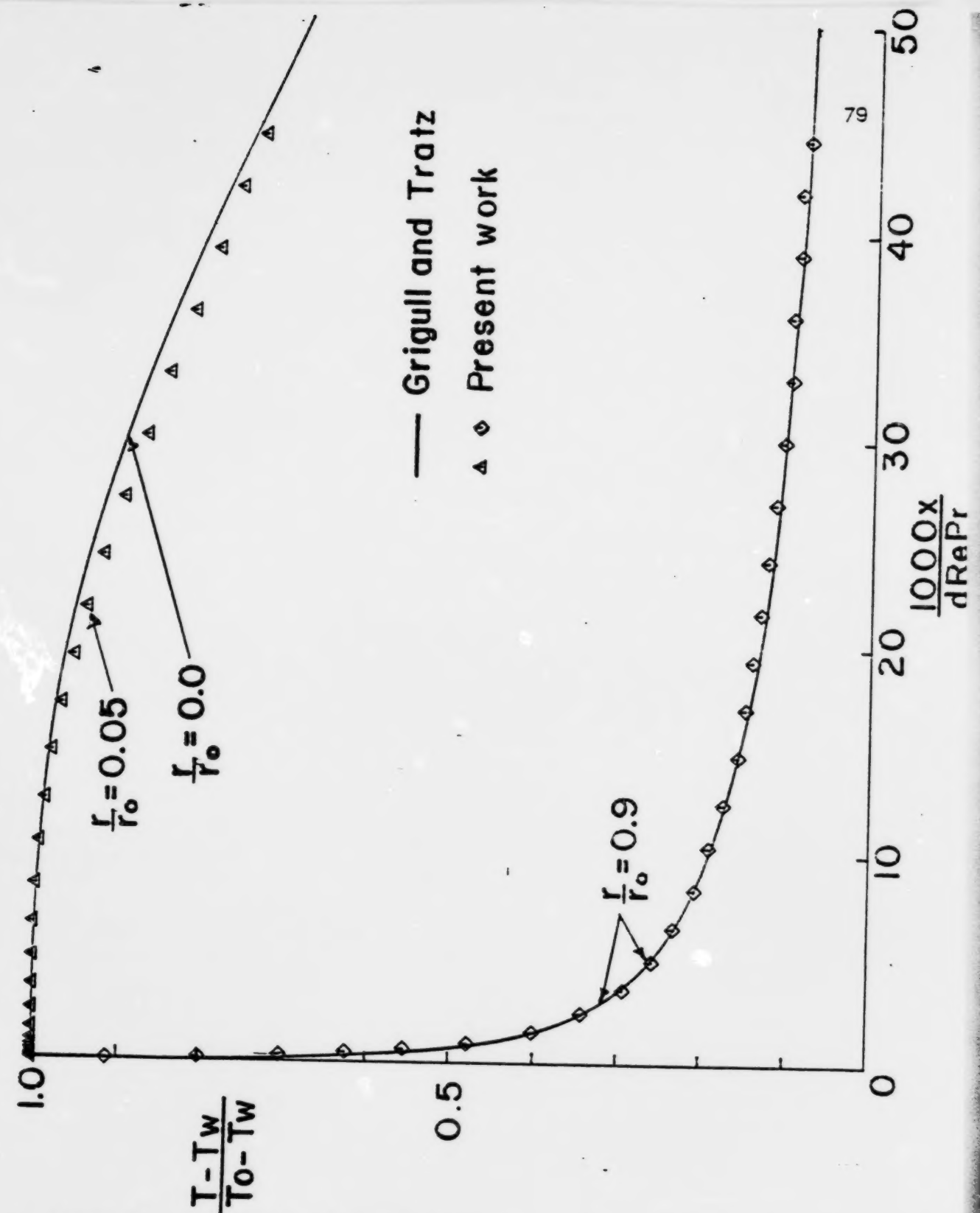

Figure 24: Comparison of Temperature – Constant Wall Temperature –Numerical Solution Calculated with Constant Properties

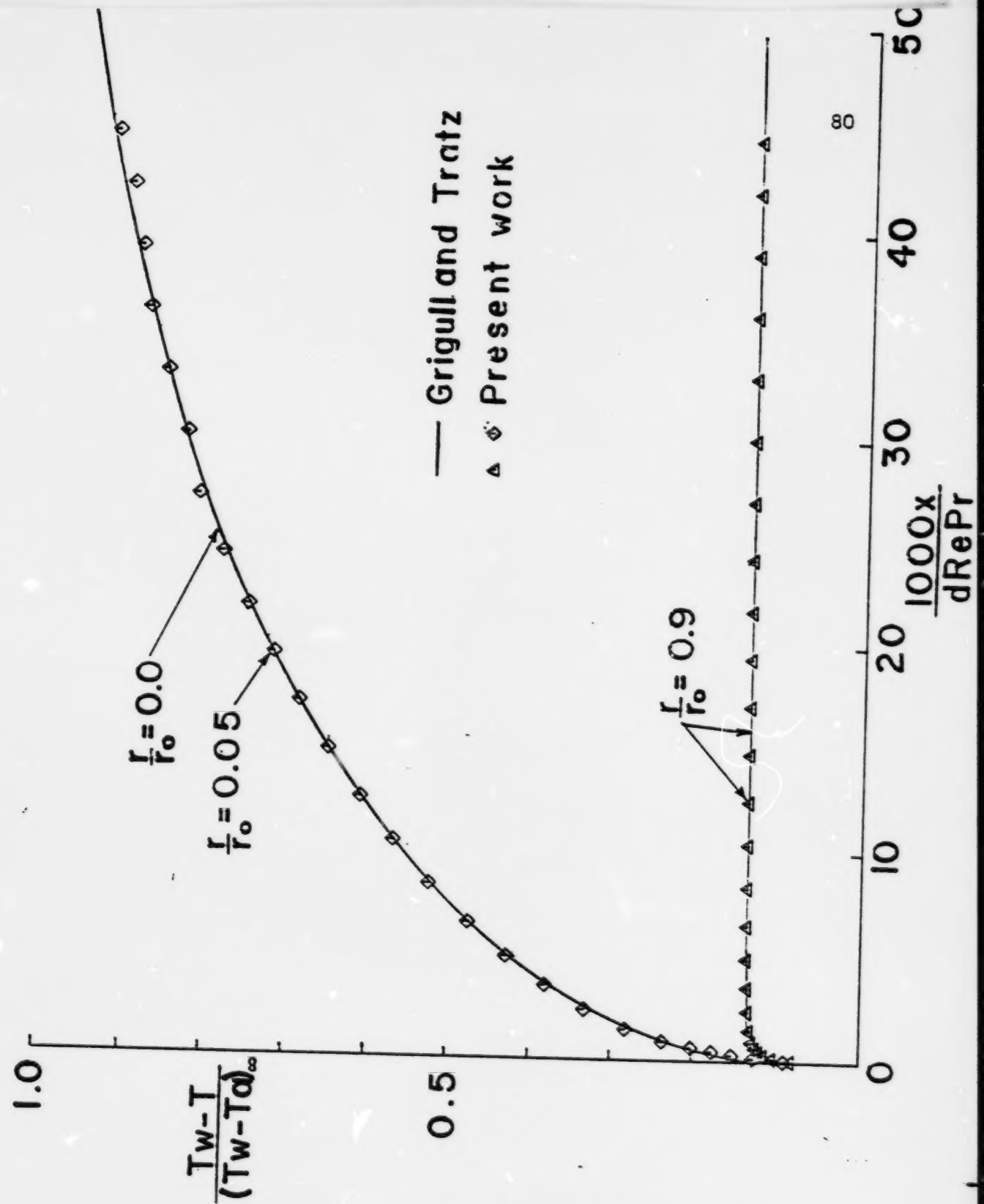

Figure 25: Comparison of Temperature – Constant Heat Flux –Numerical Solution Calculated with Constant Properties

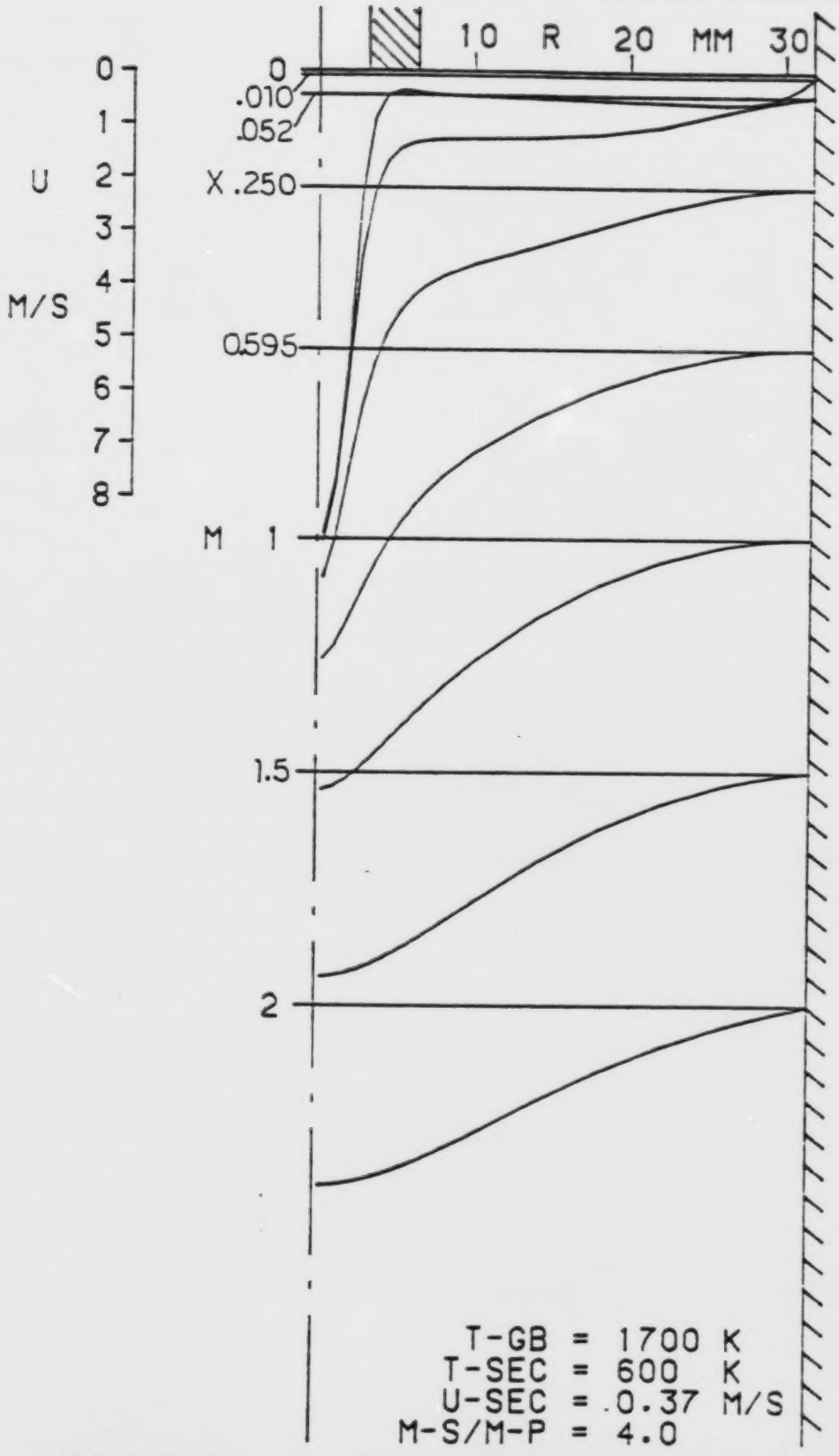

Figure 26: Velocity Profiles – Tgb=1700 K, Tinsec=600 K, M-S/M-P=4.0 – Coal Feed Rate = 1.0 g/min, Primary Mass Flow = 10.0 g/min, Secondary Mass Flow = 40.0 g/min

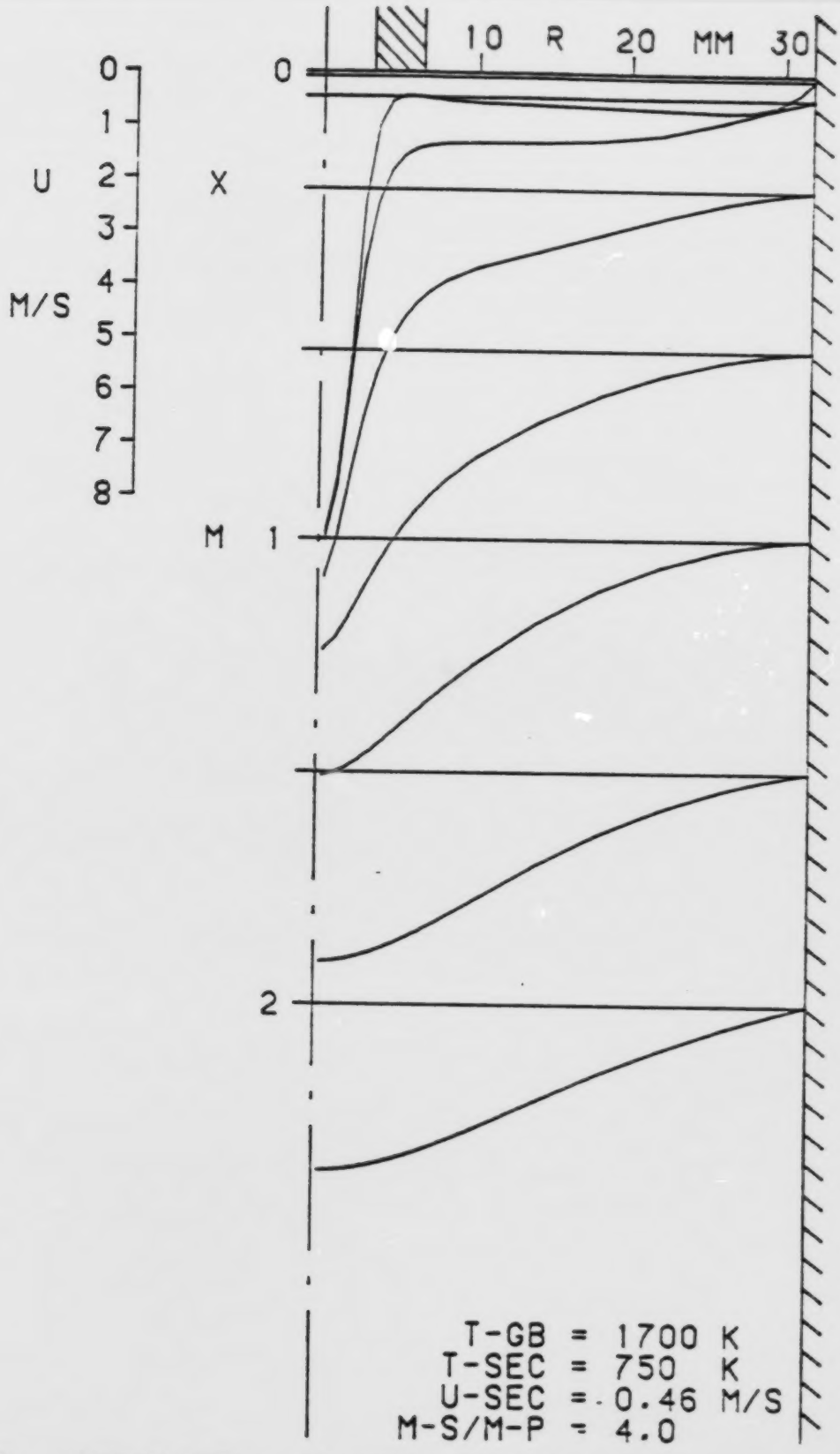

Figure 27: Velocity Profiles – Tgb=1700 K, Tinsec=750 K, M-S/M-P=4.0 – Coal Feed Rate = 1.0 g/min, Primary Mass Flow = 10.0 g/min, Secondary Mass Flow = 40.0 g/min

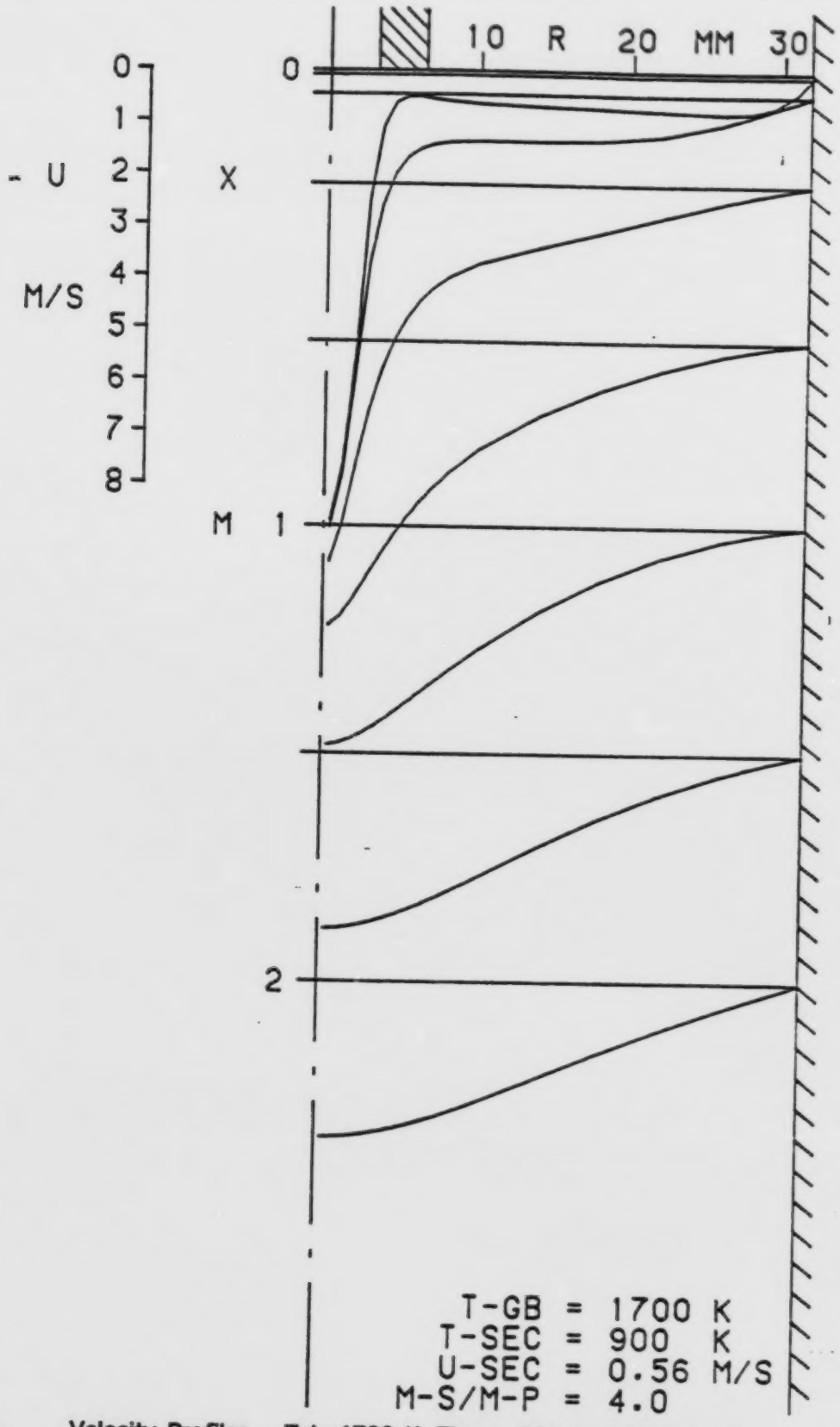

Figure 28: Velocity Profiles – Tgb=1700 K, Tinsec=900 K, M-S/M-P=4.0 – Coal Feed Rate = 1.0 g/min, Primary Mass Flow = 10.0 g/min, Secondary Mass Flow = 40.0 g/min

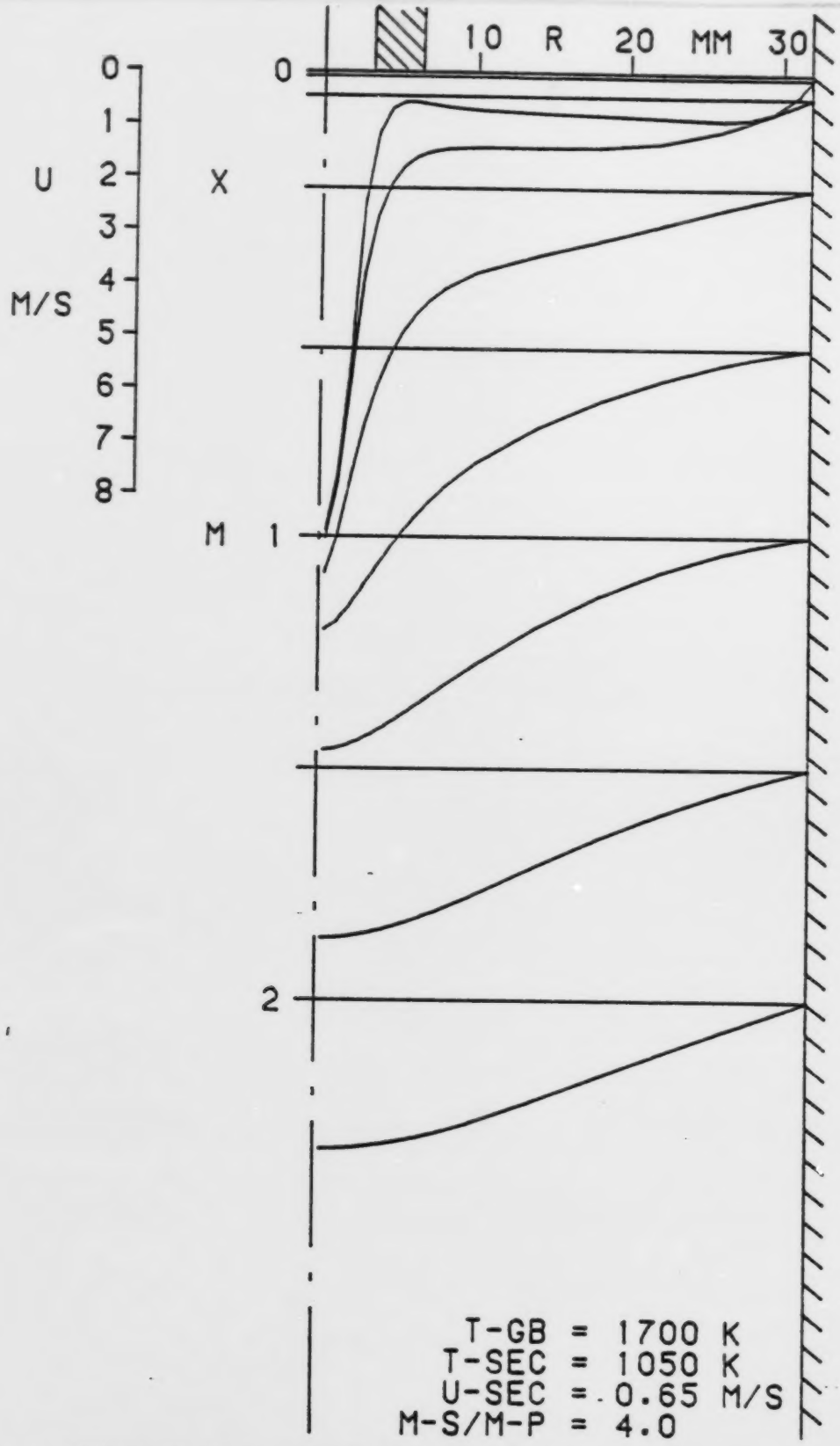

Figure 29: Velocity Profiles – Tgb=1700 K, Tinsec=1050 K, M-S/M-P=4.0 – Coal Feed Rate = 1.0 g/min, Primary Mass Flow = 10.0 g/min, Secondary Mass Flow = 40.0 g/min

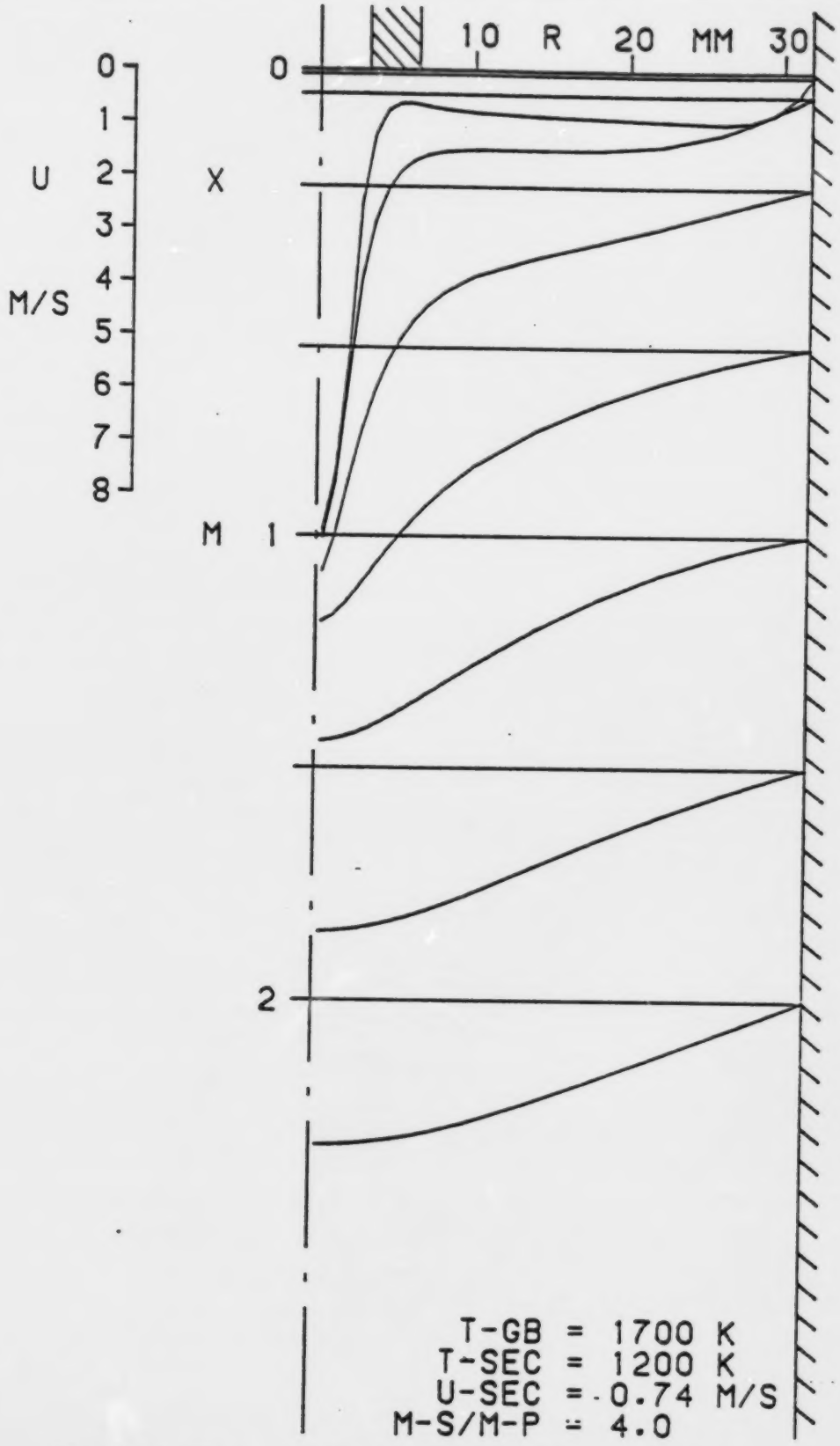

Figure 30: Velocity Profiles – Tgb=1700 K, Tinsec=1200 K, M-S/M-P=4.0 – Coal Feed Rate = 1.0 g/min, Primary Mass Flow = 10.0 g/min, Secondary Mass Flow = 40.0 g/min

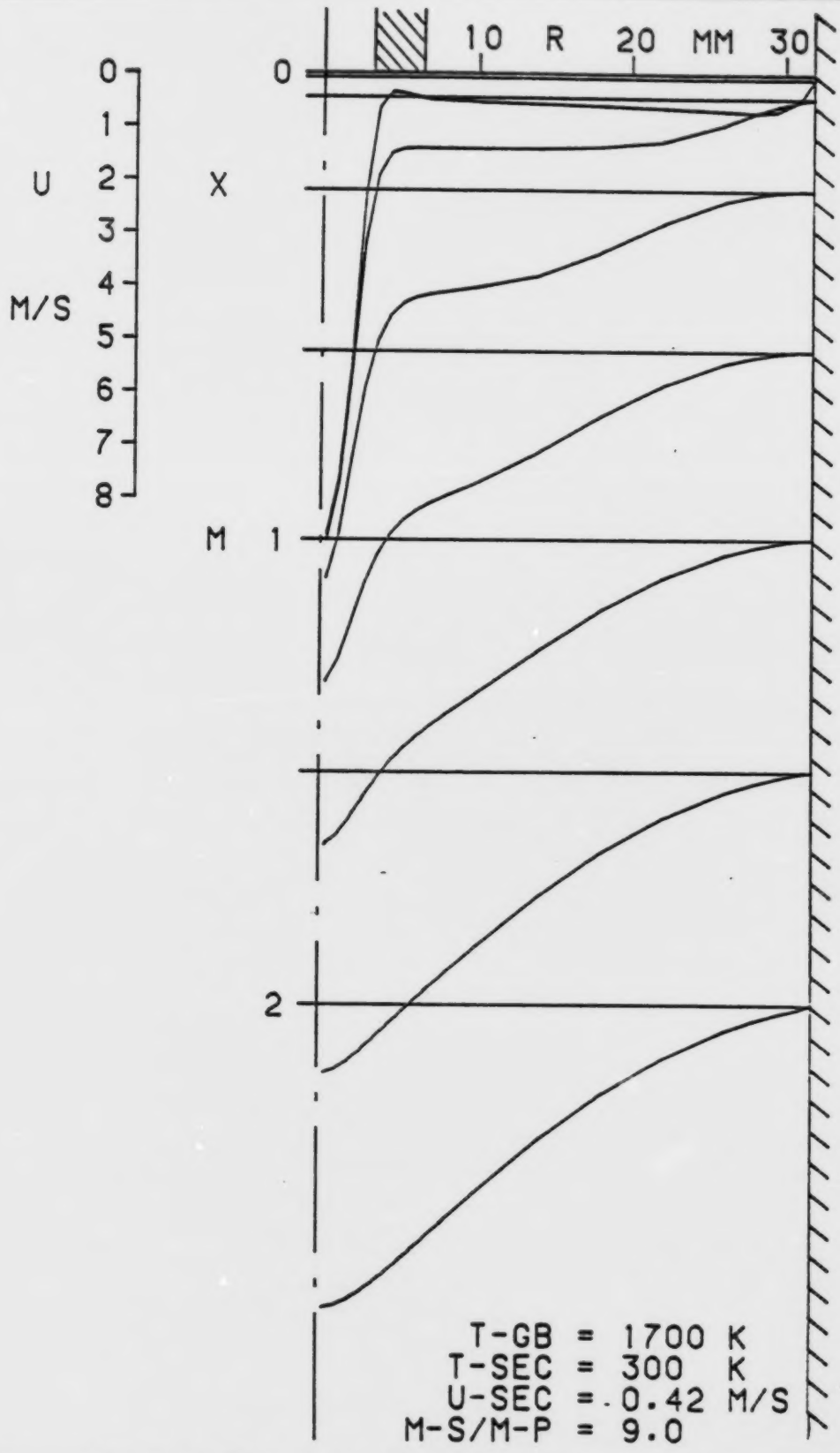

Figure 31: Velocity Profiles – Tgb=1700 K, Tinsec=300 K, M-S/M-P=9.0 – Coal Feed Rate = 1.0 g/min, Primary Mass Flow = 10.0 g/min, Secondary Mass Flow = 90.0 g/min

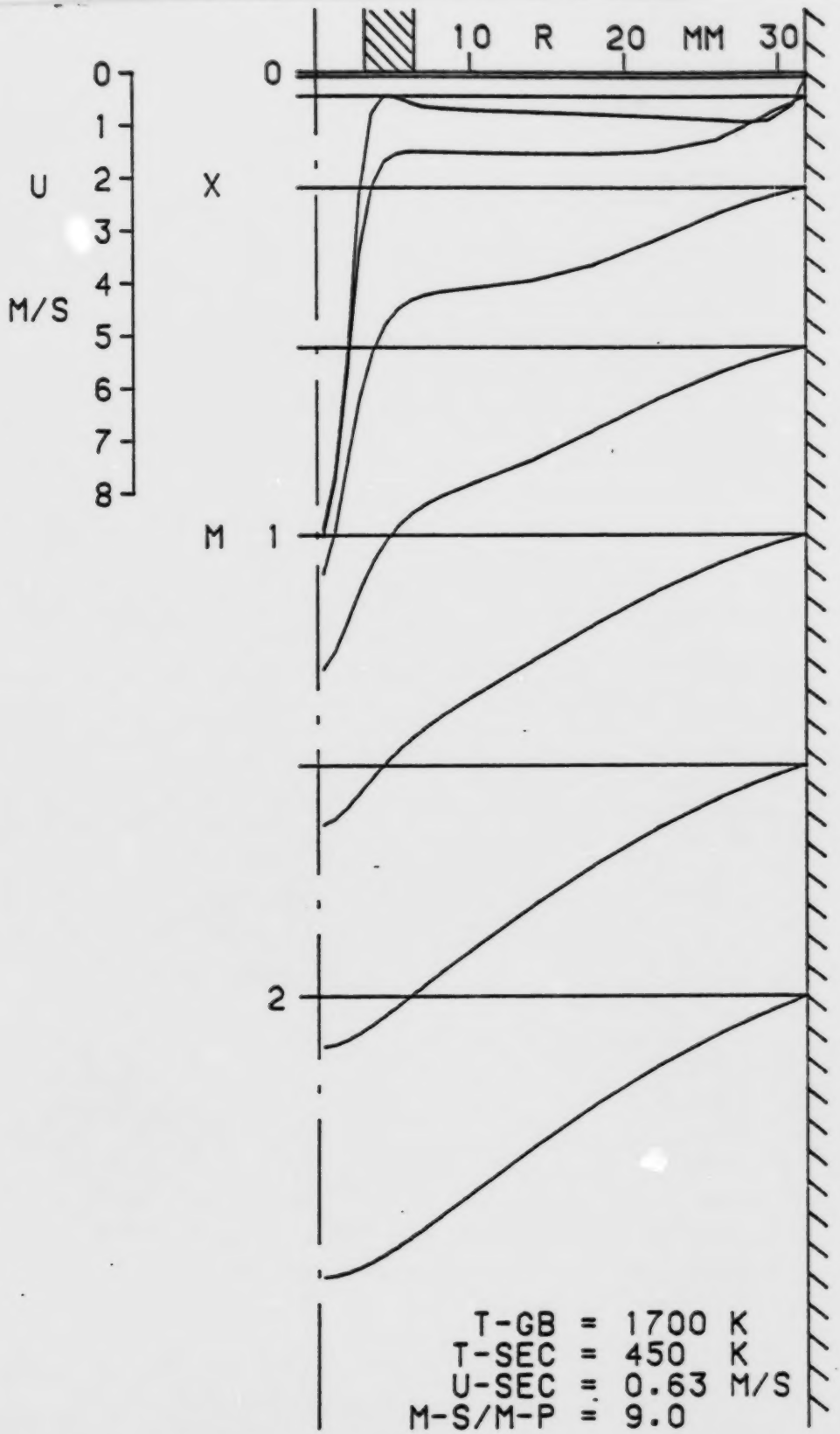

Figure 32: Velocity Profiles – Tgb=1700 K, Tinsec=450 K, M-S/M-P=9.0 – Coal Feed Rate = 1.0 g/min, Primary Mass Flow = 10.0 g/min, Secondary Mass Flow = 90.0 g/min

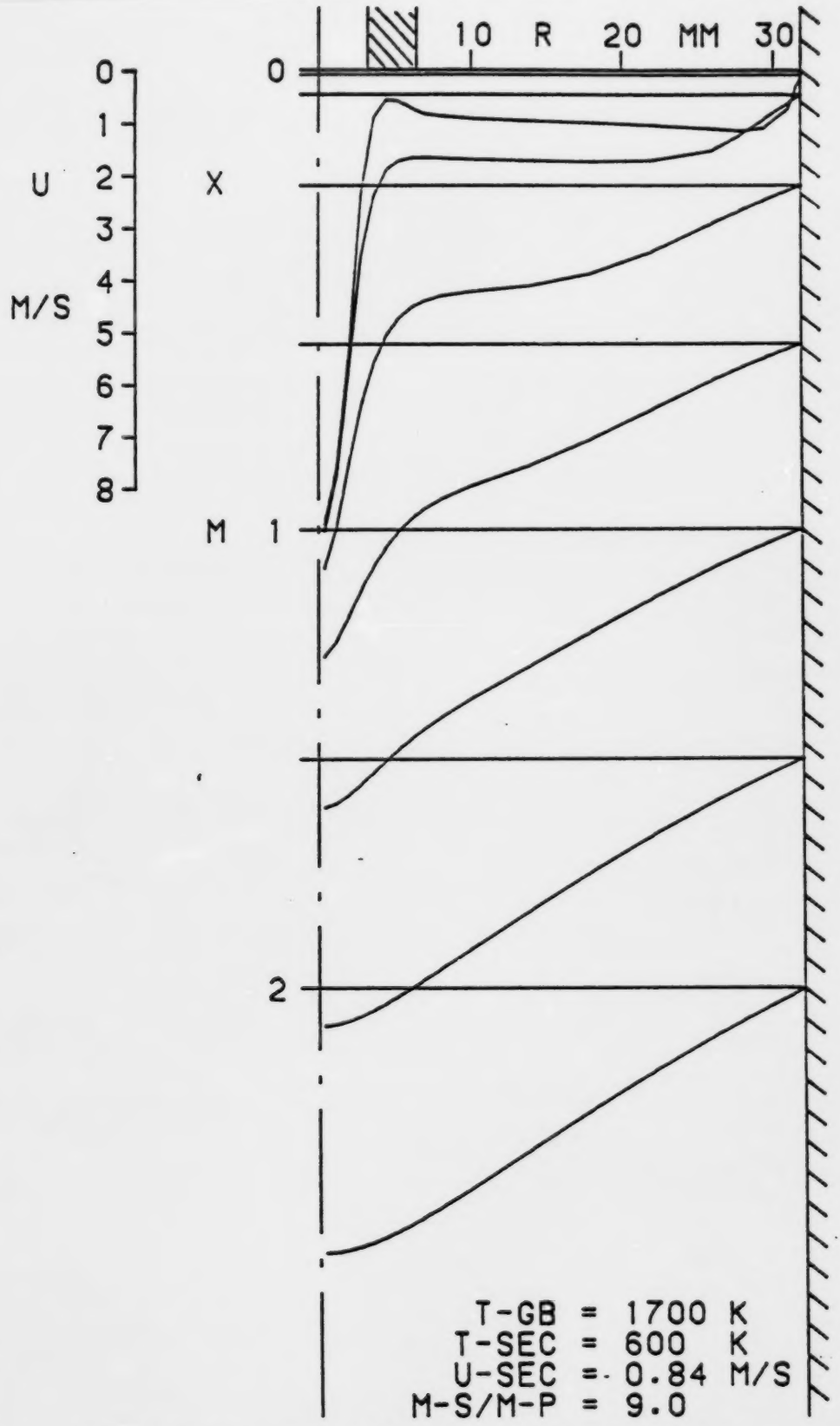

Figure 33: Velocity Profiles – Tgb=1700 K, Tinsec=600 K, M-S/M-P=9.0 – Coal Feed Rate = 1.0 g/min, Primary Mass Flow = 10.0 g/min, Secondary Mass Flow = 90.0 g/min

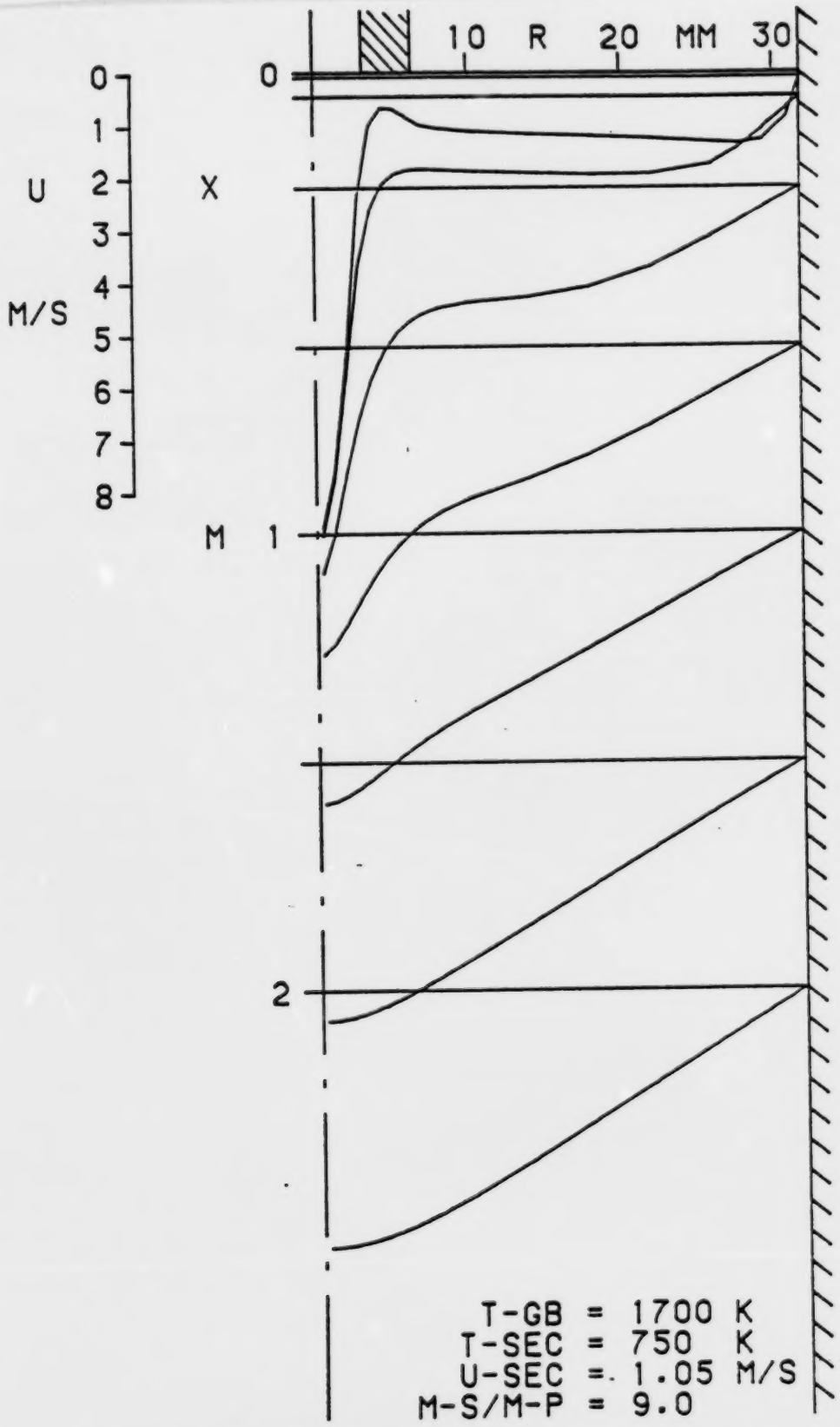

Figure 34: Velocity Profiles – Tgb=1700 K, Tinsec=750 K, M-S/M-P=9.0 – Coal Feed Rate = 1.0 g/min, Primary Mass Flow = 10.0 g/min, Secondary Mass Flow = 90.0 g/min

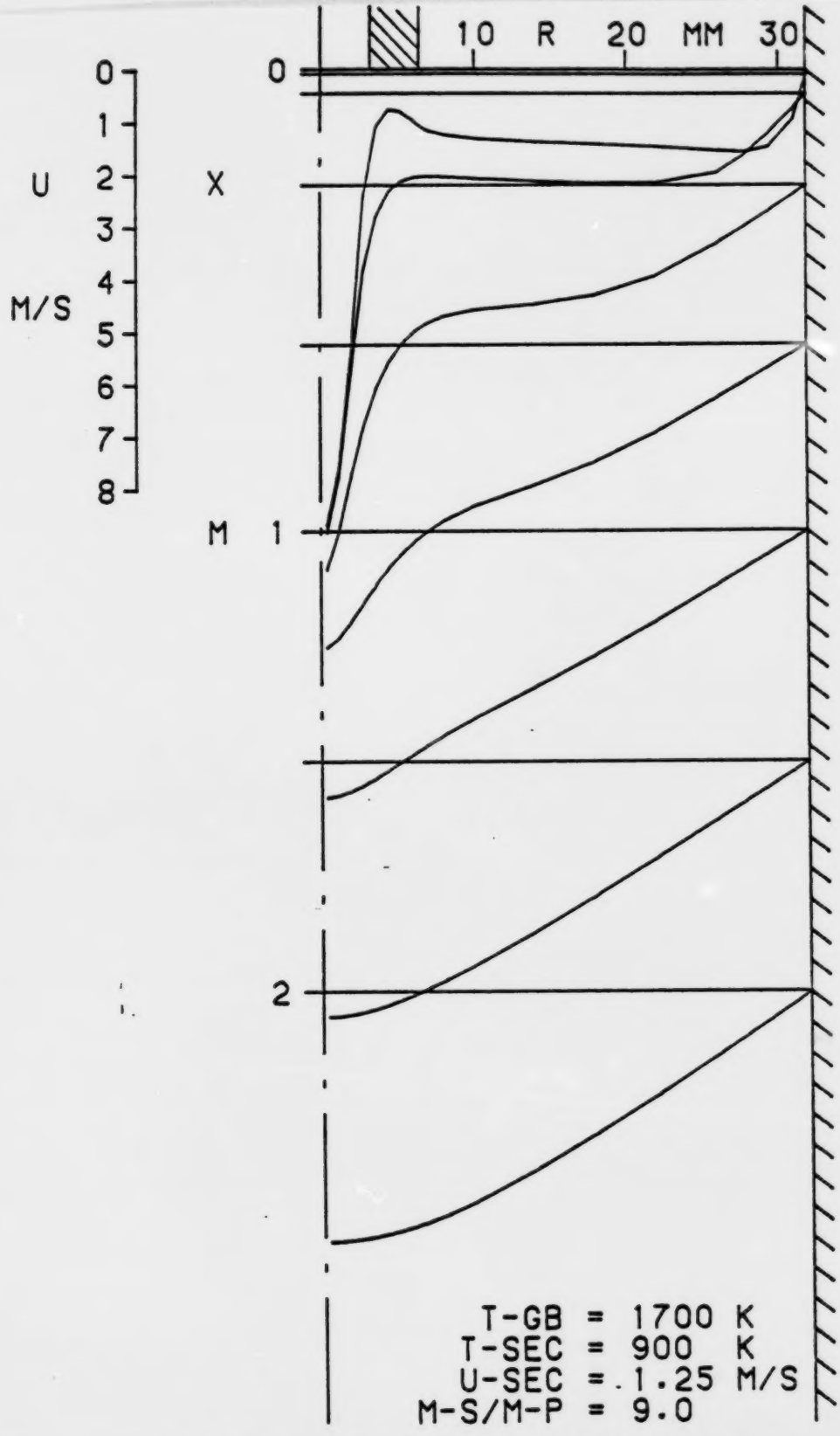

Figure 35: Velocity Profiles – Tgb=1700 K, Tinsec=900 K, M-S/M-P=9.0 – Coal Feed Rate = 1.0 g/min, Primary Mass Flow = 10.0 g/min, Secondary Mass Flow = 90.0 g/min

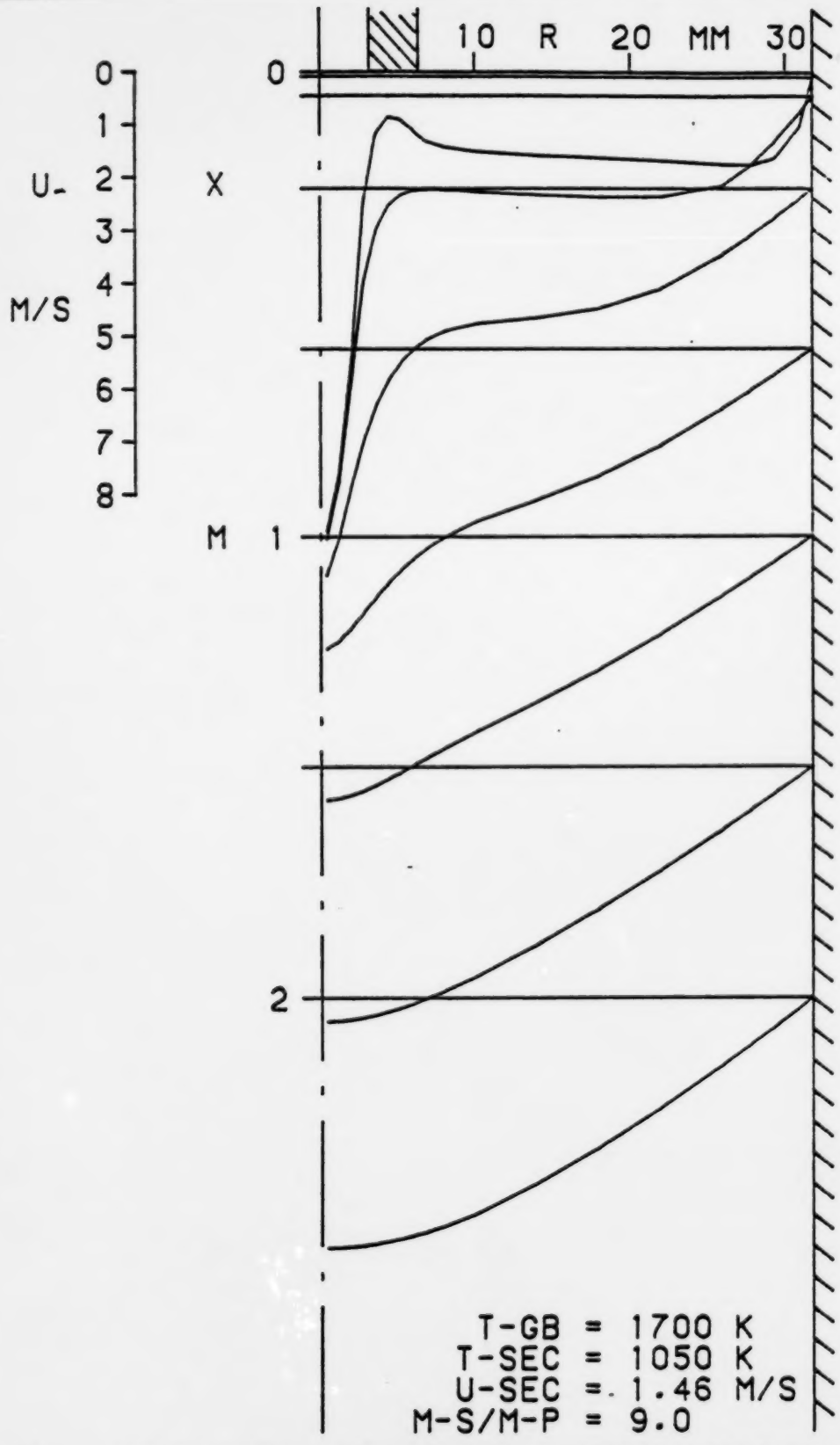

Figure 36: Velocity Profiles - Tgb=1700 K, Tinsec=1050 K, M-S/M-P=9.0 - Coal Feed Rate = 1.0 g/min, Primary Mass Flow = 10.0 g/min, Secondary Mass Flow = 90.0 g/min

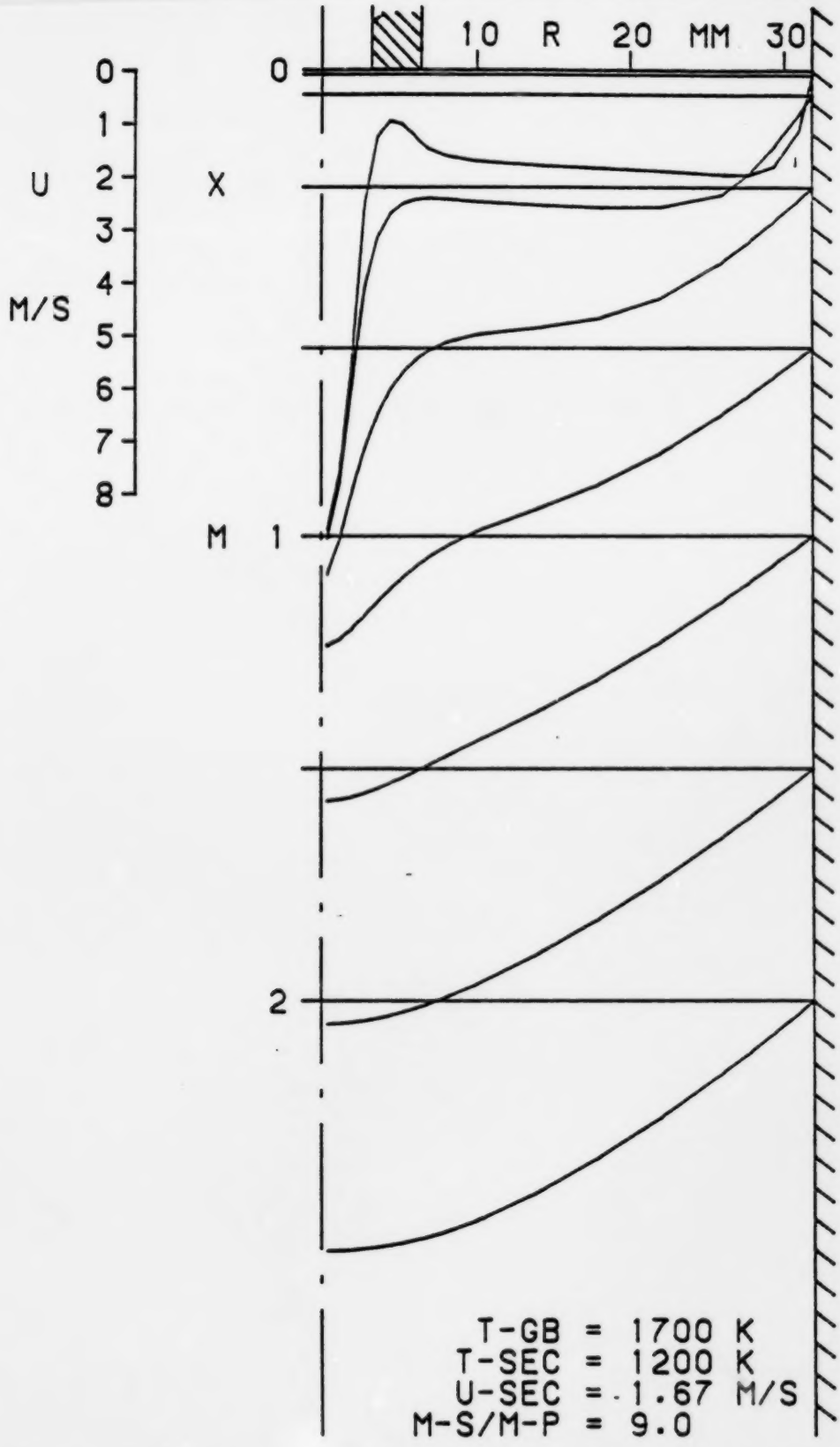

Figure 37: Velocity Profiles – Tgb=1700 K, Tinsec=1200 K, M-S/M-P=9.0 – Coal Feed Rate = 1.0 g/min, Primary Mass Flow = 10.0 g/min, Secondary Mass Flow = 90.0 g/min

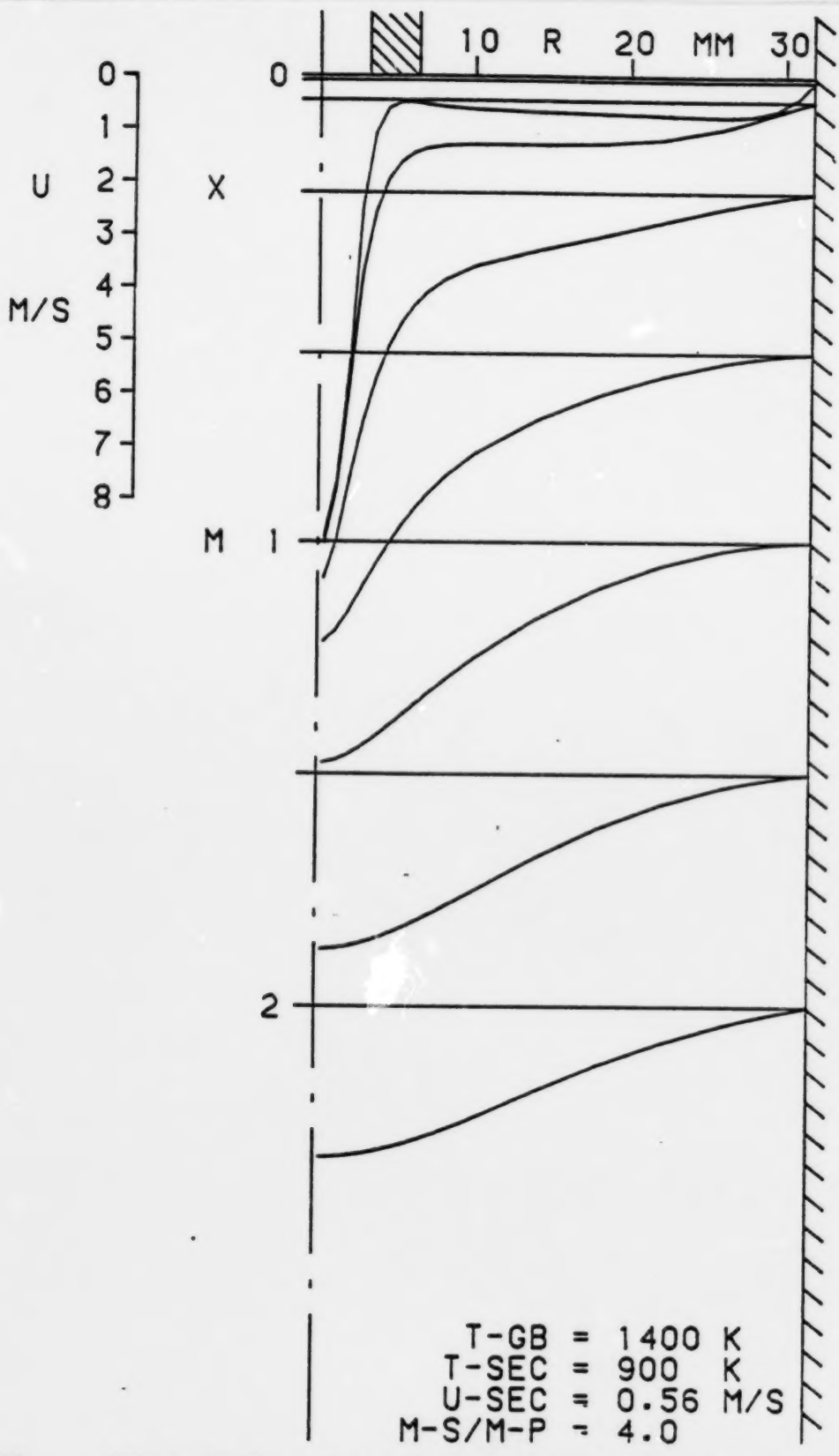

Figure 38: Velocity Profiles – Tgb=1400 K, Tinsec=900 K, M-S/M-P=4.0 – Coal Feed Rate = 1.0 g/min, Primary Mass Flow = 10.0 g/min, Secondary Mass Flow = 40.0 g/min

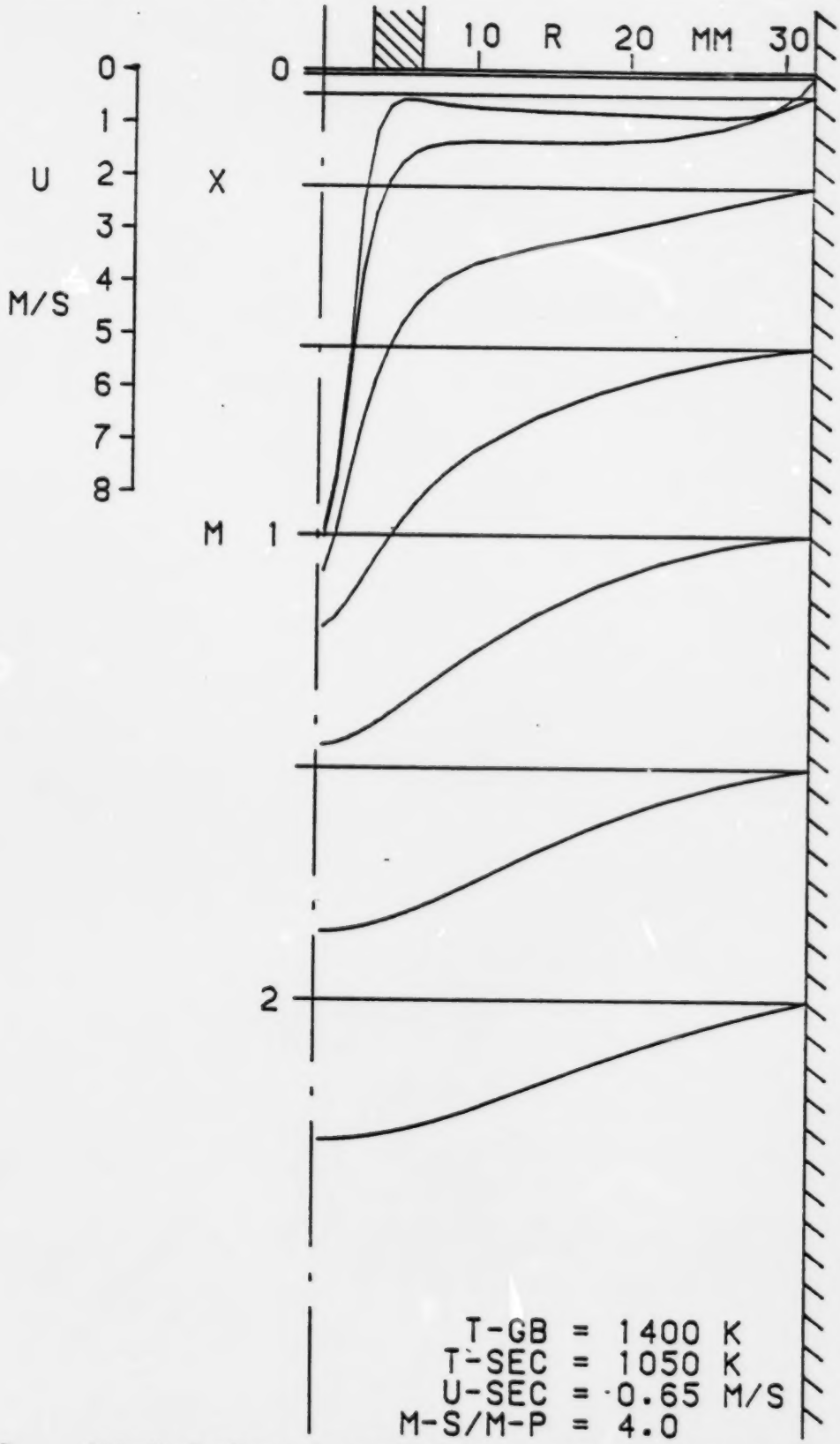

Figure 39: Velocity Profiles – Tgb=1400 K, Tinsec=1050 K, M-S/M-P=4.0 – Coal Feed Rate = 1.0 g/min, Primary Mass Flow = 10.0 g/min, Secondary Mass Flow = 40.0 g/min

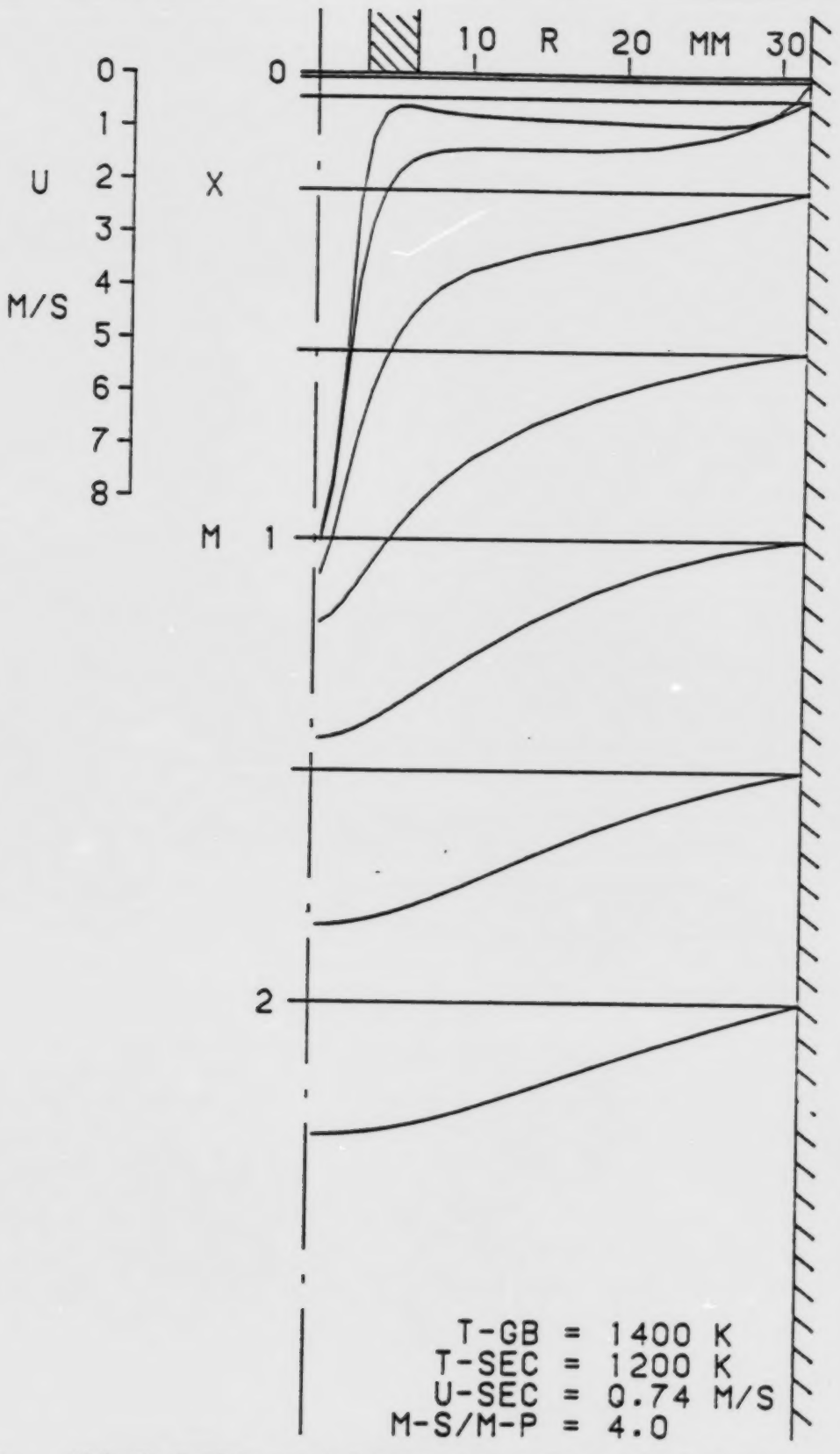

Figure 40: Velocity Profiles – Tgb=1400 K, Tinsec=1200 K, M-S/M-P=4.0 – Coal Feed Rate = 1.0 g/min, Primary Mass Flow = 10.0 g/min, Secondary Mass Flow = 40.0 g/min

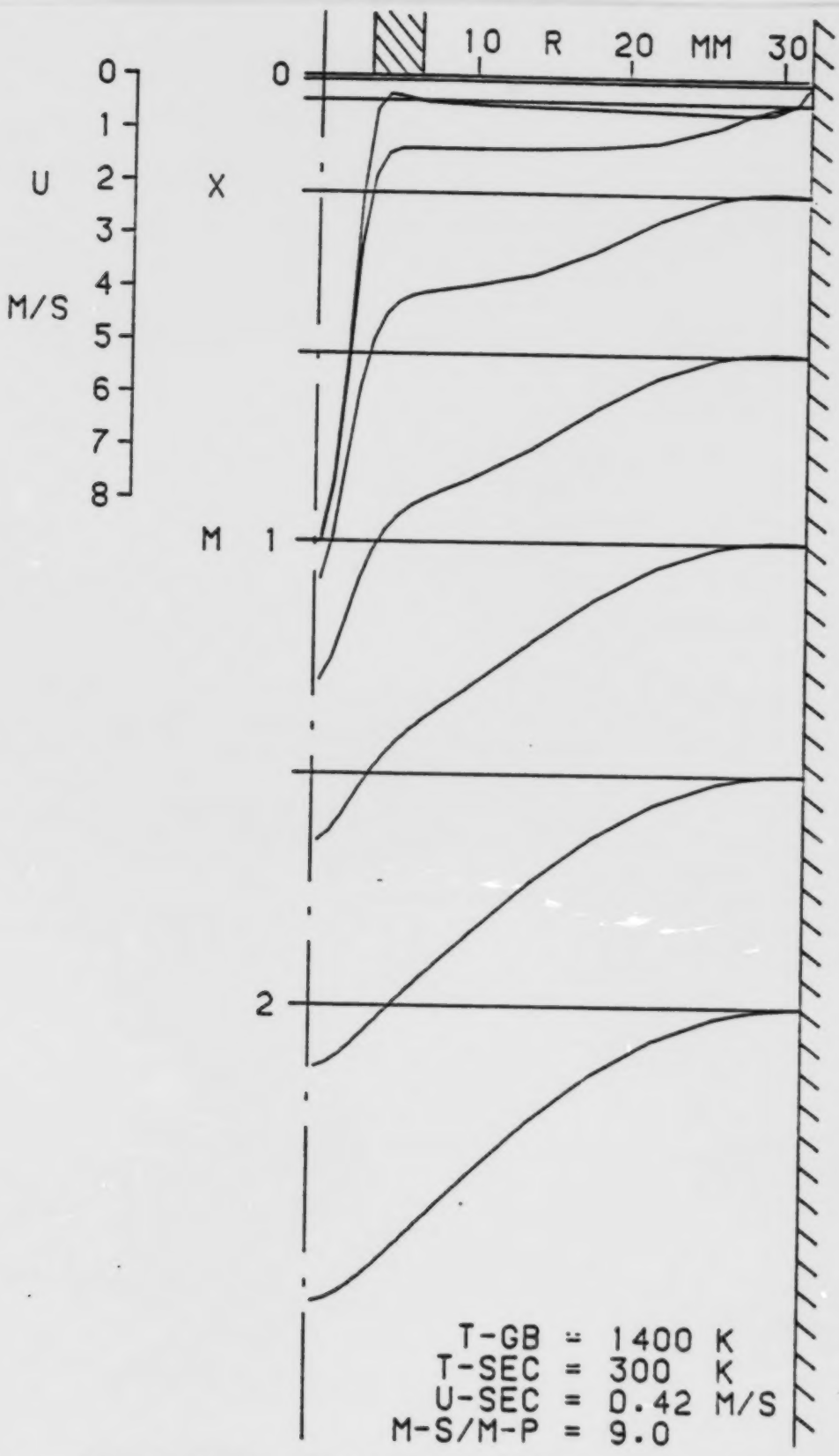

Figure 41: Velocity Profiles – Tgb=1400 K, Tinsec=300 K, M-S/M-P=9.0 – Coal Feed Rate = 1.0 g/min, Primary Mass Flow = 10.0 g/min, Secondary Mass Flow = 90.0 g/min

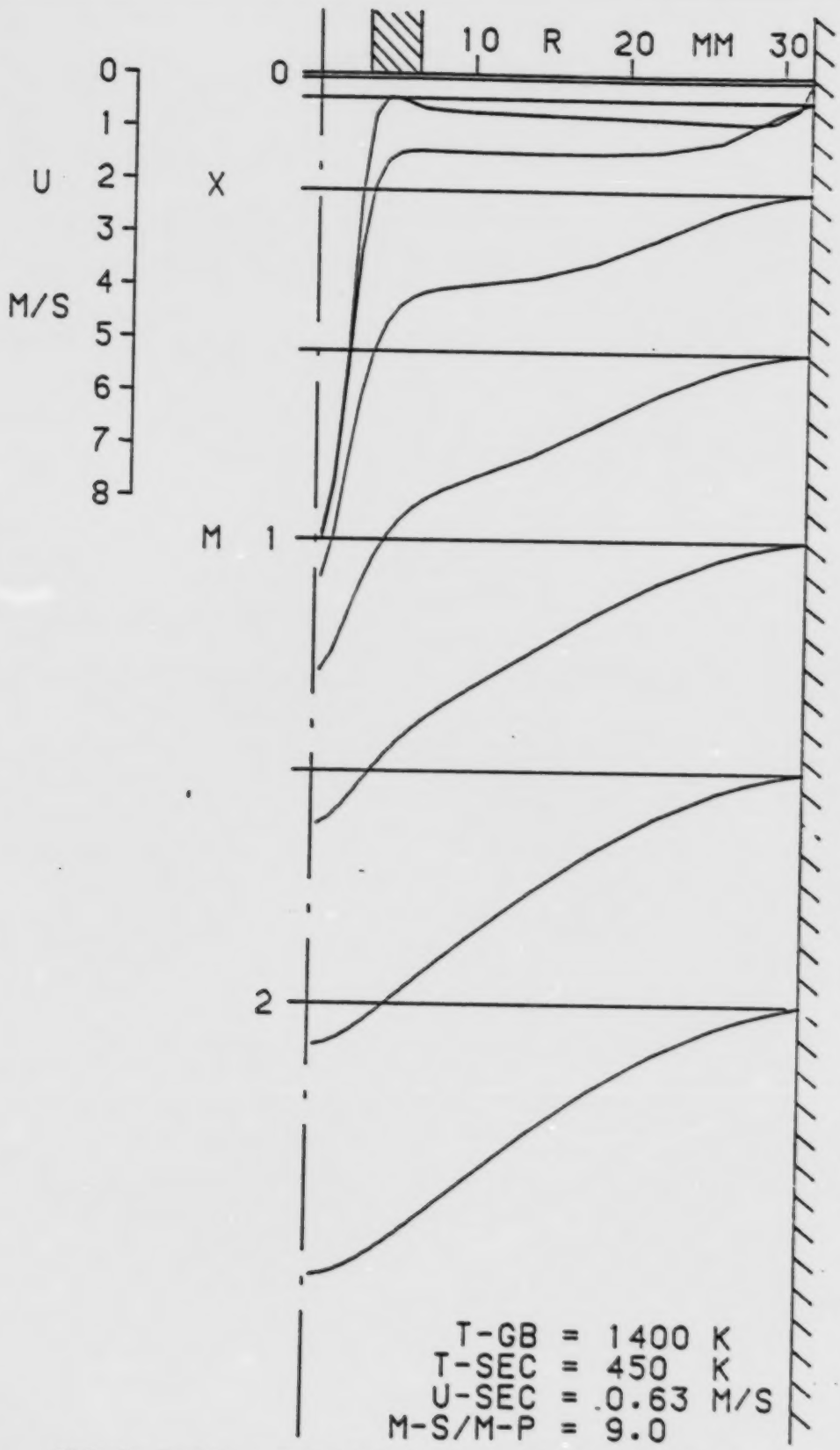

Figure 42: Velocity Profiles – Tgb=1400 K, Tinsec=450 K, M-S/M-P=9.0 – Coal Feed Rate = 1.0 g/min, Primary Mass Flow = 10.0 g/min, Secondary Mass Flow = 90.0 g/min

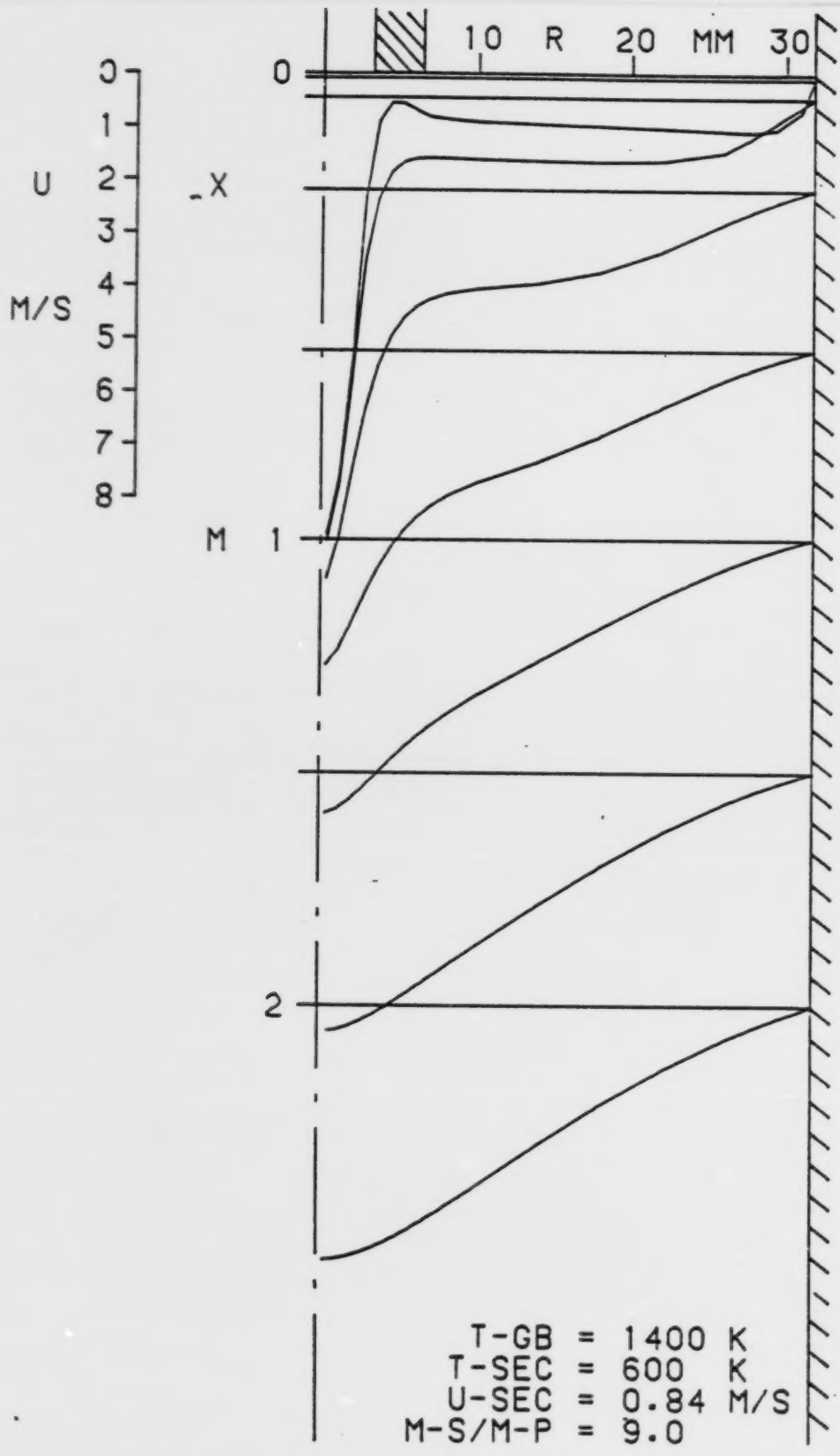

Figure 43: Velocity Profiles – Tgb=1400 K, Tinsec=600 K, M-S/M-P=9.0 – Coal Feed Rate = 1.0 g/min, Primary Mass Flow = 10.0 g/min, Secondary Mass Flow = 90.0 g/min

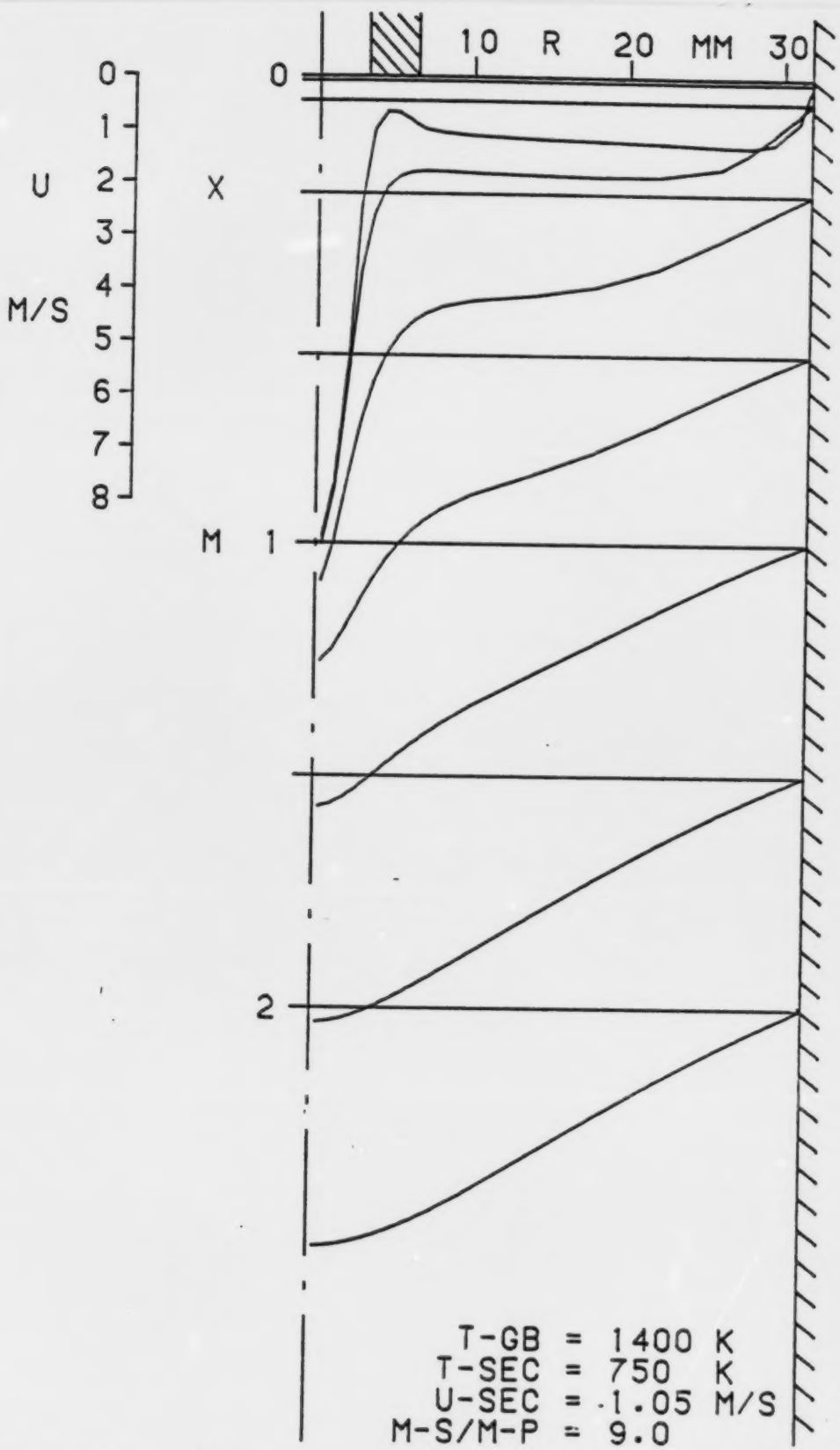

Figure 44: Velocity Profiles – Tgb=1400 K, Tinsec=750 K, M-S/M-P=9.0 – Coal Feed Rate = 1.0 g/min, Primary Mass Flow = 10.0 g/min, Secondary Mass Flow = 90.0 g/min

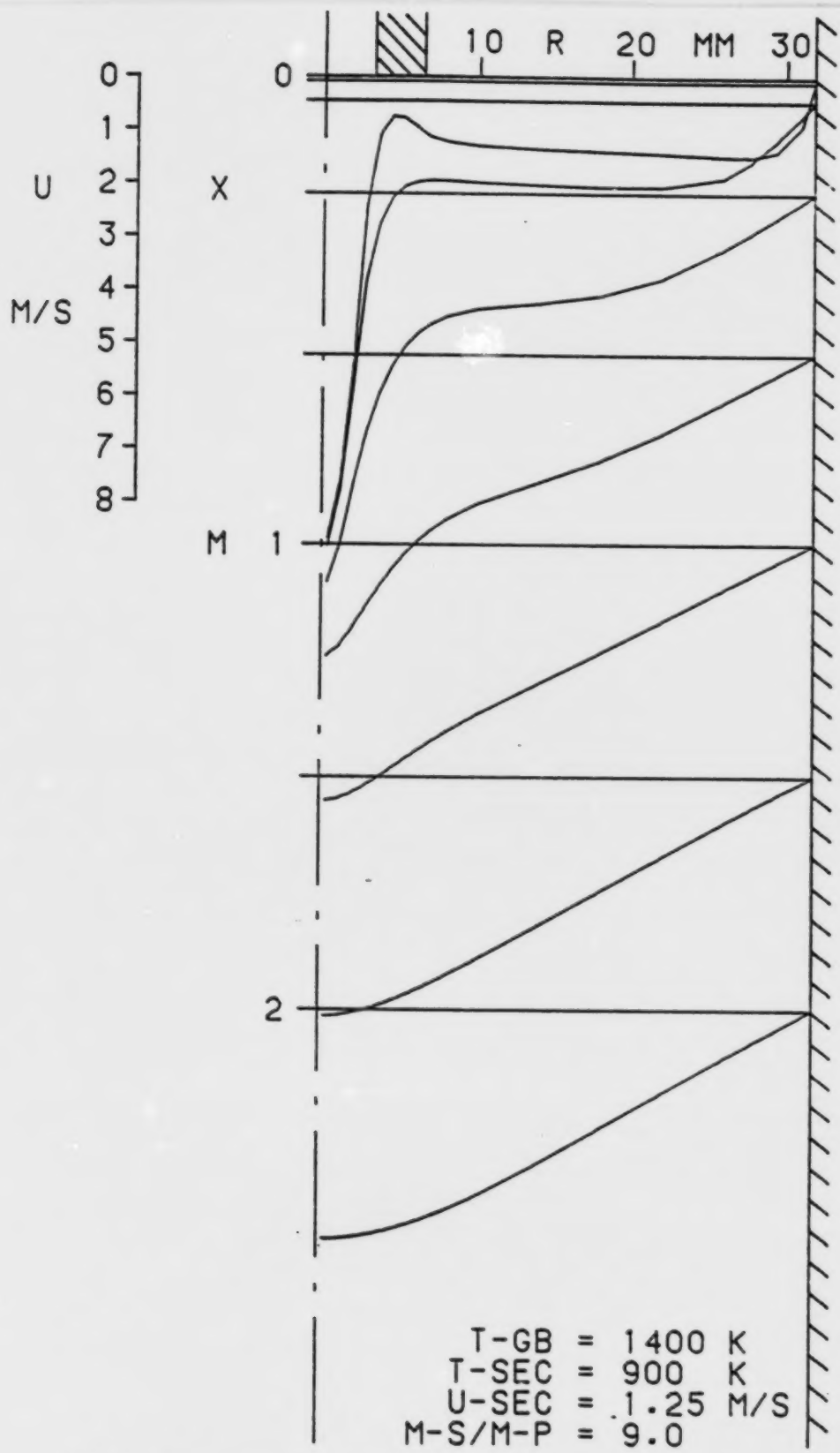

Figure 45: Velocity Profiles – Tgb=1400 K, Tinsec=900 K, M-S/M-P=9.0 – Coal Feed Rate = 1.0 g/min, Primary Mass Flow = 10.0 g/min, Secondary Mass Flow = 90.0 g/min

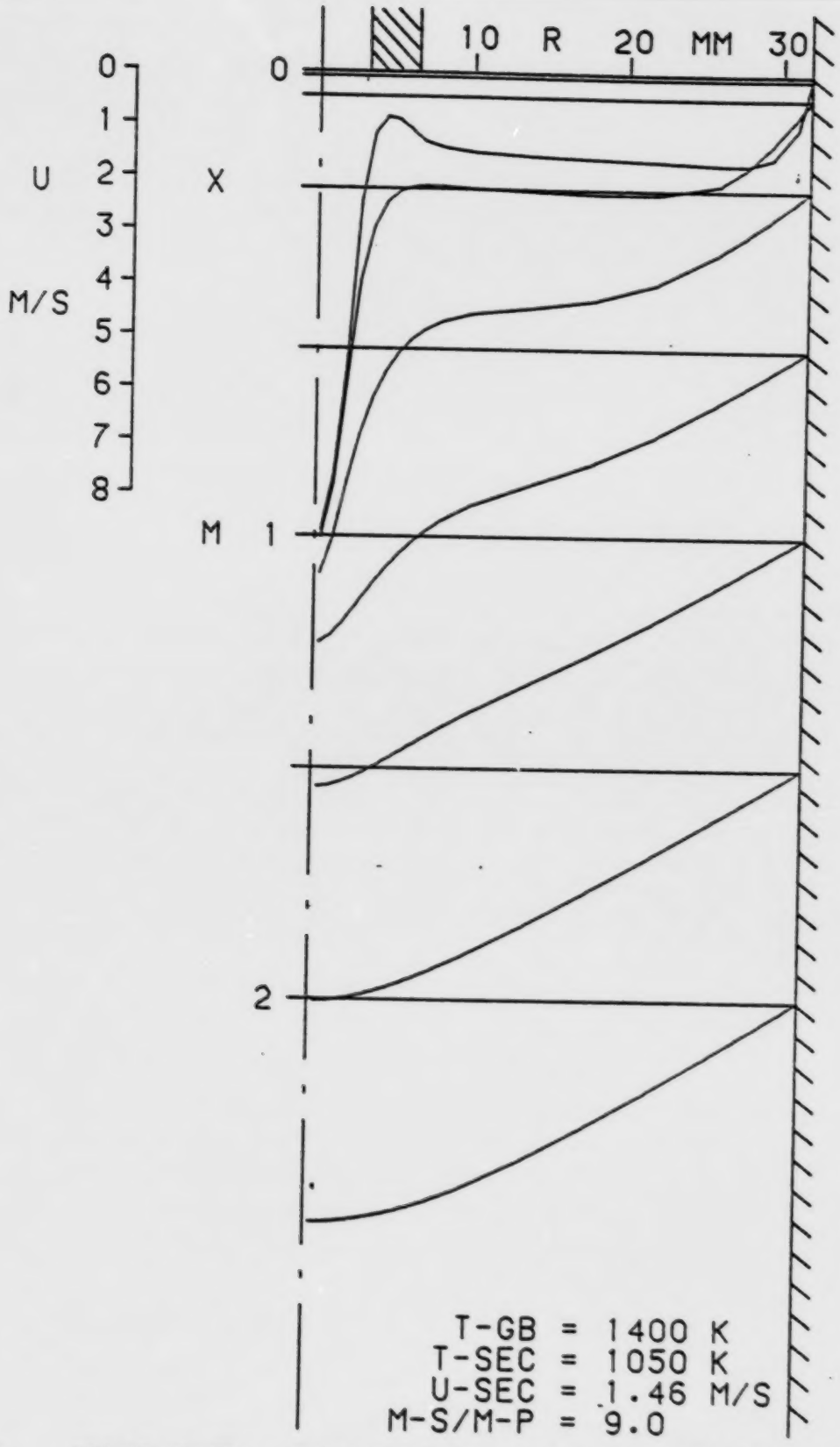

Figure 46: Velocity Profiles – Tgb=1400 K, Tinsec=1050 K, M-S/M-P=9.0 – Coal Feed Rate = 1.0 g/min, Primary Mass Flow = 10.0 g/min, Secondary Mass Flow = 90.0 g/min

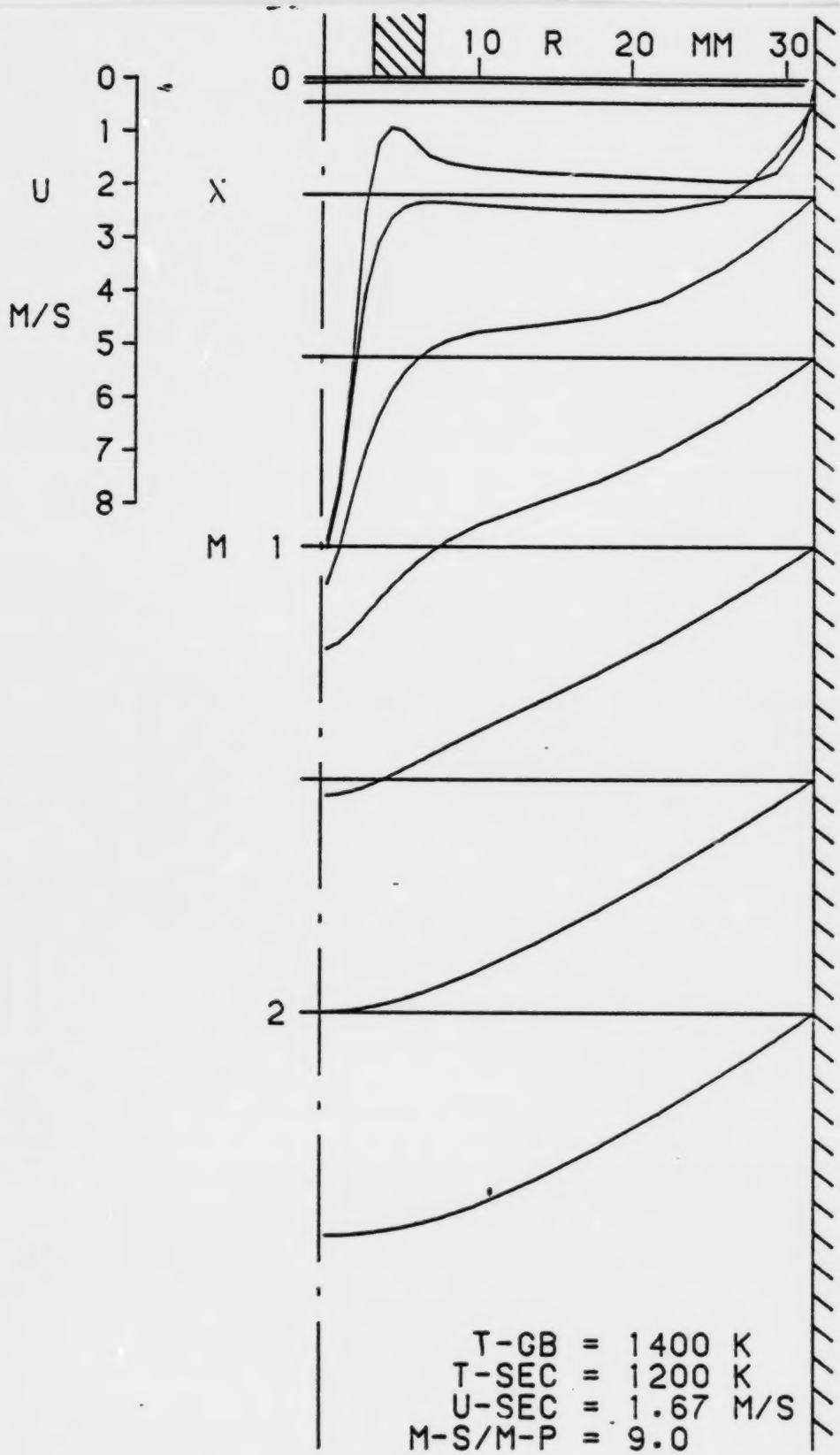

Figure 47: Velocity Profiles – Tgb=1400 K, Tinsec=1200 K, M-S/M-P=9.0 – Coal Feed Rate = 1.0 g/min, Primary Mass Flow = 10.0 g/min, Secondary Mass Flow = 90.0 g/min

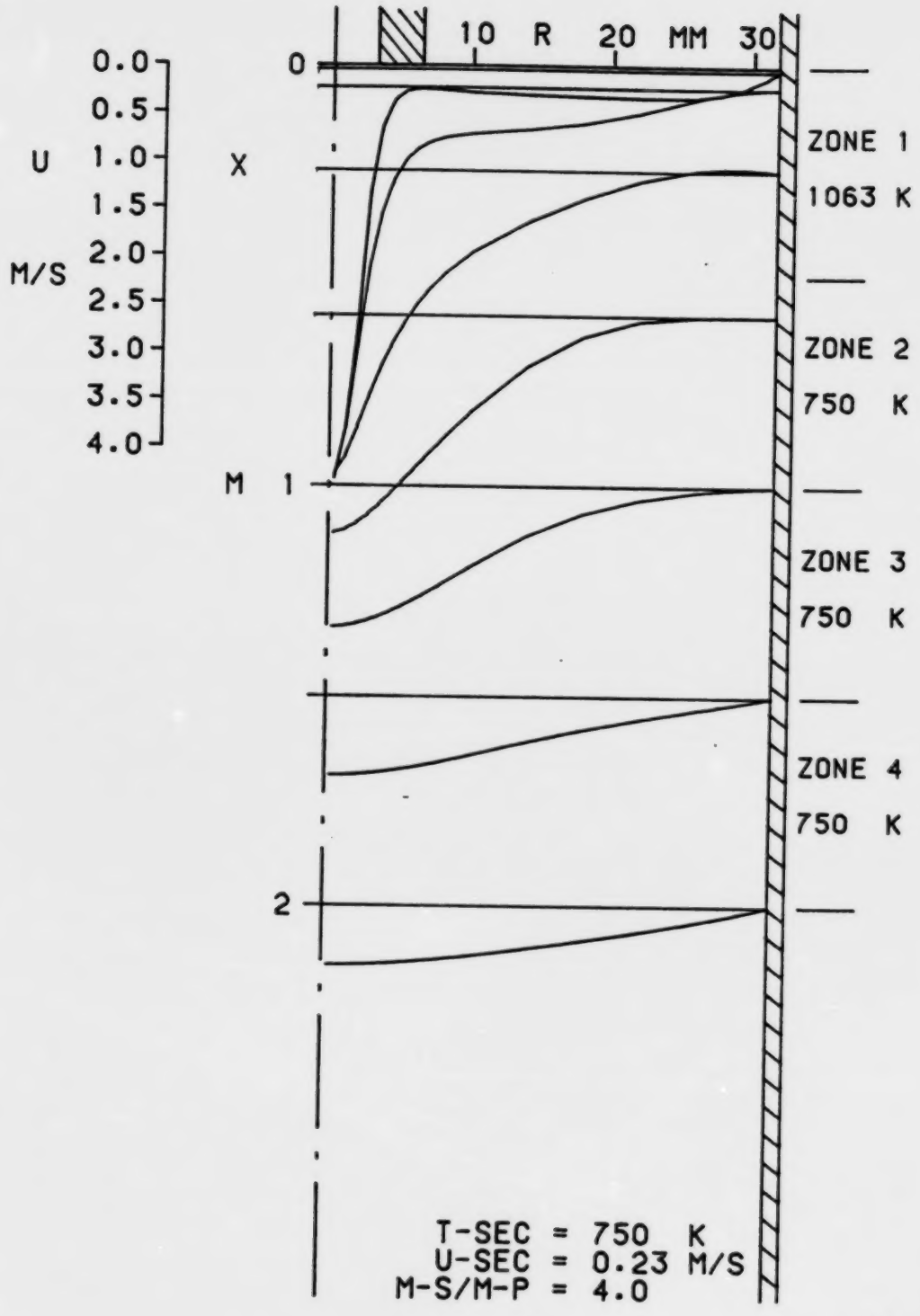

Figure 48: Velocity Profiles – Variable Zone Temp., Tinsec = 750 K – Coal Feed Rate = 0.5 g/min, Primary Mass Flow = 5.0 g/min, Secondary Mass Flow = 20.0 g/min

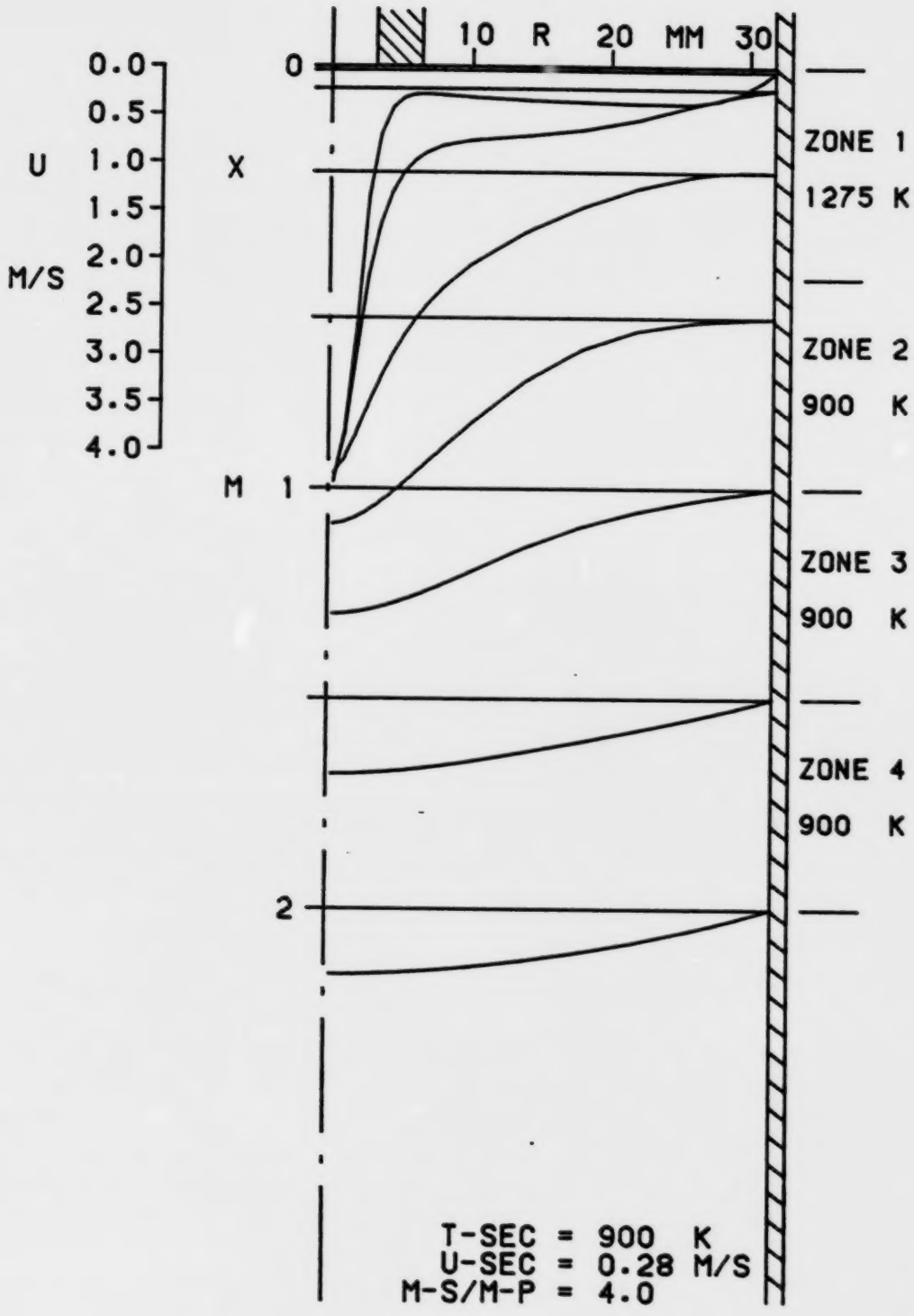

Figure 49: Velocity Profiles – Variable Zone Temp., Tinsec = 900 K – Coal Feed Rate = 0.5 g/min, Primary Mass Flow = 5.0 g/min, Secondary Mass Flow = 20.0 g/min

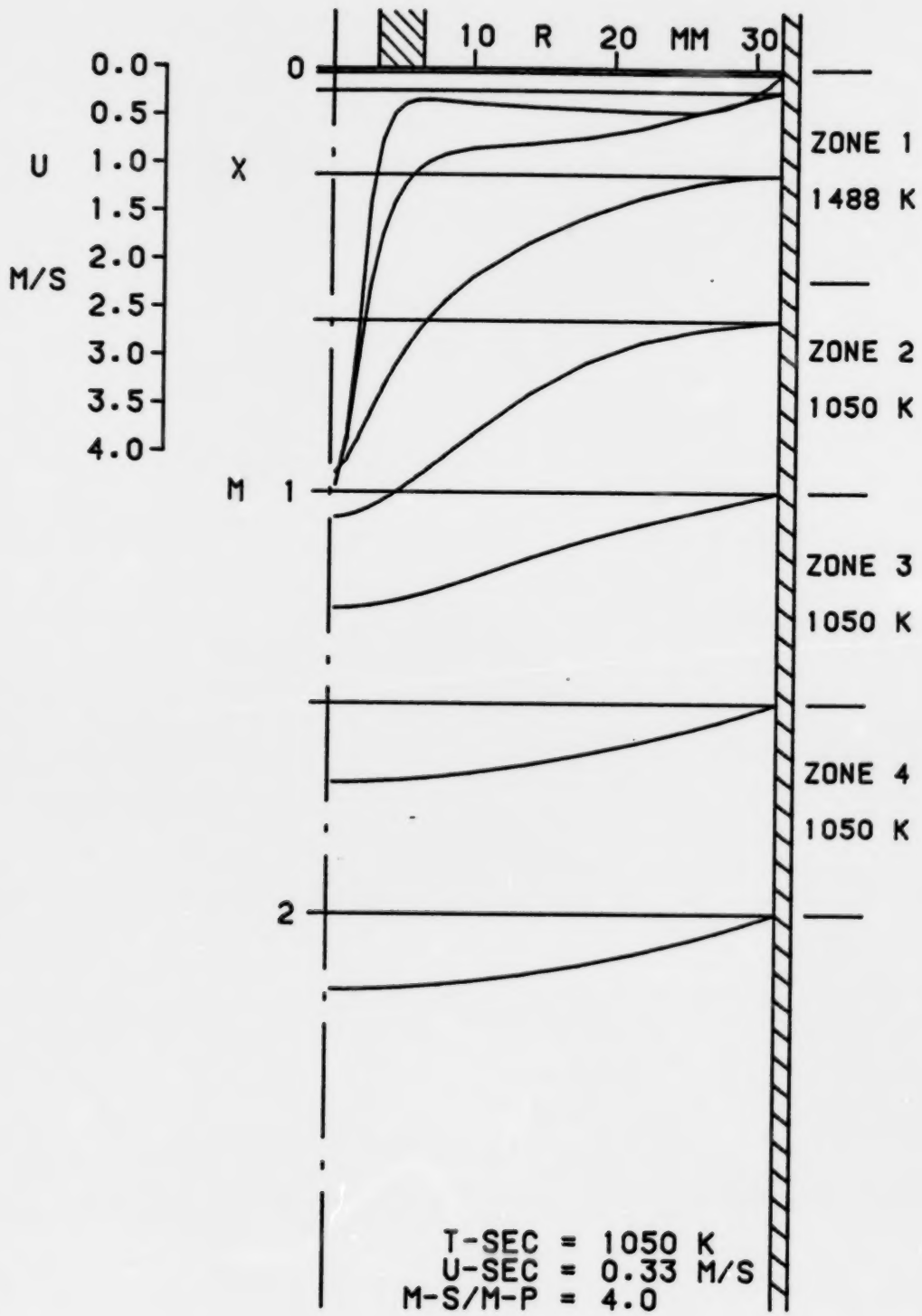

Figure 50: Velocity Profiles – Variable Zone Temp., Tinsec = 1050 K – Coal Feed Rate = 0.5 g/min, Primary Mass Flow = 5.0 g/min, Secondary Mass Flow = 20.0 g/min

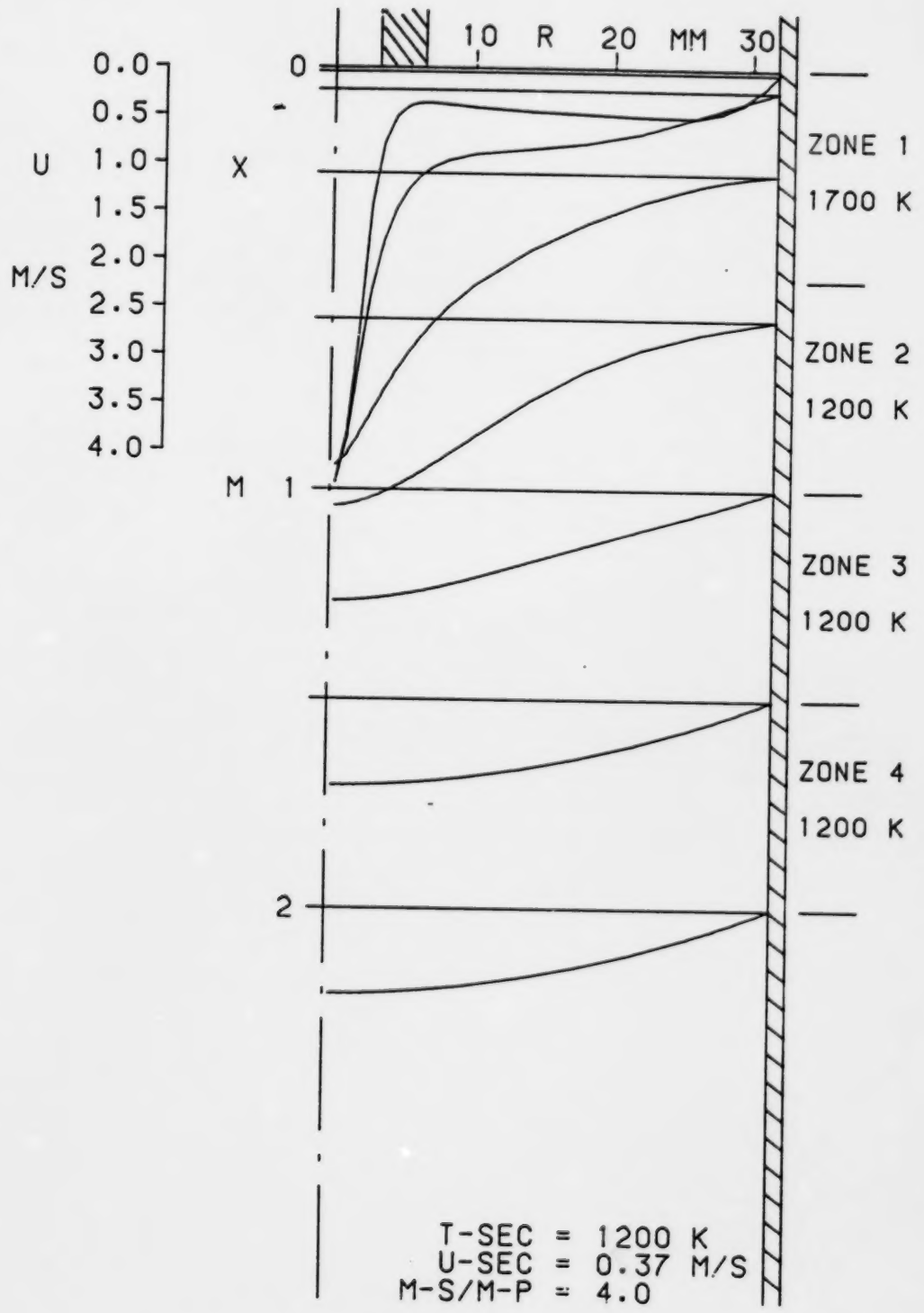

Figure 51: Velocity Profiles – Variable Zone Temp., Tinsec = 1200 K – Coal Feed Rate = 0.5 g/min., Primary Mass Flow = 5.0 g/min, Secondary Mass Flow = 20.0 g/min

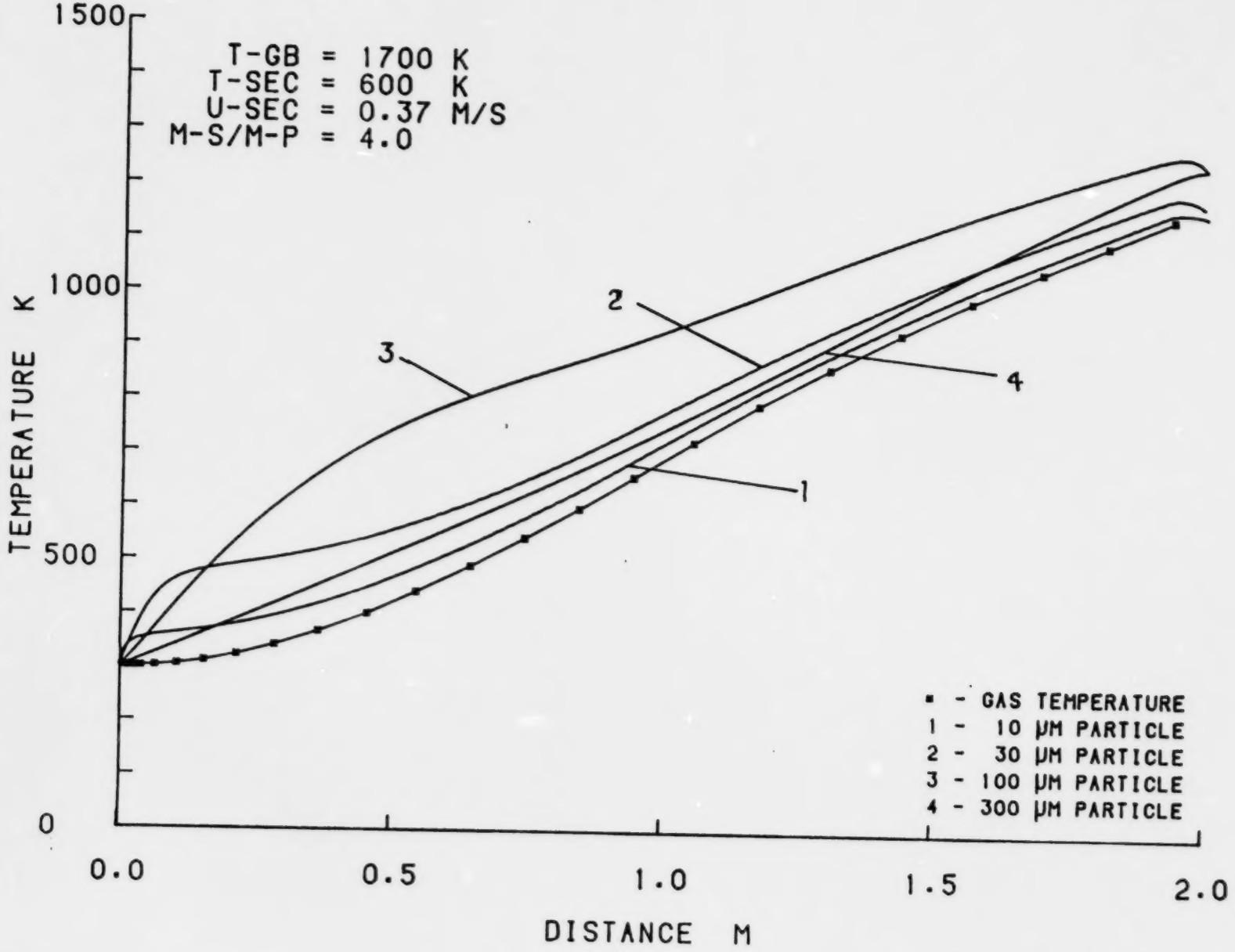

Figure 52: Particle Heating - Tgb=1700 K, Tinsec=600 K, M-S/M-P=4.0 - Coal Feed Rate = 1.0 g/min, Primary Mass Flow = 10.0 g/min, Secondary Mass Flow = 40.0 g/min

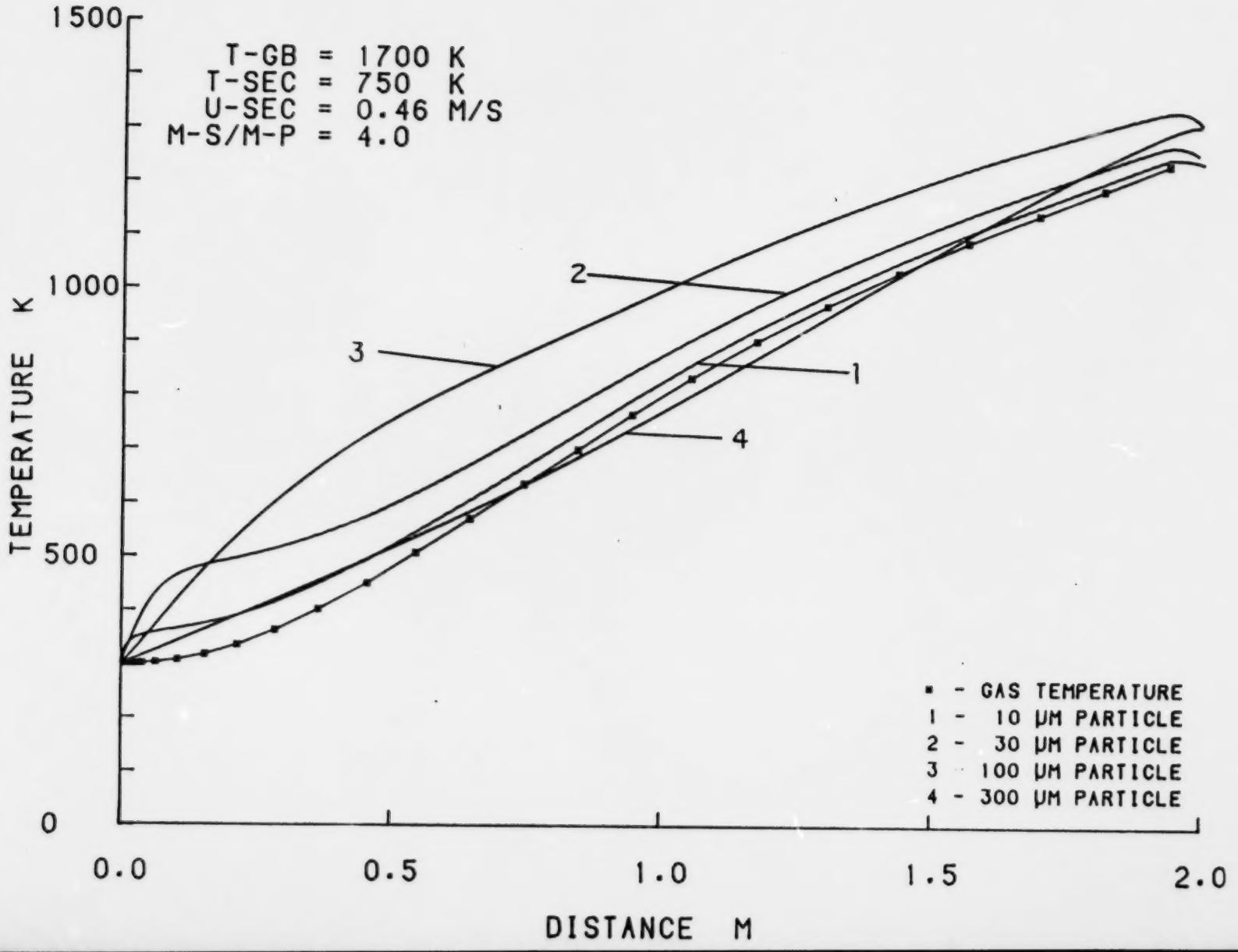

Figure 53: Particle Heating - Tgb=1700 K, Tinsec=750 K, M-S/M-P=4.0 - Coal Feed Rate = 1.0 g/min, Primary Mass Flow = 10.0 g/min, Secondary Mass Flow = 40.0 g/min

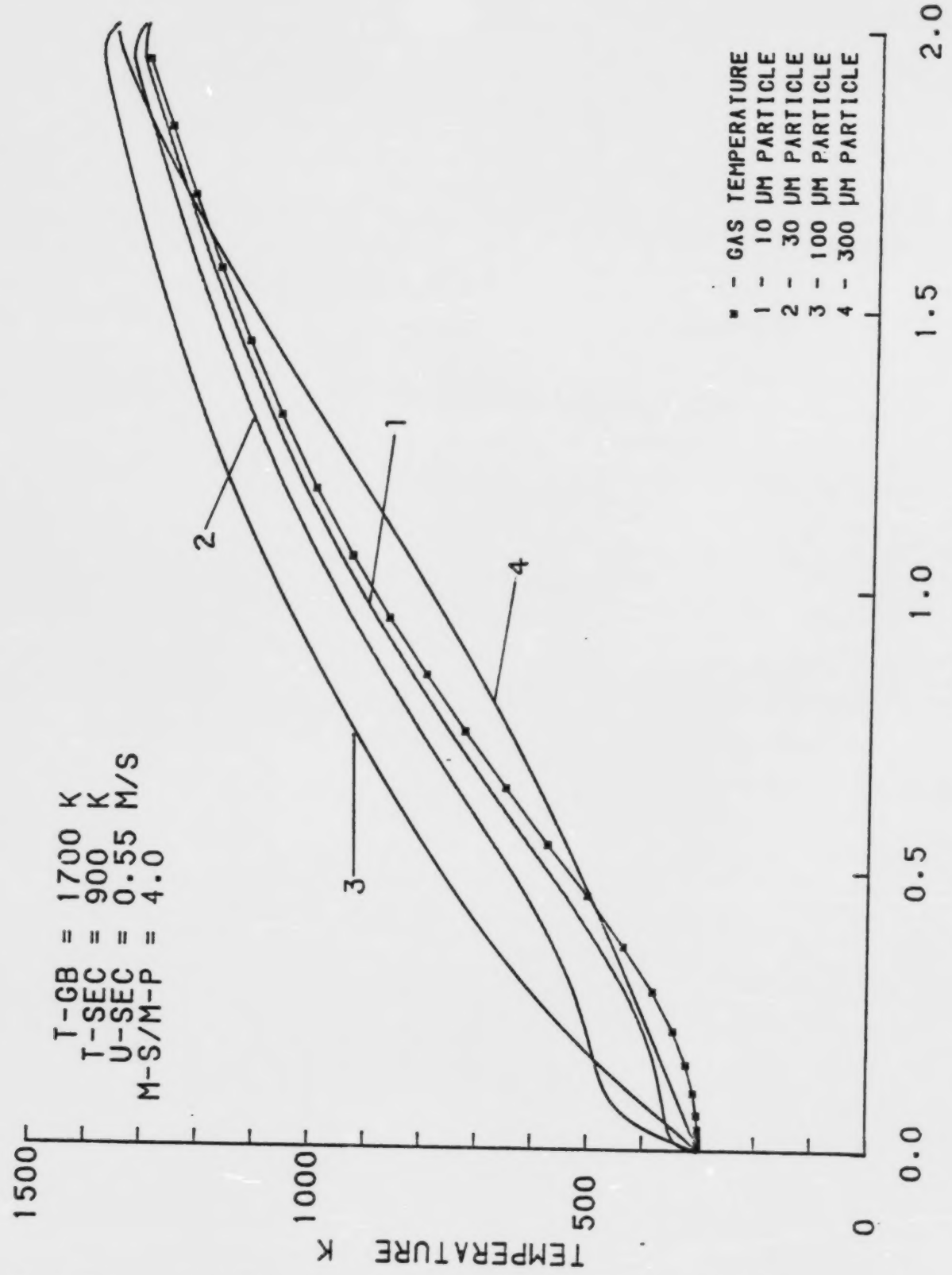

Figure 54: Particle Heating – Tgb=1700 K, Tinsec=900 K, M-S/M-P=4.0 – Coal Feed Rate = 1.0 g/min, Primary Mass Flow = 10.0 g/min, Secondary Mass Flow = 40.0 g/min

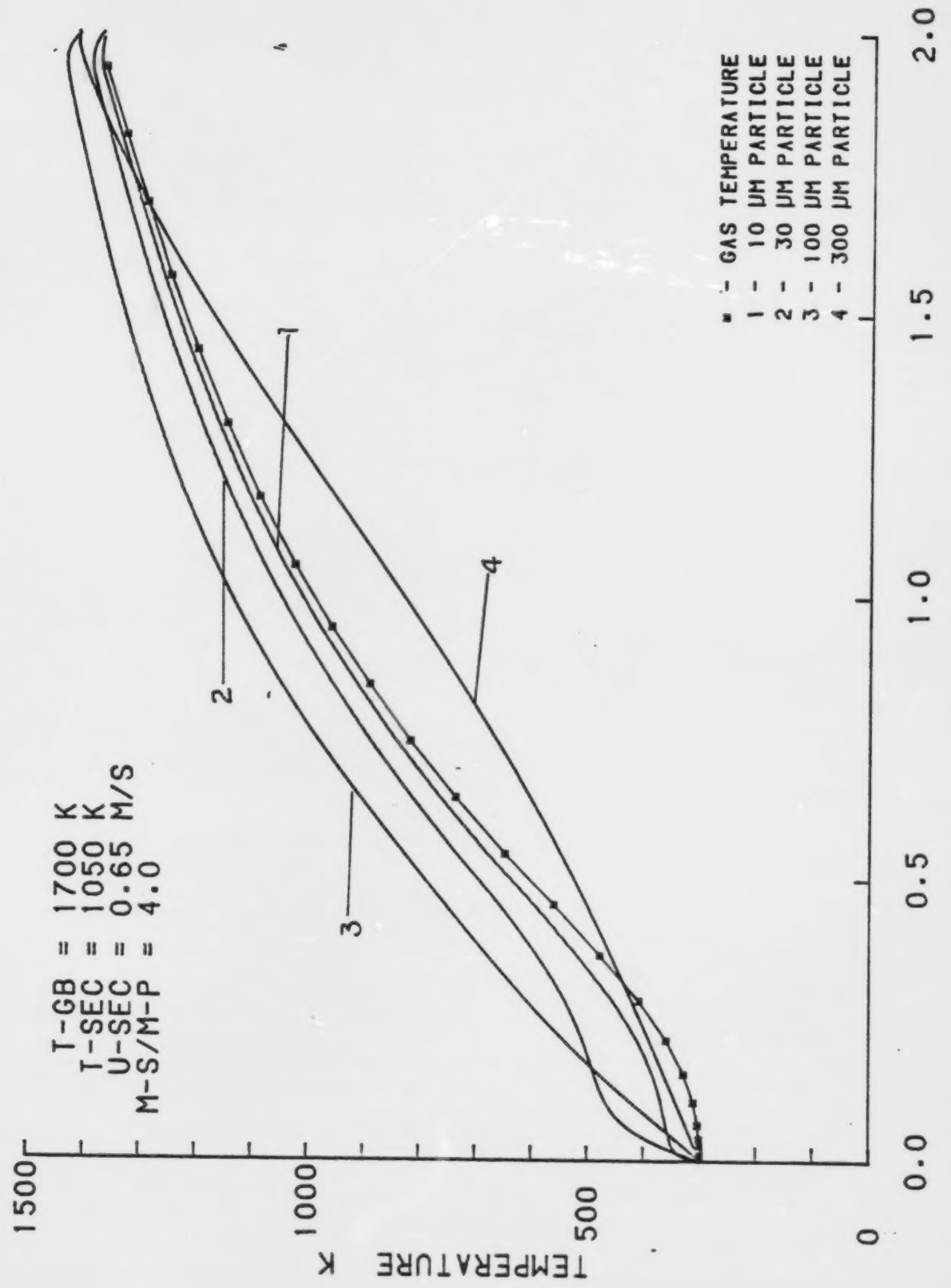

Figure 55: Particle Heating – Tgb=1700 K, Tinsec=1050 K, M-S/M-P=4.0 – Coal Feed Rate = 1.0 g/min, Primary Mass Flow = 10.0 g/min, Secondary Mass Flow = 40.0 g/min

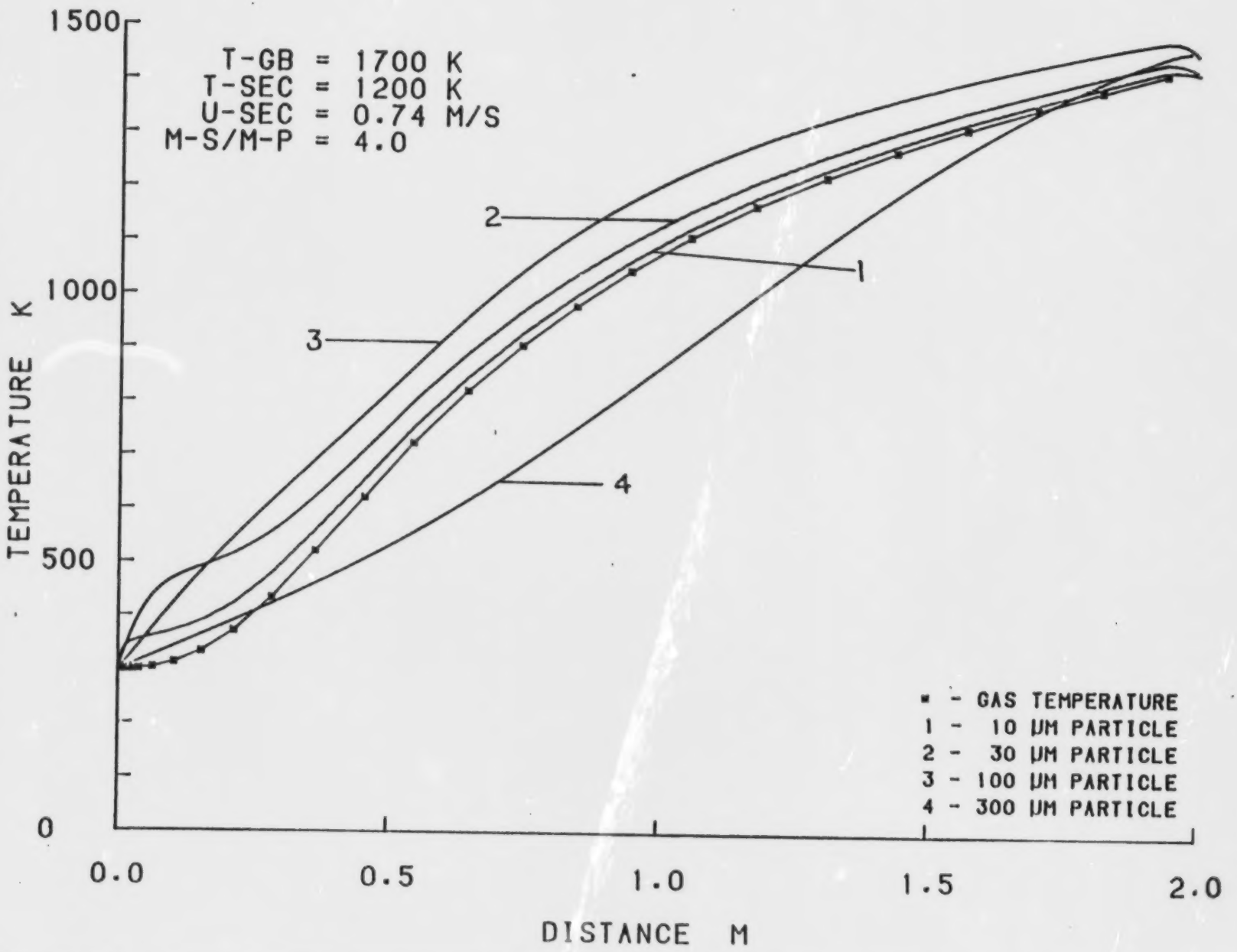

Figure 56: Particle Heating - Tgb=1700 K, Tinsec=1200 K, M-S/M-P=4.0 - Coal Feed Rate = 1.0 g/min, Primary Mass Flow = 10.0 g/min, Secondary Mass Flow = 40.0 g/min

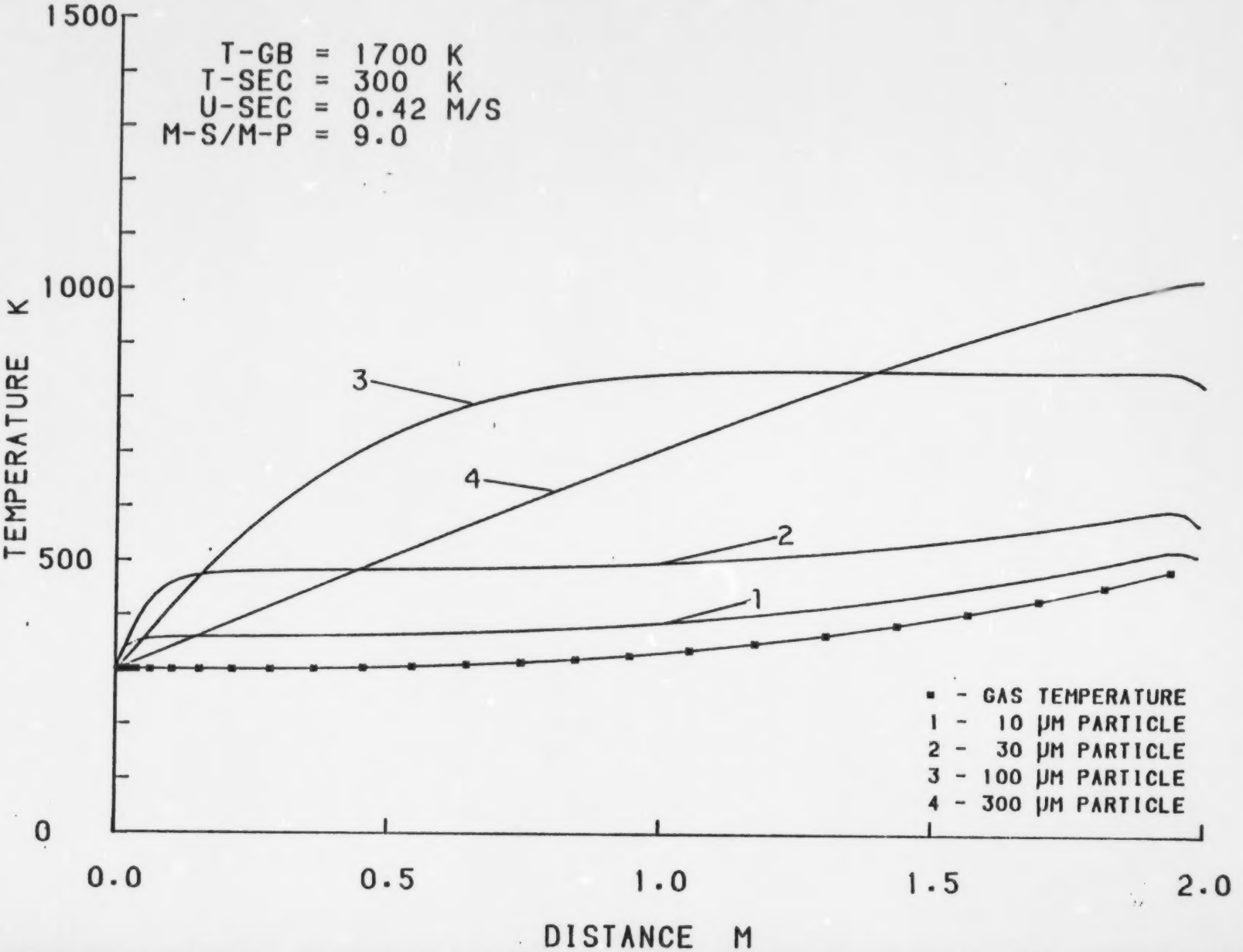

Figure 57: Particle Heating - Tgb=1700 K, Tinsec=300 K, M-S/M-P=9.0 - Coal Feed Rate = 1.0 g/min, Primary Mass Flow = 10.0 g/min, Secondary Mass Flow = 90.0 g/min

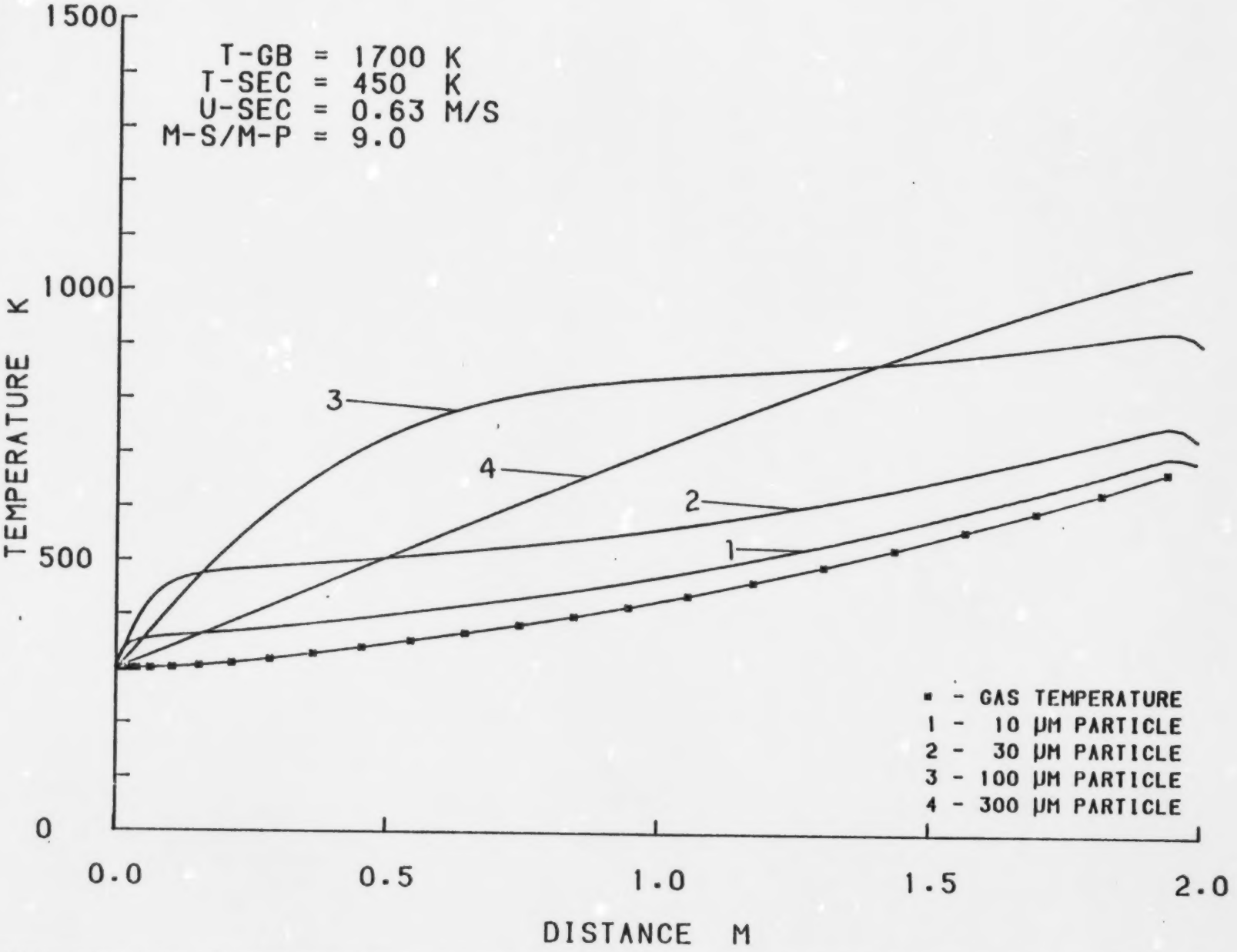

Figure 58: Particle Heating - Tgb=1700 K, Tinsec=450 K, M-S/M-P=9.0 - Coal Feed Rate = 1.0 g/min, Primary Mass Flow = 10.0 g/min, Secondary Mass Flow = 90.0 g/min

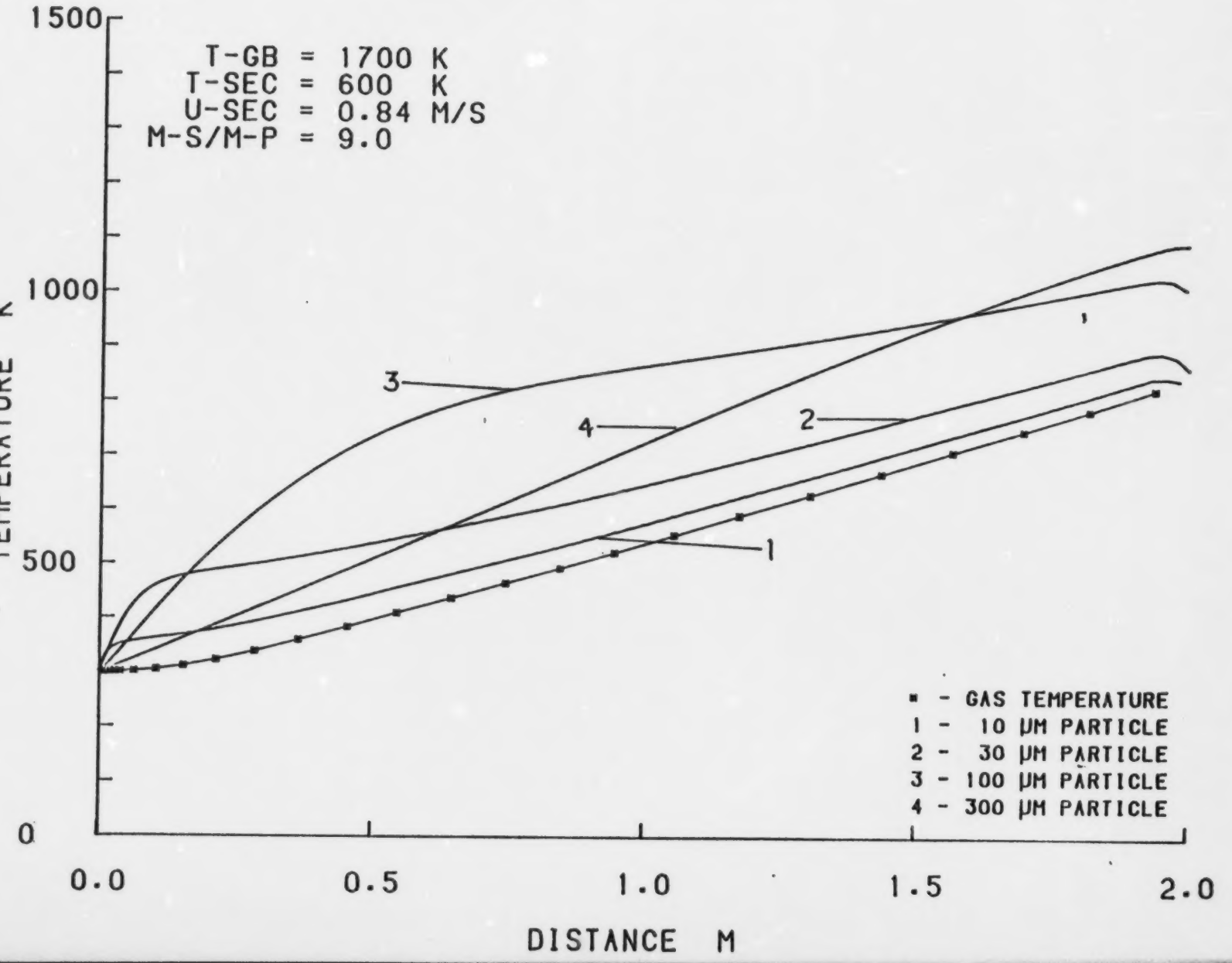

Figure 59: Particle Heating - Tgb=1700 K, Tinsec=600 K, M-S/M-P=9.0 - Coal Feed Rate = 1.0 g/min, Primary Mass Flow = 10.0 g/min, Secondary Mass Flow = 90.0 g/min

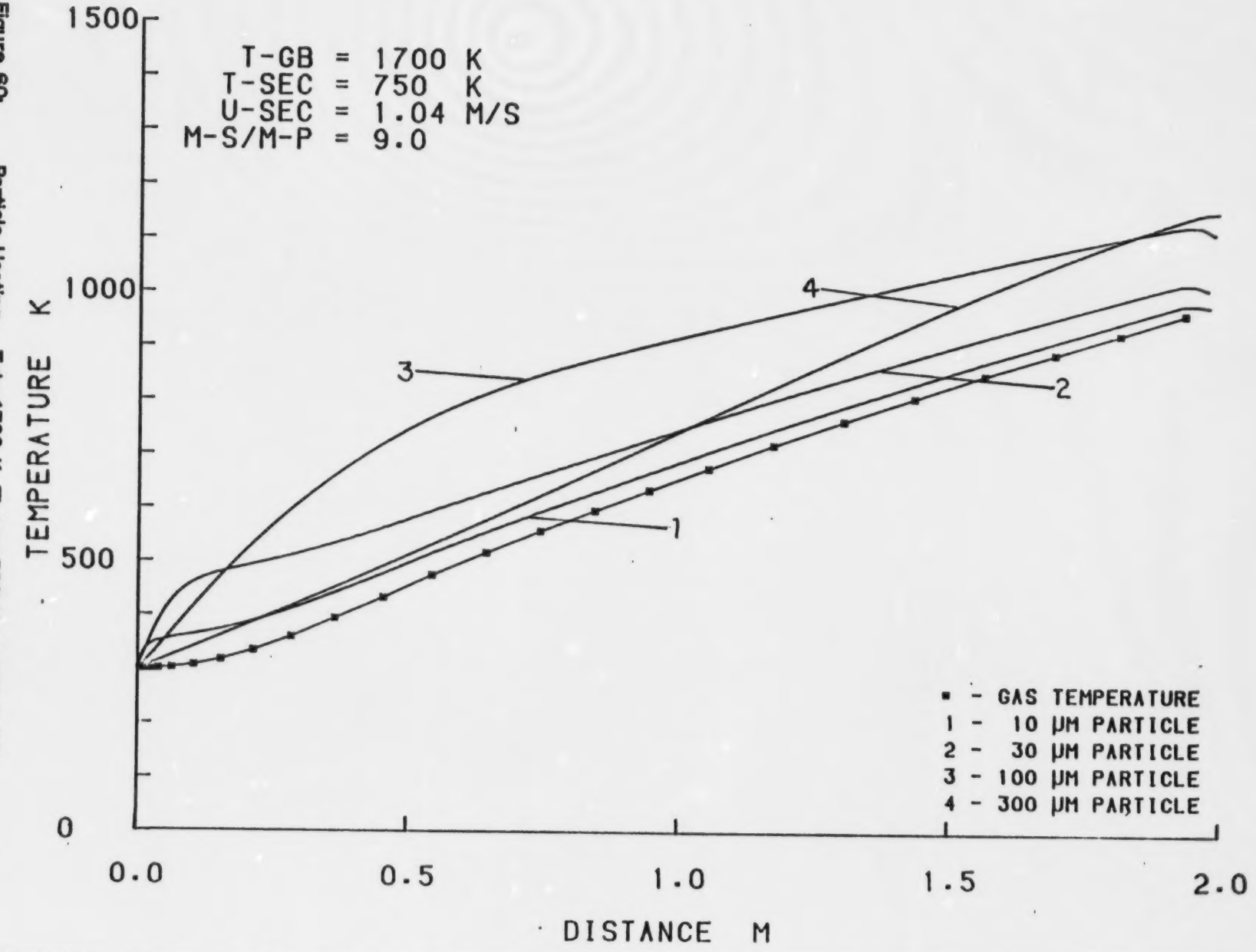

Figure 60: Particle Heating - Tgb=1700 K, Tinsec=750 K, M-S/M-P=9.0 - Coal Feed Rate = 1.0 g/min, Primary Mass Flow = 10.0 g/min, Secondary Mass Flow = 90.0 g/min

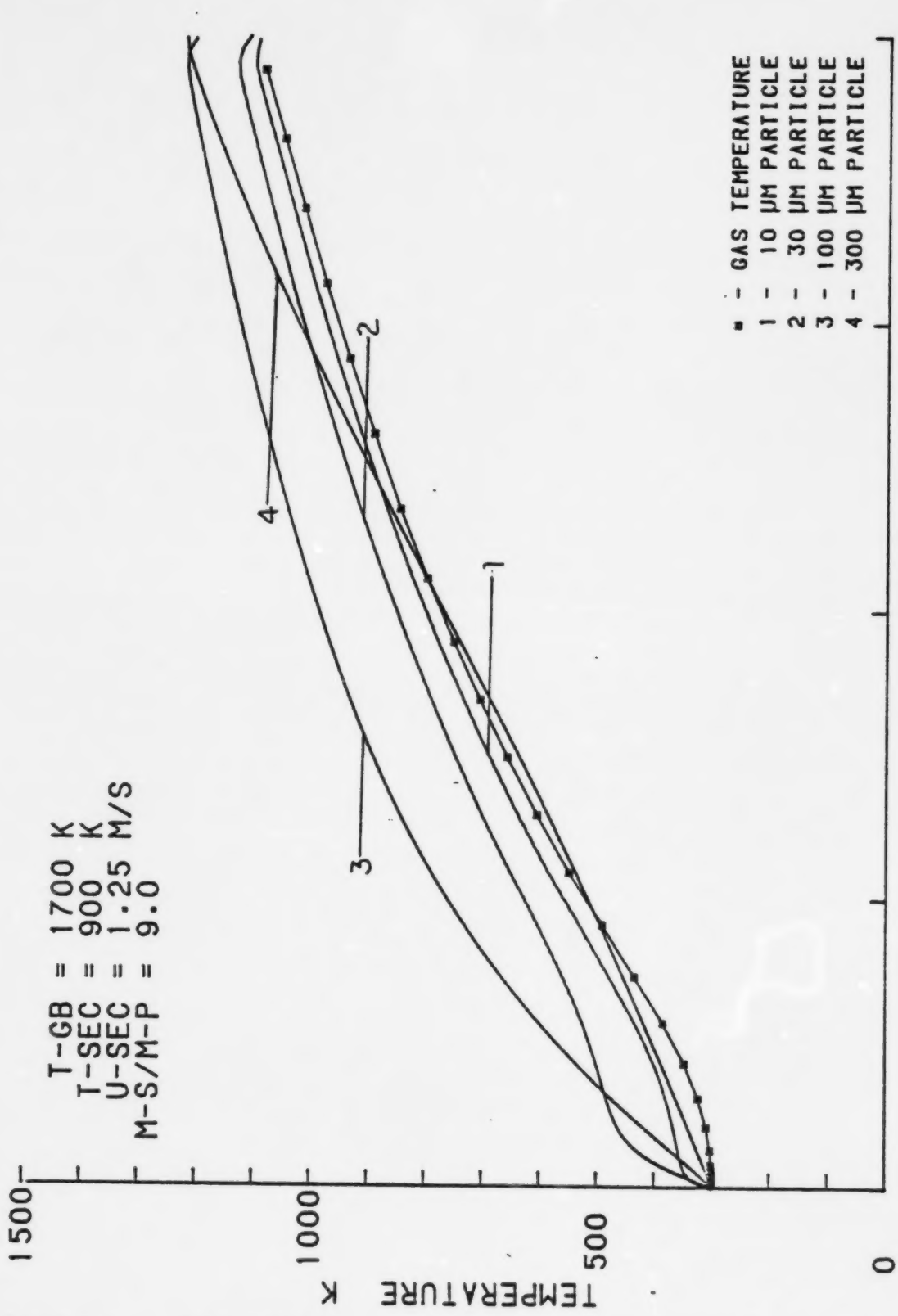

Figure 61: Particle Heating – Tgb=1700 K, Tinsec=900 K, M-S/M-P=9.0 – Coal Feed Rate = 1.0 g/min, Primary Mass Flow = 10.0 g/min, Secondary Mass Flow = 90.0 g/min

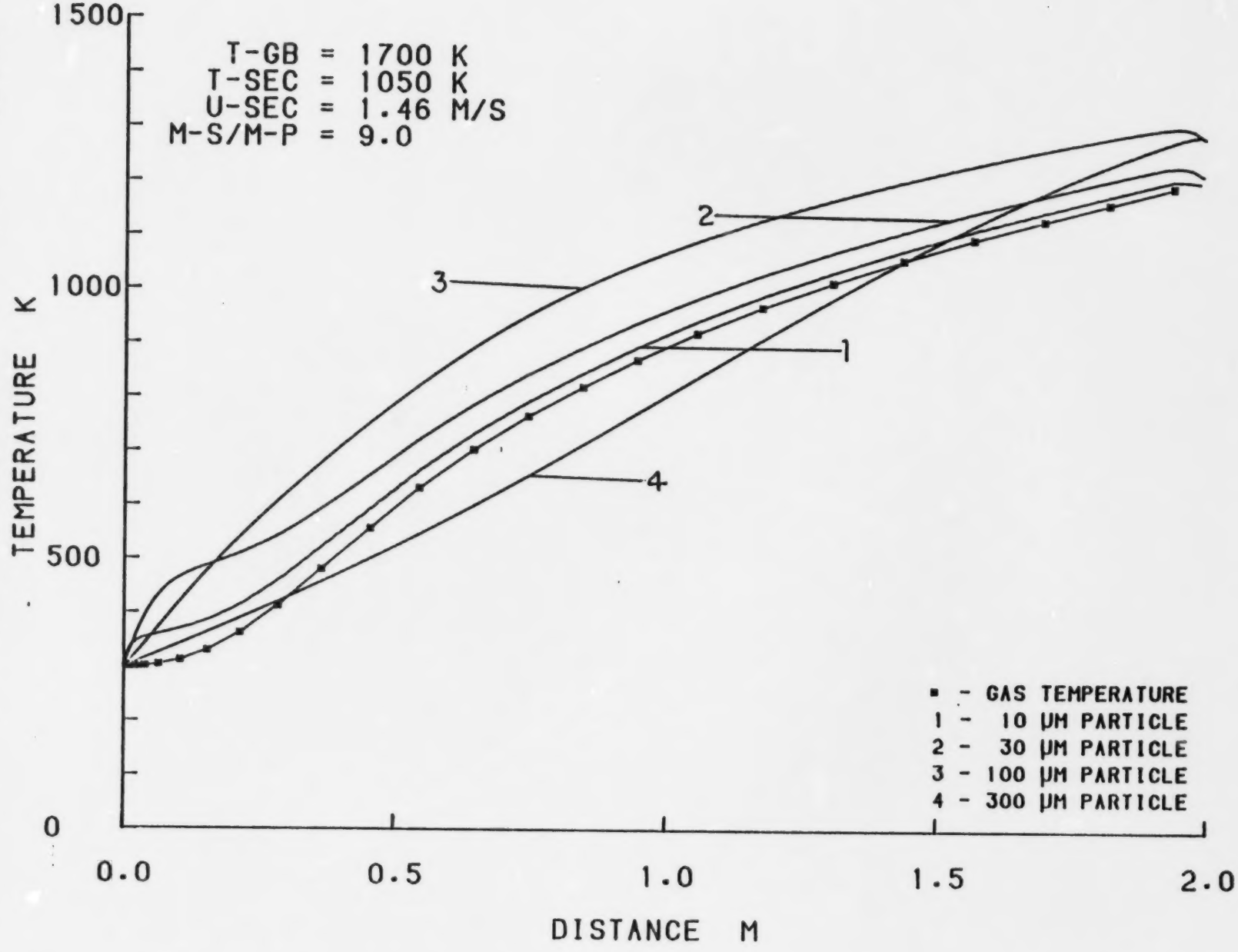

Figure 62: Particle Heating - Tgb=1700 K, Tinsec=1050 K, M-S/M-P=9.0 - Coal Feed Rate = 1.0 g/min, Primary Mass Flow = 10.0 g/min, Secondary Mass Flow = 90.0 g/min

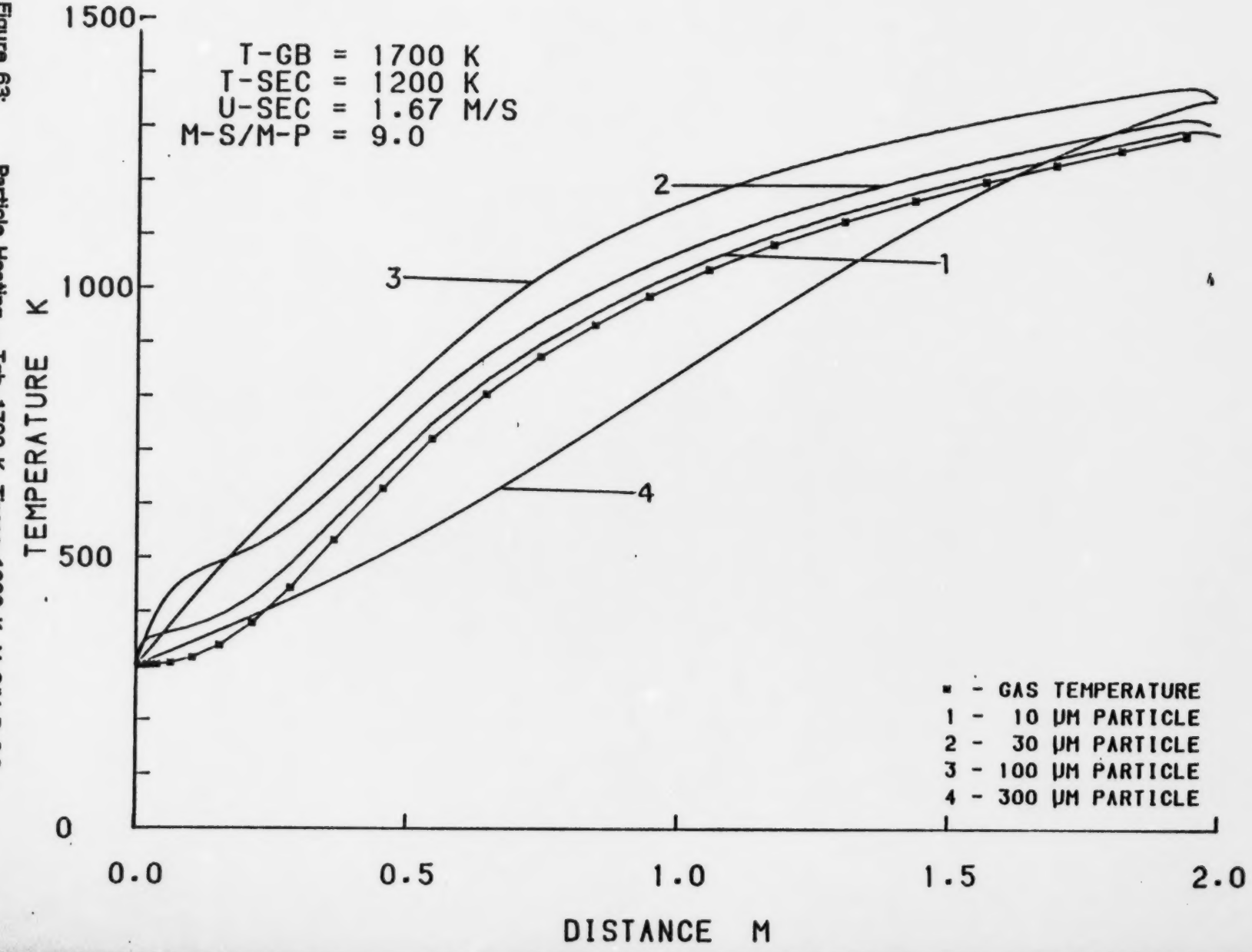

Figure 63: Particle Heating - Tgb=1700 K, Tinsec=1200 K, M-S/M-P=9.0 - Coal Feed Rate = 1.0 g/min, Primary Mass Flow = 10.0 g/min, Secondary Mass Flow = 90.0 g/min

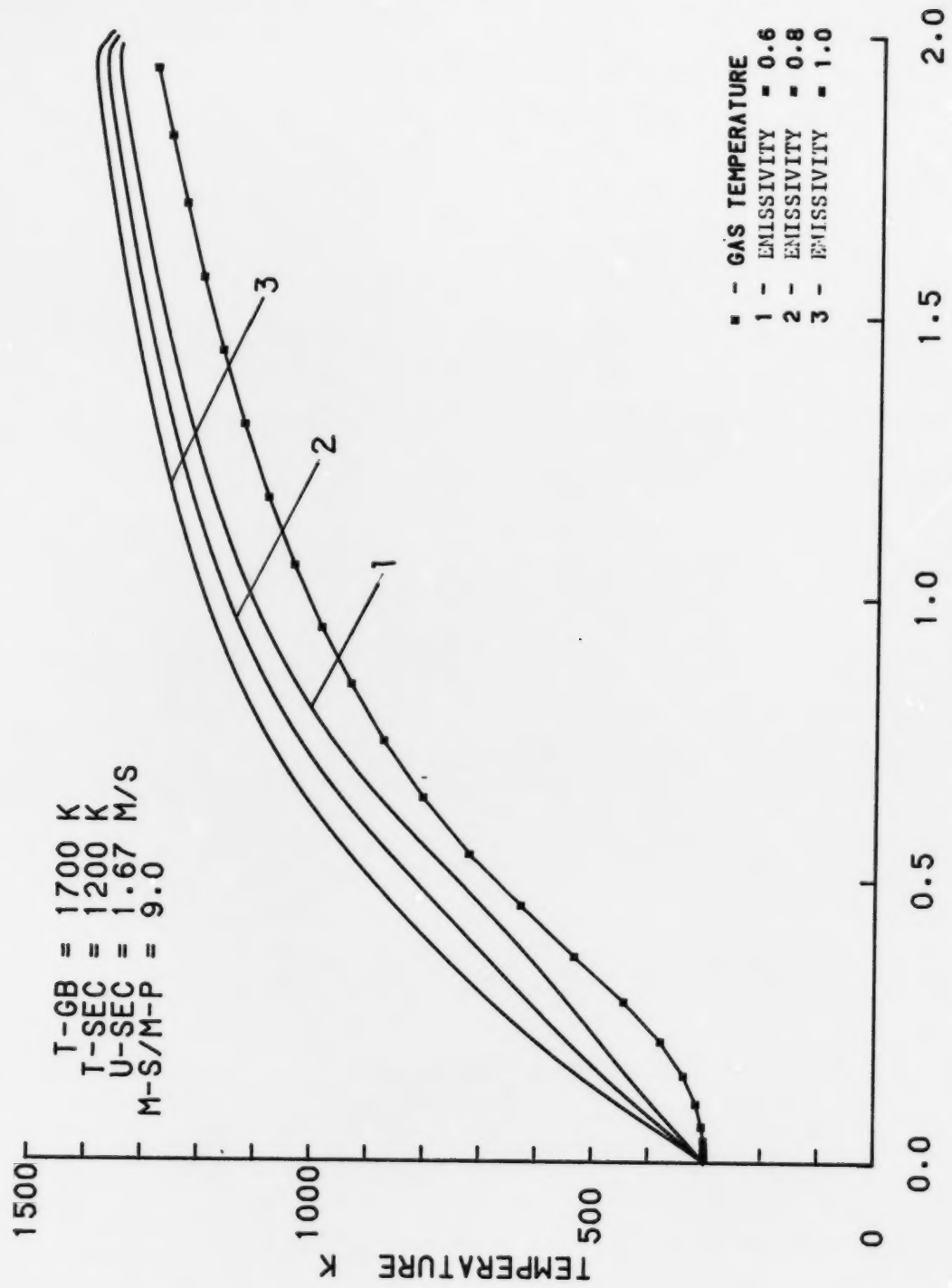

Figure 64: Effect of Emissivity on Particle Heating – Comparison of Heating for a 100 μm Particle with Various Emissivities

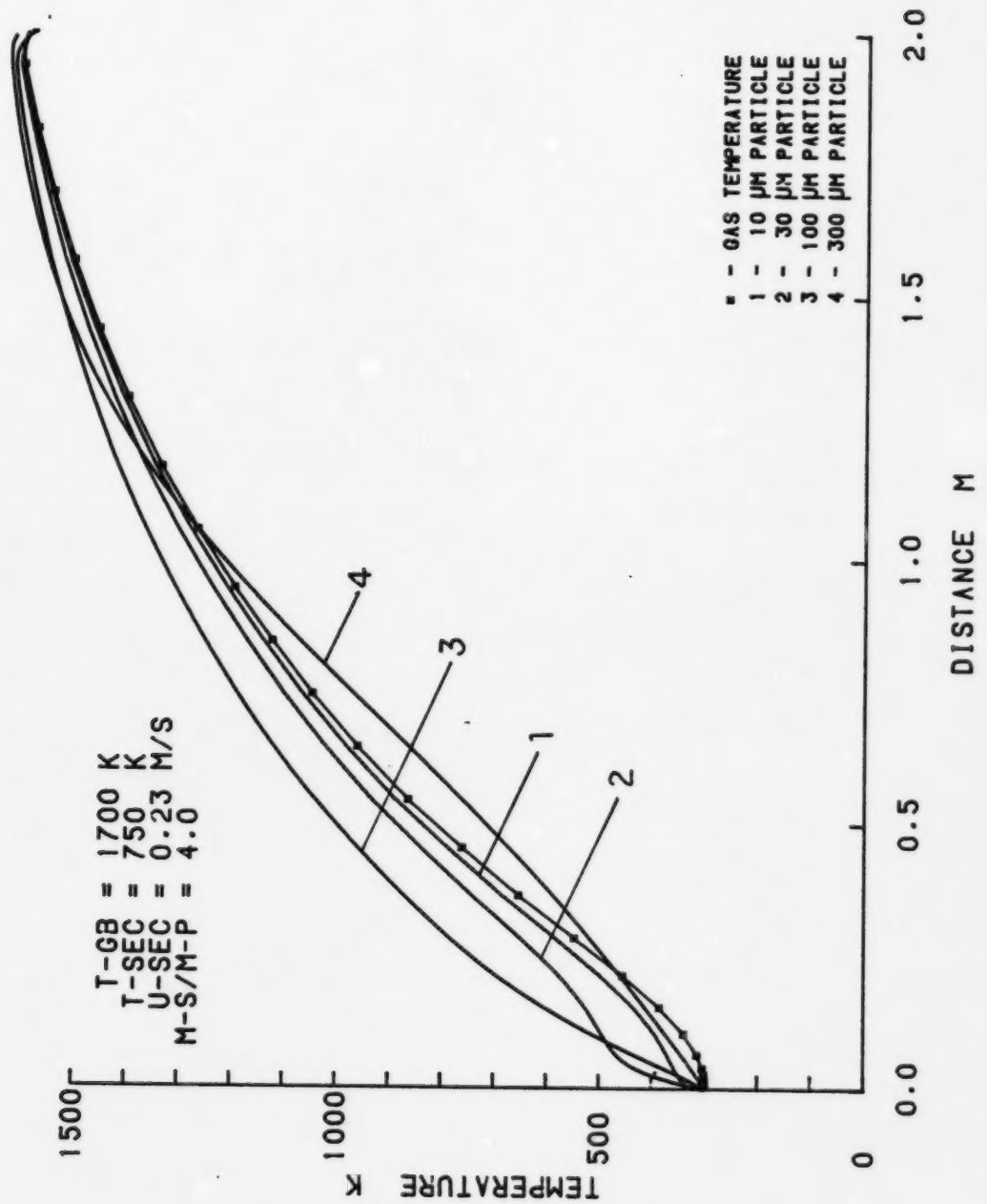

Figure 65: Particle Heating, Coal = 0.5 g/min, 1700 / 750 / 4.0 – (Glow Bar Temp./Secondary Inlet Temp./M-S/M-P), Primary Mass Flow = 5.0 g/min, Secondary Mass Flow = 20.0 g/min

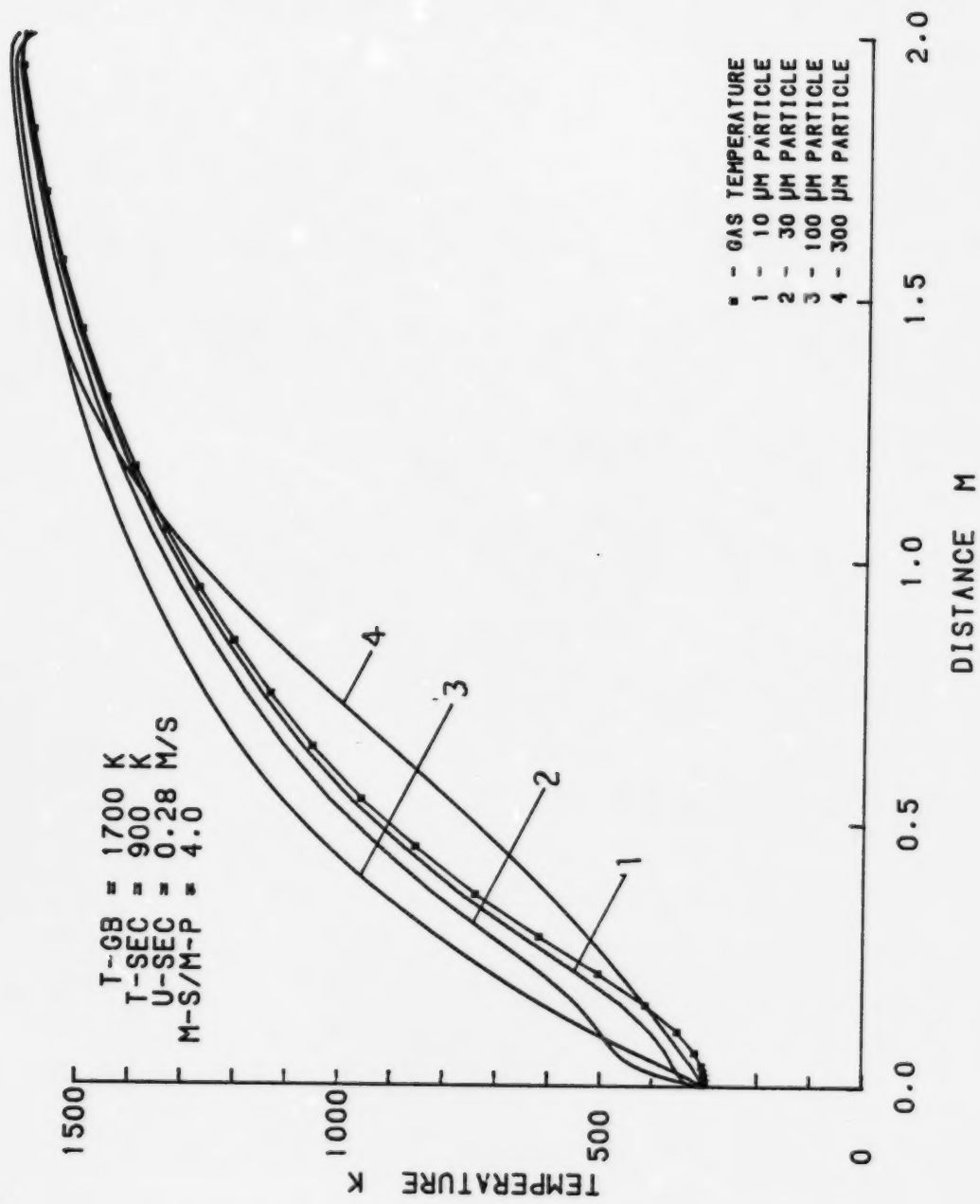

Figure 66: Particle Heating, Coal = 0.5 g/min, 1700 / 900 / 4.0 – (Glow Bar Temp./Secondary Inlet Temp./M-S/M-P), Primary Mass Flow = 5.0 g/min, Secondary Mass Flow = 20.0 g/min

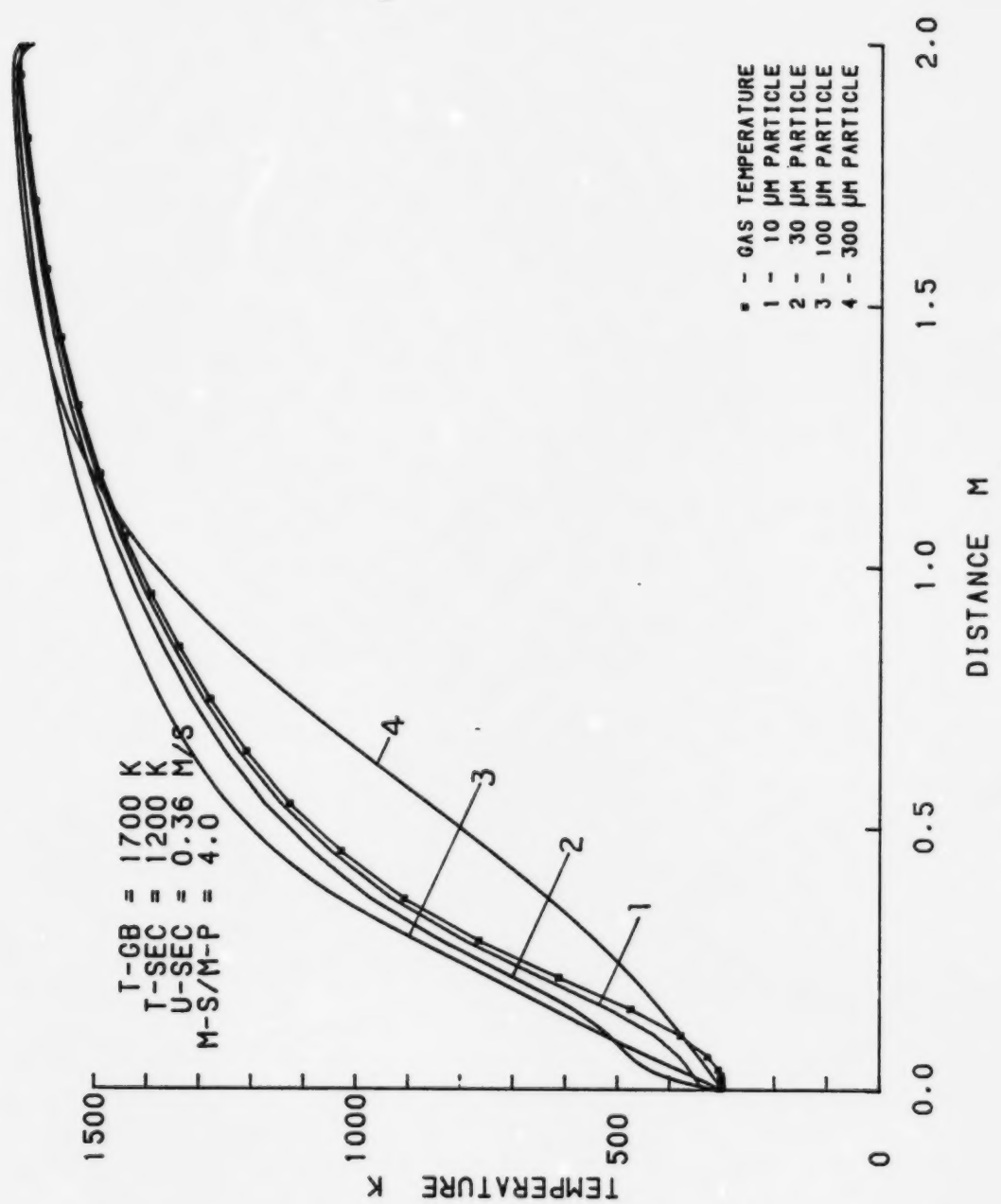

Figure 67: Particle Heating, Coal = 0.5 g/min, 1700 / 1200 / 4.0 – (Glow Bar Temp./Secondary Inlet Temp./M-S/M-P), Primary Mass Flow = 5.0 g/min, Secondary Mass Flow = 20.0 g/min

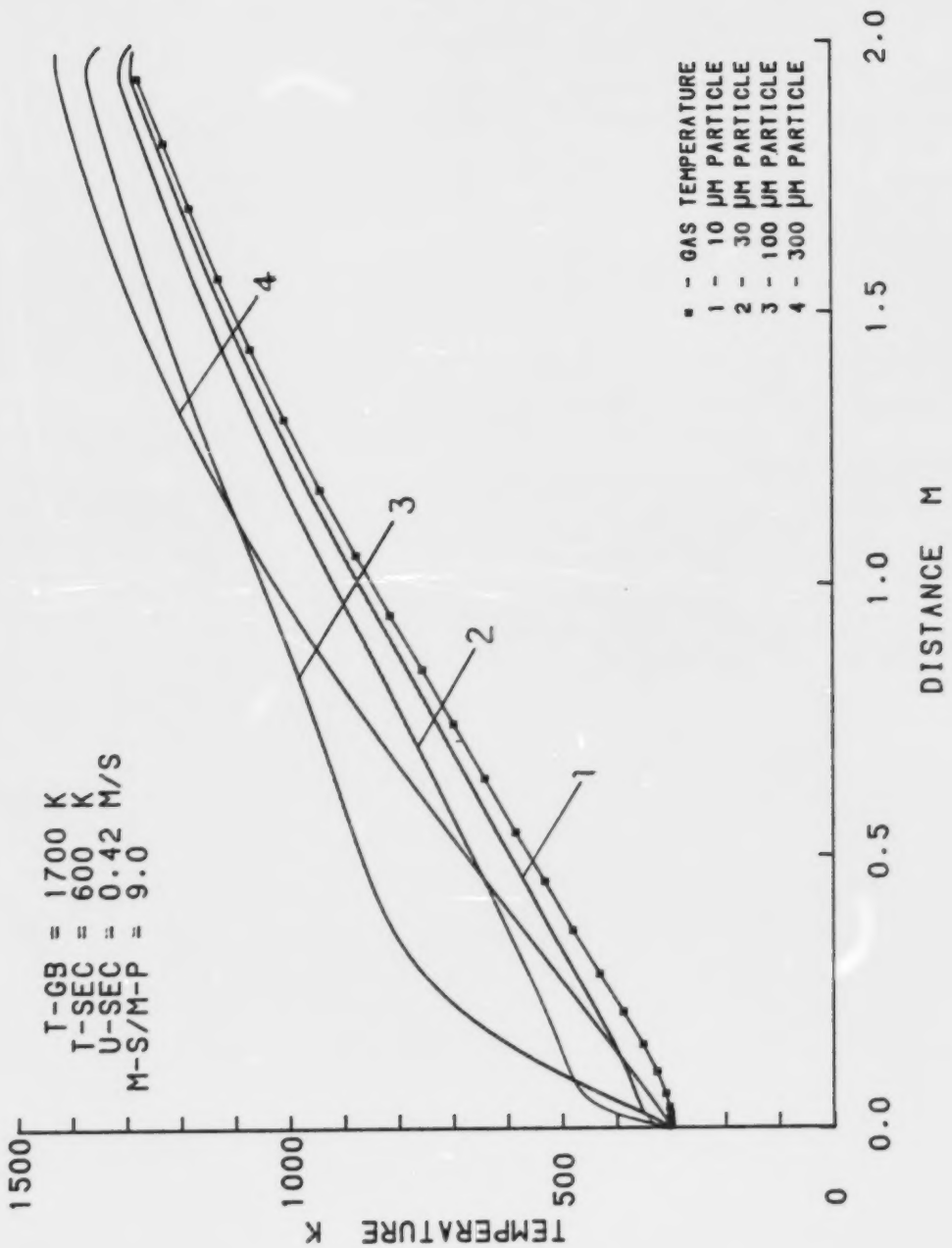

Figure 68: Particle Heating, Coal = 0.5 g/min, 1700 / 600 / 9.0 – (Glow Bar Temp./Secondary Inlet Temp./M–S/M–P), Primary Mass Flow = 5.0 g/min, Secondary Mass Flow = 45.0 g/min

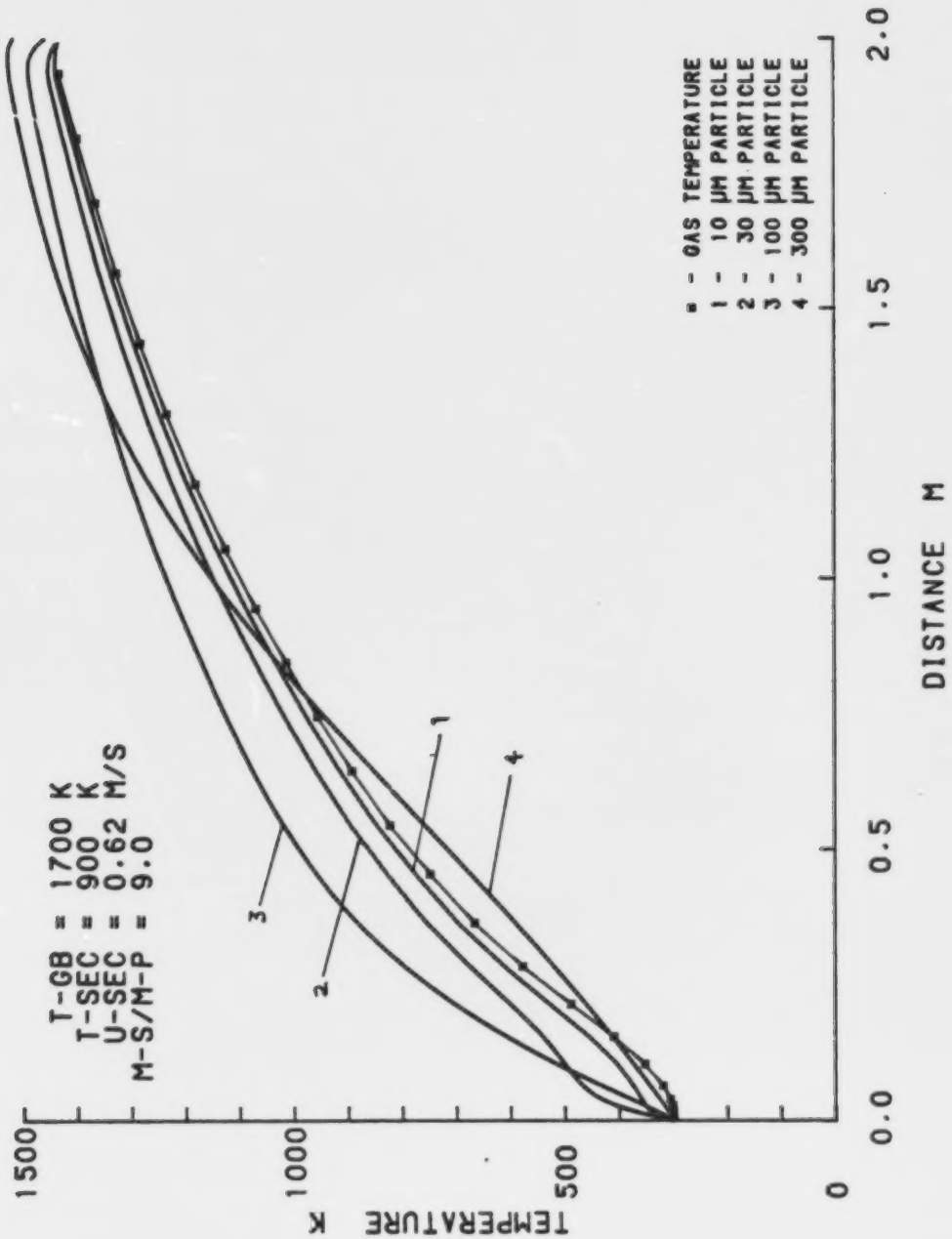

Figure 69: Particle Heating, Coal = 0.5 g/min, 1700 / 900 / 9.0 – (Glow Bar Temp./Secondary Inlet Temp./M–S/M–P), Primary Mass Flow = 5.0 g/min, Secondary Mass Flow = 45.0 g/min

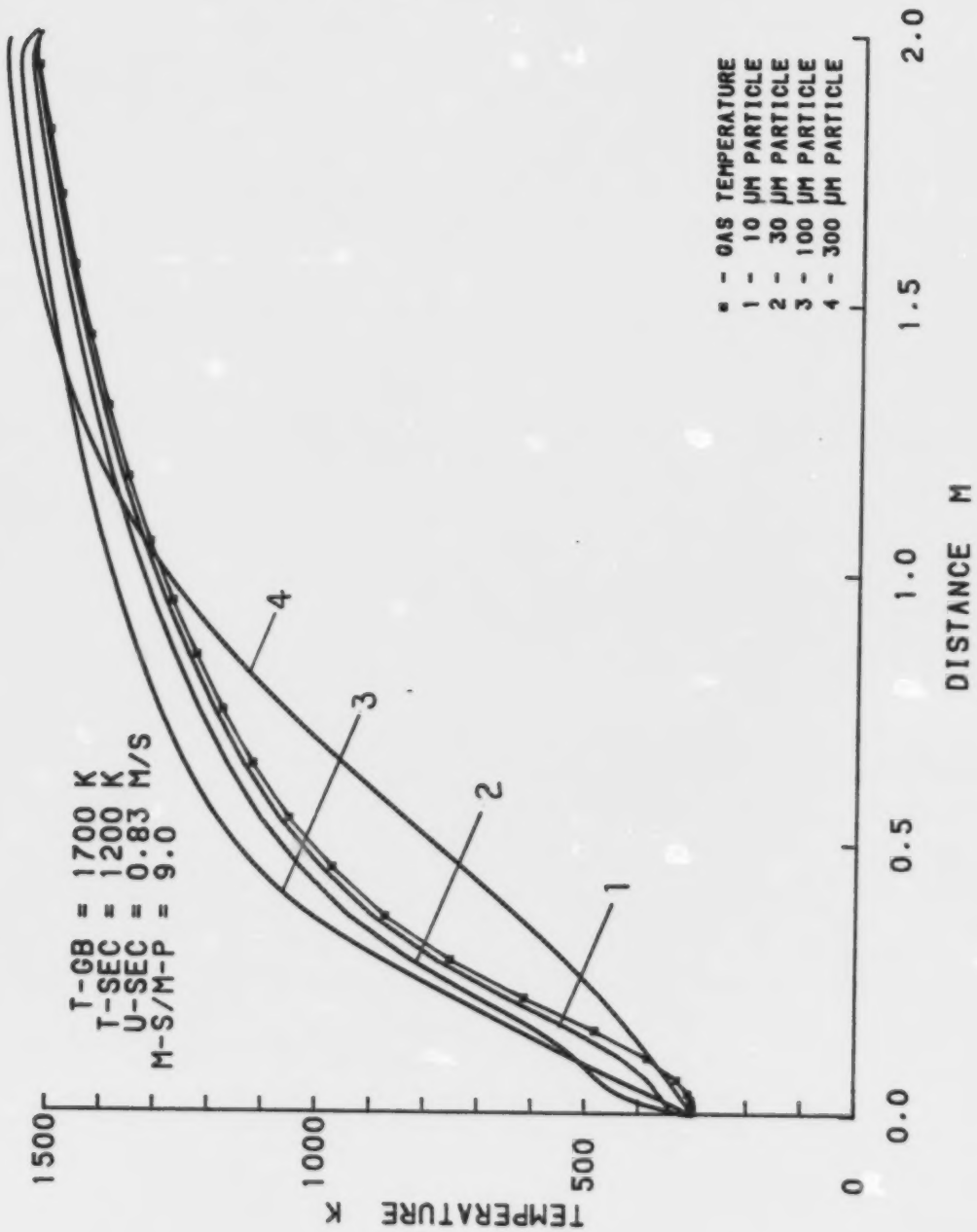

Figure 70: Particle Heating, Coal = 0.5 g/min, 1700 / 1200 / 9.0 – (Glow Bar Temp./Secondary Inlet Temp./M-S/M-P), Primary Mass Flow = 5.0 g/min, Secondary Mass Flow = 45.0 g/min

Figure 71: Particle Heating – Tgb=1400 K, Tinsec=900 K, M-S/M-P=4.0 – Coal Feed Rate = 1.0 g/min, Primary Mass Flow = 10.0 g/min, Secondary Mass Flow = 40.0 g/min

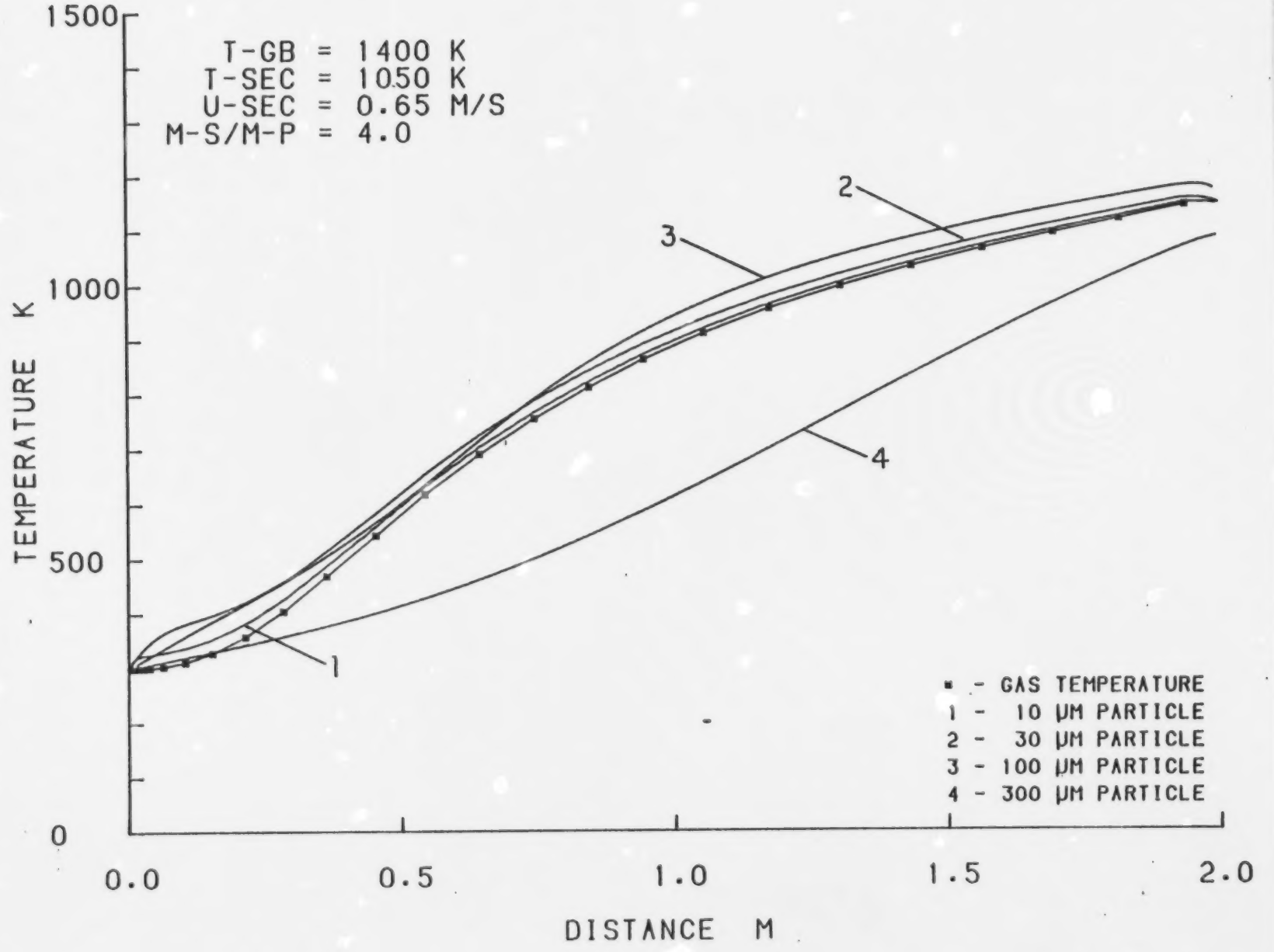

Figure 72: Particle Heating - Tgb=1400 K, Tinsec=1050 K, M-S/M-P=4.0 - Coal Feed Rate = 1.0 g/min, Primary Mass Flow = 10.0 g/min, Secondary Mass Flow = 40.0 g/min

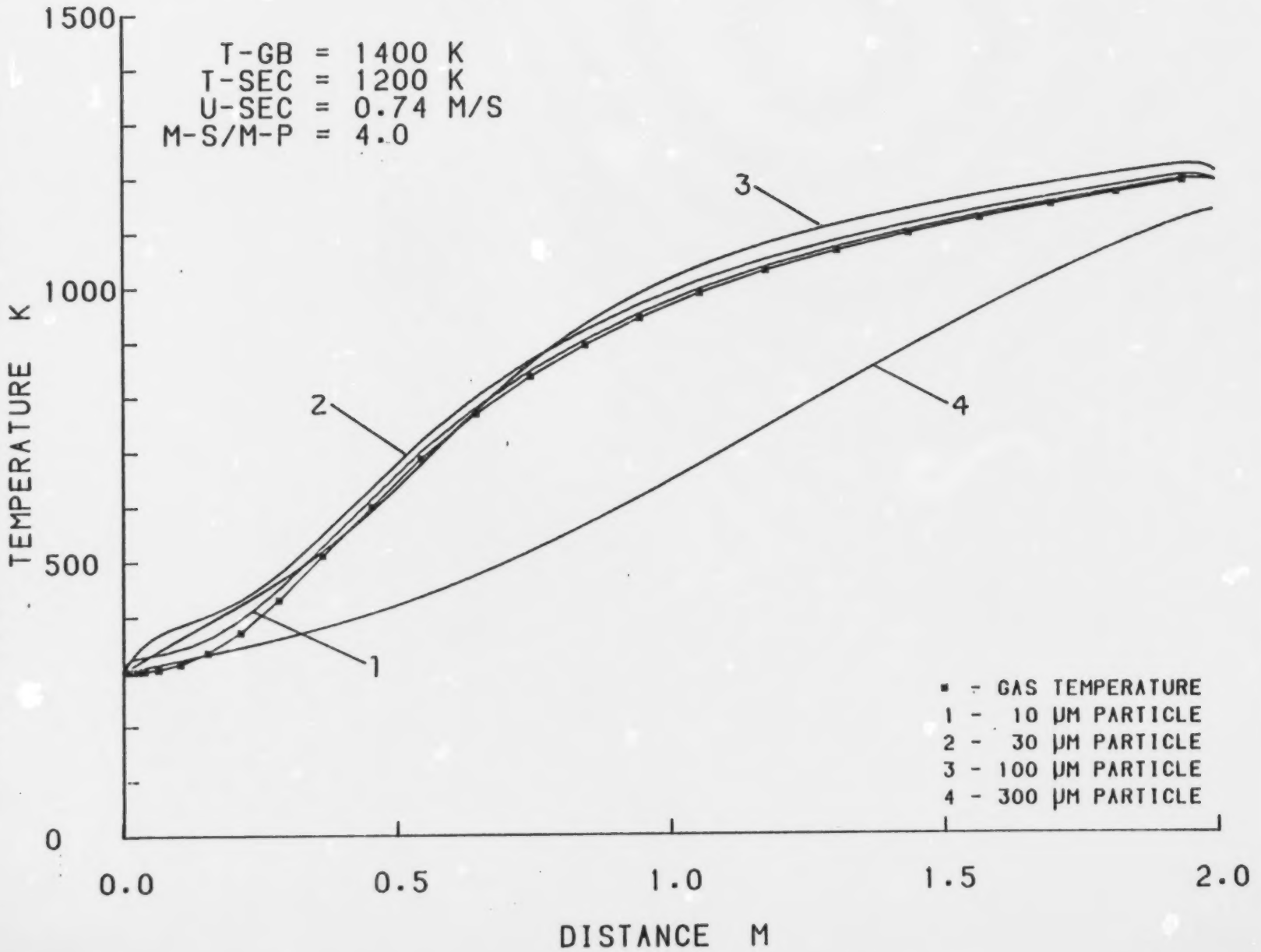

Figure 73: Particle Heating - Tgb=1400 K, Tinsec=1200 K, M-S/M-P=4.0 - Coal Feed Rate = 1.0 g/min, Primary Mass Flow = 10.0 g/min, Secondary Mass Flow = 40.0 g/min

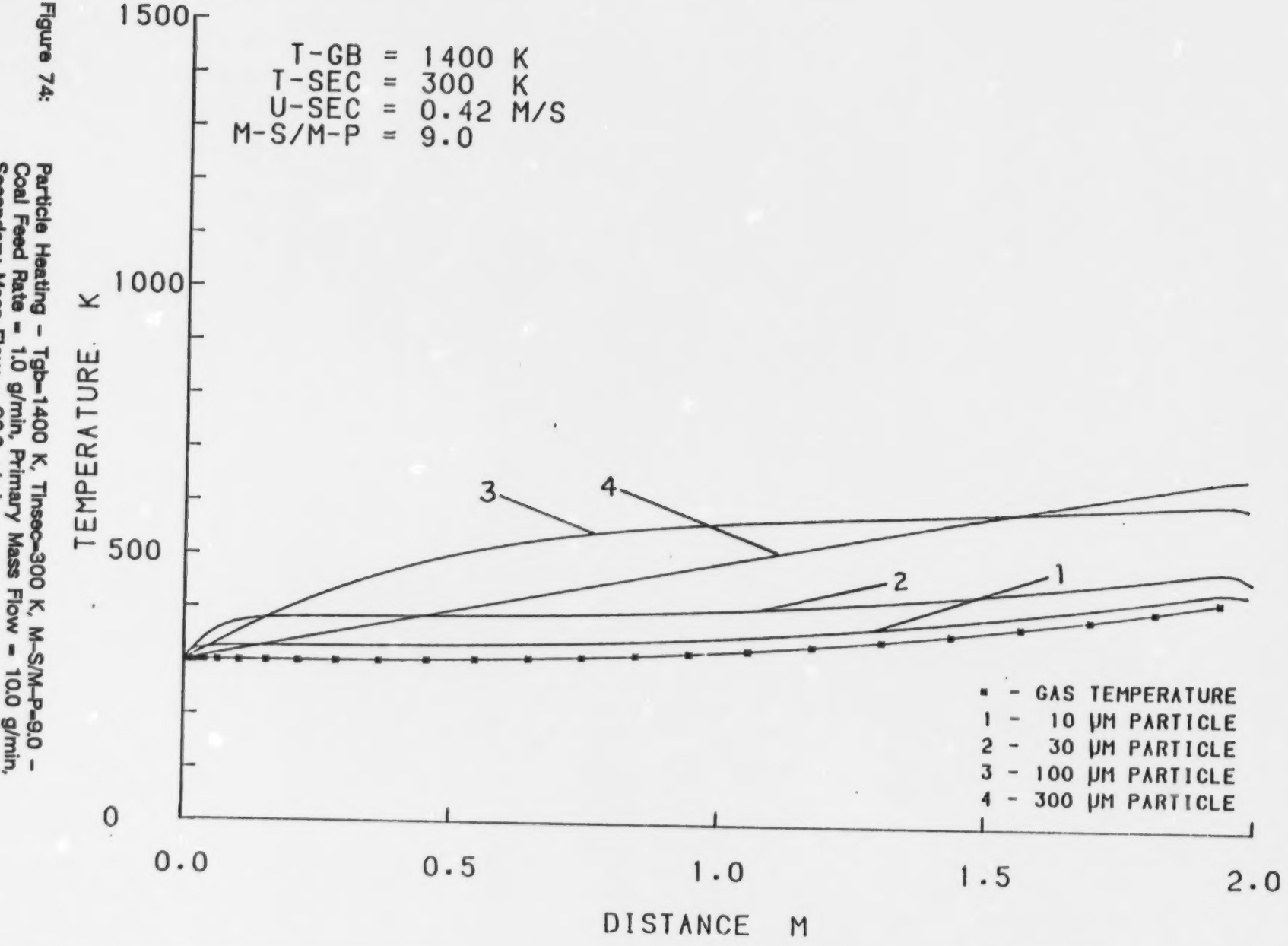

Figure 74: Particle Heating - Tgb=1400 K, Tinsec=300 K, M-S/M-P=9.0 - Coal Feed Rate = 1.0 g/min, Primary Mass Flow = 10.0 g/min, Secondary Mass Flow = 90.0 g/min

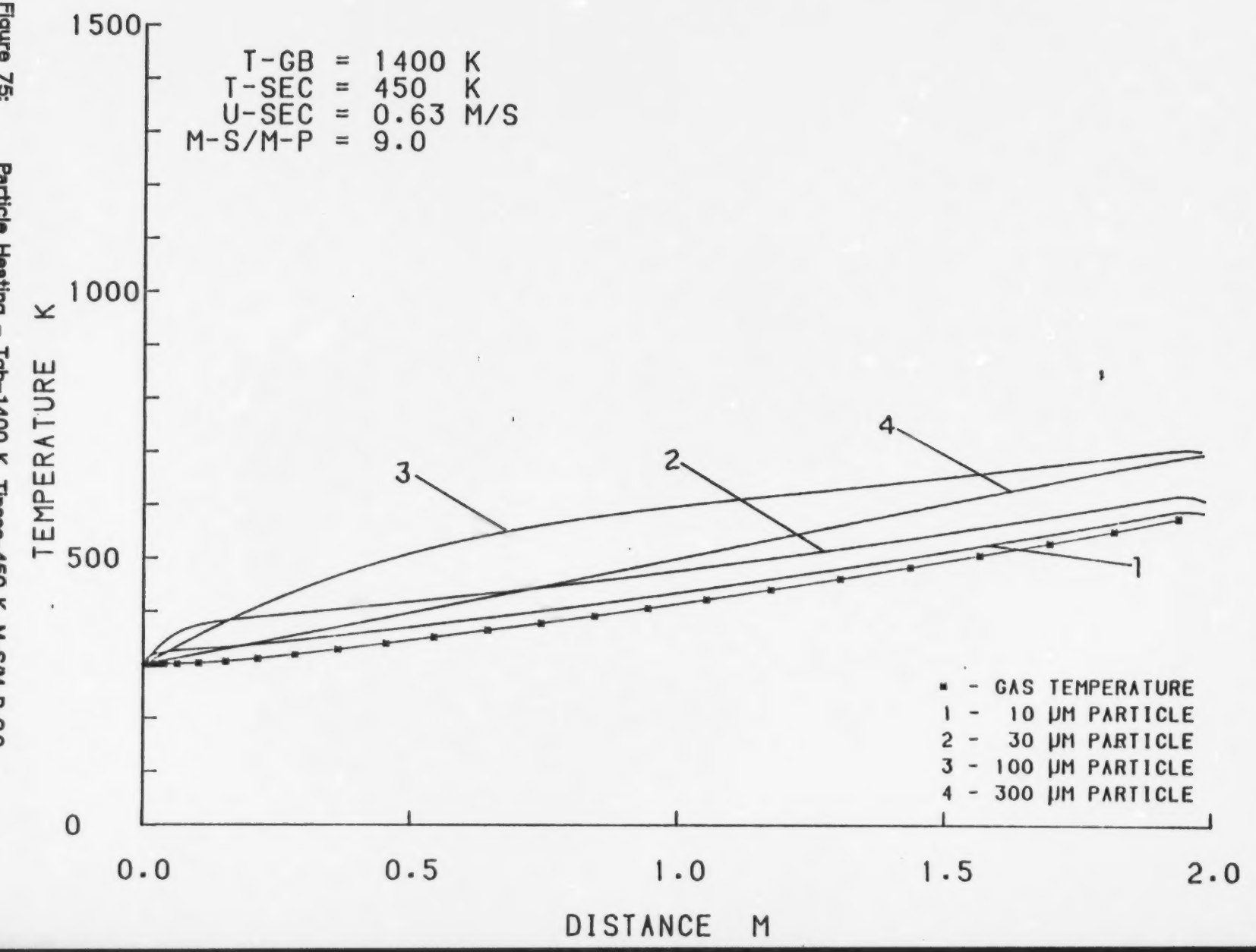

Figure 75: Particle Heating - Tgb=1400 K, Tinsec=450 K, M-S/M-P=9.0 - Coal Feed Rate = 1.0 g/min, Primary Mass Flow = 10.0 g/min, Secondary Mass Flow = 90.0 g/min

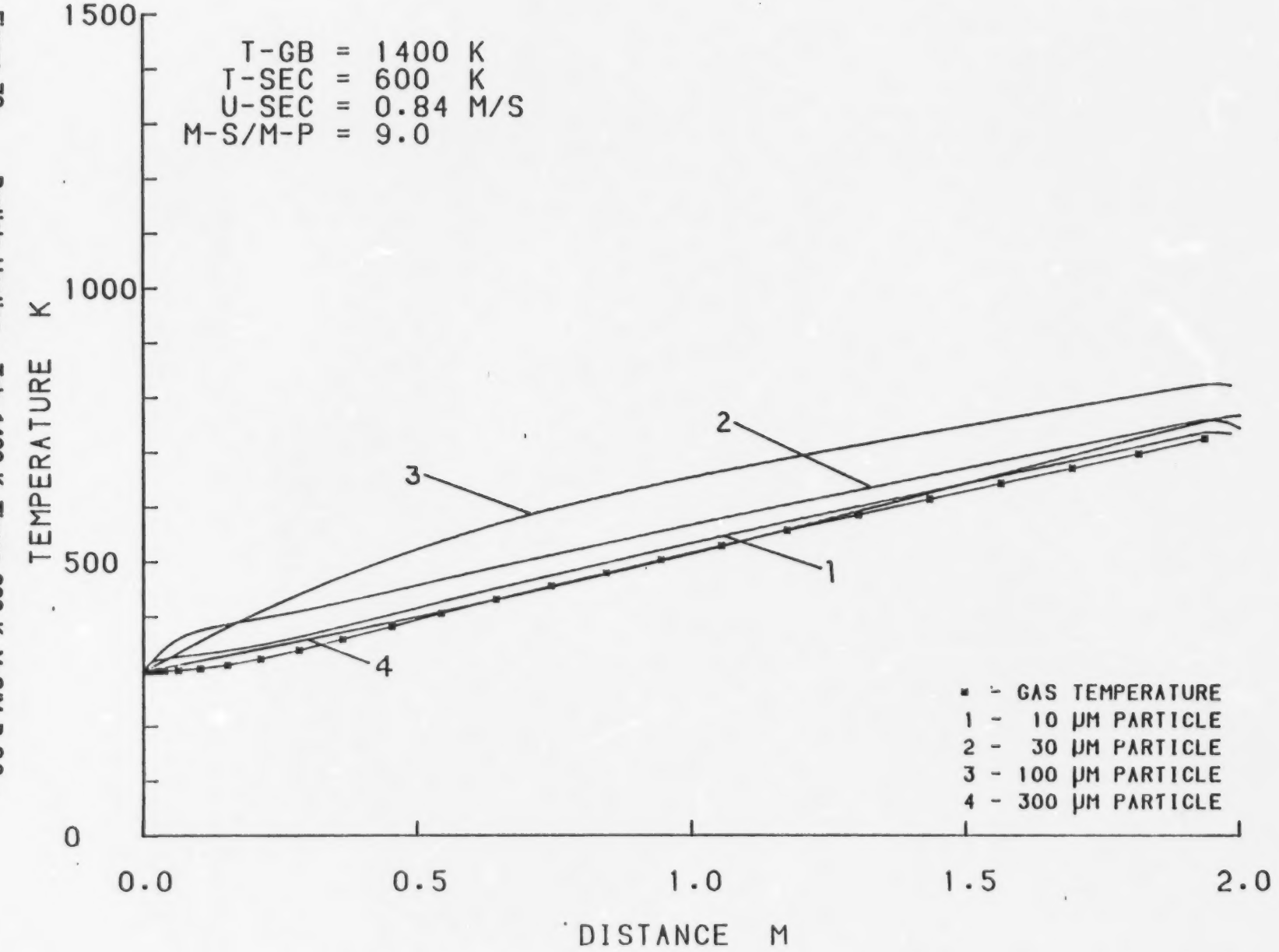

Figure 76: Particle Heating - Tgb=1400 K, Tinsec=600 K, M-S/M-P=9.0 - Coal Feed Rate = 1.0 g/min, Primary Mass Flow = 10.0 g/min, Secondary Mass Flow = 90.0 g/min

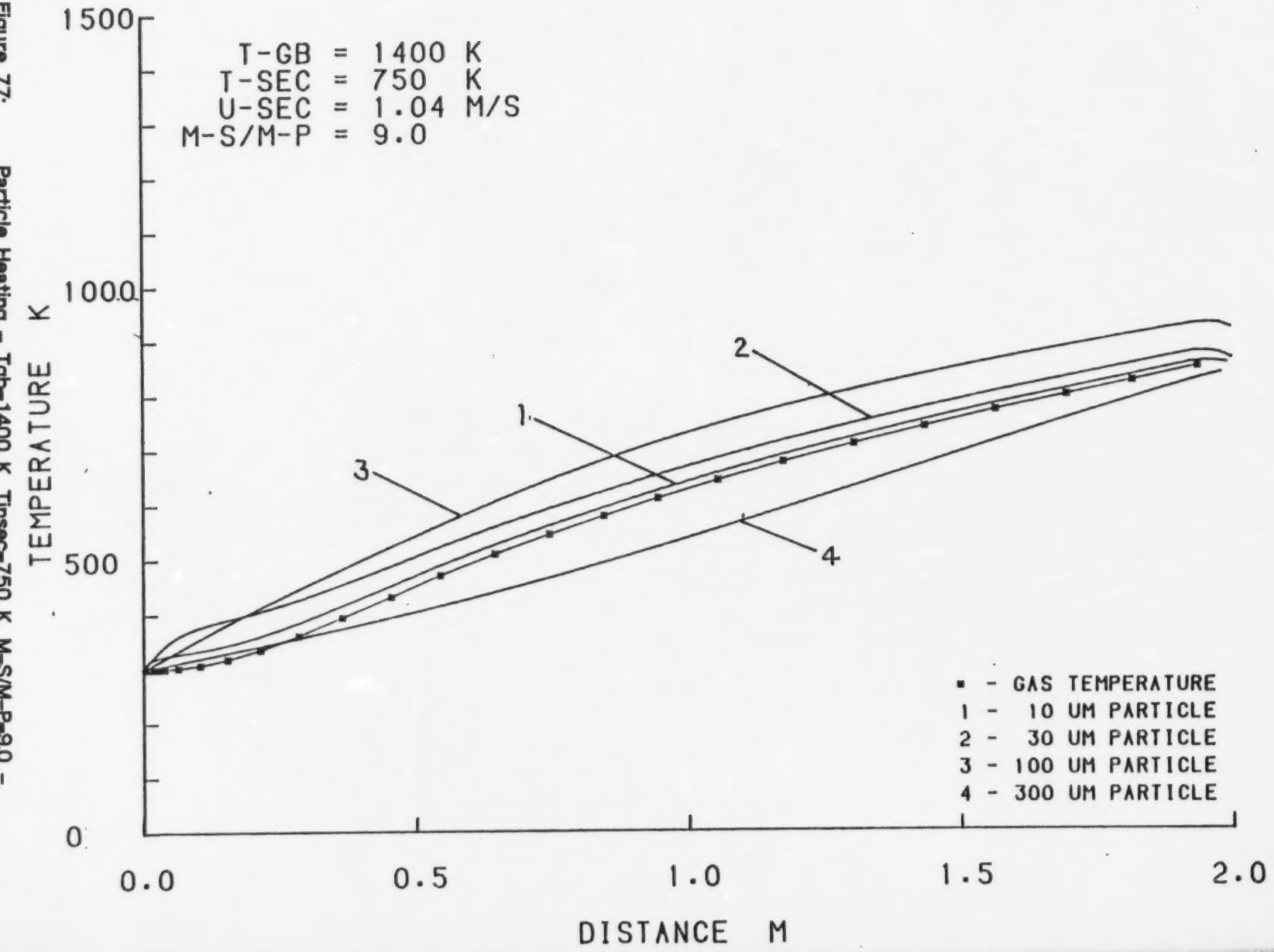

Figure 77: Particle Heating - Tgb=1400 K, Tinsec=750 K, M-S/M-P=9.0 - Coal Feed Rate = 1.0 g/min, Primary Mass Flow = 10.0 g/min, Secondary Mass Flow = 90.0 g/min

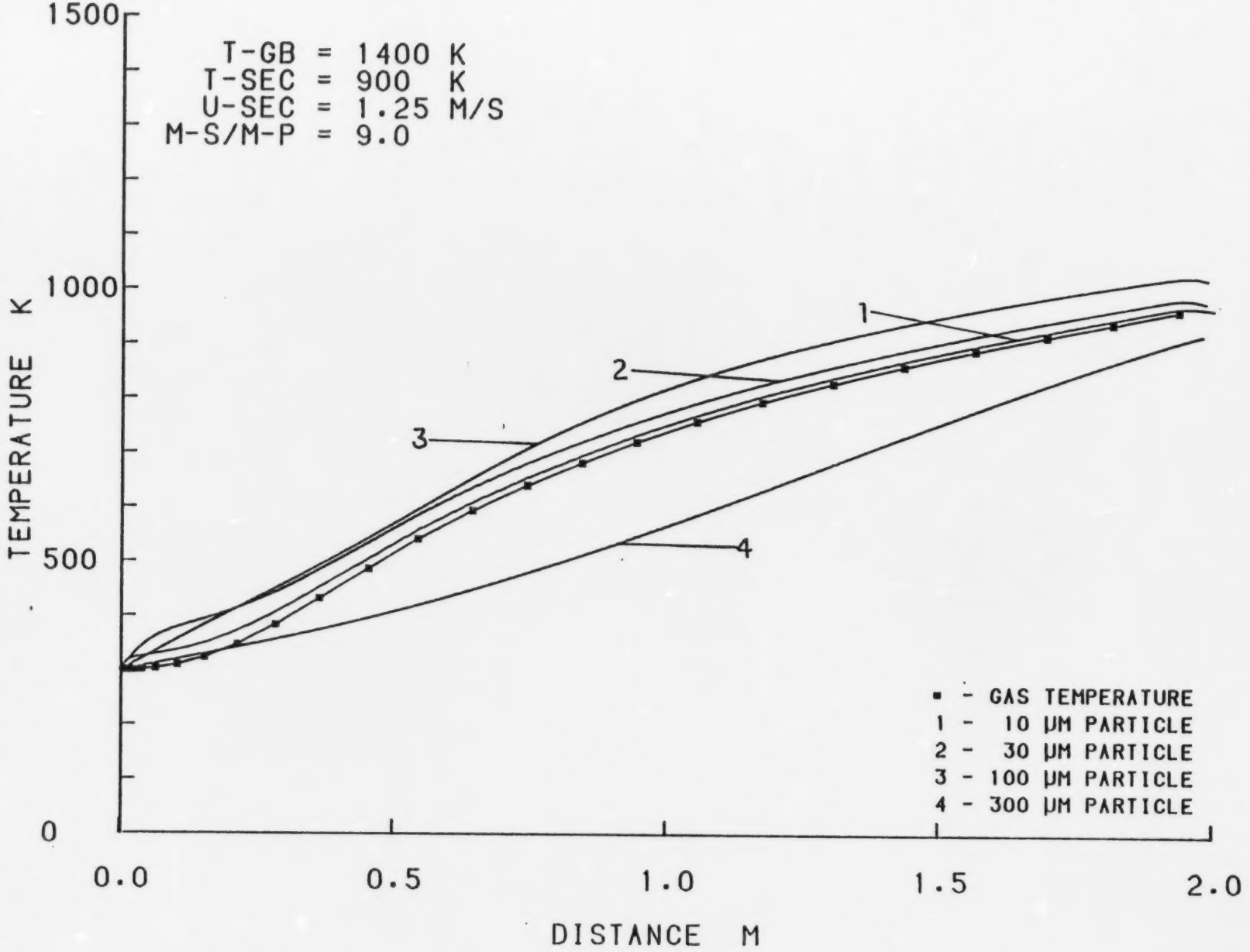

Figure 78: Particle Heating - Tgb=1400 K, Tinsec=900 K, M-S/M-P=9.0 - Coal Feed Rate = 1.0 g/min, Primary Mass Flow = 10.0 g/min, Secondary Mass Flow = 90.0 g/min

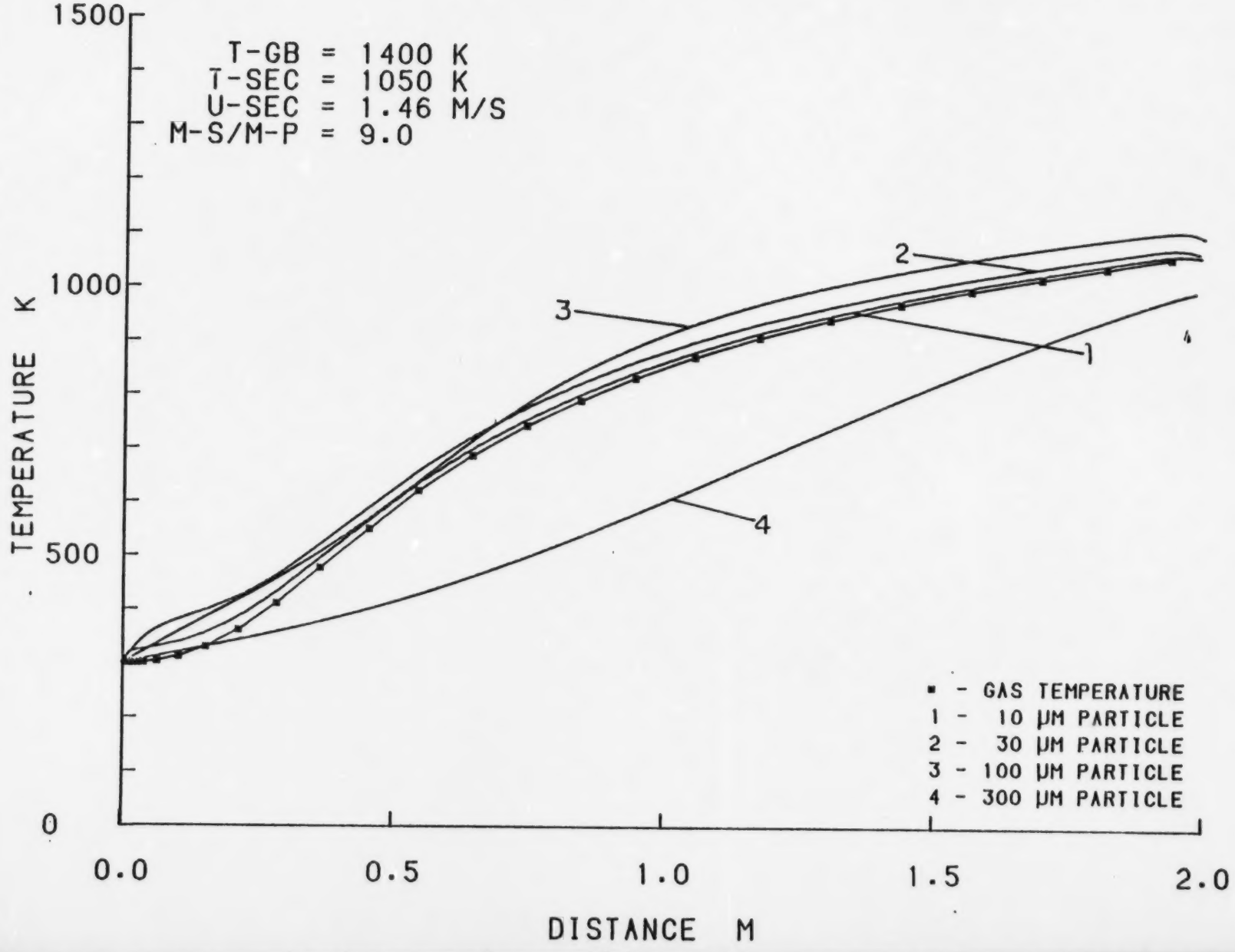

Figure 79: Particle Heating - Tgb=1400 K, Tinsec=1050 K, M-S/M-P=9.0 - Coal Feed Rate = 1.0 g/min, Primary Mass Flow = 10.0 g/min, Secondary Mass Flow = 90.0 g/min

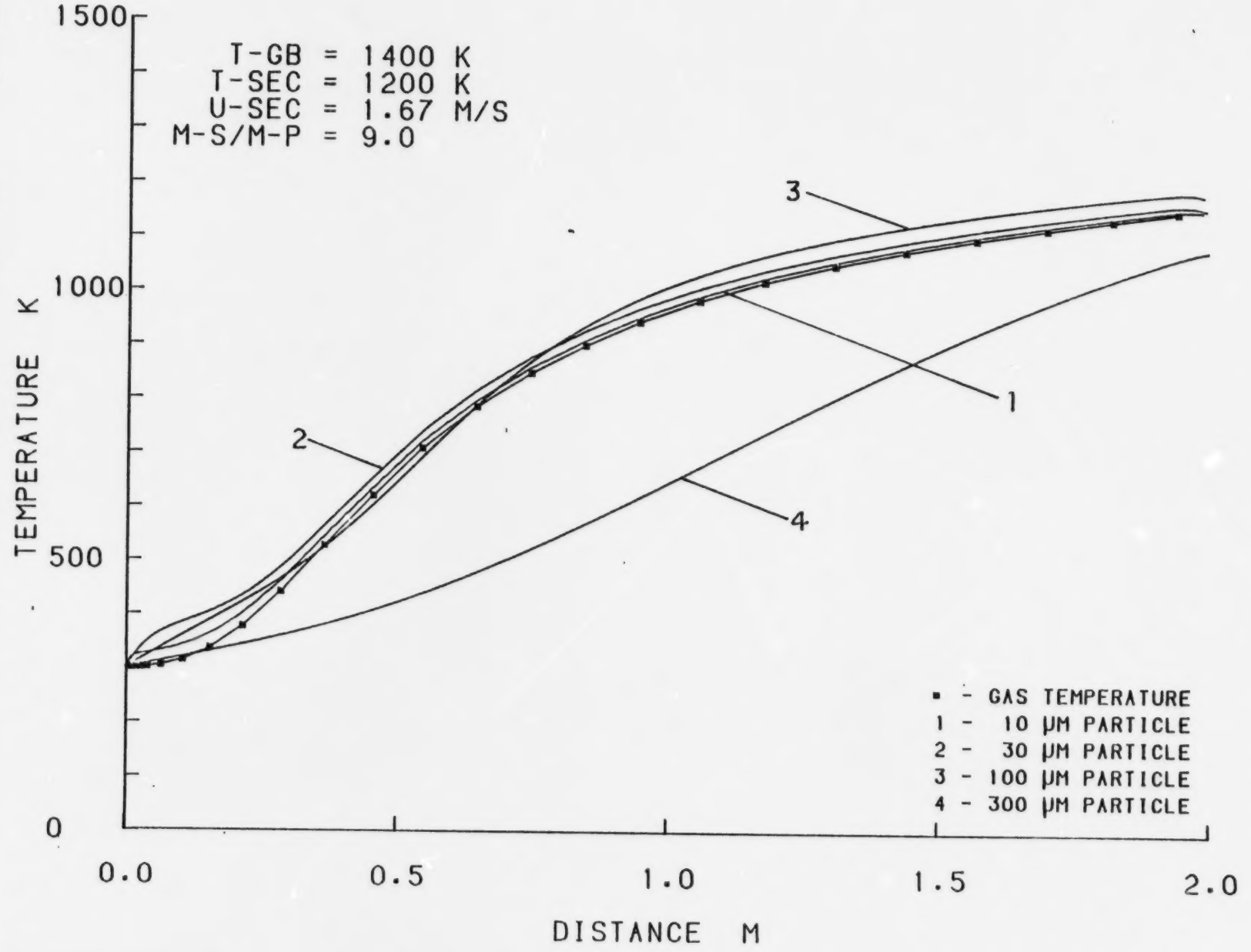

Figure 80: Particle Heating - Tgb=1400 K, Tinsec=1200 K, M-S/M-P=9.0 - Coal Feed Rate = 1.0 g/min, Primary Mass Flow = 10.0 g/min, Secondary Mass Flow = 90.0 g/min

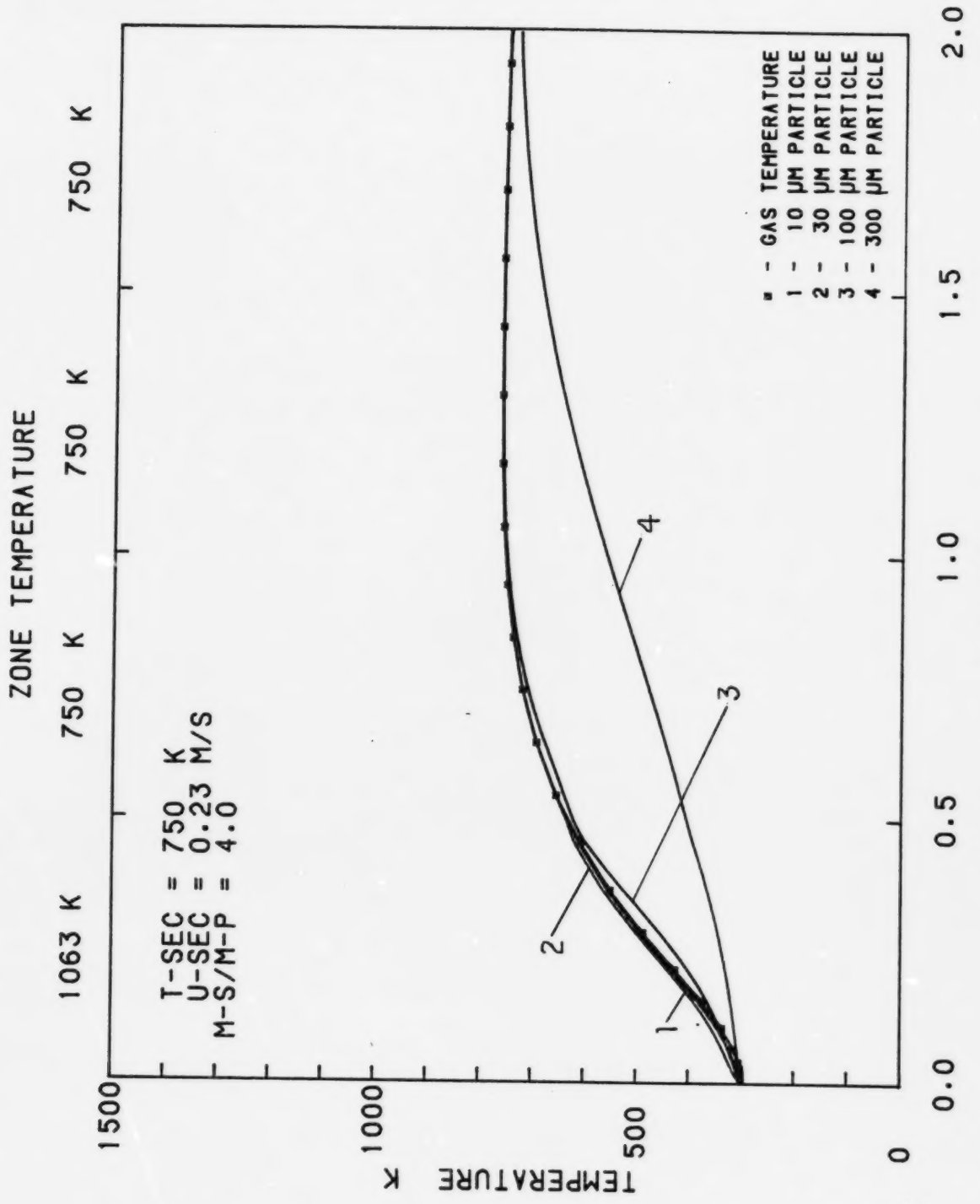

Figure 81: Variable Zone Temperature, Tinsec=750 K, M-S/M-P=4.0 – Coal Feed Rate = 0.5 g/min, Primary Mass Flow = 5.0 g/min, Secondary Mass Flow = 20.0 g/min

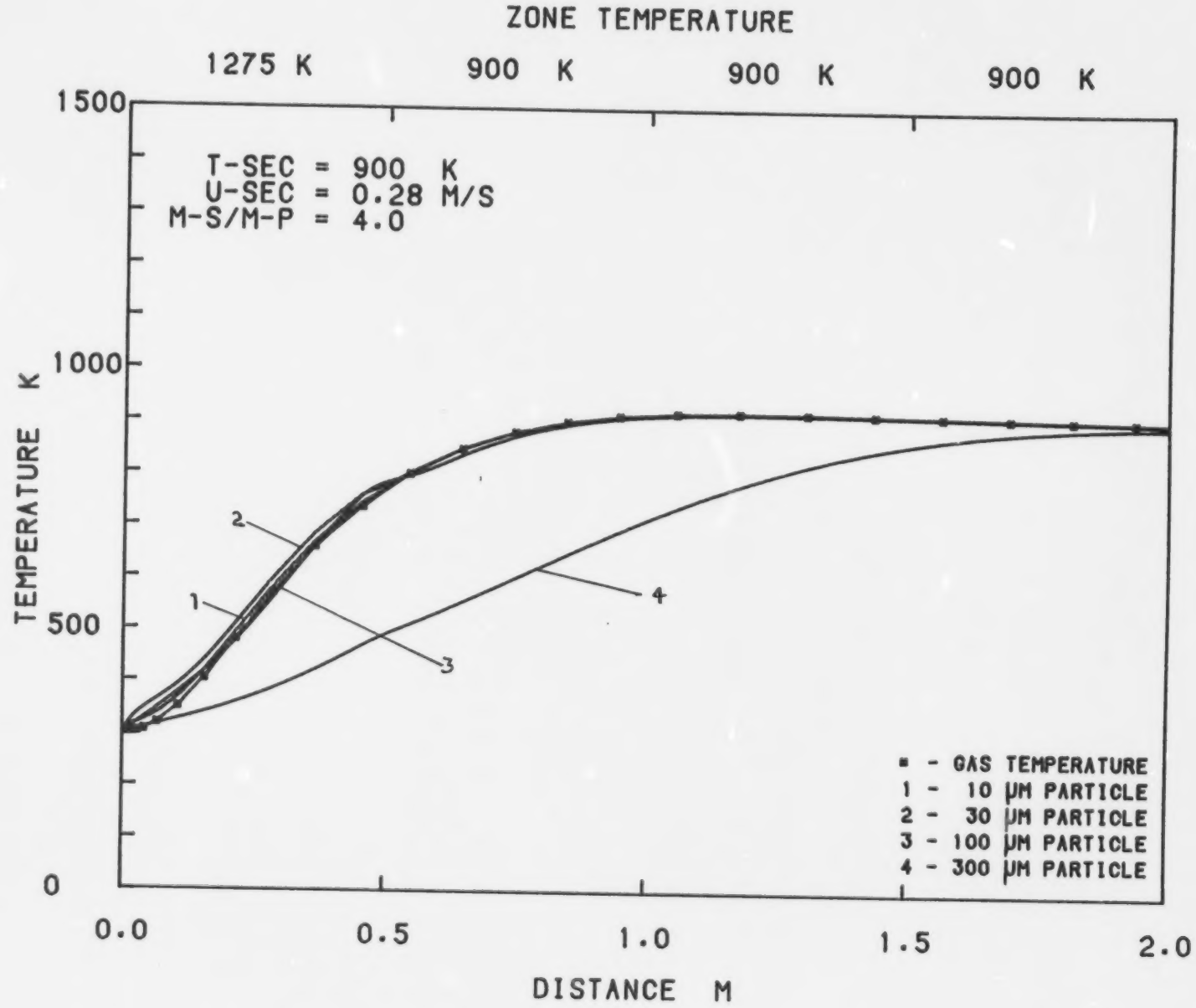

Figure 82: Variable Zone Temperature, Tinsec=900 K, M-S/M-P=4.0 - Coal Feed Rate = 0.5 g/min, Primary Mass Flow = 5.0 g/min, Secondary Mass Flow = 20.0 g/min

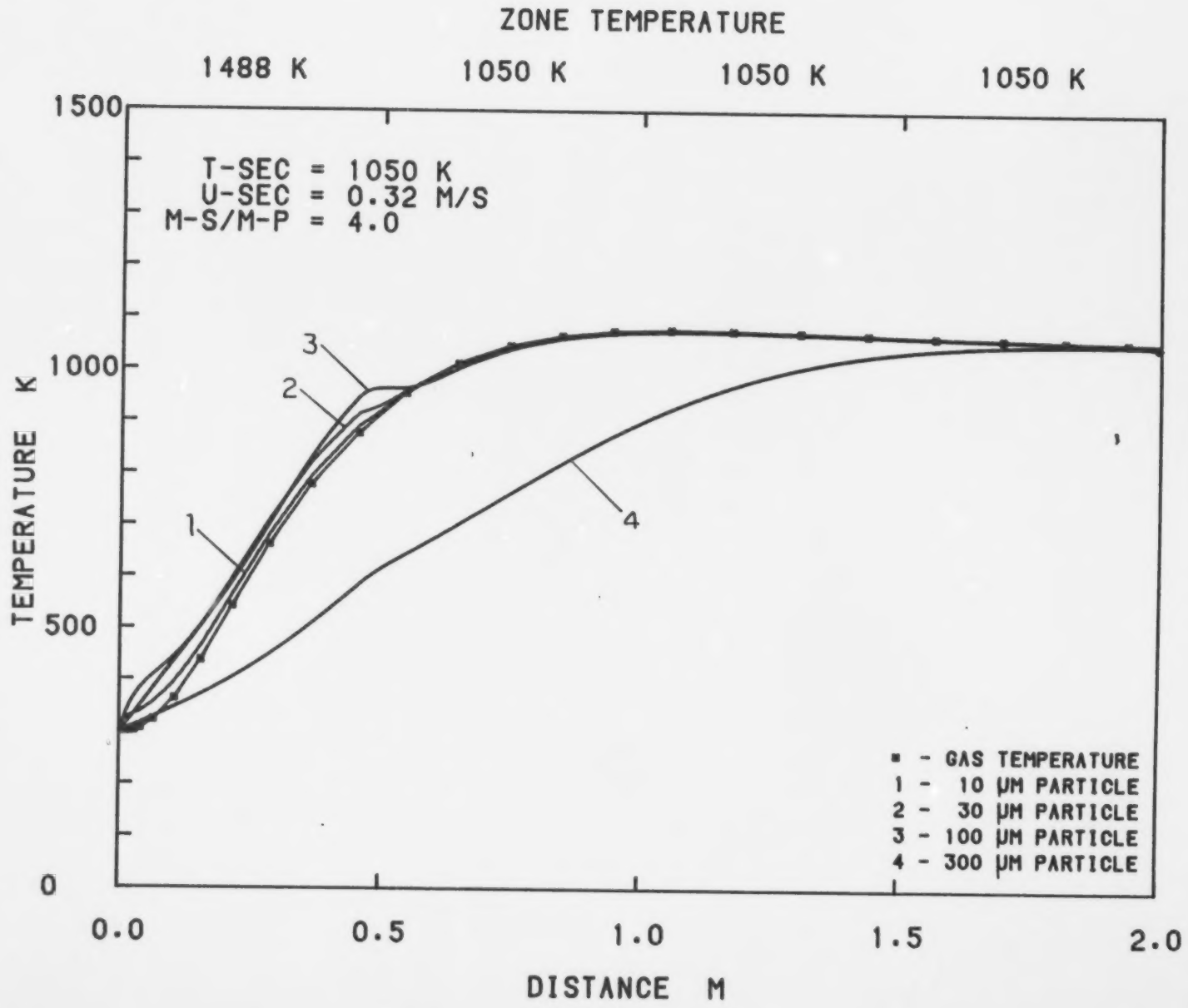

Figure 83: Variable Zone Temperature, Tinsec=1050 K, M-S/M-P=4.0 - Coal Feed Rate = 0.5 g/min, Primary Mass Flow = 5.0 g/min, Secondary Mass Flow = 20.0 g/min

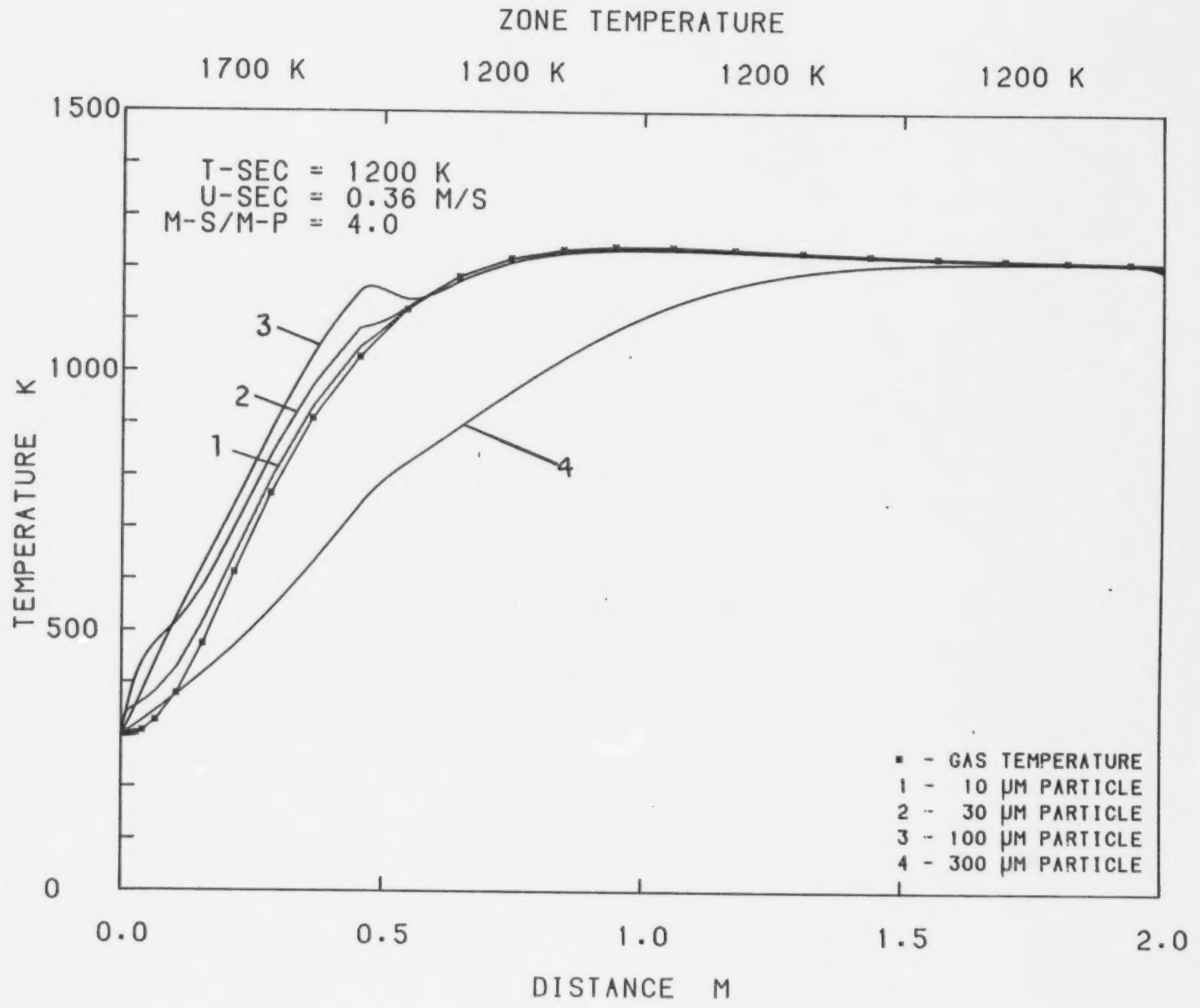

Figure 84: Variable Zone Temperature, Tinsec=1200 K, M-S/M-P=4.0 - Coal Feed Rate = 0.5 g/min, Primary Mass Flow = 5.0 g/min, Secondary Mass Flow = 20.0 g/min

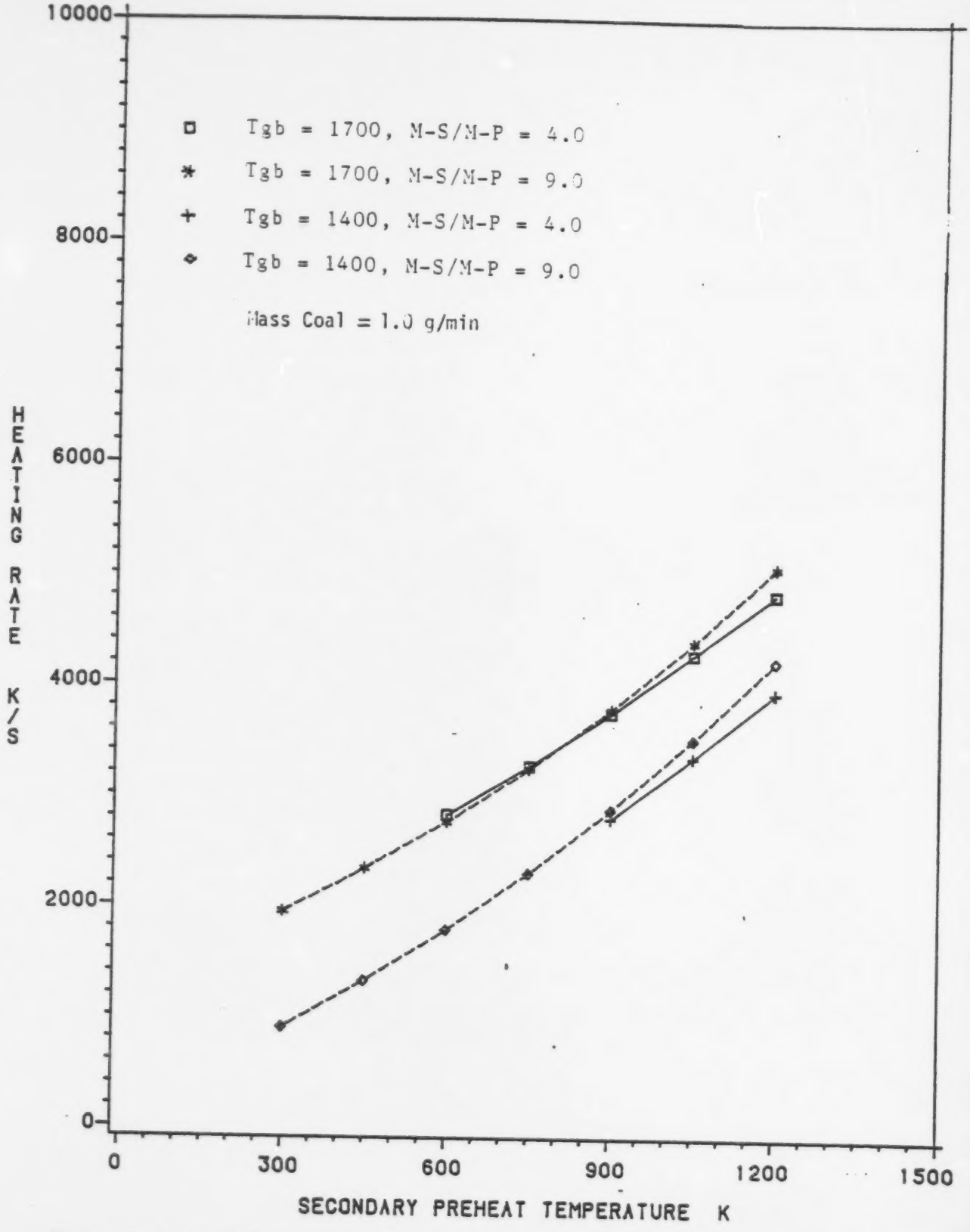

Figure 85: Rate of Temperature Rise for a 10 μm Particle – Heating Rate vs. Secondary Preheat Temperature

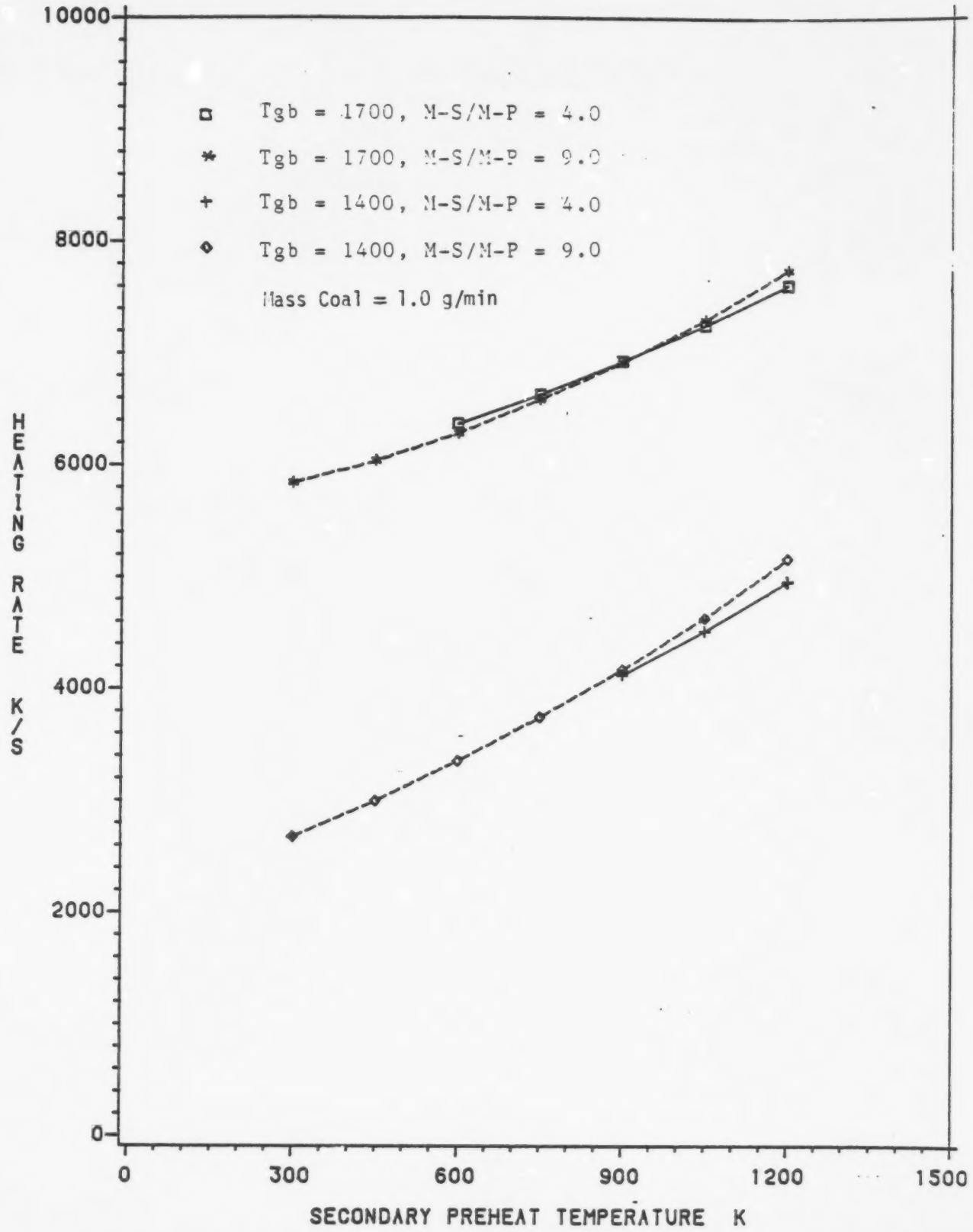

Figure 86: Rate of Temperature Rise for a 30 μm Particle – Heating Rate vs. Secondary Preheat Temperature

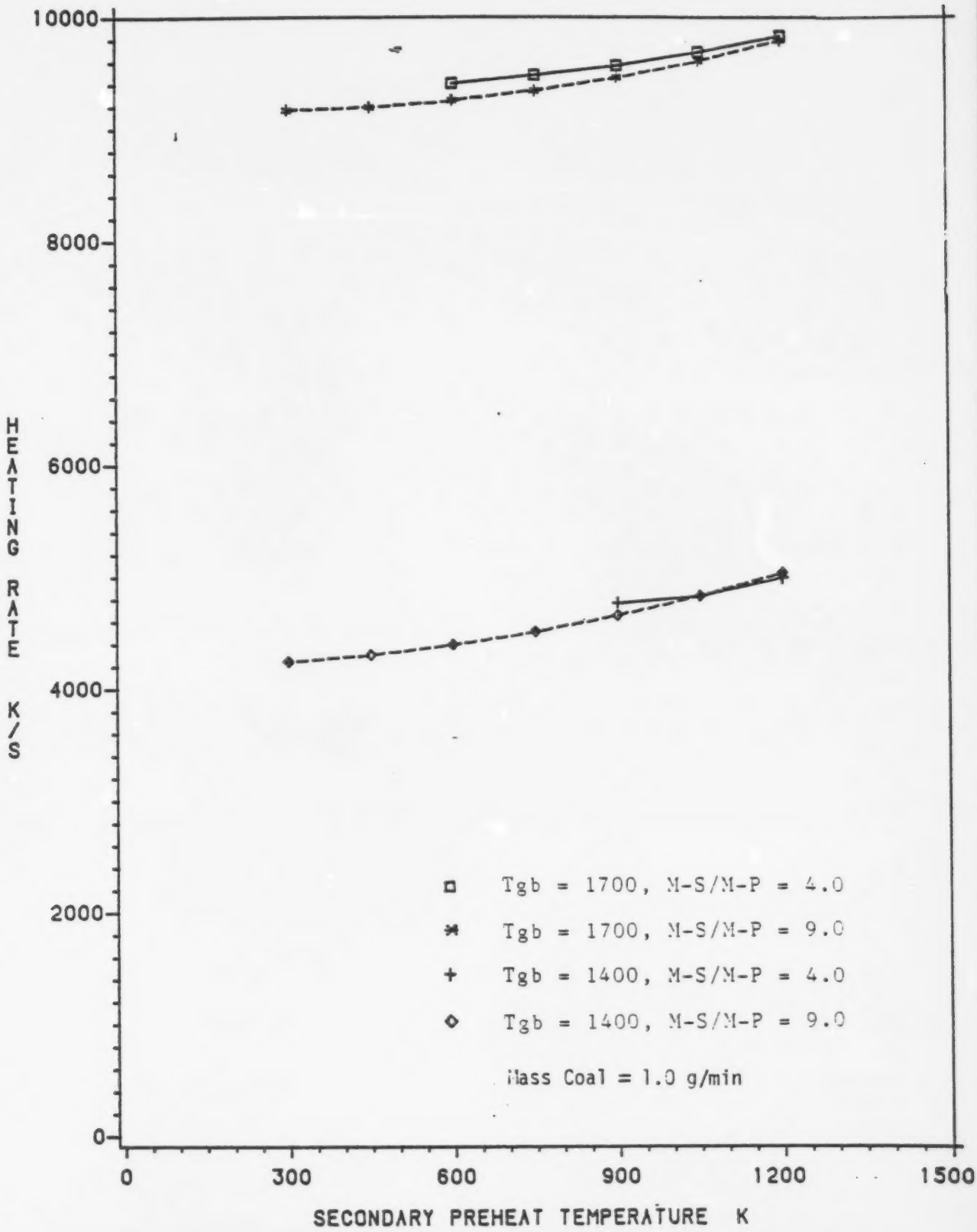

Figure 87: Rate of Temperature Rise for a 100 μm Particle – Heating Rate vs. Secondary Preheat Temperature

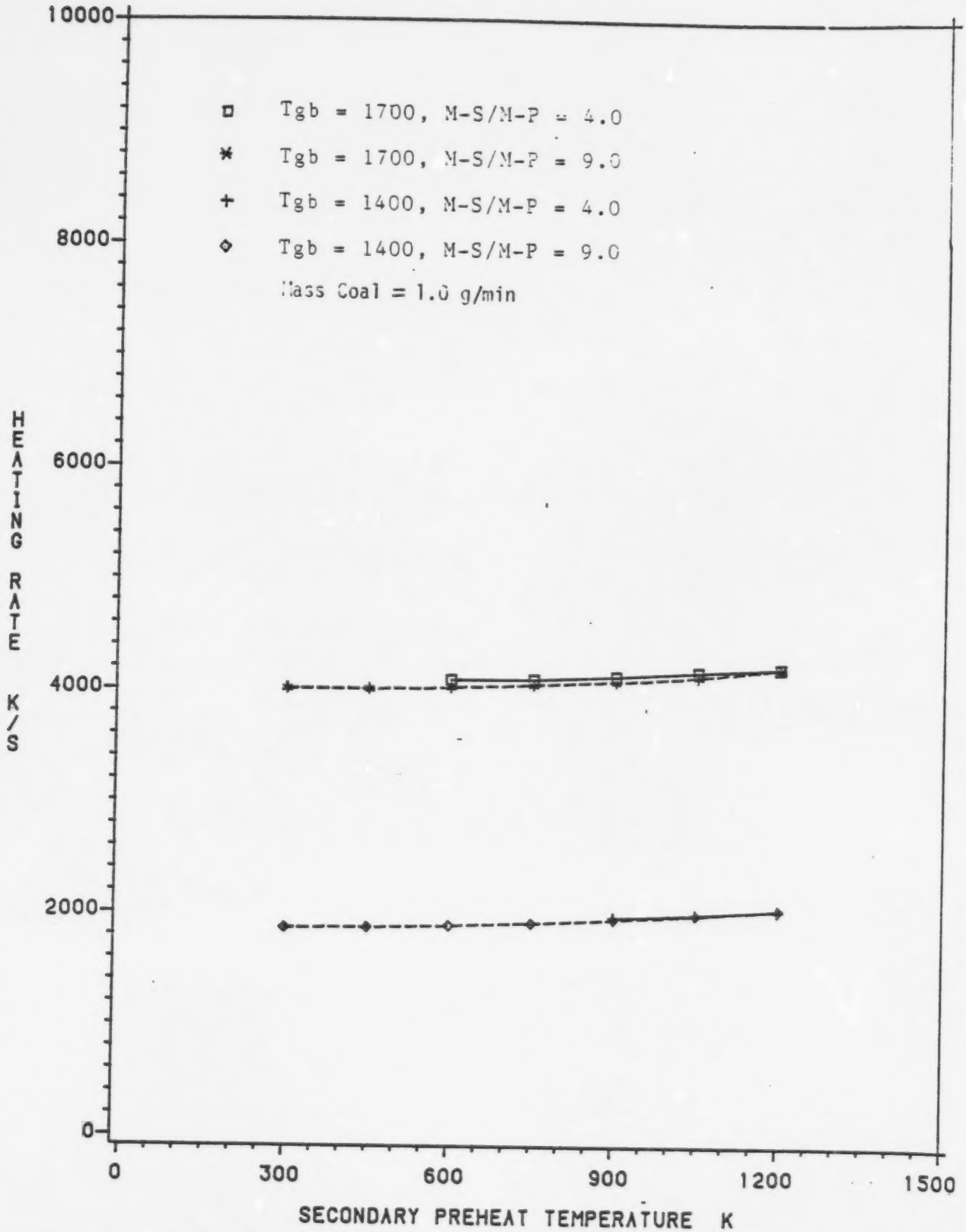

Figure 88: Rate of Temperature Rise for a 300 μm Particle – Heating Rate vs. Secondary Preheat Temperature

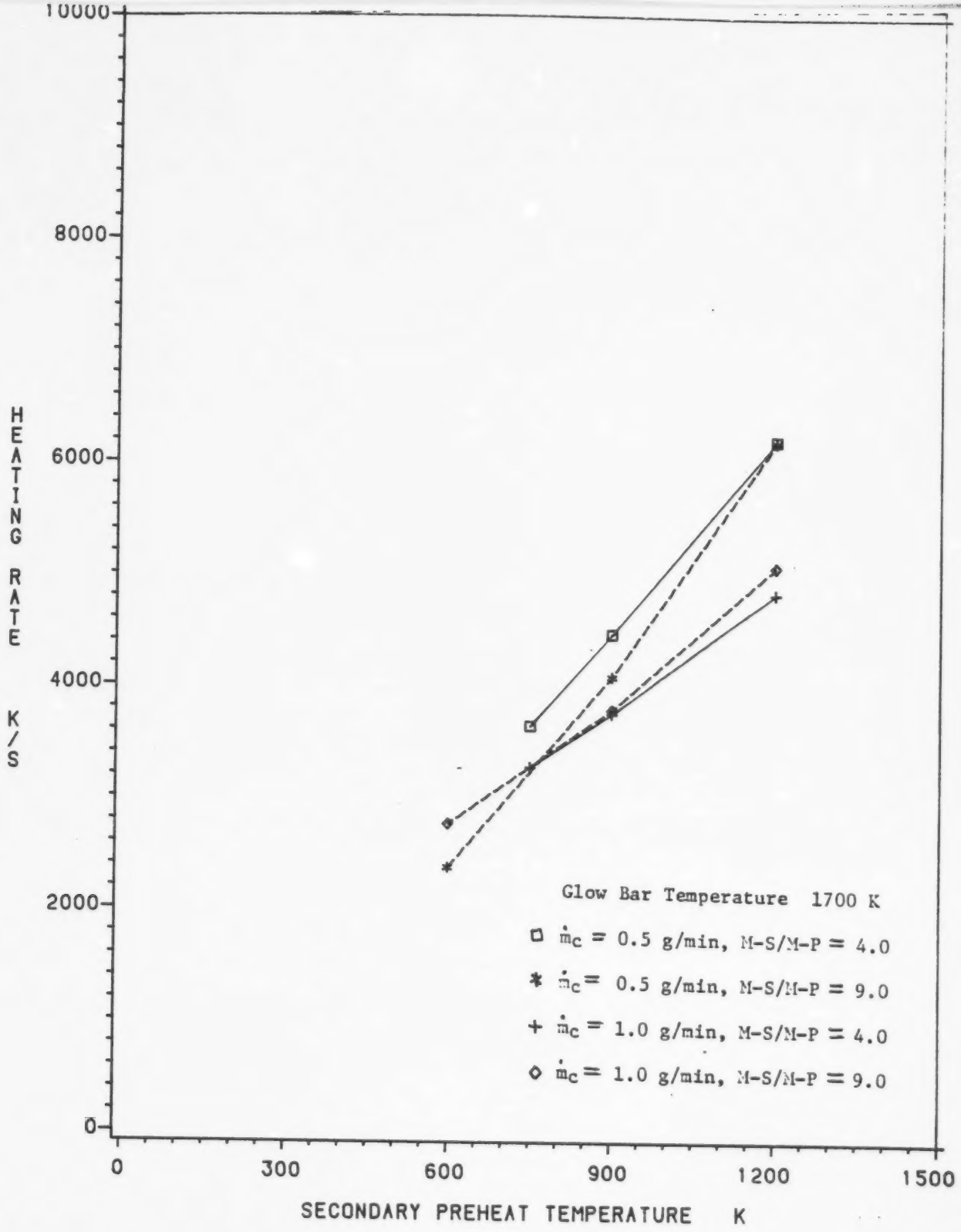

Figure 89: **Heating Rate for a 10 µm particle, 0.5 and 1.0 g/min Coal – Heating Rate vs.** Secondary Preheat Temperature

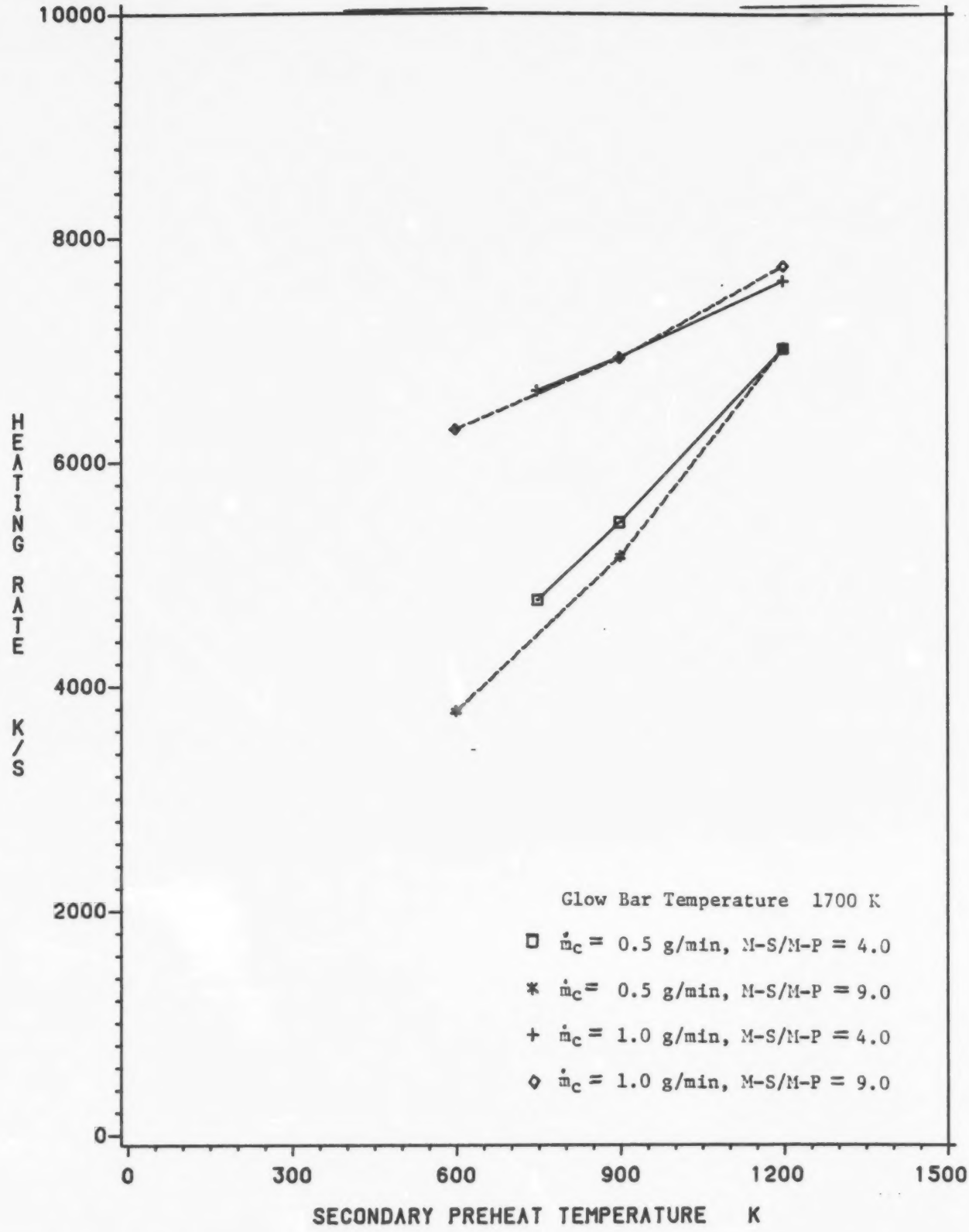

Figure 90: **Heating Rate for a 30 µm particle, 0.5 and 1.0 g/min Coal – Heating Rate vs.** Secondary Preheat Temperature

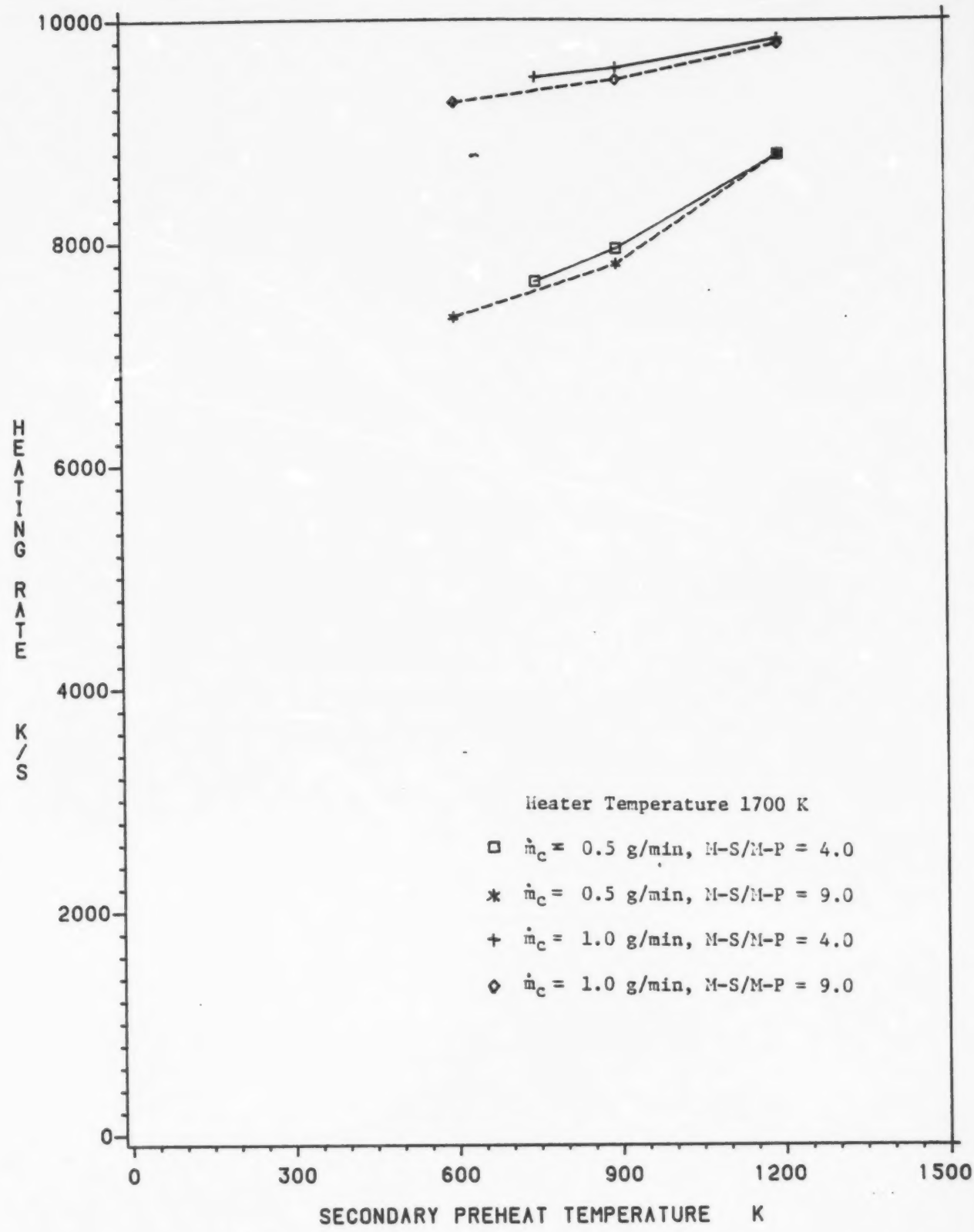

Figure 91: **Heating Rate for a 100 μm Particle, 0.5 and 1.0 g/min Coal – Heating Rate vs.** Secondary Preheat Temperature

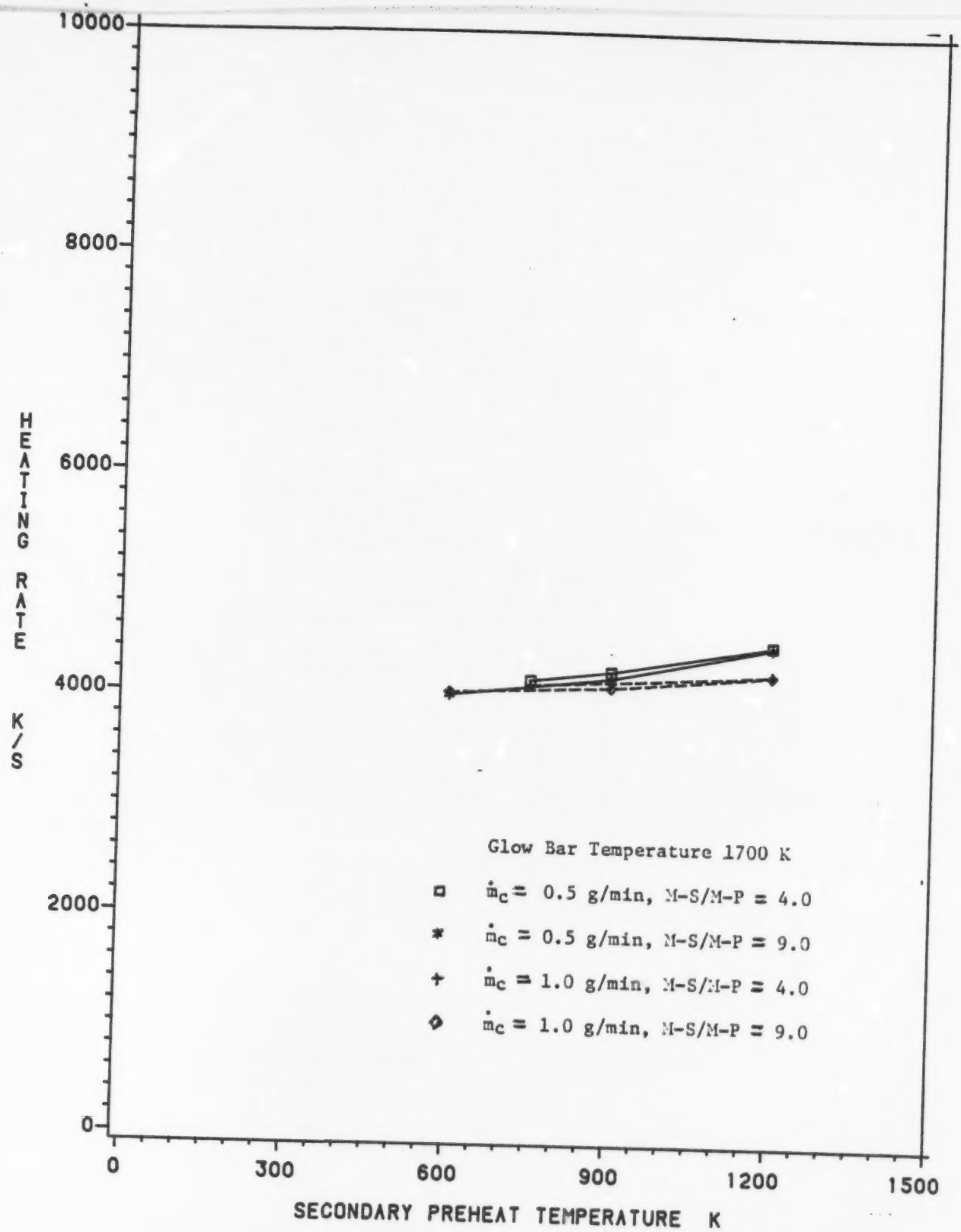

Figure 92: Heating Rate for a 300 µm particle, 0.5 and 1.0 g/min Coal – Heating Rate vs. Secondary Preheat Temperature

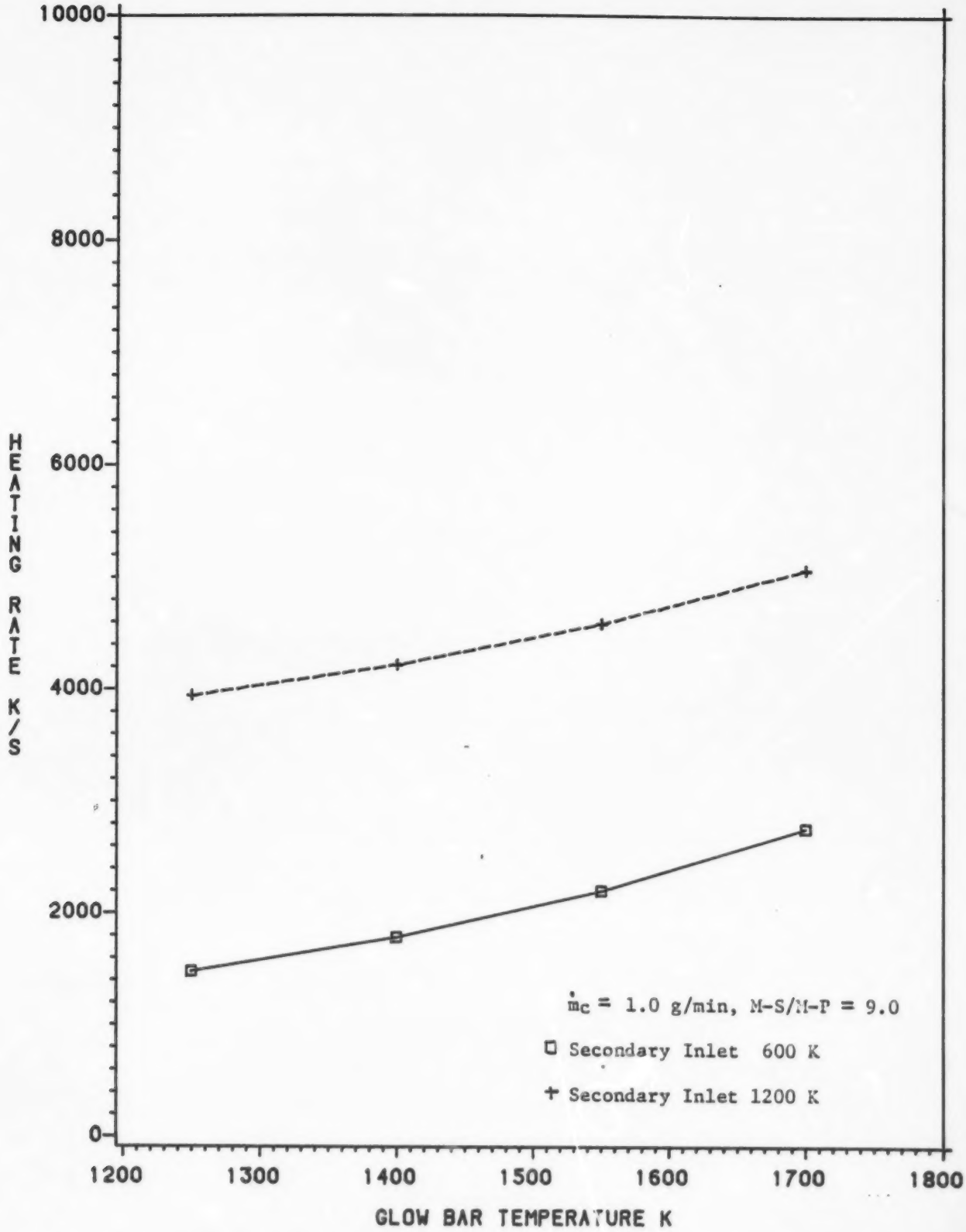

Figure 93: Heating Rate vs. Glow Bar Temperature for a 10 μm Particle – Coal Feed Rate = 1.0 g/min

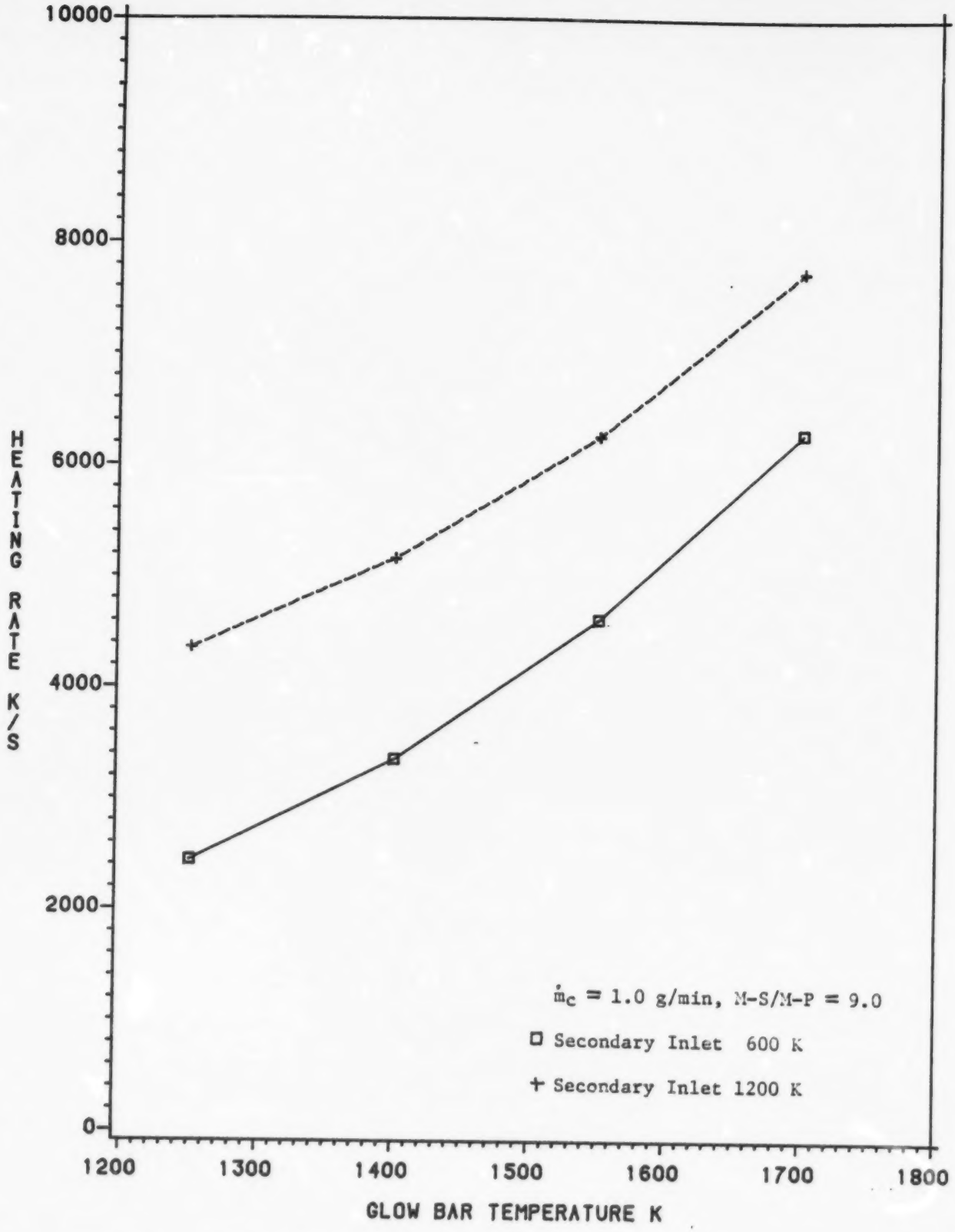

Figure 94: Heating Rate vs. Glow Bar Temperature for a 30 μm Particle – Coal Feed Rate = 1.0 g/min

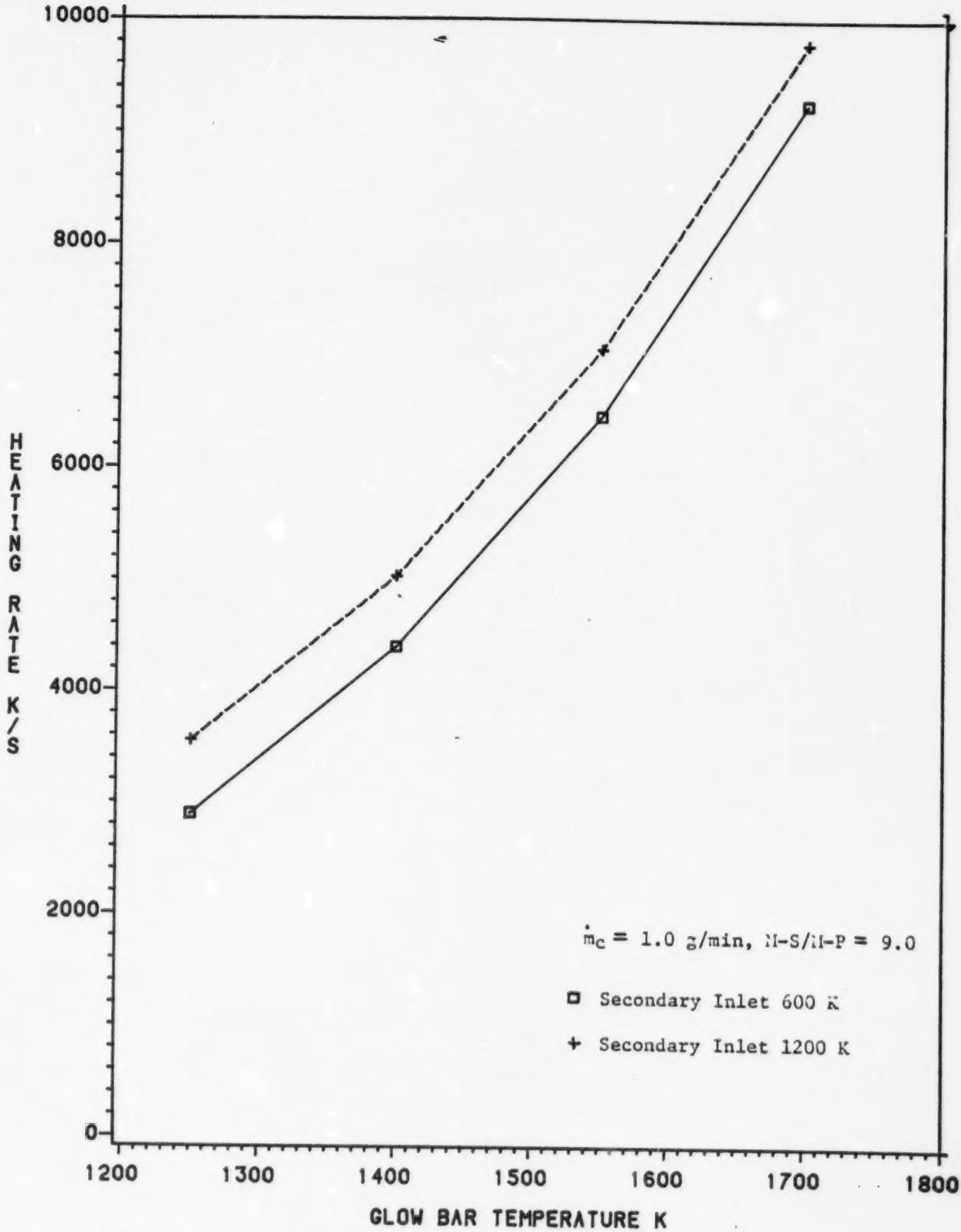

Figure 95: Heating Rate vs. Glow Bar Temperature for a 100 μm Particle – Coal Feed Rate = 1.0 g/min

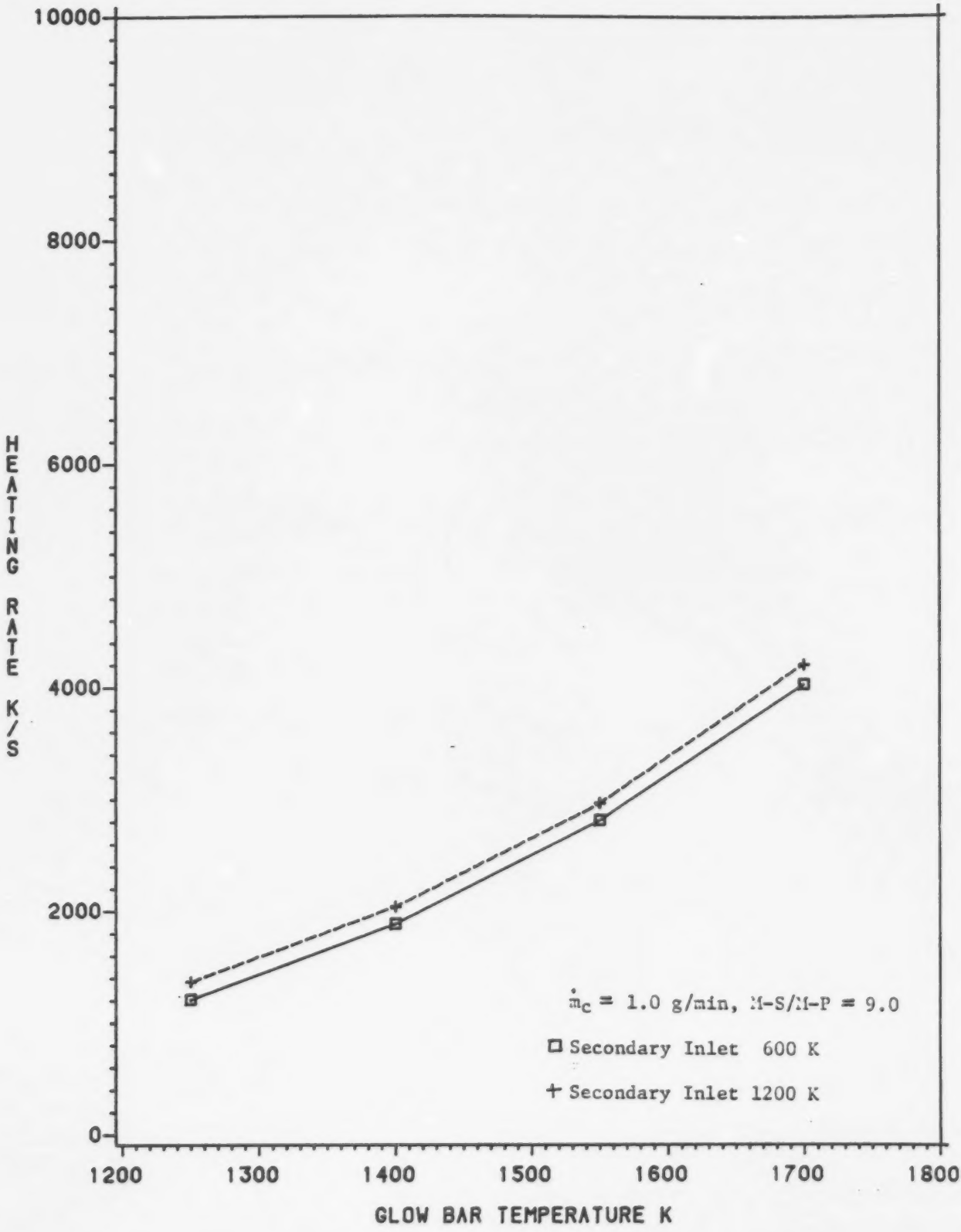

Figure 96: Heating Rate vs. Glow Bar Temperature for a 300 μm Particle - Coal Feed Rate = 1.0 g/min

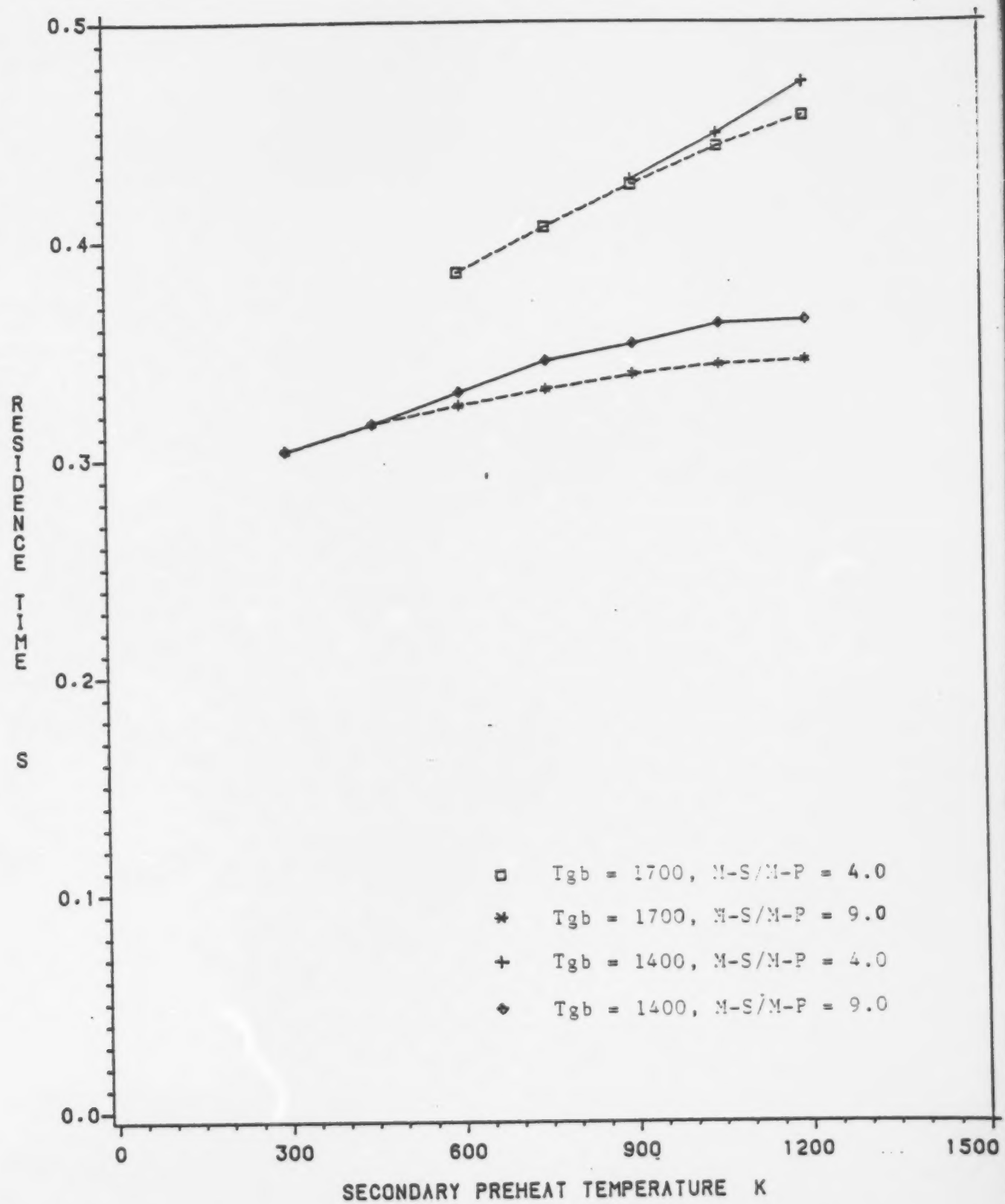

Figure 97: Residence Time vs. Preheat Temp. for a 100 μm Particle – Coal Feed Rate = 1.0 g/min

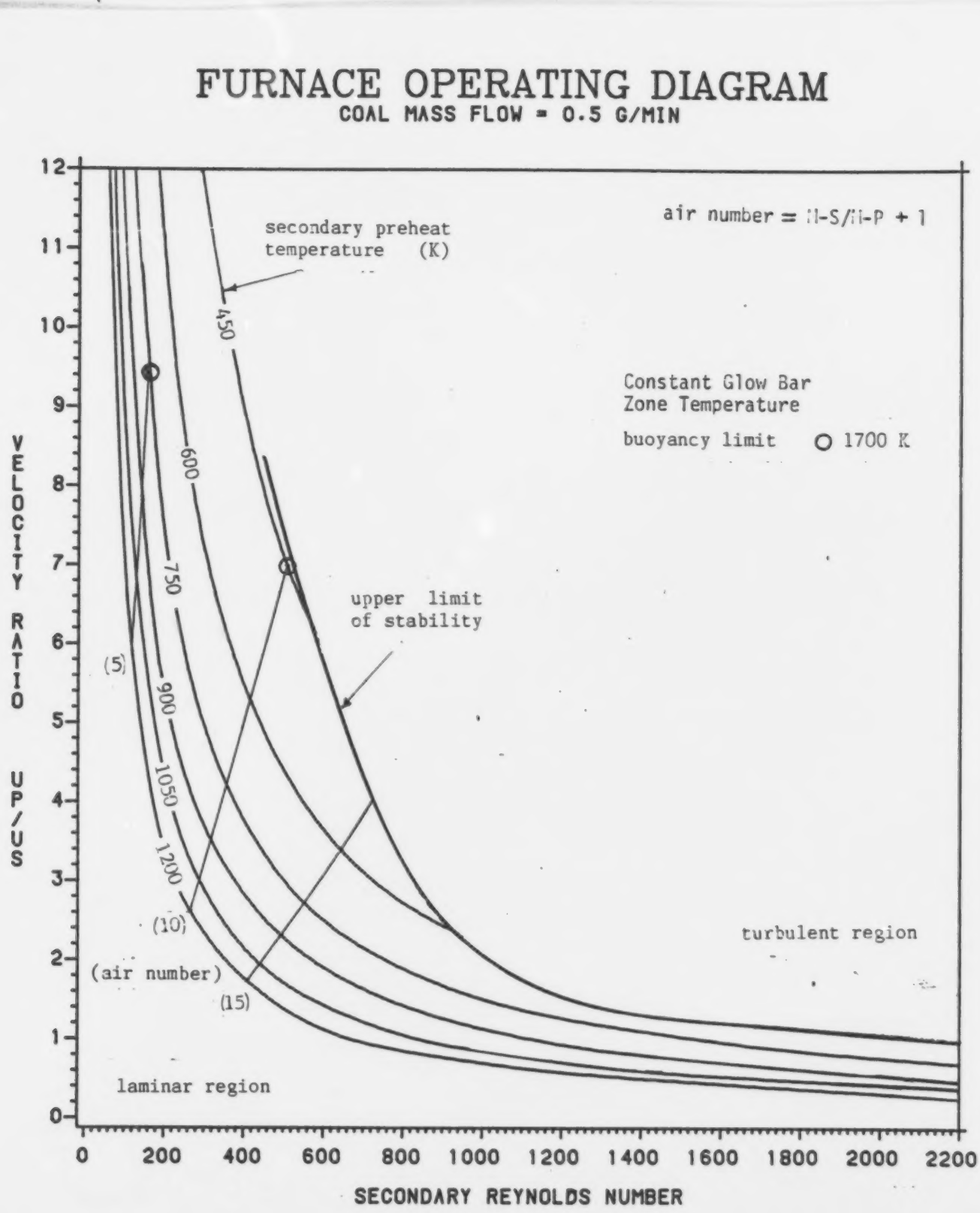

Figure 98: Furnace Operating Diagram – 0.5 g/min Coal – Based on Stability Curve Found with Flow Visualization Experiments and on Numerical Results

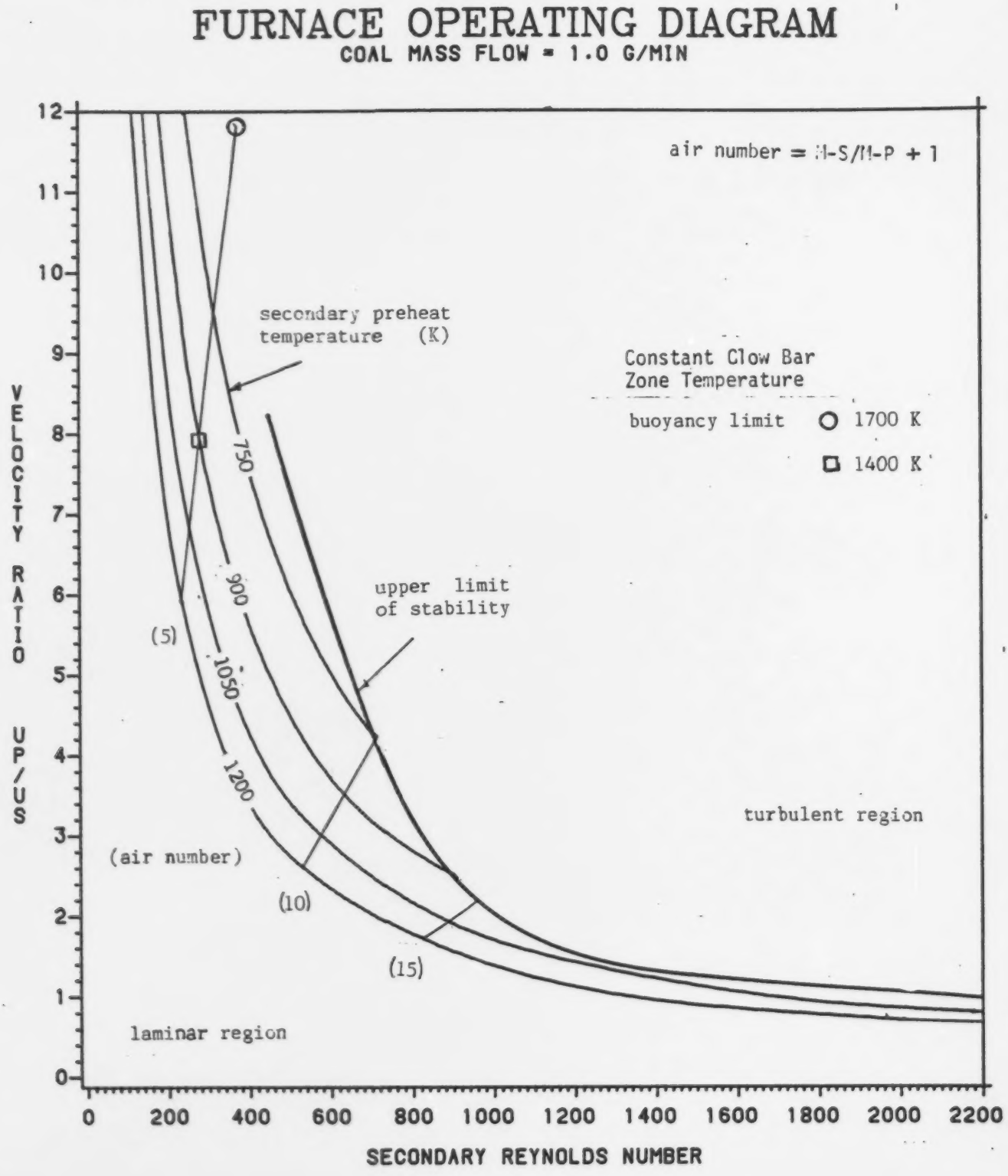

Figure 99: Furnace Operating Diagram – 1.0 g/min Coal – Based on Stability Curve Found with Flow Visualization Experiments and on Numerical Results

Chapter 6

CONCLUSIONS AND RECOMMENDATIONS

The objective of this study was to develop a numerical model for the CCRL drop tube furnace. The model examined the effect of the secondary air mass flow rate, secondary preheat temperature, the glow bar (heating element) temperature and coal feed rate. Inert, spherical particles (representing coal particles) with diameters of 10, 30, 100, and 300 μm were introduced into the furnace model and their velocities, temperatures and heating rates were computed.

The first section of this report examined experimental results obtained from isothermal flow visualization tests. These results yielded two conclusions:

1. The use of a flow straightener at the secondary air inlet and elimination of the water-cooled jacket between primary and secondary flows are necessary to obtain the desired flow pattern with low dispersion of the central primary jet.
2. The furnace should be operated within the range of Reynolds numbers indicated by the stability diagram (Figure 7) to achieve a steady laminar flow with low dispersion of the central jet. This diagram is strictly speaking only valid for isothermal conditions in the furnace.

The finite difference model of the drop tube furnace was used in a parametric study to determine the effects of secondary mass flow, secondary preheat temperature and glow bar temperature. The results led to the following conclusions:

1. Higher glow bar temperatures result in greater centre-line velocities and temperatures and reduced buoyancy effects.
2. Higher secondary air mass flows result in larger centre-line velocities but lower centre-line temperatures; buoyancy effects are reduced.
3. Increasing the secondary preheat temperature results in reduced buoyancy effects, higher centre-line temperatures and lower centre-line velocities.
4. Reducing the coal mass flow (hence decreasing the primary and secondary air quantity necessary for a given stoichiometry) results in greater centre-line temperatures, lower centre-line velocities and increased buoyancy effects.
5. Isothermal furnace operation was obtained by setting the glow bar temperatures of zones two to four equal to the secondary preheat temperature; the zone one temperature was set higher to achieve initial rapid heating (see equation, Section 5.3.3).

The introduction of the four different particle sizes into the furnace flow field under various flow conditions showed certain trends:

1. Particle heating rates increase with rising secondary preheat temperatures; the effect being strongest for small particles.
2. The mass flow rate of the secondary air has a very slight effect on the heating rates.
3. Higher glow bar temperatures significantly increase particle heating rates.
4. Heating rates are most strongly affected by radiant heat transfer from the furnace wall.

5. Heating rates rise with larger particle diameters up to a diameter of approximately 100 μm; further increases in particle diameters result in lower heating rates.
6. Higher particle temperatures were achieved by reducing the coal mass feed rate; however, the particle heating rates are lower. The difference between the temperature histories experienced by different sized particles decreases as the coal feed is reduced.
7. Each 0.1 change in the emissivity of the particle can result in temperature differences of 2 to 40 K ; the effect becomes more significant with larger diameters.
8. A lower isothermal operating temperature results in lower particle heating rates.

The residence time of a 100 μm particle was examined under various flow conditions. The following conclusions were drawn from the results:

1. A longer particle residence time is observed with larger preheat temperatures.
2. A larger secondary mass flow gives a decrease in particle residence time.
3. A higher glow bar temperature gives a small increase in particle residence time.

From this, certain recommendations can be made for choosing operating conditions for the furnace. Use of a low coal feed rate has certain advantages: it reduces the difference in temperature histories between particle sizes (an advantage if the coal cannot be closely sized) and requires less power for secondary air preheating. On the other hand, very low flow rates will lead to buoyancy driven recirculation. A coal feed rate of about 0.5 g/min (primary air

5.0 g/min) seems to be the best compromise. The secondary flow rate has very little effect on particle heating, and should therefore simply be made large enough to absorb the expected heat release from the coal sample; an overall stoichiometry of 10 times the theoretical air should be sufficient. The primary means of control of the particle heating rates is the glow bar zone temperature, and recommendations are made in Section 5.3.3 for achieving rapid heating to isothermal conditions for various final gas temperatures. The heating zone temperature settings given in that section are particularly recommended, as they give nearly all identical heating histories for all particle sizes of 100 μm or less. Use of particles much larger than 100 μm is not recommended because large particles have significant thermal inertia, causing their temperature histories to depart considerably from those of smaller particles. Finally, the operating diagrams (Figures (98) and (99)) give the range of Reynolds numbers in which the furnace must be operated to avoid unsteady flow, turbulence, or buoyancy-induced recirculation.

The model developed here is only valid if the flow in the furnace is laminar and steady. Because the eddy shedding and fluctuations observed in the furnace with the original burner design (with water-cooled jacket), this numerical model cannot make reliable predictions for this configuration. Extension of the model on such flows would require a model for the exchange caused by the unsteady motion; no such model currently exists. Turbulence models in present use are only valid for fully-developed turbulent flow, at Reynolds numbers greater than 10,000.

This model has been developed in conjunction with the actual drop tube furnace at the CANMET research laboratories. This numerical model will allow a parametric study to be performed on the CMCH furnace, examining the effects

of changing zone temperatures, air mass flow rates, air preheat temperatures, and the coal feed rate. The program developed here can easily be expanded to include a devolatilization or combustion model for future research.

REFERENCES

1. Abarbanel, S., Bennett, S., Brandt, A., Gillis, J., Velocity Profiles of Flow at Low Reynolds Numbers. Journal of Applied Mathematics, Trans. of the ASME, March 1970, pp. 2–4

2. Abdelrehim, Z.E., Heat Transfer in Turbulent Recirculatory Flows Affected by Buoyancy Forces in Rectangular Cavities. University of Ottawa, MASc thesis, 1979, 107pp.

3. Badzioch, S., Hawksley, G.W., Kinetics of Thermal Decomposition of Pulverized Coal Particles. Ind. Eng. Chem. Process Des. Develop., Vol. 9, No. 4, 1970, pp. 521–530

4. Baum, M.M., Street, P.J., Predicting the Combustion Behaviour of Coal Particles. Combustion Science and Technology, Vol. 3, 1971, pp. 231–243

5. Bergman, P.D., Koppel, L.B., Uniform Flux Heat Transfer to a Gas in Laminar Forced Convection in a Circular Tube. A.I.Ch.E. Journal, Vol. 12, No. 4, July 1966, pp. 648–655

6. Biggs, R.C., Stachiewicz, J.W., Combined Free and Forced Convection Heat Transfer of Gases 4th Inter. Ht. Tr. Conf., Paris, Heat Transfer, Vol. 4, 1970, N.C. 3.1

7. Bird, R.B., Stewart, W.E., Lightfoot, E.N., Transport Phenomena., John Wiley and Sons, Inc., 1960, 780 pp.

8. Bolz, R.E., Tuve, G.L., Handbook of Tables for Applied Engineering Science CRC Press, Inc., 1983, 2nd ed., 1166 pp.

9. Brown, C.K., Gauvin, H., Combined Free and Forced Convection I. Heat Transfer in Aiding Flow
   II. Heat Transfer in Opposing Flow. Can. J. Chem. Eng., Dec. 1965, pp. 306–318

10. Collins, M.W., Combined Convection in Vertical Tubes Heat and Mass Transfer by Combined Forced and Natural Convection, Institute of Mechanical Engineers, Westminster, London, 1971, pp 17–25

11. Eddinger, R.T., Friedman, L.D., Rau, E., Devolatilization of Coal in a Transport Reactor. Fuel, No. 45, 1966, pp. 245–252

12. Eckert, E.R.G., Drake, R.M., Analysis of Heat and Mass Transfer., McGraw-Hill Book Co., Inc., 1972, 806 pp.

13. Fargie,D., Martin, B.W. Developing Laminar Flow in a Pipe of Circular Cross-Section. Proc. Eng. Soc. Lond., A. 321, 1971, pp. 461–476

14. Field, M.A., Rate of Combustion of Size-Graded Fractions of Char from a Low-Rank Coal between 1200 K and 2000 K. Combustion and Flame, Vol. 13, June 1969, pp. 237–252

15. Friedman, M., Gillis, J., Liron, N, Laminar Flow in a Pipe at Low and Moderate Reynolds Numbers Appl. Sci. Res., Vol. 19, Nov. 1968, pp. 426–438

16. Grigull, U., Tratz, H., Thermischer Einlauf in Ausgebildeter Laminarer Rohrstromung Int J. Heat Mass Transfer, Vol. 8, 1965, pp. 669–678

17. Hanratty, T.J., Rosen, E.M., Kabel, R.L., Effect of Heat Transfer on Flow Field at Low Reynolds Numbers in Vertical Tubes Ind. Eng. Chem., Vol. 50, No. 5, May 1958, pp. 815–820

18. Hasan, Q., Natarajan, R., Seshadri, V., Finite Element Analysis of Flow Development in the Entrance Region of a Tube at Moderate Reynolds Numbers with Different Inlet Velocity Profiles. Finite Element Flow Analysis, Proc. 4th Int. Symp. Finite Element Methods in Flow Problems, Tokyo, editor T. Kawai, Univ. Tokyo Press, North-Holland Pub. Co., 1982, pp.145–152

19. Hebert, L.S., Sterns, U.J., Heat Transfer in Vertical Tubes – interaction of Forced and Free Convection. Chem. Eng. J., No. 4, 1972, pp. 46–52

20. Holman, J.P., Heat Transfer McGraw-Hill Book Co., Inc., 1981, 5th ed., 570 pp.

21. Hottel, H.C., Sarofim, A.F., Radiative Transfer., McGraw-Hill Book Co., 1967, 520 pp.

22. Howard, J.B., Essenhigh, R.H., Pyrolysis of Coal Particles in Pulverized Fuel Flames. Ind. Eng. Chem. Proc. Des. Devel., Vol. 6, No.1, Jan. 1967, pp.74–84

23. Jorgensen, F.R.A., Zuiderwyk, M., Two – Colour Pyrometer Measurement of the Temperature of Individual Combusting Particles. J. Phys. E. Sci. Instrum., Vol. 18, 1985, pp. 486–491

24. Kays, W.M., Numerical Solutions for Laminar Flow Heat Transfer in Circular Tubes. Trans. ASME, Vol. 77, Nov. 1955, pp. 1265–1274

25. Kobayashi, H., Howard, J.B., Sarofim, F., Coal Devolatilization at High Temperatures. 16th Symp. (Int.) Comb., The Combustion Institute, Pittsburgh, PA., 1977, pp. 411–425

26. Lilley, D.G., Rhode, D.L., A Computer Code for Swirling Turbulent Axisymmetric Recirculating Flows in Practical Isothermal Combustor Geometries. NASA Contractor Report 3442, Prepared for Lewis Research Center, 1982, 130 pp.

27. McDonald, J.W., Denny, V.E., Mills, A.F., Numerical Solutions of the Navier-Stokes Equations in Inlet Regions. Journal of Applied Mathematics, Trans. ASME, Dec 1972, pp. 873-878

28. Mitchell, R.E., McLean, W.J., On the Temperature and Reaction Rate of Burning Pulverized Fuels. 19th Symp. (Int.) Comb., The Combustion Institute, 1982, pp. 1113-1122

29. Patankar, S.V., Numerical Heat Transfer and Fluid Flow., Hemisphere Publishing Co., 1980, 197 pp.

30. Scheele, G.F., Hanratty, T.J., Effect of Natural Convection on Stability of Flow in a Vertical Pipe. J. Fluid Mech., Vol. 14, 1962, pp. 244-256

31. Scheele, G.F., Hanratty, T.J., Effect of Natural Convection Instabilities on Rates of Heat Transfer at Low Reynolds Numbers. A.I.Ch.J., Vol. 9, No. 2, Mar. 1963, pp. 183-185

32. Scaroni, A.W., Walker (Jr.), P.L., Essenhigh, R.H., Kinetics of Lignite Pyrolysis in an Entrained-Flow, Isothermal Furnace Fuel, Vol. 60, Jan. 1981, pp. 71-76

33. Schmidt, F.W., Zelder, B., Laminar Flows in Inlet Sections of Tubes and Ducts. A.I.Ch.E. Journal, Vol. 15, No. 4, July 1964, pp. 612-614

34. Siegel, R., Howell, J.R., Thermal Radiation Heat Transfer., Hemisphere Publishing Co., 1981, 2nd ed., 862 pp.

35. Smoot, L.D., Pratt, D.T., Pulverized Coal Combustion and Gasification., Plenum, New York, 1979

36. Sciomon, P.R., Hamblen, D.G., Carengelo, R.M., Krause, J.L., Coal Thermal Decomposition in an Entrained Flow Reactor: Experiments and Theory. 19th Symp. (Int.) Comb., The Combustion Institute, 1982, pp. 1139-1149

37. Spalding, D.B., GENMIX - A General Computer Program for Two-Dimensional Parabolic Phenomena The Science and Applications of Heat and Mass Transfer, Pergamon Press, 1977, 380 pp.

38. Sparrow, E.M., Lin, S.H., Lundgren, T.S. Flow Development in the Hydrodynamic Entrance Region of Tubes and Ducts. Phys. Fluids, Vol. 7, No. 3, Mar. 1964, pp.

39. Streeter, V.L., Wylie, E.B., Fluid Mechanics McGraw-Hill Book Co., Inc., 1979, 7th ed., 562 pp.

40. Timothy, L.D., Sarofim, A.F., Beer, J.M., Characteristics of a Single Particle Coal Combustion. 19th Symp. (Int.) Comb., The Combustion Institute, 1982, pp. 1123-1130

41. Wagner, M.H., Developing Flow in Circular Conduits: Transition from Plug Flow to Tube Flow. J. Fluid Mech., Vol. 72, part 2, 1975, pp. 257-268

Appendix A

PARTICLE DENSITY

One of the assumptions made in developing the particle heating model was that the concentration of particles was small and that the effect of the particles on each other could be neglected. The furnace is a long narrow 2m long, 0.064m I.D. cylinder through which coal and air are passed. The mass flow of air was based on a stoichiometric quantity (primary flow) plus an amount of excess air (secondary flow). In order to determine if the concentration of particles is small, the volume and the number of particles in the furnace needs to be known; a 100 μm particle was chosen for this analysis.

The heating of the particles was studied under a number of different flow conditions. Typical flow conditions were used to estimate the particle concentration.

Typical values: coal feed rate = 0.01667 g/s

average residence time = 0.45 s

density of coal = 1300 kg/m**3

therefore

total mass of coal in furnace at any time:

= (0.01667)(0.45)

= 7.576 *10**-3 g

= 5.828 *10**-9 m**3

Volume of a 100 μm spherical particle:

100 μm = 5.236 *10**-13 m**3

therefore, number of 100 μm particles in furnace at any time

= (5.828 *10**-9)/(5.236 *10**-13)

= 1.113 *10**4 particles

The furnace consists of a 2m long cylinder. If the furnace is sliced into a series of disks, then a certain number of particles can be said to occupy each disk. If the thickness of a slice is large compared to the diameter of the particle, then the concentration of the particles is small and cloud effects can be neglected.

For a 100 μm particle:

thickness of slice = (furnace length)/(number of particles)

=(2m)/(1.113 *10**4 particles)

=0.000180 m

number of particle diameters/slice

=(0.000180)/(0.000100)

=1.8

Thickness of slice is 1.8 particle diameters and one 100 μm particle occupies each slice. The assumption that the particles are spaced sufficiently apart with low particle concentration can be said to be valid.

Similarly,

10 μm particle = 0.018 particle diameters/slice thickness

30 μm particle = 0.16 particle diameters/slice thickness

300 μm particle = 16 particle diameters/slice thickness

For the 10 and 30 μm particle sizes, the slice thickness is smaller than the particle diameter; therefore, more than one particle will have to occupy each slice.

10 μm = 56 particles/slice thickness

30 μm = 6.3 particles/slice thickness

The concentration of the 10 and 30 μm particle is still relatively small when spread out over the cross-sectional area of the slice (slice diameter based on diameter of primary inlet = 6400 μm).

Appendix B

VIEW FACTORS

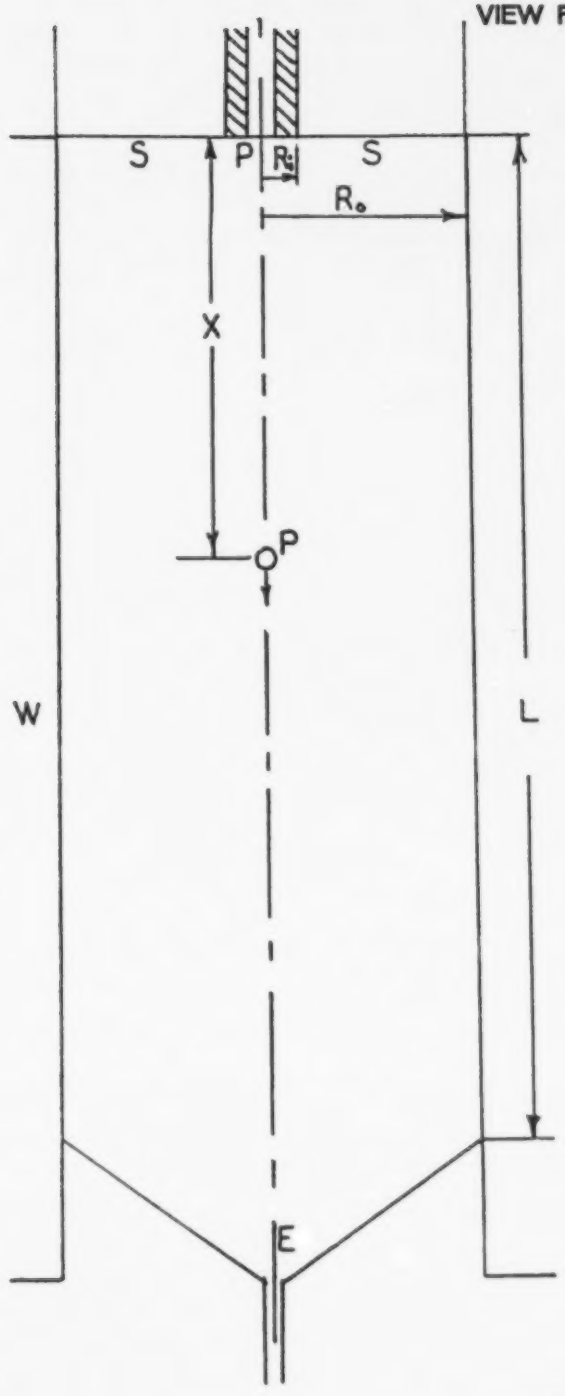

$$F_{PP} = \frac{1}{2}\left[1 - \frac{1}{\sqrt{1 + \frac{R_o^2}{x^2}}}\right]$$

$$F_{PE} = \frac{1}{2}\left[1 - \frac{1}{\sqrt{1 + \frac{R_o^2}{(L-x)^2}}}\right]$$

$$F_{PS} = \frac{1}{2}\left[1 - \frac{1}{\sqrt{1 + \frac{R_o^2}{x^2}}}\right] - F_{PP}$$

$$F_{PW} = 1 - F_{PP} - F_{PS} - F_{PE}$$

Appendix C

LISTING OF THE FORTRAN COMPUTER PROGRAM

```
C------CCRL COAL DROP FURNACE NUMERICAL MODEL------EMR CONTRACT                CCR00010
C                                                                              CCR00020
C------WRITTEN BY ROBERT J. FLAXMAN ------ MASC MECH. ENG. THESIS              CCR00030
C                                                                              CCR00040
C------THIS PROGRAM PREDICTS THE VELOCITY AND TEMPERATURE PROFILES INSIDECCR00050
C     A LAMINAR COAL DROP FURNACE UNDER SPECIFIED FLOW CONDITIONS.             CCR00060
C     THE PROGRAM USES THESE CALCULATED VALUES TO SOLVE TEMPERATURES           CCR00070
C     AND VELOCITIES OF SIZE GRADED PARTICLES AS THEY TRAVEL THROUGH           CCR00080
C     THE FURNACE.                                                             CCR00090
C                                                                              CCR00100
C------------------------------------------------------------------------------ CCR00110
C                                                                              CCR00120
      DIMENSION HEDU(9),HEDV(9),HEDP(9),HEDT(9),HEDM(9),HEDD(9)                CCR00130
      COMMON                                                                   CCR00140
     1/UVEL/RESORU,NSWPU,URFU,DXEPU(32),DXPWU(32),SEWU(32)                     CCR00150
     1/VVEL/RESORV,NSWPV,URFV,DYNPV(32),DYPSV(32),SNSV(32)                     CCR00160
     1/PCOR/RESORM,NSWPP,URFP,DU(30,30),DV(30,30),IPREF,JPREF                  CCR00170
     1/VAR/U(30,30),V(30,30),P(30,30),PP(30,30)                                CCR00180
     1/ALL/IT,JT,NI,NJ,NIM1,NJM1,GREAT                                         CCR00190
      COMMON                                                                   CCR00200
     1/GEOM/X(32),Y(32),DXEP(32),DXPW(32),DYNP(32),DYPS(32),                   CCR00210
     1       SNS(32),SEW(32),XU(32),YV(32),R(32),RV(32),RCV(32)                CCR00220
     1/FLUPR/VISSEC,DENSEC,PRANDL,DEN(30,30),VIS(30,30),CONST,                 CCR00230
     1        VISPRM,DENPRM,SECMAS,PRMMAS,SPRAT                                CCR00240
      COMMON                                                                   CCR00250
     1/PROB1/UINPRM,UINSEC,GRAVTY,FLOWIN,NITER                                 CCR00260
     1/COEF/AP(30,30),AN(30,30),AS(30,30),AE(30,30),AW(30,30),SU(30,30),CCR00270
     1       SP(30,30)                                                         CCR00280
      COMMON                                                                   CCR00290
     1/TEMP/T(30,30),GAMH(30,30),RESORT,NSWPT,URFT,                            CCR00300
     2      TINPRM,TINSEC,TGB(30),HTFLX(30),HFXOLD(30)                         CCR00310
      LOGICAL INCALU,INCALV,INCALP,INPRO,INCALT,INCLUP                         CCR00320
      READ(5,010) HEDU,HEDV,HEDP,HEDT,HEDM,HEDD                               CCR00330
  010 FORMAT(9A4)                                                              CCR00340
C                                                                              CCR00350
C------------------------  CCRL   FORTRAN  ------------------------------- CCCR00360
C                                                                              CCR00370
CHAPTER  1  1  1  1  1  PARAMETERS AND CONTROL INDICES  1  1  1  1  1  1CCR00380
C                                                                              CCR00390
C------GRID                                                                    CCR00400
C------THE GRID CONSISTS OF 28 AXIAL POSITIONS AND 20 RADIAL POSITIONS.        CCR00410
C                                                                              CCR00420
      GREAT=1.E30                                                              CCR00430
      NITER=0                                                                  CCR00440
```

```
      IT=30                                                          CCR00450
      JT=30                                                          CCR00460
      IMON=5                                                         CCR00470
      JMON=5                                                         CCR00480
      JPREF=2                                                        CCR00490
      IPREF=2                                                        CCR00500
      NSWPU=3                                                        CCR00510
      NSWPV=3                                                        CCR00520
      NSWPP=5                                                        CCR00530
      NSWPT=3                                                        CCR00540
C-----THIS GIVES THE NUMBER OF NODE POINTS IN THE X AND Y DIRECTION  CCR00550
      NI=28                                                          CCR00560
      NJ=20                                                          CCR00570
C**   NJ=29                                                          CCR00580
C                                                                    CCR00590
      NIM1=NI-1                                                      CCR00600
      NJM1=NJ-1                                                      CCR00610
C                                                                    CCR00620
C-----THE FOLLOWING ARE THE AXIAL POSITIONS OF THE GRID IN METERS.   CCR00630
C                                                                    CCR00640
      X(1)=-0.002                                                    CCR00650
      X(2)=0.002                                                     CCR00660
      X(3)=0.007                                                     CCR00670
      X(4)=0.013                                                     CCR00680
      X(5)=0.020                                                     CCR00690
      X(6)=0.028                                                     CCR00700
      X(7)=0.040                                                     CCR00710
      X(8)=0.065                                                     CCR00720
      X(9)=0.105                                                     CCR00730
      X(10)=0.155                                                    CCR00740
      X(11)=0.215                                                    CCR00750
      X(12)=0.285                                                    CCR00760
      X(13)=0.365                                                    CCR00770
      X(14)=0.455                                                    CCR00780
      X(15)=0.545                                                    CCR00790
      X(16)=0.645                                                    CCR00800
      X(17)=0.745                                                    CCR00810
      X(18)=0.845                                                    CCR00820
      X(19)=0.945                                                    CCR00830
      X(20)=1.055                                                    CCR00840
      X(21)=1.175                                                    CCR00850
      X(22)=1.305                                                    CCR00860
      X(23)=1.435                                                    CCR00870
      X(24)=1.565                                                    CCR00880
      X(25)=1.695                                                    CCR00890
      X(26)=1.815                                                    CCR00900
      X(27)=1.935                                                    CCR00910
      X(28)=2.065                                                    CCR00920
C                                                                    CCR00930
C-----THE FOLLOWING ARE THE RADIAL POSITIONS OF THE MOD. GRID IN METRES CCR00940
C                                                                    CCR00950
      Y(1)=-0.0004                                                   CCR00960
      Y(2)=0.0004                                                    CCR00970
      Y(3)=0.0012                                                    CCR00980
```

```
      Y(4)=0.0020                                                       CCR00990
      Y(5)=0.0028                                                       CCR01000
      Y(6)=0.0036                                                       CCR01010
      Y(7)=0.0044                                                       CCR01020
      Y(8)=0.0052                                                       CCR01030
      Y(9)=0.0060                                                       CCR01040
      Y(10)=0.0068                                                      CCR01050
      Y(11)=0.0080                                                      CCR01060
      Y(12)=0.0100                                                      CCR01070
      Y(13)=0.0140                                                      CCR01080
      Y(14)=0.0180                                                      CCR01090
      Y(15)=0.0220                                                      CCR01100
      Y(16)=0.0260                                                      CCR01110
      Y(17)=0.0278                                                      CCR01120
      Y(18)=0.0294                                                      CCR01130
      Y(19)=0.0310                                                      CCR01140
      Y(20)=0.0326                                                      CCR01150
C                                                                       CCR01160
C-----THE FOLLOWING IS THE GRID SPACING IN THE RADIAL DIRECTION OF THE  CCR01170
C     ORIGINAL BURNER                                                   CCR01180
C                                                                       CCR01190
C     Y(1)=-0.0004                                                      CCR01200
C     Y(2)=0.0004                                                       CCR01210
C     Y(3)=0.0012                                                       CCR01220
C     Y(4)=0.0020                                                       CCR01230
C     Y(5)=0.0028                                                       CCR01240
C     Y(6)=0.0036                                                       CCR01250
C     Y(7)=0.0044                                                       CCR01260
C     Y(8)=0.0052                                                       CCR01270
C     Y(9)=0.0060                                                       CCR01280
C     Y(10)=0.0068                                                      CCR01290
C     Y(11)=0.0080                                                      CCR01300
C     Y(12)=0.0100                                                      CCR01310
C     Y(13)=0.0120                                                      CCR01320
C     Y(14)=0.0152                                                      CCR01330
C     Y(15)=0.0164                                                      CCR01340
C     Y(16)=0.0174                                                      CCR01350
C     Y(17)=0.0184                                                      CCR01360
C     Y(18)=0.0196                                                      CCR01370
C     Y(19)=0.0208                                                      CCR01380
C     Y(20)=0.0220                                                      CCR01390
C     Y(21)=0.0231                                                      CCR01400
C     Y(22)=0.0243                                                      CCR01410
C     Y(23)=0.0256                                                      CCR01420
C     Y(24)=0.0268                                                      CCR01430
C     Y(25)=0.0280                                                      CCR01440
C     Y(26)=0.0292                                                      CCR01450
C     Y(27)=0.0304                                                      CCR01460
C     Y(28)=0.0314                                                      CCR01470
C     Y(29)=0.0322                                                      CCR01480
C                                                                       CCR01490
C-----DEPENDENT VARIABLE SELECTION                                      CCR01500
C-----THIS DETERMINES WHICH SUBROUTINES ARE TO BE USED                  CCR01510
C                                                                       CCR01520
```

```
      INCALU=.TRUE.                                                     CCR01530
      INCALV=.TRUE.                                                     CCR01540
      INCALP=.TRUE.                                                     CCR01550
      INCALT=.TRUE.                                                     CCR01560
      INCLUP=.TRUE.                                                     CCR01570
      INPRO=.TRUE.                                                      CCR01580
C                                                                       CCR01590
CC----INLET FLUID PROPERTIES-------------------------------------------CCR01600
C                                                                       CCR01610
C-----INLET TEMPERATURE IN K                                            CCR01620
C                                                                       CCR01630
      TINPRM=300.0                                                      CCR01640
      TINSEC=1200.0                                                     CCR01650
C                                                                       CCR01660
C-----DENSITY IN KG/M**3 AND VISCOSITY IN KG/M*S (DYNAMIC)              CCR01670
C                                                                       CCR01680
      DENSEC=101325.0/(287.0*TINSEC)                                    CCR01690
      VISSEC=1.5E-6*TINSEC**1.5/(TINSEC+130.0)                          CCR01700
      DENPRM=101325.0/(287.0*TINPRM)                                    CCR01710
      VISPRM=1.5E-6*TINPRM**1.5/(TINPRM+130.0)                          CCR01720
C                                                                       CCR01730
C-----AVERAGE PRANDTL NUMBER FROM 800-1200 K, ATMOSPHERIC PRESSURE      CCR01740
C     (PATM) IN KPA AND GAS CONSTANT (RR) IN KJ/KG K                    CCR01750
C                                                                       CCR01760
      PRANDL=0.700                                                      CCR01770
      PATM=101325.0                                                     CCR01780
      RR=287.0                                                          CCR01790
      CONST=RR/PATM                                                     CCR01800
C                                                                       CCR01810
CC----INITIALIZE GLOW BAR (HEATING ELEMENT) ZONE TEMPERATURE            CCR01820
C                                                                       CCR01830
C-----TEMPERATURES IN K                                                 CCR01840
C                                                                       CCR01850
      ZONE1=1700.0                                                      CCR01860
      ZONE2=1200.0                                                      CCR01870
      ZONE3=1200.0                                                      CCR01880
      ZONE4=1200.0                                                      CCR01890
C                                                                       CCR01900
      DO 211 I=2,NIM1                                                   CCR01910
      IF(I.LT.15) TGB(I)=ZONE1                                          CCR01920
      IF((I.GE.15).AND.(I.LT.20)) TGB(I)=ZONE2                          CCR01930
      IF((I.GE.20).AND.(I.LT.24)) TGB(I)=ZONE3                          CCR01940
      IF(I.GE.24) TGB(I)=ZONE4                                          CCR01950
 211  CONTINUE                                                          CCR01960
C                                                                       CCR01970
C-----PROGRAM CONTROL AND MONITOR                                       CCR01980
C                                                                       CCR01990
      MAXIT=300                                                         CCR02000
      URFU=0.5                                                          CCR02010
      URFV=0.5                                                          CCR02020
      URFP=0.25                                                         CCR02030
      URFT=0.75                                                         CCR02040
      SORMAX=0.010                                                      CCR02050
      GRAVTY=9.806                                                      CCR02060
```

```
C                                                                       CCR02070
CHAPTER  2  2  2  2  2  2  INITIAL OPERATIONS  2  2  2  2  2  2  2  2 2CCR02080
C                                                                       CCR02090
C**---THE C** COMMENTS WERE THE TERMS USED TO PREDICT THE FLOW          CCR02100
C**   FIELD USING THE ORIGINAL BURNER AND SUPPLIED FLOW RATES           CCR02110
C**   AND TEMPERATURE DATA                                              CCR02120
C                                                                       CCR02130
C-----COAL FEED RATE AND AIR MASS FLOWS IN KG/SEC                       CCR02140
C                                                                       CCR02150
      CMAS=0.001/60.0                                                   CCR02160
      PRIMAS=10.0*CMAS                                                  CCR02170
C**   PRIMAS=5.53378E-4                                                 CCR02180
C                                                                       CCR02190
C-----SECONDARY/PRIMARY MASS RATIO (M-S/M-P)                            CCR02200
C                                                                       CCR02210
      SPRAT=4.0                                                         CCR02220
      SECMAS=SPRAT*PRIMAS                                               CCR02230
C**   SECMAS=(4.7096E-3)/4.0                                            CCR02240
      RATIO=1.0+SPRAT                                                   CCR02250
C                                                                       CCR02260
C-----CALCULATE GEOMETRICAL QUANTITIES AND SET VARIABLES TO ZERO        CCR02270
      CALL INIT                                                         CCR02280
C                                                                       CCR02290
CC----CALCULATE AREAS                                                   CCR02300
C                                                                       CCR02310
      C=1.0                                                             CCR02320
      PI=4.0*ATAN(C)                                                    CCR02330
C                                                                       CCR02340
C**---THE ORIGINAL OR MODIFIED BURNER AREA MUST BE SPECIFIED             CCR02350
C                                                                       CCR02360
C-----AREA OF PRIMARY FLOW INLET                                        CCR02370
      APRM=(RV(6)**2)*PI                                                CCR02380
C                                                                       CCR02390
C-----AREA OF SECONDARY FLOW INLET                                      CCR02400
      ASEC=(RV(NJ)**2-RV(10)**2)*PI                                     CCR02410
C**   ASEC=(RV(26)**2-RV(18)**2)*PI                                     CCR02420
C                                                                       CCR02430
C-----SPECIFY INLET CONDITIONS - VELOCITIES IN (M/S)                    CCR02440
C                                                                       CCR02450
      UINPRM=PRIMAS/(APRM*DENPRM)                                       CCR02460
      UINSEC=SECMAS/(ASEC*DENSEC)                                       CCR02470
C                                                                       CCR02480
C**   RK=RV(18)/RV(26)                                                  CCR02490
C**   RKCST=(((1.0-RK**4)/(1.0-RK**2))-((1.0-RK**2)/ALOG(1.0/RK)))     CCR02500
C                                                                       CCR02510
      DO 203 I=1,NI                                                     CCR02520
      DO 200 J=10,NJM1                                                  CCR02530
      U(I,J)=UINSEC                                                     CCR02540
C**   DO 200 J=18,25                                                    CCR02550
C**   U(I,J)=(1.0-(R(J)/RV(26))**2+((1.0-RK**2)/(ALOG(1.0/RK)))        CCR02560
C**  @       *ALOG(R(J)/RV(26)))*2.0*UINSEC/RKCST                      CCR02570
 200  CONTINUE                                                          CCR02580
C                                                                       CCR02590
      DO 202 J=2,9                                                      CCR02600
```

```
C**   DO 202 J=2,17                                                    CCR02610
      IF(J.LE.5) U(I,J)=2.0*UINPRM*(1.0-(R(J)/RV(6))**2)               CCR02620
      IF(J.GT.5) U(I,J)=0.0                                            CCR02630
 202  CONTINUE                                                         CCR02640
 203  CONTINUE                                                         CCR02650
C                                                                      CCR02660
C-----INITIAL OUTPUT                                                   CCR02670
C                                                                      CCR02680
      WRITE(6,213) RATIO                                               CCR02690
      WRITE(6,219) UINPRM                                              CCR02700
      WRITE(6,220) UINSEC                                              CCR02710
      WRITE(6,221) TINPRM                                              CCR02720
      WRITE(6,217) TINSEC                                              CCR02730
      WRITE (6,711) ZONE1                                              CCR02740
      WRITE (6,712) ZONE2                                              CCR02750
      WRITE (6,713) ZONE3                                              CCR02760
      WRITE (6,714) ZONE4                                              CCR02770
C                                                                      CCR02780
C-----CALCULATE INLET REYNOLDS NUMBERS                                 CCR02790
C-----HYDRAULIC DIAMETER IS USED BELOW IE HYD DIA = 4*XS-AREA/WET PERMTRCCR02800
C                                                                      CCR02810
      REPRM=UINPRM*0.0032*2*DENPRM/VISPRM                              CCR02820
      RESEC=UINSEC*(4.0*ASEC/0.24)*DENSEC/VISSEC                       CCR02830
C**   RESEC=UINSEC*(4.0*ASEC/0.299)*DENSEC/VISSEC                      CCR02840
C                                                                      CCR02850
      WRITE(6,223) PRANDL                                              CCR02860
      WRITE(6,229) REPRM                                               CCR02870
      WRITE(6,230) RESEC                                               CCR02880
      WRITE(6,250) VISSEC                                              CCR02890
      WRITE(6,260) DENSEC                                              CCR02900
C                                                                      CCR02910
      IF(INCALU) CALL PRINT(2,2,NI,NJ,IT,JT,XU,Y,U,HEDU)               CCR02920
C     IF(INCALV) CALL PRINT(2,2,NI,NJ,IT,JT,X,YV,V,HEDV)               CCR02930
C     IF(INCALP) CALL PRINT(2,2,NI,NJ,IT,JT,X,Y,P,HEDP)                CCR02940
C     IF(INCALT) CALL PRINT(2,2,NI,NJ,IT,JT,X,Y,T,HEDT)                CCR02950
C     IF(INPRO ) CALL PRINT(1,1,NI,NJ,IT,JT,X,Y,VIS,HEDM)              CCR02960
C     IF(INPRO ) CALL PRINT(1,1,NI,NJ,IT,JT,X,Y,DEN,HEDD)              CCR02970
C                                                                      CCR02980
C----------CALCULATE RESIDUAL SOURCE-NORMALIZATION FACTORS----------CCR02990
C                                                                      CCR03000
CHAPTER  3  3  3  3  3  3  3  ITERATION LOOP  3  3  3  3  3  3  3  3  3 CCR03010
C                                                                      CCR03020
  300 NITER=NITER+1                                                    CCR03030
C-----UPDATE MAIN DEPENDENT VARIABLES                                  CCR03040
      IF(INCALU) CALL CALCU                                            CCR03050
      IF(INCALV) CALL CALCV                                            CCR03060
      IF(INCALP) CALL CALCP                                            CCR03070
      IF(INCALT) CALL CALCT                                            CCR03080
C                                                                      CCR03090
C-----THIS CALCULATES THE MASS FLOW ENTERING THE FURNACE               CCR03100
      FLOWIN=0.0                                                       CCR03110
      XMOMIN=0.0                                                       CCR03120
      DO 111 J=2,NJM1                                                  CCR03130
      ARDEN=0.5*(DEN(2,J)+DEN(1,J))*RCV(J)*SNS(J)                      CCR03140
```

```
      XMONIN=XMONIN+ARDEN*U(2,J)*U(2,J)                                 CCR03150
      FLOWIN=FLOWIN+ARDEN*U(2,J)                                        CCR03160
  111 CONTINUE                                                          CCR03170
C                                                                       CCR03180
C-----THIS CALCULATES THE MASS FLOW LEAVING THE FURNACE                 CCR03190
C                                                                       CCR03200
      ARDENT=0.0                                                        CCR03210
      FLOW=0.0                                                          CCR03220
      DO 196 J=2,NJM1                                                   CCR03230
      ARDEN=0.5*(DEN(NIM1,J)+DEN(NIM1-1,J))*RCV(J)*SNS(J)               CCR03240
      ARDENT=ARDENT+ARDEN                                               CCR03250
  196 FLOW=FLOW+ARDEN*U(NIM1,J)                                         CCR03260
C                                                                       CCR03270
C-----THIS ADJUSTS THE FINAL VELOCITY IN ORDER TO CONSERVE MASS         CCR03280
      UINC=(FLOWIN-FLOW)/ARDENT                                         CCR03290
      DO 197 J=2,NJM1                                                   CCR03300
  197 U(NI,J)=U(NIM1,J)+UINC                                            CCR03310
C                                                                       CCR03320
C-----THIS CALCULATES THE AMOUNT OF RECIRCULATING FLOW                  CCR03330
C                                                                       CCR03340
      REFLOT=0.0                                                        CCR03350
      DO 169 I=2,NIM1                                                   CCR03360
      REFLO=0.0                                                         CCR03370
      DO 168 J=2,NJM1                                                   CCR03380
      REFL=0.5*(DEN(I,J)+DEN(I-1,J))*RCV(J)*SNS(J)*                     CCR03390
     *     0.5*(ABS(U(I,J))-U(I,J))                                     CCR03400
      REFLO=REFL+REFLO                                                  CCR03410
  168 CONTINUE                                                          CCR03420
      IF(REFLO.GT.REFLOT) REFLOT=REFLO                                  CCR03430
  169 CONTINUE                                                          CCR03440
C-----UPDATE FLUID PROPERITIES                                          CCR03450
      IF(INPRO) CALL PROPS                                              CCR03460
C                                                                       CCR03470
C-----INTERMEDIATE OUTPUT                                               CCR03480
C-----THE VALUES ARE NORMALIZED WITH THE INLET CONDITIONS               CCR03490
      RESORM=RESORM/FLOWIN                                              CCR03500
      RESORU=RESORU/XMONIN                                              CCR03510
      RESORV=RESORV/XMONIN                                              CCR03520
      RESORT=RESORT/(FLOWIN*TINPRM)                                     CCR03530
      REFLOT=REFLOT/FLOWIN                                              CCR03540
C                                                                       CCR03550
C-----AFTER EACH ITERATION, THE RESIDUAL SOURCE TERMS, A MONITORED      CCR03560
C     GRID POINT (5,5) AND THE HEAT FLUX IS PRINTED                     CCR03570
C                                                                       CCR03580
      WRITE(6,199)NITER,RESORU,RESORV,RESORM,RESORT,U(5,5),V(5,5),P(5,5)CCR03590
     *           ,HTFLX(2),HTFLX(NIM1)                                  CCR03600
  199 FORMAT(I5,7F11.5,2F14.5)                                          CCR03610
C-----INTERMEDIATE OUTPUT AFTER 40 ITERATIONS                           CCR03620
      IF(MOD(NITER,40).NE.0) GO TO 301                                  CCR03630
C     IF(INCALU) CALL PRINT(2,1,NI,NJ,IT,JT,XU,Y,U,HEDU)                CCR03640
C     IF(INCALV) CALL PRINT(1,2,NI,NJ,IT,JT,X,YV,V,HEDV)                CCR03650
C     IF(INCALP) CALL PRINT(2,2,NI,NJ,IT,JT,X,Y,P,HEDP)                 CCR03660
C     IF(INCALT) CALL PRINT(2,2,NI,NJ,IT,JT,X,Y,T,HEDT)                 CCR03670
C     IF(INPRO ) CALL PRINT(1,1,NI,NJ,IT,JT,X,Y,VIS,HEDM)               CCR03680
```

```
C     IF(INPRO ) CALL PRINT(1,1,NI,NJ,IT,JT,X,Y,DEN,HEDD)                CCR03690
 301  CONTINUE                                                           CCR03700
C                                                                       CCR03710
C-----TERMINATION TEST-------------------------------------------------- CCR03720
C                                                                       CCR03730
      SORCE=AMAX1(RESORM,RESORU,RESORV,RESORT)                          CCR03740
      IF(SORCE.LT.SORMAX) GO TO 302                                     CCR03750
      IF(NITER.EQ.25.AND.SORCE.GT.1.0E4*SORMAX) GO TO 302               CCR03760
      IF(NITER.EQ.MAXIT) GO TO 302                                      CCR03770
C                                                                       CCR03780
      GO TO 300                                                         CCR03790
 302  CONTINUE                                                          CCR03800
C                                                                       CCR03810
C-----FINAL OPERATIONS AND OUTPUT                                       CCR03820
C                                                                       CCR03830
      WRITE(6,311) NITER,RESORU,RESORV,RESORM,RESORT,UINC,REFLOT        CCR03840
      IF(INCALU) CALL PRINT(2,1,NI,NJ,IT,JT,XU,Y,U,HEDU)                CCR03850
      IF(INCALV) CALL PRINT(1,2,NI,NJ,IT,JT,X,YV,V,HEDV)                CCR03860
C     IF(INCALP) CALL PRINT(2,2,NI,NJ,IT,JT,X,Y,P,HEDP)                 CCR03870
      IF(INCALT) CALL PRINT(2,2,NI,NJ,IT,JT,X,Y,T,HEDT)                 CCR03880
C     IF(INPRO ) CALL PRINT(1,1,NI,NJ,IT,JT,X,Y,VIS,HEDM)               CCR03890
C     IF(INPRO ) CALL PRINT(1,1,NI,NJ,IT,JT,X,Y,DEN,HEDD)               CCR03900
C                                                                       CCR03910
CC----*NOTE - THIS SUBROUTINE IS SPECIFICALLY FOR THE CALCOMP PLOTTER   CCR03920
C                                                                       CCR03930
C-----PLOT SUBROUTINE----VELOCITY PROFILES                              CCR03940
C                                                                       CCR03950
C                                                                       CCR03960
C     XAXIS=32.0                                                        CCR03970
C     IF(INCLUP) XAXIS=60.0                                             CCR03980
C     CALL PLOTS(XAXIS,27.5)                                            CCR03990
C     CALL FACTOR(0.90)                                                 CCR04000
C                                                                       CCR04010
C-----DEVELOPING  VELOCITY PROFILES----RADIAL VS. AXIAL DISTANCE        CCR04020
C                                                                       CCR04030
C     CALL PLOT(2.0,2.0,-3)                                             CCR04040
C                                                                       CCR04050
C-----THIS DRAWS THE FURNACE WALL                                       CCR04060
C                                                                       CCR04070
C     CALL PLOT(22.0,15.95,3)                                           CCR04080
C     CALL PLOT(-1.0,15.95,2)                                           CCR04090
C     DO 166 I=1,46                                                     CCR04100
C     TIC=(I-1)*0.5-1.0                                                 CCR04110
C     TAC=I*0.5-1.25                                                    CCR04120
C     CALL PLOT(TIC,15.95,3)                                            CCR04130
C     CALL PLOT(TAC,16.25,2)                                            CCR04140
C 166 CONTINUE                                                          CCR04150
C     CALL PLOT(22.0,16.25,3)                                           CCR04160
C     CALL PLOT(-1.0,16.25,2)                                           CCR04170
C     DO 161 K=1,5                                                      CCR04180
C     AAA=(K-1)*3.75                                                    CCR04190
C     CALL PLOT(AAA,17.5,3)                                             CCR04200
C     CALL PLOT(AAA,16.5,2)                                             CCR04210
C 161 CONTINUE                                                          CCR04220
```

```
C     CALL SYMBOL(1.4,16.5,0.32,'ZONE 1',90.0,6)                    CCR04230
C     CALL NUMBER(2.4,16.5,0.32,ZONE1,90.0,-1)                      CCR04240
C     CALL SYMBOL(2.4,18.1,0.32,'K',90.0,1)                         CCR04250
C     CALL SYMBOL(5.1,16.5,0.32,'ZONE 2',90.0,6)                    CCR04260
C     CALL NUMBER(6.1,16.5,0.32,ZONE2,90.0,-1)                      CCR04270
C     CALL SYMBOL(6.1,18.1,0.32,'K',90.0,1)                         CCR04280
C     CALL SYMBOL(8.9,16.5,0.32,'ZONE 3',90.0,6)                    CCR04290
C     CALL NUMBER(9.9,16.5,0.32,ZONE3,90.0,-1)                      CCR04300
C     CALL SYMBOL(9.9,18.1,0.32,'K',90.0,1)                         CCR04310
C     CALL SYMBOL(12.6,16.5,0.32,'ZONE 4',90.0,6)                   CCR04320
C     CALL NUMBER(13.6,16.5,0.32,ZONE4,90.0,-1)                     CCR04330
C     CALL SYMBOL(13.6,18.1,0.32,'K',90.0,1)                        CCR04340
CC    CALL SYMBOL(13.0,16.5,.35,'FURNACE   WALL',0.0,14)            CCR04350
C                                                                   CCR04360
C-----THIS DRAWS THE CENTRE LINE                                    CCR04370
C                                                                   CCR04380
C     DO 165 I=1,8                                                  CCR04390
C     SPC1=3.0*I-4.0                                                CCR04400
C     DASH=SPC1+2.0                                                 CCR04410
C     SPC2=DASH+0.45                                                CCR04420
C     DOT=SPC2+0.1                                                  CCR04430
C     CALL PLOT(SPC1,8.0,3)                                         CCR04440
C     CALL PLOT(DASH,8.0,2)                                         CCR04450
C     CALL PLOT(SPC2,8.0,3)                                         CCR04460
C     IF(I.LT.8) CALL PLOT(DOT,8.0,2)                               CCR04470
C 165 CONTINUE                                                      CCR04480
C     DO 177 I=1,3                                                  CCR04490
C     PEP=(I-1)*7.5+0.18                                            CCR04500
C     PEP1=(I-1)*1.0                                                CCR04510
C     CALL NUMBER(PEP,7.2,0.35,PEP1,90.0,-1)                        CCR04520
C 177 CONTINUE                                                      CCR04530
C     CALL SYMBOL(2.0,6.2,0.35,'X',90.0,1)                          CCR04540
C     CALL SYMBOL(7.68,6.2,0.35,'M',90.0,1)                         CCR04550
C                                                                   CCR04560
C-----THIS DRAWS THE BURNER MOUTH                                   CCR04570
C                                                                   CCR04580
C     CALL PLOT(-1.0,8.80,3)                                        CCR04590
C     CALL PLOT(0.0,8.80,2)                                         CCR04600
C     CALL PLOT(0.0,9.60,2)                                         CCR04610
C     CALL PLOT(-1.0,9.60,2)                                        CCR04620
C                                                                   CCR04630
C     DO 701 J=1,3                                                  CCR04640
C     TICA=(J*2.5)+8.0                                              CCR04650
C     TICB=TICA-0.25                                                CCR04660
C     RRNUM=J*10.0                                                  CCR04670
C     CALL PLOT(0.0,TICA,3)                                         CCR04680
C     CALL PLOT(-0.3,TICA,2)                                        CCR04690
C     CALL NUMBER(-0.4,TICB,0.35,RRNUM,90.0,-1)                     CCR04700
C701  CONTINUE                                                      CCR04710
C     CALL SYMBOL(-0.4,11.6,0.35,'R',90.0,1)                        CCR04720
C     CALL SYMBOL(-0.4,14.0,0.35,'MM',90.0,2)                       CCR04730
C                                                                   CCR04740
C     CALL PLOT(0.0,15.95,3)                                        CCR04750
C     CALL PLOT(0.0,7.7,2)                                          CCR04760
```

```
C     DO 98 I=4,NI,4                                                    CCR04770
C     XX=XU(I)*7.5                                                      CCR04780
C     CALL PLOT(XX,15.95,3)                                             CCR04790
C     CALL PLOT(XX,7.7,2)                                               CCR04800
C     NX=XX+0.25                                                        CCR04810
C     RR=R(2)*250.0+8.0                                                 CCR04820
C     UU=(U(I,2)/UINPRM)*3.75+XX                                        CCR04830
C     CALL PLOT(UU,RR,3)                                                CCR04840
C     DO 99 J=3,NJM1                                                    CCR04850
C     RR=R(J)*250.0+8.0                                                 CCR04860
C     UU=(U(I,J)/UINPRM)*3.75+XX                                        CCR04870
C     CALL PLOT(UU,RR,2)                                                CCR04880
C 99  CONTINUE                                                          CCR04890
C     CALL PLOT(XX,15.95,2)                                             CCR04900
C 98  CONTINUE                                                          CCR04910
C     CALL PLOT(6.82,5.0,3)                                             CCR04920
C     CALL PLOT(0.0,5.0,2)                                              CCR04930
C     DO 101 K=1,9                                                      CCR04940
C     D=(K-1)*0.8523                                                    CCR04950
C     CALL PLOT(D,5.0,3)                                                CCR04960
C     CALL PLOT(D,4.8,2)                                                CCR04970
C     DD=D+0.18                                                         CCR04980
C     IF(UINPRM.GT.3.0) DND=(K-1)*1.0                                   CCR04990
C     IF(UINPRM.LT.3.0) DND=(K-1)*0.5                                   CCR05000
C     CALL NUMBER(DD,3.7,0.35,DND,90.0,1)                               CCR05010
C 101 CONTINUE                                                          CCR05020
C     CALL SYMBOL(2.0,2.65,0.35,'U',90.0,1)                             CCR05030
C     CALL SYMBOL(4.0,2.3,0.35,'M/S',90.0,3)                            CCR05040
C     CALL SYMBOL(22.0,9.5,0.35,'M-S/M-P =       ',90.0,16)             CCR05050
C     CALL SYMBOL(20.5,9.5,0.35,'   T-GB =      K',90.0,16)             CCR05060
C     CALL SYMBOL(21.0,9.5,0.35,'  T-SEC =      K',90.0,16)             CCR05070
C     CALL SYMBOL(21.5,9.5,0.35,'  U-SEC =      M/S',90.0,18)           CCR05080
C     CALL NUMBER(21.5,13.0,0.35,UINSEC,90.0,2)                         CCR05090
C     CALL NUMBER(20.5,13.0,0.35,TMPGLB,90.0,-1)                        CCR05100
C     CALL NUMBER(21.0,13.0,0.35,TINSEC,90.0,-1)                        CCR05110
C     CALL NUMBER(22.0,13.0,0.35,SPRAT,90.0,1)                          CCR05120
C                                                                       CCR05130
C     CALL SYMBOL(0.5,23.0,.84,'CCRL FURNACE VELOCITY PROFILES',0.0,30) CCR05140
C     CALL SYMBOL(0.5,21.5,.35,'AVG. PRIMARY INLET VELOCITY       M/S', CCR05150
C    *            0.0,37)                                               CCR05160
C     CALL NUMBER(10.3,21.5,.35,UINPRM,0.0,3)                           CCR05170
C     CALL SYMBOL(0.5,21.0,.35,'AVG. SECONDARY INLET VELOCITY       M/S'CCR05180
C    *            ,0.0,39)                                              CCR05190
C     CALL NUMBER(11.0,21.0,.35,UINSEC,0.0,3)                           CCR05200
C     CALL SYMBOL(0.5,20.0,.35,'PRIMARY INLET TEMPERATURE      K',.0,32)CCR05210
C     CALL NUMBER(9.9,20.0,.35,TINPRM,0.0,-1)                           CCR05220
C     CALL SYMBOL(0.5,19.5,.35,'SECONDARY INLET TEMPERATURE     K', .0 CCR05230
C    *            ,34)                                                  CCR05240
C     CALL NUMBER(10.2,19.5,.35,TINSEC,0.0,-1)                          CCR05250
C     CALL SYMBOL(0.5,18.5,.35,'PRIMARY INLET REYNOLDS NUMBER',0.0,29)  CCR05260
C     CALL NUMBER(11.2,18.5,.35,REPRM,0.0,-1)                           CCR05270
C     CALL SYMBOL(0.5,18.0,.35,'SECONDARY INLET REYNOLDS NUMBER',0.0,31)CCR05280
C     CALL NUMBER(11.9,18.0,.35,RESEC,0.0,-1)                           CCR05290
C                                                                       CCR05300
```

```
C-----THIS SECTION MUST BE CHANGED MANUALLY FOR CHF OR CWT                CCR05310
C                                                                        CCR05320
C     CALL SYMBOL(16.5,21.5,.35,'ZONE #1  TEMPERATURE  1700   K',0.0,30)CCR05330
C     CALL SYMBOL(16.5,21.0,.35,'ZONE #2  TEMPERATURE  1700   K',0.0,30)CCR05340
C     CALL SYMBOL(16.5,20.5,.35,'ZONE #3  TEMPERATURE  1700   K',0.0,30)CCR05350
C     CALL SYMBOL(16.5,20.0,.35,'ZONE #4  TEMPERATURE  1700   K',0.0,30)CCR05360
C                                                                        CCR05370
C-----THE FOLLOWING STATEMENT CALLS THE PARTICLE HEATING SUBROUTINE       CCR05380
C                                                                        CCR05390
C-----THIS CALLS THE PARTICLE HEATING SUBROUTINE                         CCR05400
C                                                                        CCR05410
      IF(INCLUP) CALL CALCUP                                             CCR05420
C     CALL PLOT(0.0,0.0,999)                                             CCR05430
      STOP                                                               CCR05440
C                                                                        CCR05450
C-----FORMAT STATEMENTS                                                  CCR05460
  213 FORMAT(1HO,5X,'LAMBDA                    ',T50,'=',1PE11.3)        CCR05470
  221 FORMAT(1H0,5X,'PRM INLET TEMPERATURE ',T50,'=',1PE11.3,2X,'K')     CCR05480
  217 FORMAT(1H0,5X,'SEC INLET TEMPERATURE ',T50,'=',1PE11.3,2X,'K')     CCR05490
  711 FORMAT(1HO,5X,'TEMPERATURE OF ZONE1',T50,'=',1PE11.3,2X,'K')       CCR05500
  712 FORMAT(1HO,5X,'TEMPERATURE OF ZONE2',T50,'=',1PE11.3,2X,'K')       CCR05510
  713 FORMAT(1HO,5X,'TEMPERATURE OF ZONE3',T50,'=',1PE11.3,2X,'K')       CCR05520
  714 FORMAT(1HO,5X,'TEMPERATURE OF ZONE4',T50,'=',1PE11.3,2X,'K')       CCR05530
  219 FORMAT(1H0,5X,'PRM INLET VELOCITY (PARB)',T50,'=',1PE11.3,2X,      CCR05540
     8       'M/S')                                                      CCR05550
  220 FORMAT(1H0,5X,'SEC INLET VELOCITY (UNFM)',T50,'=',1PE11.3,2X,      CCR05560
     *       'M/S')                                                      CCR05570
  223 FORMAT(1H0,5X,'AVG. PRANDTL NUMBER',T50,'=',1PE11.3)               CCR05580
  229 FORMAT(1H0,5X,'PRM REYNOLDS NO.',T50,'=',1PE11.3,2X,'(INLET)')     CCR05590
  230 FORMAT(1H0,5X,'SEC REYNOLDS NO.',T50,'=',1PE11.3,2X,'(INLET)')     CCR05600
  250 FORMAT(1H0,5X,'LAMINAR VISCOSITY ',T50,'=',1PE11.3,2X,             CCR05610
     *       'KG/M*S (INLET)')                                           CCR05620
  260 FORMAT(1H0,5X,'FLUID DENSITY ',T50,'=',1PE11.3,2X,                 CCR05630
     *       'KG/M**3 (INLET)')                                          CCR05640
  311 FORMAT(//1H0,5X,'NUMBER OF ITERATIONS',T50,'=',I3,/,1H0,5X,        CCR05650
     *       'U VEL RESIDUAL',T50,'=',1PE11.3,/,1H0,5X,'V VEL RESIDUAL',CCR05660
     *       T50,'=',1PE11.3,/,1H0,5X,'MASS RESIDUAL',T50,'=',1PE11.3,  CCR05670
     *       /,1H0,5X,'TEMP RESIDUAL',T50,'=',1PE11.3,/,1H0,5X,         CCR05680
     *       'FINAL U VELOCITY DIFFERENCE',T50,'=',1PE11.3,             CCR05690
     *       /,1H0,5X,'RECIRCULATED MASS',T50,'=',1PE11.3)              CCR05700
      END                                                                CCR05710
C                                                                        CCR05720
C                                                                        CCR05730
      SUBROUTINE INIT                                                    CCR05740
C                                                                        CCR05750
CHAPTER  0  0  0  0  0  0  0  0  PRELIMINARIES  0  0  0  0  0  0  0  0   CCR05760
C                                                                        CCR05770
      COMMON                                                             CCR05780
     1/UVEL/RESORU,NSWPU,URFU,DXEPU(32),DXPWU(32),SEWU(32)               CCR05790
     1/VVEL/RESORV,NSWPV,URFV,DYNPV(32),DYPSV(32),SNSV(32)               CCR05800
     1/PCOR/RESORM,NSWPP,URFP,DU(30,30),DV(30,30),IPREF,JPREF            CCR05810
     1/VAR/U(30,30),V(30,30),P(30,30),PP(30,30)                          CCR05820
     1/ALL/IT,JT,NI,NJ,NIM1,NJM1,GREAT                                   CCR05830
      COMMON                                                             CCR05840
```

```
     1/GEOM/X(32),Y(32),DXEP(32),DXPW(32),DYNP(32),DYPS(32),                CCR05850
     1       SNS(32),SEW(32),XU(32),YV(32),R(32),RV(32),RCV(32)             CCR05860
     1/FLUPR/VISSEC,DENSEC,PRANDL,DEN(30,30),VIS(30,30),CONST,              CCR05870
     1        VISPRM,DENPRM,SECMAS,PRMMAS,SPRAT                             CCR05880
      COMMON                                                                CCR05890
     1/PROB1/UINPRM,UINSEC,GRAVTY,FLOWIN,NITER                              CCR05900
     1/COEF/AP(30,30),AN(30,30),AS(30,30),AE(30,30),AW(30,30),SU(30,30),    CCR05910
     1       SP(30,30)                                                      CCR05920
      COMMON                                                                CCR05930
     1/TEMP/T(30,30),GAMH(30,30),RESORT,NSWPT,URFT,                         CCR05940
     2       TINPRM,TINSEC,TGB(30),HTFLX(30),HFXOLD(30)                     CCR05950
C                                                                           CCR05960
CHAPTER  1  1  1  1  1  CALCULATE GEOMETRIC COEFFICIENTS  1  1  1  1 1      CCR05970
C                                                                           CCR05980
      DO 100 J=1,NJ                                                         CCR05990
  100 R(J)=Y(J)                                                             CCR06000
      DXPW(1)=0.0                                                           CCR06010
      DXEP(NI)=0.0                                                          CCR06020
      DO 101 I=1,NIM1                                                       CCR06030
      DXEP(I)=X(I+1)-X(I)                                                   CCR06040
  101 DXPW(I+1)=DXEP(I)                                                     CCR06050
      DYPS(1)=0.0                                                           CCR06060
      DYNP(NJ)=0.0                                                          CCR06070
      DO 102 J=1,NJM1                                                       CCR06080
      DYNP(J)=Y(J+1)-Y(J)                                                   CCR06090
  102 DYPS(J+1)=DYNP(J)                                                     CCR06100
      SEW(1)=0.0                                                            CCR06110
      SEW(NI)=0.0                                                           CCR06120
      DO 103 I=2,NIM1                                                       CCR06130
  103 SEW(I)=0.5*(DXEP(I)+DXPW(I))                                          CCR06140
      SNS(1)=0.0                                                            CCR06150
      SNS(NJ)=0.0                                                           CCR06160
      DO 104 J=2,NJM1                                                       CCR06170
  104 SNS(J)=0.5*(DYNP(J)+DYPS(J))                                          CCR06180
      XU(1)=0.0                                                             CCR06190
      DO 105 I=2,NI                                                         CCR06200
  105 XU(I)=0.5*(X(I)+X(I-1))                                               CCR06210
      DXPWU(1)=0.0                                                          CCR06220
      DXPWU(2)=0.0                                                          CCR06230
      DXEPU(1)=0.0                                                          CCR06240
      DXEPU(NI)=0.0                                                         CCR06250
      DO 106 I=2,NIM1                                                       CCR06260
      DXEPU(I)=XU(I+1)-XU(I)                                                CCR06270
  106 DXPWU(I+1)=DXEPU(I)                                                   CCR06280
      SEWU(1)=0.0                                                           CCR06290
      DO 107 I=2,NI                                                         CCR06300
  107 SEWU(I)=X(I)-X(I-1)                                                   CCR06310
      YV(1)=0.0                                                             CCR06320
      RV(1)=0.0                                                             CCR06330
      DO 108 J=2,NJ                                                         CCR06340
      RV(J)=0.5*(R(J)+R(J-1))                                               CCR06350
  108 YV(J)=0.5*(Y(J)+Y(J-1))                                               CCR06360
      RCV(1)=R(1)                                                           CCR06370
      RCV(NJ)=R(NJ)                                                         CCR06380
```

```
      DO 113 J=2,NJM1                                                   CCR06390
  113 RCV(J)=0.5*(RV(J+1)+RV(J))                                        CCR06400
      DYPSV(1)=0.0                                                      CCR06410
      DYPSV(2)=0.0                                                      CCR06420
      DYNPV(NJ)=0.0                                                     CCR06430
      DO 109 J=2,NJM1                                                   CCR06440
      DYNPV(J)=YV(J+1)-YV(J)                                            CCR06450
  109 DYPSV(J+1)=DYNPV(J)                                               CCR06460
      SNSV(1)=0.0                                                       CCR06470
      DO 110 J=2,NJ                                                     CCR06480
  110 SNSV(J)=Y(J)-Y(J-1)                                               CCR06490
C                                                                       CCR06500
CHAPTER  2  2  2  2  2  2  SET VARIABLES TO ZERO  2  2  2  2  2  2       CCR06510
C                                                                       CCR06520
      DO 201 I=1,NI                                                     CCR06530
      DO 200 J=1,NJ                                                     CCR06540
      U(I,J)=0.0                                                        CCR06550
      V(I,J)=0.0                                                        CCR06560
      P(I,J)=0.0                                                        CCR06570
      IF(J.GE.10) T(I,J)=TINSEC                                         CCR06580
      IF(J.LT.10) T(I,J)=TINPRM                                         CCR06590
      PP(I,J)=0.0                                                       CCR06600
      IF(J.GE.10) DEN(I,J)=DENSEC                                       CCR06610
      IF(J.GE.10) VIS(I,J)=VISSEC                                       CCR06620
      IF(J.LT.10) DEN(I,J)=DENPRM                                       CCR06630
      IF(J.LT.10) VIS(I,J)=VISPRM                                       CCR06640
      IF(J.GE.10) GAMH(I,J)=VISSEC/PRANDL                               CCR06650
      IF(J.LT.10) GAMH(I,J)=VISPRM/PRANDL                               CCR06660
      DU(I,J)=0.0                                                       CCR06670
      DV(I,J)=0.0                                                       CCR06680
      SU(I,J)=0.0                                                       CCR06690
      SP(I,J)=0.0                                                       CCR06700
  200 CONTINUE                                                          CCR06710
  201 CONTINUE                                                          CCR06720
      DO 202 I=1,NI                                                     CCR06730
      HTFLX(I)=0.0                                                      CCR06740
  202 HFXOLD(I)=0.0                                                     CCR06750
      RETURN                                                            CCR06760
      END                                                               CCR06770
C                                                                       CCR06780
C                                                                       CCR06790
      SUBROUTINE PROPS                                                  CCR06800
C                                                                       CCR06810
CHAPTER  0  0  0  0  0  0  0  0  PRELIMINARIES  0  0  0  0  0  0  0  0  CCR06820
C                                                                       CCR06830
      COMMON                                                            CCR06840
     1/FLUPR/VISSEC,DENSEC,PRANDL,DEN(30,30),VIS(30,30),CONST,          CCR06850
     1       VISPRM,DENPRM,SECMAS,PRMMAS,SPRAT                          CCR06860
     1/VAR/U(30,30),V(30,30),P(30,30),PP(30,30)                         CCR06870
     1/ALL/IT,JT,NI,NJ,NIM1,NJM1,GREAT                                  CCR06880
     1/TEMP/T(30,30),GAMH(30,30),RESORT,NSWPT,URFT,                     CCR06890
     2     TINPRM,TINSEC,TGB(30),HTFLX(30),HFXOLD(30)                   CCR06900
C                                                                       CCR06910
C                                                                       CCR06920
```

```
C---- SUTHERLAND EQUATION; B AND S CONSTANTS                          CCR06930
      B=1.5E-6                                                        CCR06940
      S=130.                                                          CCR06950
      DO 100 I=1,NI                                                   CCR06960
      DO 100 J=1,NJM1                                                 CCR06970
      DEN(I,J)=1.0/(T(I,J)*CONST)                                     CCR06980
      VIS(I,J)=B*(T(I,J)**(1.5))/(S+T(I,J))                           CCR06990
      GAMH(I,J)=VIS(I,J)/PRANDL                                       CCR07000
  100 CONTINUE                                                        CCR07010
      RETURN                                                          CCR07020
      END                                                             CCR07030
C                                                                     CCR07040
      SUBROUTINE CALCU                                                CCR07050
C                                                                     CCR07060
CHAPTER  0  0  0  0  0  0  0  0  PRELIMINARIES  0  0  0  0  0  0  0  0 CCR07070
C                                                                     CCR07080
      COMMON                                                          CCR07090
     1/UVEL/RESORU,NSWPU,URFU,DXEPU(32),DXPWU(32),SEWU(32)            CCR07100
     1/VVEL/RESORV,NSWPV,URFV,DYNPV(32),DYPSV(32),SNSV(32)            CCR07110
     1/PCOR/RESORM,NSWPP,URFP,DU(30,30),DV(30,30),IPREF,JPREF         CCR07120
     1/VAR/U(30,30),V(30,30),P(30,30),PP(30,30)                       CCR07130
     1/ALL/IT,JT,NI,NJ,NIM1,NJM1,GREAT                                CCR07140
      COMMON                                                          CCR07150
     1/GEOM/X(32),Y(32),DXEP(32),DXPW(32),DYNP(32),DYPS(32),          CCR07160
     1       SNS(32),SEW(32),XU(32),YV(32),R(32),RV(32),RCV(32)       CCR07170
     1/FLUPR/VISSEC,DENSEC,PRANDL,DEN(30,30),VIS(30,30),CONST,        CCR07180
     1        VISPRM,DENPRM,SECMAS,PRMMAS,SPRAT                       CCR07190
      COMMON                                                          CCR07200
     1/COEF/AP(30,30),AN(30,30),AS(30,30),AE(30,30),AW(30,30),SU(30,30),CCR07210
     1       SP(30,30)                                                CCR07220
     1/PROB1/UINPRM,UINSEC,GRAVTY,FLOWIN,NITER                        CCR07230
      COMMON                                                          CCR07240
     1/TEMP/T(30,30),GAMH(30,30),RESORT,NSWPT,URFT,                   CCR07250
     2       TINPRM,TINSEC,TGB(30),HTFLX(30),HFXOLD(30)               CCR07260
C                                                                     CCR07270
CHAPTER  1  1  1  1  1  1  ASSEMBLY OF COEFFICIENTS  1  1  1  1  1  1CCR07280
C                                                                     CCR07290
      DO 100 I=3,NIM1                                                 CCR07300
      DO 101 J=2,NJM1                                                 CCR07310
C-----COMPUTE AREAS AND VOLUME                                        CCR07320
      AREAN=RV(J+1)*SEWU(I)                                           CCR07330
      AREAS=RV(J)*SEWU(I)                                             CCR07340
      AREAEW=RCV(J)*SNS(J)                                            CCR07350
      VOL=RCV(J)*SEWU(I)*SNS(J)                                       CCR07360
C-----CALCULATE CONVECTION COEFFICIENTS                               CCR07370
      GN=0.5*(DEN(I,J+1)+DEN(I,J))*V(I,J+1)                           CCR07380
      GS=0.5*(DEN(I,J-1)+DEN(I,J))*V(I,J)                             CCR07390
      GNW=0.5*(DEN(I-1,J)+DEN(I-1,J+1))*V(I-1,J+1)                    CCR07400
      GSW=0.5*(DEN(I-1,J)+DEN(I-1,J-1))*V(I-1,J)                      CCR07410
      GE=0.5*(DEN(I+1,J)+DEN(I,J))*U(I+1,J)                           CCR07420
      GP=0.5*(DEN(I,J)+DEN(I-1,J))*U(I,J)                             CCR07430
      GW=0.5*(DEN(I-1,J)+DEN(I-2,J))*U(I-1,J)                         CCR07440
      CN=0.5*(GN+GNW)*AREAN                                           CCR07450
      CS=0.5*(GS+GSW)*AREAS                                           CCR07460
```

```
      CE=0.5*(GE+GP)*AREAEW                                              CCR07470
      CW=0.5*(GP+GW)*AREAEW                                              CCR07480
C-----CALCULATE DIFFUSION COEFFICIENTS                                   CCR07490
      VISN=0.25*(VIS(I,J)+VIS(I,J+1)+VIS(I-1,J)+VIS(I-1,J+1))            CCR07500
      VISS=0.25*(VIS(I,J)+VIS(I,J-1)+VIS(I-1,J)+VIS(I-1,J-1))            CCR07510
      DN=VISN*AREAN/DYNP(J)                                              CCR07520
      DS=VISS*AREAS/DYPS(J)                                              CCR07530
      DE=VIS(I,J)*AREAEW/DXEPU(I)                                        CCR07540
      DW=VIS(I-1,J)*AREAEW/DXPWU(I)                                      CCR07550
C-----CALCULATE COEFFICIENTS OF SOURCE TERMS                             CCR07560
      SMP=CN-CS+CE-CW                                                    CCR07570
      CP=AMAX1(0.0,SMP)                                                  CCR07580
      CPO=CP                                                             CCR07590
C-----ASSEMBLE MAIN COEFFICIENTS                                         CCR07600
C     IF(DS.EQ.0.0) DS=1.0E-25                                           CCR07610
      AN(I,J)=AMAX1(ABS(0.5*CN),DN)-0.5*CN                               CCR07620
      AS(I,J)=AMAX1(ABS(0.5*CS),DS)+0.5*CS                               CCR07630
      AW(I,J)=AMAX1(ABS(0.5*CW),DW)+0.5*CW                               CCR07640
      AE(I,J)=AMAX1(ABS(0.5*CE),DE)-0.5*CE                               CCR07650
C     AN(I,J)=DN*AMAX1(0.0,(1.0-0.1*ABS(CN/DN))**5)+AMAX1(-CN,0.0)       CCR07660
C     AS(I,J)=DS*AMAX1(0.0,(1.0-0.1*ABS(CS/DS))**5)+AMAX1(CS,0.0)        CCR07670
C     AE(I,J)=DE*AMAX1(0.0,(1.0-0.1*ABS(CE/DE))**5)+AMAX1(-CE,0.0)       CCR07680
C     AW(I,J)=DW*AMAX1(0.0,(1.0-0.1*ABS(CW/DW))**5)+AMAX1(CW,0.0)        CCR07690
      DU(I,J)=AREAEW                                                     CCR07700
      DUDXE=(U(I+1,J)-U(I,J))/DXEPU(I)                                   CCR07710
      DUDXW=(U(I,J)-U(I-1,J))/DXPWU(I)                                   CCR07720
      SORCE1=(DUDXE*VIS(I,J)-DUDXW*VIS(I-1,J))/SEWU(I)                   CCR07730
      DVDXN=(V(I,J+1)-V(I-1,J+1))/SEWU(I)                                CCR07740
      DVDXS=(V(I,J)-V(I-1,J))/SEWU(I)                                    CCR07750
      DYVDYE=(RV(J+1)*V(I,J+1)-RV(J)*V(I,J))/SNS(J)                      CCR07760
      DYVDYW=(RV(J+1)*V(I-1,J+1)-RV(J)*V(I-1,J))/SNS(J)                  CCR07770
      SORCE2=(RV(J+1)*VISN*DVDXN-RV(J)*VISS*DVDXS)/(RCV(J)*DYNPV(J))     CCR07780
      SORCE3=0.0                                                         CCR07790
C     SORCE3=-(2.0/3.0)*((VIS(I,J)*(DYVDYE/R(J)+DUDXE)-VIS(I-1,J)*       CCR07800
C    *         (DYVDYW/R(J)+DUDXW))/SEWU(I))                           CCR07810
      SU(I,J)=CPO*U(I,J)+DU(I,J)*(P(I-1,J)-P(I,J))                       CCR07820
      SU(I,J)=SU(I,J)+(SORCE1+SORCE2+SORCE3)*VOL                         CCR07830
      SP(I,J)=-CP                                                        CCR07840
      DENU=(DEN(I,J)+DEN(I-1,J))/2.                                      CCR07850
      DENA=(DEN(I,2)+DEN(I-1,2))/2.                                      CCR07860
      SU(I,J)=SU(I,J)+GRAVTY*(DENU-DENA)*VOL                             CCR07870
  101 CONTINUE                                                           CCR07880
  100 CONTINUE                                                           CCR07890
C                                                                        CCR07900
CHAPTER  2  2  2  2  2  2  2  PROBLEM MODIFICATIONS  2  2  2  2  2  2 2CCR07910
C                                                                        CCR07920
      CALL MODU                                                          CCR07930
C                                                                        CCR07940
CHAPTER  3  FINAL COEFF. ASSEMBLY AND RESIDUAL SOURCE CALCULATION  3  3 CCR07950
C                                                                        CCR07960
      RESORU=0.0                                                         CCR07970
      DO 300 I=3,NIM1                                                    CCR07980
      DO 301 J=2,NJM1                                                    CCR07990
      AP(I,J)=AN(I,J)+AS(I,J)+AE(I,J)+AW(I,J)-SP(I,J)                    CCR08000
```

```
      DU(I,J)=DU(I,J)/AP(I,J)                                          CCR08010
      RESOR=AN(I,J)*U(I,J+1)+AS(I,J)*U(I,J-1)+AE(I,J)*U(I+1,J)         CCR08020
     1     +AW(I,J)*U(I-1,J)-AP(I,J)*U(I,J)+SU(I,J)                    CCR08030
      VOL=RCV(J)*SEWU(I)*SNS(J)                                        CCR08040
      SORVOL=GREAT*VOL                                                 CCR08050
      IF(-SP(I,J).GT.0.5*SORVOL)  RESOR=RESOR/SORVOL                   CCR08060
      RESORU=RESORU+ABS(RESOR)                                         CCR08070
C-----UNDER-RELAXATION                                                 CCR08080
      AP(I,J)=AP(I,J)/URFU                                             CCR08090
      SU(I,J)=SU(I,J)+(1.-URFU)*AP(I,J)*U(I,J)                         CCR08100
      DU(I,J)=DU(I,J)*URFU                                             CCR08110
  301 CONTINUE                                                         CCR08120
  300 CONTINUE                                                         CCR08130
C                                                                      CCR08140
CHAPTER  4  4  4  SOLUTION OF DIFFERENCE EQUATION  4  4  4  4  4  4  4 CCR08150
C                                                                      CCR08160
      DO 400 N=1,NSWPU                                                 CCR08170
  400 CALL LISOLV(3,2,NI,NJ,IT,JT,U)                                   CCR08180
      RETURN                                                           CCR08190
      END                                                              CCR08200
C                                                                      CCR08210
      SUBROUTINE CALCV                                                 CCR08220
C                                                                      CCR08230
CHAPTER  0  0  0  0  0  0  0  0  PRELIMINARIES  0  0  0  0  0  0  0  0 CCR08240
C                                                                      CCR08250
      COMMON                                                           CCR08260
     1/UVEL/RESORU,NSWPU,URFU,DXEPU(32),DXPWU(32),SEWU(32)             CCR08270
     1/VVEL/RESORV,NSWPV,URFV,DYNPV(32),DYPSV(32),SNSV(32)             CCR08280
     1/PCOR/RESORM,NSWPP,URFP,DU(30,30),DV(30,30),IPREF,JPREF          CCR08290
     1/VAR/U(30,30),V(30,30),P(30,30),PP(30,30)                        CCR08300
      COMMON                                                           CCR08310
     1/GEOM/X(32),Y(32),DXEP(32),DXPW(32),DYNP(32),DYPS(32),           CCR08320
     1       SNS(32),SEW(32),XU(32),YV(32),R(32),RV(32),RCV(32)        CCR08330
     1/ALL/IT,JT,NI,NJ,NIM1,NJM1,GREAT                                 CCR08340
     1/FLUPR/VISSEC,DENSEC,PRANDL,DEN(30,30),VIS(30,30),CONST,         CCR08350
     1        VISPRM,DENPRM,SECMAS,PRMMAS,SPRAT                        CCR08360
      COMMON                                                           CCR08370
     1/COEF/AP(30,30),AN(30,30),AS(30,30),AE(30,30),AW(30,30),SU(30,30),CCR08380
     1       SP(30,30)                                                 CCR08390
     1/PROB1/UINPRM,UINSEC,GRAVTY,FLOWIN,NITER                         CCR08400
C                                                                      CCR08410
CHAPTER  1  1  1  1  1  1  ASSEMBLY OF COEFFICIENTS  1  1  1  1  1  1 CCR08420
C                                                                      CCR08430
      DO 100 I=2,NIM1                                                  CCR08440
      DO 101 J=3,NJM1                                                  CCR08450
C-----COMPUTE AREAS AND VOLUME                                         CCR08460
      AREAN=R(J)*SEW(I)                                                CCR08470
      AREAS=R(J-1)*SEW(I)                                              CCR08480
      AREAEW=RV(J)*SNSV(J)                                             CCR08490
      VOL=RV(J)*SEW(I)*SNSV(J)                                         CCR08500
C-----CALCULATE CONVECTION COEFFICIENTS                                CCR08510
      GN=0.5*(DEN(I,J+1)+DEN(I,J))*V(I,J+1)                            CCR08520
      GP=0.5*(DEN(I,J)+DEN(I,J-1))*V(I,J)                              CCR08530
      GS=0.5*(DEN(I,J-1)+DEN(I,J-2))*V(I,J-1)                          CCR08540
```

```
      GE=0.5*(DEN(I+1,J)+DEN(I,J))*U(I+1,J)                              CCR08550
      GSE=0.5*(DEN(I,J-1)+DEN(I+1,J-1))*U(I+1,J-1)                       CCR08560
      GW=0.5*(DEN(I,J)+DEN(I-1,J))*U(I,J)                                CCR08570
      GSW=0.5*(DEN(I,J-1)+DEN(I-1,J-1))*U(I,J-1)                         CCR08580
      CN=0.5*(GN+GP)*AREAN                                               CCR08590
      CS=0.5*(GP+GS)*AREAS                                               CCR08600
      CE=0.5*(GE+GSE)*AREAEW                                             CCR08610
      CW=0.5*(GW+GSW)*AREAEW                                             CCR08620
C-----CALCULATE DIFFUSION COEFFICIENTS                                   CCR08630
      VISE=0.25*(VIS(I,J)+VIS(I+1,J)+VIS(I,J-1)+VIS(I+1,J-1))            CCR08640
      VISW=0.25*(VIS(I,J)+VIS(I-1,J)+VIS(I,J-1)+VIS(I-1,J-1))            CCR08650
      DN=VIS(I,J)*AREAN/DYNPV(J)                                         CCR08660
      DS=VIS(I,J-1)*AREAS/DYPSV(J)                                       CCR08670
      DE=VISE*AREAEW/DXEP(I)                                             CCR08680
      DW=VISW*AREAEW/DXPW(I)                                             CCR08690
C-----CALCULATE COEFFICIENTS OF SOURCE TERMS                             CCR08700
      SMP=CN-CS+CE-CW                                                    CCR08710
      CP=AMAX1(0.0,SMP)                                                  CCR08720
      CPO=CP                                                             CCR08730
C-----ASSEMBLE MAIN COEFFICIENTS                                         CCR08740
C     IF(DS.EQ.0.0) DS=1.0E-25                                           CCR08750
      AN(I,J)=AMAX1(ABS(0.5*CN),DN)-0.5*CN                               CCR08760
      AS(I,J)=AMAX1(ABS(0.5*CS),DS)+0.5*CS                               CCR08770
      AE(I,J)=AMAX1(ABS(0.5*CE),CE)-0.5*CE                               CCR08780
      AW(I,J)=AMAX1(ABS(0.5*CW),CW)+0.5*CW                               CCR08790
C     AN(I,J)=DN*AMAX1(0.0,(1.0-0.1*ABS(CN/DN))**5)+AMAX1(-CN,0.0)       CCR08800
C     AE(I,J)=DE*AMAX1(0.0,(1.0-0.1*ABS(CE/DE))**5)+AMAX1(-CE,0.0)       CCR08810
C     AS(I,J)=DS*AMAX1(0.0,(1.0-0.1*ABS(CS/DS))**5)+AMAX1(CS,0.0)        CCR08820
C     AW(I,J)=DW*AMAX1(0.0,(1.0-0.1*ABS(CW/DW))**5)+AMAX1(CW,0.0)        CCR08830
      DV(I,J)=0.5*(AREAN+AREAS)                                          CCR08840
      DUDYE=(U(I+1,J)-U(I+1,J-1))/SNSV(J)                                CCR08850
      DUDYW=(U(I,J)-U(I,J-1))/SNSV(J)                                    CCR08860
      SORCE1=(DUDYE*VISE-DUDYW*VISW)/DXEPU(I)                            CCR08870
      DVDYN=(V(I,J+1)-V(I,J))/DYNPV(J)                                   CCR08880
      DVDYS=(V(I,J)-V(I,J-1))/DYPSV(J)                                   CCR08890
      SORCE2=(VIS(I,J)*RCV(J)*DVDYN-VIS(I,J-1)*RCV(J-1)*DVDYS)           CCR08900
     #      /(RV(J)*SNSV(J))                                             CCR08910
      DYVDYN=(RV(J+1)*V(I,J+1)-RV(J)*V(I,J))/DYNPV(J)                    CCR08920
      DYVDYS=(RV(J)*V(I,J)-RV(J-1)*V(I,J-1))/DYPSV(J)                    CCR08930
      DUDXN=(U(I+1,J)-U(I,J))/SEW(I)                                     CCR08940
      DUDXS=(U(I+1,J-1)-U(I,J-1))/SEW(I)                                 CCR08950
      SORCE3=0.0                                                         CCR08960
C     SORCE3=(2.0/3.0)*(VIS(I,J)*(DYVDYN/RCV(J)+DUDXN)-VIS(I,J-1)*       CCR08970
C    #       (DYVDYS/RCV(J-1)+DUDXS))/SNSV(J)                           CCR08980
      SU(I,J)=CPO*V(I,J)+DV(I,J)*(P(I,J-1)-P(I,J))                       CCR08990
      SU(I,J)=SU(I,J)+(SORCE1+SORCE2+SORCE3)*VOL                         CCR09000
      SP(I,J)=-CP                                                        CCR09010
      SP(I,J)=SP(I,J)-(VIS(I,J)+VIS(I,J-1))*VOL/RV(J)**2                 CCR09020
  101 CONTINUE                                                           CCR09030
  100 CONTINUE                                                           CCR09040
C                                                                        CCR09050
CHAPTER  2  2  2  2  2  2  2  PROBLEM MODIFICATIONS  2  2  2  2  2  2 2CCR09060
C                                                                        CCR09070
      CALL MODV                                                          CCR09080
```

```
C                                                                       CCR09090
CHAPTER  3  FINAL COEFF. ASSEMBLY AND RESIDUAL SOURCE CALCULATION  3  3 CCR09100
C                                                                       CCR09110
      RESORV=0.0                                                        CCR09120
      DO 300 I=2,NIM1                                                   CCR09130
      DO 301 J=3,NJM1                                                   CCR09140
      AP(I,J)=AN(I,J)+AS(I,J)+AE(I,J)+AW(I,J)-SP(I,J)                   CCR09150
      RESOR=AN(I,J)*V(I,J+1)+AS(I,J)*V(I,J-1)+AE(I,J)*V(I+1,J)          CCR09160
     1     +AW(I,J)*V(I-1,J)-AP(I,J)*V(I,J)+SU(I,J)                     CCR09170
      DV(I,J)=DV(I,J)/AP(I,J)                                           CCR09180
      VOL=RV(J)*SEW(I)*SNSV(J)                                          CCR09190
      SORVOL=GREAT*VOL                                                  CCR09200
      IF(-SP(I,J).GT.0.5*SORVOL)  RESOR=RESOR/SORVOL                    CCR09210
      RESORV=RESORV+ABS(RESOR)                                          CCR09220
C-----UNDER-RELAXATION                                                  CCR09230
      AP(I,J)=AP(I,J)/URFV                                              CCR09240
      SU(I,J)=SU(I,J)+(1.-URFV)*AP(I,J)*V(I,J)                          CCR09250
      DV(I,J)=DV(I,J)*URFV                                              CCR09260
  301 CONTINUE                                                          CCR09270
  300 CONTINUE                                                          CCR09280
C                                                                       CCR09290
CHAPTER  4  4  4  SOLUTION OF DIFFERENCE EQUATION  4  4  4  4  4  4  4  CCR09300
C                                                                       CCR09310
      DO 400 N=1,NSWPV                                                  CCR09320
  400 CALL LISOLV(2,3,NI,NJ,IT,JT,V)                                    CCR09330
      RETURN                                                            CCR09340
      END                                                               CCR09350
      SUBROUTINE CALCP                                                  CCR09360
C                                                                       CCR09370
CHAPTER  0  0  0  0  0  0  0  0  PRELIMINARIES  0  0  0  0  0  0  0  0  CCR09380
C                                                                       CCR09390
      COMMON                                                            CCR09400
     1/PCOR/RESORM,NSWPP,URFP,DU(30,30),DV(30,30),IPREF,JPREF           CCR09410
     1/VAR/U(30,30),V(30,30),P(30,30),PP(30,30)                         CCR09420
     1/ALL/IT,JT,NI,NJ,NIM1,NJM1,GREAT                                  CCR09430
      COMMON                                                            CCR09440
     1/GEOM/X(32),Y(32),DXEP(32),DXPW(32),DYNP(32),DYPS(32),            CCR09450
     1       SNS(32),SEW(32),XU(32),YV(32),R(32),RV(32),RCV(32)         CCR09460
     1/FLUPR/VISSEC,DENSEC,PRANDL,DEN(30,30),VIS(30,30),CONST,          CCR09470
     1        VISPRM,DENPRM,SECMAS,PRMMAS,SPRAT                         CCR09480
     1/COEF/AP(30,30),AN(30,30),AS(30,30),AE(30,30),AW(30,30),SU(30,30),CCR09490
     1       SP(30,30)                                                  CCR09500
      RESORM=0.0                                                        CCR09510
C                                                                       CCR09520
CHAPTER  1  1  1  1  1  1  ASSEMBLY OF COEFFICIENTS  1  1  1  1  1  1  1CCR09530
C                                                                       CCR09540
      DO 100 I=2,NIM1                                                   CCR09550
      DO 101 J=2,NJM1                                                   CCR09560
C-----COMPUTE AREAS AND VOLUME                                          CCR09570
      AREAN=RV(J+1)*SEW(I)                                              CCR09580
      AREAS=RV(J)*SEW(I)                                                CCR09590
      AREAEW=RCV(J)*SNS(J)                                              CCR09600
      VOL=RCV(J)*SNS(J)*SEW(I)                                          CCR09610
C-----CALCULATE COEFFICIENTS                                            CCR09620
```

```
      DENN=0.5*(DEN(I,J)+DEN(I,J+1))                                    CCR09630
      DENS=0.5*(DEN(I,J)+DEN(I,J-1))                                    CCR09640
      DENE=0.5*(DEN(I,J)+DEN(I+1,J))                                    CCR09650
      DENW=0.5*(DEN(I,J)+DEN(I-1,J))                                    CCR09660
      AN(I,J)=DENN*AREAN*DV(I,J+1)                                      CCR09670
      AS(I,J)=DENS*AREAS*DV(I,J)                                        CCR09680
      AE(I,J)=DENE*AREAEW*DU(I+1,J)                                     CCR09690
      AW(I,J)=DENW*AREAEW*DU(I,J)                                       CCR09700
C-----CALCULATE SOURCE TERMS                                            CCR09710
      CN=DENN*V(I,J+1)*AREAN                                            CCR09720
      CS=DENS*V(I,J)*AREAS                                              CCR09730
      CE=DENE*U(I+1,J)*AREAEW                                           CCR09740
      CW=DENW*U(I,J)*AREAEW                                             CCR09750
      SMP=CN-CS+CE-CW                                                   CCR09760
      SP(I,J)=0.0                                                       CCR09770
      SU(I,J)=-SMP                                                      CCR09780
C-----COMPUTE SUM OF ABSOLUTE MASS SOURCES                              CCR09790
      RESORM=RESORM+ABS(SMP)                                            CCR09800
  101 CONTINUE                                                          CCR09810
  100 CONTINUE                                                          CCR09820
C                                                                       CCR09830
CHAPTER  2  2  2  2  2  2  2  PROBLEM MODIFICATIONS  2  2  2  2  2  2  2CCR09840
C                                                                       CCR09850
      CALL MODP                                                         CCR09860
C                                                                       CCR09870
CHAPTER  3  3  3  3  3  FINAL COEFFICIENT ASSEMBLY  3  3  3  3  3  3  3 CCR09880
C                                                                       CCR09890
      DO 300 I=2,NIM1                                                   CCR09900
      DO 301 J=2,NJM1                                                   CCR09910
  301 AP(I,J)=AN(I,J)+AS(I,J)+AE(I,J)+AW(I,J)-SP(I,J)                   CCR09920
  300 CONTINUE                                                          CCR09930
C                                                                       CCR09940
CHAPTER  4  4  4  4  4  SOLUTION OF DIFFERENCE EQUATIONS  4  4  4  4  4 CCR09950
C                                                                       CCR09960
C                                                                       CCR09970
CHAPTER  5  5  5  5  CORRECT VELOCITIES AND PRESSURE  5  5  5  5  5  5  CCR09980
      DO 400 N=1,NSWPP                                                  CCR09990
  400 CALL LISOLV(2,2,NI,NJ,IT,JT,PP)                                   CCR10000
C                                                                       CCR10010
C-----VELOCITIES                                                        CCR10020
      DO 500 I=2,NIM1                                                   CCR10030
      DO 501 J=2,NJM1                                                   CCR10040
      IF(I.NE.2) U(I,J)=U(I,J)+DU(I,J)*(PP(I-1,J)-PP(I,J))              CCR10050
      IF(J.NE.2) V(I,J)=V(I,J)+DV(I,J)*(PP(I,J-1)-PP(I,J))              CCR10060
  501 CONTINUE                                                          CCR10070
  500 CONTINUE                                                          CCR10080
C-----PRESSURES (WITH PROVISION FOR UNDER-RELAXATION)                   CCR10090
      PPREF=PP(IPREF,JPREF)                                             CCR10100
      DO 502 I=2,NIM1                                                   CCR10110
      DO 503 J=2,NJM1                                                   CCR10120
      P(I,J)=P(I,J)+URFP*(PP(I,J)-PPREF)                                CCR10130
      PP(I,J)=0.0                                                       CCR10140
  503 CONTINUE                                                          CCR10150
  502 CONTINUE                                                          CCR10160
```

```
      RETURN                                                            CCR10170
      END                                                               CCR10180
      SUBROUTINE CALCT                                                  CCR10190
      COMMON                                                            CCR10200
     1/VAR/U(30,30),V(30,30),P(30,30),PP(30,30)                         CCR10210
     1/ALL/IT,JT,NI,NJ,NIM1,NJM1,GREAT                                  CCR10220
      COMMON                                                            CCR10230
     1/GEOM/X(32),Y(32),DXEP(32),DXPW(32),DYNP(32),DYPS(32),            CCR10240
     1       SNS(32),SEW(32),XU(32),YV(32),R(32),RV(32),RCV(32)         CCR10250
     1/FLUPR/VISSEC,DENSEC,PRANDL,DEN(30,30),VIS(30,30),CONST,          CCR10260
     1        VISPRM,DENPRM,SECMAS,PRMMAS,SPRAT                         CCR10270
      COMMON                                                            CCR10280
     1/PROB1/UINPRM,UINSEC,GRAVTY,FLOWIN,NITER                          CCR10290
     1/COEF/AP(30,30),AN(30,30),AS(30,30),AE(30,30),AW(30,30),SU(30,30),CCR10300
     1       SP(30,30)                                                  CCR10310
      COMMON                                                            CCR10320
     1/TEMP/T(30,30),GAMH(30,30),RESORT,NSWPT,URFT,                     CCR10330
     2      TINPRM,TINSEC,TGB(30),HTFLX(30),HFXOLD(30)                  CCR10340
C                                                                       CCR10350
CHAPTER  1  1  1  1  1  1  ASSEMBLY OF COEFFICIENTS  1  1  1  1  1  1   CCR10360
C                                                                       CCR10370
      DO 100 I=2,NIM1                                                   CCR10380
      DO 101 J=2,NJM1                                                   CCR10390
C_____COMPUTE AREAS VOLUME                                              CCR10400
      AREAN=RV(J+1)*SEW(I)                                              CCR10410
      AREAS=RV(J)*SEW(I)                                                CCR10420
      AREAEW=RCV(J)*SNS(J)                                              CCR10430
      VOL=RCV(J)*SNS(J)*SEW(I)                                          CCR10440
C     CALCULATE CONVECTION COEFFICIENTS                                 CCR10450
      GN=0.5*(DEN(I,J)+DEN(I,J+1))*V(I,J+1)                             CCR10460
      GS=0.5*(DEN(I,J)+DEN(I,J-1))*V(I,J)                               CCR10470
      GE=0.5*(DEN(I,J)+DEN(I+1,J))*U(I+1,J)                             CCR10480
      GW=0.5*(DEN(I,J)+DEN(I-1,J))*U(I,J)                               CCR10490
      CN=GN*AREAN                                                       CCR10500
      CS=GS*AREAS                                                       CCR10510
      CE=GE*AREAEW                                                      CCR10520
      CW=GW*AREAEW                                                      CCR10530
C     CALCULATE DIFFUSION COEFFICIENTS                                  CCR10540
      GAMN=0.5*(GAMH(I,J)+GAMH(I,J+1))                                  CCR10550
      GAMS=0.5*(GAMH(I,J)+GAMH(I,J-1))                                  CCR10560
      GAME=0.5*(GAMH(I,J)+GAMH(I+1,J))                                  CCR10570
      GAMW=0.5*(GAMH(I,J)+GAMH(I-1,J))                                  CCR10580
      DN=GAMN*AREAN/DYNP(J)                                             CCR10590
      DS=GAMS*AREAS/DYPS(J)                                             CCR10600
      DE=GAME*AREAEW/DXEP(I)                                            CCR10610
      DW=GAMW*AREAEW/DXPW(I)                                            CCR10620
C     SOURCE TERMS                                                      CCR10630
      SMP=CN-CS+CE-CW                                                   CCR10640
      CP=AMAX1(0.0,SMP)                                                 CCR10650
      CPO=CP                                                            CCR10660
C     ASSEMBLE MAIN COEFFICIENTS                                        CCR10670
C     IF(DS.EQ.0.0) DS=1.0E-25                                          CCR10680
      AN(I,J)=AMAX1(ABS(0.5*CN),DN)-0.5*CN                              CCR10690
      AS(I,J)=AMAX1(ABS(0.5*CS),DS)+0.5*CS                              CCR10700
```

```
      AE(I,J)=AMAX1(ABS(0.5*CE),DE)-0.5*CE                              CCR10710
      AW(I,J)=AMAX1(ABS(0.5*CW),DW)+0.5*CW                              CCR10720
C     AN(I,J)=DN*AMAX1(0.0,(1.0-0.1*ABS(CN/DN))**5)+AMAX1(-CN,0.0)      CCR10730
C     AS(I,J)=DS*AMAX1(0.0,(1.0-0.1*ABS(CS/DS))**5)+AMAX1(CS,0.0)       CCR10740
C     AE(I,J)=DE*AMAX1(0.0,(1.0-0.1*ABS(CE/DE))**5)+AMAX1(-CE,0.0)      CCR10750
C     AW(I,J)=DW*AMAX1(0.0,(1.0-0.1*ABS(CW/DW))**5)+AMAX1(CW,0.0)       CCR10760
      SU(I,J)=CPO*T(I,J)                                                CCR10770
      SP(I,J)=-CP                                                       CCR10780
  101 CONTINUE                                                          CCR10790
  100 CONTINUE                                                          CCR10800
C                                                                       CCR10810
CHAPTER  2  2  2  2  2  2  PROBLEM MODIFICATIONS  2  2  2  2  2  2      CCR10820
C                                                                       CCR10830
      CALL MODT                                                         CCR10840
CHAPTER 3 FINAL COEFFICIENT ASSEMBLY AND RESIDUAL SOURCE CALCULATION 3  CCR10850
C                                                                       CCR10860
      RESORT=0.0                                                        CCR10870
      DO 300 I=2,NIM1                                                   CCR10880
      DO 301 J=2,NJM1                                                   CCR10890
      AP(I,J)=AN(I,J)+AS(I,J)+AE(I,J)+AW(I,J)-SP(I,J)                   CCR10900
      RESOR=AN(I,J)*T(I,J+1)+AS(I,J)*T(I,J-1)+AE(I,J)*T(I+1,J)          CCR10910
     1       +AW(I,J)*T(I-1,J)-AP(I,J)*T(I,J)+SU(I,J)                   CCR10920
      VOL=RCV(J)*SEW(I)*SNS(J)                                          CCR10930
      SORVOL=GREAT*VOL                                                  CCR10940
      IF(-SP(I,J).GT.0.5*SORVOL) RESOR=RESOR/SORVOL                     CCR10950
      RESORT=RESORT+ABS(RESOR)                                          CCR10960
C     UNDER-RELAXATION                                                  CCR10970
      AP(I,J)=AP(I,J)/URFT                                              CCR10980
      SU(I,J)=SU(I,J)+(1.0-URFT)*AP(I,J)*T(I,J)                         CCR10990
  301 CONTINUE                                                          CCR11000
  300 CONTINUE                                                          CCR11010
C                                                                       CCR11020
CHAPTER  4  4  4  4  4  SOLUTION OF DIFFERENCE EQUATIONS  4  4  4  4  4 CCR11030
C                                                                       CCR11040
      DO 400 N=1,NSWPT                                                  CCR11050
  400 CALL LISOLV(2,2,NI,NJ,IT,JT,T)                                    CCR11060
      RETURN                                                            CCR11070
      END                                                               CCR11080
C                                                                       CCR11090
      SUBROUTINE LISOLV(ISTART,JSTART,NI,NJ,IT,JT,PHI)                  CCR11100
C                                                                       CCR11110
CHAPTER  0  0  0  0  0  0  0  0  PRELIMINARIES  0  0  0  0  0  0  0  0  CCR11120
C                                                                       CCR11130
      DIMENSION PHI(IT,JT),A(32),B(32),C(32),D(32)                      CCR11140
      COMMON                                                            CCR11150
     1/COEF/AP(30,30),AN(30,30),AS(30,30),AE(30,30),AW(30,30),SU(30,30),CCR11160
     1       SP(30,30)                                                  CCR11170
      NIM1=NI-1                                                         CCR11180
      NJM1=NJ-1                                                         CCR11190
      JSTM1=JSTART-1                                                    CCR11200
      A(JSTM1)=0.0                                                      CCR11210
C-----COMMENCE W-E SWEEP                                                CCR11220
      DO 100 I=ISTART,NIM1                                              CCR11230
      C(JSTM1)=PHI(I,JSTM1)                                             CCR11240
```

```
C-----COMMENCE S-N TRAVERSE                                          CCR11250
      DO 101 J=JSTART,NJM1                                           CCR11260
C-----ASSEMBLE TDMA COEFFICIENTS                                     CCR11270
      A(J)=AN(I,J)                                                   CCR11280
      B(J)=AS(I,J)                                                   CCR11290
      C(J)=AE(I,J)*PHI(I+1,J)+AW(I,J)*PHI(I-1,J)+SU(I,J)             CCR11300
      D(J)=AP(I,J)                                                   CCR11310
C-----CALCULATE COEFFICIENTS OF RECURRENCE FORMULA                   CCR11320
      TERM=1./(D(J)-B(J)*A(J-1))                                     CCR11330
      A(J)=A(J)*TERM                                                 CCR11340
  101 C(J)=(C(J)+B(J)*C(J-1))*TERM                                   CCR11350
C-----OBTAIN NEW PHI'S                                               CCR11360
      DO 102 JJ=JSTART,NJM1                                          CCR11370
      J=NJ+JSTM1-JJ                                                  CCR11380
  102 PHI(I,J)=A(J)*PHI(I,J+1)+C(J)                                  CCR11390
  100 CONTINUE                                                       CCR11400
      RETURN                                                         CCR11410
      END                                                            CCR11420
C                                                                    CCR11430
      SUBROUTINE PRINT(ISTART,JSTART,NI,NJ,IT,JT,X,Y,PHI,HEAD)       CCR11440
      DIMENSION PHI(IT,JT),X(IT),Y(JT),HEAD(9),STORE(50)             CCR11450
      DIMENSION F(7),F4(11)                                          CCR11460
      DATA F/4H(1H ,4H,A4,,4HI3, ,4H11I ,4H10, ,4H7X, ,              CCR11470
     14HA6) /                                                        CCR11480
      DATA F4/4H 1I ,4H 2I ,4H 3I ,4H 4I ,4H 5I ,4H 6I ,             CCR11490
     1        4H 7I ,4H 8I ,4H 9I ,4H10I ,4H11I /                    CCR11500
      DATA HI,HY/4H  I=,4H Y =/                                      CCR11510
      ISKIP=1                                                        CCR11520
      JSKIP=1                                                        CCR11530
      WRITE(6,110)HEAD                                               CCR11540
      ISTA=ISTART-12                                                 CCR11550
  100 CONTINUE                                                       CCR11560
      ISTA=ISTA+12                                                   CCR11570
      IEND=ISTA+11                                                   CCR11580
      IEND=MIN0(NI,IEND)                                             CCR11590
      F(4)=F4(IEND-ISTA)                                             CCR11600
      WRITE(6,F) HI, (I,I=ISTA,IEND,ISKIP), HY                       CCR11610
      WRITE(6,112)                                                   CCR11620
      DO 101 JJ=JSTART,NJ,JSKIP                                      CCR11630
      J=JSTART+NJ-JJ                                                 CCR11640
      DO 120 I=ISTA,IEND                                             CCR11650
      A=PHI(I,J)                                                     CCR11660
      IF(ABS(A).LT.1.E-20) A=0.0                                     CCR11670
  120 STORE(I)=A                                                     CCR11680
      WRITE(6,113)  J,(STORE(I),I=ISTA,IEND,ISKIP),Y(J)              CCR11690
  101 CONTINUE                                                       CCR11700
      WRITE(6,114) (X(I),I=ISTA,IEND,ISKIP)                          CCR11710
      IF(IEND.LT.NI)GO TO 100                                        CCR11720
  110 FORMAT(1H0,20(2H*-),7X,9A4,7X,20(2H-*))                        CCR11730
  112 FORMAT(3H  J)                                                  CCR11740
  113 FORMAT(1H ,I3,1P12E10.2,0PF7.3)                                CCR11750
  114 FORMAT(6H0X=    ,F7.3,11F10.3)                                 CCR11760
      RETURN                                                         CCR11770
      END                                                            CCR11780
```

```
C                                                                       CCR11790
      SUBROUTINE PROMOD                                                 CCR11800
C                                                                       CCR11810
CHAPTER  0  0  0  0  0  0  0  PRELIMINARIES  0  0  0  0  0  0  0  0  0  CCR11820
C                                                                       CCR11830
      COMMON                                                            CCR11840
     1/VVEL/RESORV,NSWPV,URFV,DYNPV(32),DYPSV(32),SNSV(32)              CCR11850
     1/UVEL/RESORU,NSWPU,URFU,DXEPU(32),DXPWU(32),SEWU(32)              CCR11860
     1/PCOR/RESORM,NSWPP,URFP,DU(30,30),DV(30,30),IPREF,JPREF           CCR11870
     1/VAR/U(30,30),V(30,30),P(30,30),PP(30,30)                         CCR11880
     1/ALL/IT,JT,NI,NJ,NIM1,NJM1,GREAT                                  CCR11890
      COMMON                                                            CCR11900
     1/GEOM/X(32),Y(32),DXEP(32),DXPW(32),DYNP(32),DYPS(32),            CCR11910
     1       SNS(32),SEW(32),XU(32),YV(32),R(32),RV(32),RCV(32)         CCR11920
     1/FLUPR/VISSEC,DENSEC,PRANDL,DEN(30,30),VIS(30,30),CONST,          CCR11930
     1        VISPRM,DENPRM,SECMAS,PRMMAS,SPRAT                         CCR11940
      COMMON                                                            CCR11950
     1/PROB1/UINPRM,UINSEC,GRAVTY,FLOWIN,NITER                          CCR11960
     1/COEF/AP(30,30),AN(30,30),AS(30,30),AE(30,30),AW(30,30),SU(30,30),CCR11970
     1       SP(30,30)                                                  CCR11980
      COMMON                                                            CCR11990
     1/TEMP/T(30,30),GAMH(30,30),RESORT,NSWPT,URFT,                     CCR12000
     2      TINPRM,TINSEC,TGB(30),HTFLX(30),HFXOLD(30)                  CCR12010
C                                                                       CCR12020
CHAPTER  1  1  1  1  1  1  1  1  PROPERTIES  1  1  1  1  1  1  1  1  1  CCR12030
C                                                                       CCR12040
      ENTRY MODPRO                                                      CCR12050
C-----NO MODIFICATIONS FOR THIS PROBLEM                                 CCR12060
C                                                                       CCR12070
      RETURN                                                            CCR12080
CHAPTER  2  2  2  2  2  2  2  2  U MOMENTUM  2  2  2  2  2  2  2  2  2  CCR12090
C                                                                       CCR12100
      ENTRY MODU                                                        CCR12110
C-----TOP WALL                                                          CCR12120
      YP=YV(NJ)-Y(NJM1)                                                 CCR12130
      J=NJM1                                                            CCR12140
      DO 210 I=3,NIM1                                                   CCR12150
      TMULT=(VIS(I-1,J)+VIS(I,J))*0.5/YP                                CCR12160
      SP(I,J)=SP(I,J)-TMULT*SEWU(I)*RV(NJ)                              CCR12170
  210 AN(I,J)=0.0                                                       CCR12180
C-----SYMMETRY AXIS                                                     CCR12190
      DO 203 I=1,NI                                                     CCR12200
      AS(I,2)=0.0                                                       CCR12210
  203 U(I,1)=U(I,2)                                                     CCR12220
C-----LEFT SIDE WALL                                                    CCR12230
      DO 207 J=2,NJM1                                                   CCR12240
  207 U(2,J)=U(1,J)*(T(2,J)+T(1,J))/(2.0*T(1,J))                        CCR12250
      DO 208 J=6,9                                                      CCR12260
  208 AW(I,J)=0.0                                                       CCR12270
C     DO 208 J=6,17                                                     CCR12280
C 208 AW(2,J)=0.0                                                       CCR12290
C     DO 212 J=26,28                                                    CCR12300
C 212 AW(2,J)=0.0                                                       CCR12310
C-----RIGHT SIDE WALL                                                   CCR12320
```

```
C                                                                       CCR12330
      DO 206 J=1,NJ                                                     CCR12340
      AE(NIM1,J)=0.0                                                    CCR12350
 206  CONTINUE                                                          CCR12360
      RETURN                                                            CCR12370
C                                                                       CCR12380
CHAPTER  3  3  3  3  3  3  3  3  V MOMENTUM  3  3  3  3  3  3  3  3  3  CCR12390
C                                                                       CCR12400
      ENTRY MODV                                                        CCR12410
C-----LEFT SIDE WALL                                                    CCR12420
      XP=X(2)-XU(2)                                                     CCR12430
      DO 303 J=6,10                                                     CCR12440
C     DO 303 J=6,18                                                     CCR12450
      TTMULT=(VIS(2,J)+VIS(2,J-1))*0.5/XP                               CCR12460
      SP(2,J)=SP(2,J)-TTMULT*RV(J)*SNSV(J)                              CCR12470
      IF(J.EQ.6)SP(2,J)=SP(2,J)-TTMULT*(R(J)**2-RV(J)**2)/2.0           CCR12480
C     IF(J.EQ.18)SP(2,J)=SP(2,J)-TTMULT*(RV(J)**2-R(J-1)**2)/2.0        CCR12490
      IF(J.EQ.10)SP(2,J)=SP(2,J)-TTMULT*(RV(J)**2-R(J-1)**2)/2.0        CCR12500
 303  AW(2,J)=0.0                                                       CCR12510
C     DO 304 J=26,29                                                    CCR12520
C     TTMULT=(VIS(2,J)+VIS(2,J-1))*0.5/XP                               CCR12530
C     SP(2,J)=SP(2,J)-TTMULT*RV(J)*SNSV(J)                              CCR12540
C     IF(J.EQ.26)SP(2,J)=SP(2,J)-TTMULT*(R(J)**2-RV(J)**2)/2.0          CCR12550
C     IF(J.EQ.29)SP(2,J)=SP(2,J)-TTMULT*(RV(J)**2-R(J-1)**2)/2.0        CCR12560
C     AW(2,J)=0.0                                                       CCR12570
C304  CONTINUE                                                          CCR12580
C-----RIGHT SIDE WALL                                                   CCR12590
C                                                                       CCR12600
      DO 312 J=2,NJM1                                                   CCR12610
  312 AE(NIM1,J)=0.0                                                    CCR12620
      RETURN                                                            CCR12630
C                                                                       CCR12640
CHAPTER  4  4  4  4  4  4  PRESSURE CORRECTION  4  4  4  4  4  4  4  4  CCR12650
C                                                                       CCR12660
      ENTRY MODP                                                        CCR12670
C                                                                       CCR12680
C-----NO MODIFICATION                                                   CCR12690
C                                                                       CCR12700
      RETURN                                                            CCR12710
C                                                                       CCR12720
C                                                                       CCR12730
      ENTRY MODT                                                        CCR12740
C-----TOP WALL (2.0 M VARIABLE WALL TEMP )                              CCR12750
      J=NJM1                                                            CCR12760
      YT=YV(NJ)-Y(J)                                                    CCR12770
      DO 500 I=2,NIM1                                                   CCR12780
C---- SPECIFIC HEAT CORRELATION                                         CCR12790
      CPP=(T(I,J)-350.0)*0.212+1000.                                    CCR12800
      TT=VIS(I,J)/(PRANDL*YT)                                           CCR12810
      RSTG=1.0/(CPP*TT)                                                 CCR12820
      TWLOUT=T(I,J)+HTFLX(I)*(RSTG+RSTW)                                CCR12830
C-----C1=RV(NJ)/(ROUT*SIG*EPS1)                                         CCR12840
C     ROUT=2.75 IN = 0.034925 M                                         CCR12850
C     EPS1=0.90 EMISSIVITY OF MULLITE ALUMINIUM/SILICON/OXYGEN          CCR12860
```

```
      C1=1.7846E7                                                        CCR12870
C-----RSTW=RV(NJ)*ALOG(ROUT/RV(NJ))/KWALL                                CCR12880
C     KWALL = 2.076 W/M K  (MULLITE - FROM CRC HANDBOOK)                 CCR12890
      RSTW=1.43585E-3                                                    CCR12900
      RSTR=C1/((TGB(I)+TWLOUT)*(TGB(I)**2+TWLOUT**2))                    CCR12910
      HTFLX(I)=(TGB(I)-T(I,J))/(RSTR+RSTW+RSTG)                          CCR12920
      HTFLX(I)=0.05*HTFLX(I)+0.95*HFXOLD(I)                              CCR12930
      HFXOLD(I)=HTFLX(I)                                                 CCR12940
      SU(I,J)=SU(I,J)+RV(NJ)*SEW(I)*HTFLX(I)/CPP                         CCR12950
      T(I,NJ)=T(I,J)+HTFLX(I)*RSTG                                       CCR12960
      AN(I,J)=0.0                                                        CCR12970
  500 CONTINUE                                                           CCR12980
C-----LEFT SIDE WALL                                                     CCR12990
C                                                                        CCR13000
      DO 501 J=6,9                                                       CCR13010
C     DO 501 J=6,17                                                      CCR13020
      XT=X(2)-XU(2)                                                      CCR13030
      XTT=VIS(2,J)/(PRANDL*XT)                                           CCR13040
      SP(2,J)=SP(2,J)-XTT*R(J)*SNS(J)                                    CCR13050
      SU(2,J)=SU(2,J)+XTT*R(J)*SNS(J)*T(1,J)                             CCR13060
  501 AW(2,J)=0.0                                                        CCR13070
C-----SYMMETRY AXIS                                                      CCR13080
      DO 502 I=2,NIM1                                                    CCR13090
      T(I,1)=T(I,2)                                                      CCR13100
  502 AS(I,2)=0.0                                                        CCR13110
C-----RIGHT SIDE WALL                                                    CCR13120
C                                                                        CCR13130
      DO 503 J=2,NJ                                                      CCR13140
      T(NI,J)=T(NIM1,J)                                                  CCR13150
  503 AE(NIM1,J)=0.0                                                     CCR13160
      RETURN                                                             CCR13170
      END                                                                CCR13180
C                                                                        CCR13190
      SUBROUTINE CALCUP                                                  CCR13200
C                                                                        CCR13210
      DIMENSION DIST(1000),UP(1000),TP(1000)                             CCR13220
      COMMON                                                             CCR13230
     1/GEOM/X(32),Y(32),DXEP(32),DXPW(32),DYNP(32),DYPS(32),             CCR13240
     1       SNS(32),SEW(32),XU(32),YV(32),R(32),RV(32),RCV(32)          CCR13250
     1/FLUPR/VISSEC,DENSEC,PRANDL,DEN(30,30),VIS(30,30),CONST,           CCR13260
     1       VISPRM,DENPRM,SECMAS,PRMMAS,SPRAT                           CCR13270
     1/VAR/U(30,30),V(30,30),P(30,30),PP(30,30)                          CCR13280
      COMMON                                                             CCR13290
     1/TEMP/T(30,30),GAMH(30,30),RESORT,NSWPT,URFT,                      CCR13300
     2      TINPRM,TINSEC,TGB(30),HTFLX(30),HFXOLD(30)                  CCR13310
C                                                                        CCR13320
      NI=28                                                              CCR13330
      NJ=20                                                              CCR13340
      NIM1=NI-1                                                          CCR13350
C                                                                        CCR13360
C-----*NOTE - THIS IS FOR USE WITH A CALCOMP PLOTTER                     CCR13370
C-----THIS PORTION DRAWS THE AXIS FOR THE TEMP VS DIST CURVE             CCR13380
C                                                                        CCR13390
C     CALL PLOT(32.0,1.0,-3)                                             CCR13400
```

```
C     CALL PLOT(20.0,15.0,3)                                                    CCR13410
C     CALL PLOT(0.0,15.0,2)                                                     CCR13420
C     CALL PLOT(0.0,0.0,2)                                                      CCR13430
C     DO 121 K=1,16                                                             CCR13440
C     PR=(K-1)*1.0                                                              CCR13450
C     PPRR=PR-0.18                                                              CCR13460
C     TMPR=100.0*(K-1)                                                          CCR13470
C     IF(AMOD(PR,5.0).EQ.0.)CALL NUMBER(-1.4,PPRR,.35,TMPR,0.0,-1)              CCR13480
C     CALL PLOT(0.0,PR,3)                                                       CCR13490
C     CALL PLOT(0.25,PR,2)                                                      CCR13500
C 121 CONTINUE                                                                  CCR13510
C     CALL SYMBOL(-1.7,5.0,0.35,'TEMPERATURE  K',90.0,14)                       CCR13520
C                                                                               CCR13530
C     CALL SYMBOL(0.8,12.65,0.35,'M-S/M-P =       ',0.0,16)                     CCR13540
C     CALL SYMBOL(0.8,14.15,0.35,'   T-GB =      K',0.0,16)                     CCR13550
C     CALL SYMBOL(0.8,13.65,0.35,'  T-SEC =      K',0.0,16)                     CCR13560
C     CALL SYMBOL(0.8,13.15,0.35,'  U-SEC =      M/S',0.0,18)                   CCR13570
C     CALL NUMBER(4.3,13.15,0.35,U(2,10),0.0,2)                                 CCR13580
C     CALL NUMBER(4.3,14.15,0.35,TMPGLB,0.0,-1)                                 CCR13590
C     CALL NUMBER(4.3,13.65,0.35,TINSEC,0.0,-1)                                 CCR13600
C     CALL NUMBER(4.3,12.65,0.35,SPRAT,0.0,1)                                   CCR13610
C                                                                               CCR13620
C     CALL SYMBOL(15.0,2.0,0.25,'1 -  10 UM PARTICLE',0.0,19)                   CCR13630
C     CALL SYMBOL(15.0,1.5,0.25,'2 -  30 UM PARTICLE',0.0,19)                   CCR13640
C     CALL SYMBOL(15.0,1.0,0.25,'3 - 100 UM PARTICLE',0.0,19)                   CCR13650
C     CALL SYMBOL(15.0,0.5,0.25,'4 - 300 UM PARTICLE',0.0,19)                   CCR13660
C     CALL SYMBOL(15.0,2.5,0.25,'  - GAS TEMPERATURE',0.0,19)                   CCR13670
C     CALL SYMBOL(15.0,2.625,0.10,11,0.0,-1)                                    CCR13680
C     CALL SYMBOL(15.0,2.0,0.25,'1 - EMISSIVITY = 0.6',0.0,21)                  CCR13690
C     CALL SYMBOL(15.0,1.5,0.25,'2 - EMISSIVITY = 0.8',0.0,21)                  CCR13700
C     CALL SYMBOL(15.0,1.0,0.25,'3 - EMISSIVITY = 1.0',0.0,21)                  CCR13710
C                                                                               CCR13720
C     CALL PLOT(20.0,15.0,3)                                                    CCR13730
C     CALL PLOT(20.0,0.0,2)                                                     CCR13740
C     CALL PLOT(0.0,0.0,2)                                                      CCR13750
C     DO 122 I=1,5                                                              CCR13760
C     PPR=(I-1)*5.0                                                             CCR13770
C     ZZ=PPR/10.0                                                               CCR13780
C     ZZP=PPR-0.40                                                              CCR13790
C     CALL NUMBER(ZZP,-1.0,.35,ZZ,0.0,1)                                        CCR13800
C     CALL PLOT(PPR,0.25,3)                                                     CCR13810
C     CALL PLOT(PPR,0.0,2)                                                      CCR13820
C 122 CONTINUE                                                                  CCR13830
C     CALL SYMBOL(8.0,-2.0,0.35,'DISTANCE  M',0.0,11)                           CCR13840
C     CALL PLOT(0.0,3.0,3)                                                      CCR13850
C     DO 134 I=3,NIM1                                                           CCR13860
C     TG=T(I,2)*0.01                                                            CCR13870
C     ZG=X(I)*10.0                                                              CCR13880
C     CALL SYMBOL(ZG,TG,0.10,11,0.0,-2)                                         CCR13890
C 134 CONTINUE                                                                  CCR13900
C     DO 133 J=1,5                                                              CCR13910
C     QQ=(J-1)*5.0                                                              CCR13920
C     CALL PLOT(QQ,15.0,3)                                                      CCR13930
C     CALL PLOT(QQ,14.75,2)                                                     CCR13940
```

```
C 133 CONTINUE                                                          CCR13950
C     CALL SYMBOL(7.2,16.6,0.35,'ZONE TEMPERATURE',0.0,16)              CCR13960
C     CALL NUMBER(1.45,15.6,0.35,TGB(7),0.0,-1)                         CCR13970
C     CALL SYMBOL(3.2,15.6,0.35,'K',0.0,1)                              CCR13980
C     CALL NUMBER(6.45,15.6,0.35,TGB(17),0.0,-1)                        CCR13990
C     CALL SYMBOL(8.2,15.6,0.35,'K',0.0,1)                              CCR14000
C     CALL NUMBER(11.45,15.6,0.35,TGB(22),0.0,-1)                       CCR14010
C     CALL SYMBOL(13.2,15.6,0.35,'K',0.0,1)                             CCR14020
C     CALL NUMBER(16.45,15.6,0.35,TGB(26),0.0,-1)                       CCR14030
C     CALL SYMBOL(18.2,15.6,0.35,'K',0.0,1)                             CCR14040
C                                                                       CCR14050
C-----THIS SUBROUTINE USES 6 DIFFERENT PARTICLE DIAMETRES               CCR14060
C                                                                       CCR14070
      DO 191 M=1,6                                                      CCR14080
C                                                                       CCR14090
      IF(M.EQ.1)DIAPAR=0.000010                                         CCR14100
      IF(M.EQ.2)DIAPAR=0.000030                                         CCR14110
      IF(M.EQ.3)DIAPAR=0.000050                                         CCR14120
      IF(M.EQ.4)DIAPAR=0.000075                                         CCR14130
      IF(M.EQ.5)DIAPAR=0.000100                                         CCR14140
      IF(M.EQ.6)DIAPAR=0.000150                                         CCR14150
C                                                                       CCR14160
      WRITE(6,11) DIAPAR                                                CCR14170
   11 FORMAT(///,'DIA M',E10.2,3X,'TIME  S',3X,'VEL M/S',5X,'DIST M',7X,CCR14180
     •  'RE',7X,'H W/M2C',2X,'QRAD W/M2',3X,'QCON W/M2',4X,'TEMP K',/)   CCR14190
C                                                                       CCR14200
C-----COAL PROPERTIES                                                   CCR14210
C                                                                       CCR14220
      CPPAR=1300.0                                                      CCR14230
      EPS=0.8                                                           CCR14240
      DENPAR=1300.0                                                     CCR14250
C                                                                       CCR14260
C-----INITIAL VALUES                                                    CCR14270
C                                                                       CCR14280
      UU=U(2,2)                                                         CCR14290
      VSC=VIS(1,2)                                                      CCR14300
      TMP=T(1,2)                                                        CCR14310
      TWL=T(2,NJ)                                                       CCR14320
      TP(1)=T(1,2)                                                      CCR14330
      TEXIT=TINPRM                                                      CCR14340
      DST=DEN(1,2)                                                      CCR14350
      DIST(1)=0.0                                                       CCR14360
C                                                                       CCR14370
C-----TEMPERATURE INCREMENT                                             CCR14380
      DELTMP=5.0                                                        CCR14390
C                                                                       CCR14400
      GRAVTY=9.806                                                      CCR14410
      SIG=5.669E-8                                                      CCR14420
C                                                                       CCR14430
C-----THIS GIVES INITIAL DISTANCE TRAVELLED                             CCR14440
C                                                                       CCR14450
      UP(1)=UU+(SQRT((576.0•VSC••2)/(DIAPAR••4•DENPAR••2)+(32.0•DST•    CCR14460
     •      GRAVTY)/(3.0•DENPAR•DIAPAR))-24.0•VSC/(DIAPAR••2•DENPAR))•  CCR14470
     •      (DENPAR•DIAPAR)/(4.0•DST)                                   CCR14480
```

```
C                                                                       CCR14490
      VFPE=0.5*(1.0-1.0/SQRT(1.0+RV(NJ)**2/XU(NI)**2))                  CCR14500
      VFPW=1.0-VFPE-0.5                                                 CCR14510
      QRAD=SIG*EPS*VFPW*(TWL**4-TP(1)**4)                               CCR14520
      RELC=0.0                                                          CCR14530
      HTC=0.0                                                           CCR14540
      QCONV=0.0                                                         CCR14550
      TIME=0.0                                                          CCR14560
      K=2                                                               CCR14570
      L=2                                                               CCR14580
C                                                                       CCR14590
   70 CONTINUE                                                          CCR14600
      DELT=DENPAR*CPPAR*DIAPAR*DELTMP/(6.0*ABS(QRAD-QCONV))             CCR14610
      IF(DELT.GT.0.005) DELT=0.005                                      CCR14620
      DIST(K)=DIST(K-1)+UP(K-1)*DELT                                    CCR14630
      WRITE(6,95) TIME,UP(K-1),DIST(K-1),RELC,HTC,QRAD,QCONV,TP(K-1)    CCR14640
   95 FORMAT(17X,F7.5,2X,E10.3,1X,E10.3,2X,E10.3,2X,E10.3,2X,F8.2,2X,E11.4,2X,CCR14650
     *       E10.4,2X,F7.1)                                             CCR14660
      IF(DIST(K).GE.XU(NI)) GO TO 80                                    CCR14670
      J=L                                                               CCR14680
C                                                                       CCR14690
      DO 90 I=J,NI                                                      CCR14700
      IF((DIST(K).LE.X(I)).AND.(DIST(K).GT.X(I-1))) L=I                 CCR14710
   90 CONTINUE                                                          CCR14720
      CST=(DIST(K)-X(L-1))/(X(L)-X(L-1))                                CCR14730
      VSC=VIS(L-1,2)+(VIS(L,2)-VIS(L-1,2))*CST                          CCR14740
      DST=DEN(L-1,2)+(DEN(L,2)-DEN(L-1,2))*CST                          CCR14750
      TMP=T(L-1,2)+(T(L,2)-T(L-1,2))*CST                                CCR14760
      TWL=T(L-1,NJ)+(T(L,NJ)-T(L-1,NJ))*CST                             CCR14770
      IF(DIST(K).LT.XU(L)) UU=U(L-1,2)+(U(L,2)-U(L-1,2))*(DIST          CCR14780
     *       (K)-XU(L-1))/(XU(L)-XU(L-1))                               CCR14790
      IF(DIST(K).GE.XU(L)) UU=U(L,2)+(U(L+1,2)-U(L,2))*(DIST(K)         CCR14800
     *       -XU(L))/(XU(L+1)-XU(L))                                    CCR14810
C                                                                       CCR14820
C-----THIS CALCULATES FILM TEMPERATURE PROPERTIES                       CCR14830
C                                                                       CCR14840
      VSCF=(1.5E-6*TP(K-1)**1.5/(TP(K-1)+130.0)+VSC)/2.0                CCR14850
      DSTF=(1.0/(CONST*TP(K-1))+DST)/2.0                                CCR14860
C                                                                       CCR14870
C-----CALCULATE PARTICLE VELOCITY                                       CCR14880
C                                                                       CCR14890
      RELC=ABS(UP(K-1)-UU)*DIAPAR*DSTF/VSCF                             CCR14900
      AUP=18.0*VSCF*(1.0+0.15*RELC**0.687)/(DENPAR*DIAPAR**2)           CCR14910
      UP(K)=UU-((GRAVTY-AUP*(UP(K-1)-UU))*EXP(-AUP*DELT)-GRAVTY)/AUP    CCR14920
C                                                                       CCR14930
C-----CALCULATE PARTICLE TEMPERATURE                                    CCR14940
C                                                                       CCR14950
      CPP=(TMP-350.0)*0.212+1000.0                                      CCR14960
      VFPP=0.5*(1.0-1.0/SQRT(1.0+RV(10)**2/DIST(K)**2))                 CCR14970
      VFPS=0.5*(1.0-1.0/SQRT(1.0+RV(NJ)**2/DIST(K)**2))-VFPP            CCR14980
      VFPE=0.5*(1.0-1.0/SQRT(1.0+RV(NJ)**2/(XU(NI)-DIST(K))**2))        CCR14990
      VFPW=1.0-VFPP-VFPS-VFPE                                           CCR15000
      VSCP=1.5E-6*TP(K-1)**1.5/(130.0+TP(K-1))                          CCR15010
      HTC=(2.0+(0.4*RELC**(1/2)+0.06*RELC**(2/3))*(PRANDL**0.4          CCR15020
```

```
     *    )*(VSC/VSCP)**0.25)*VSC*CPP/(PRANDL*DIAPAR)                    CCR15030
          HPP=SIG*EPS*VFPP*(TINPRM+TP(K-1))*(TINPRM**2+TP(K-1)**2)       CCR15040
          HPS=SIG*EPS*VFPS*(TINSEC+TP(K-1))*(TINSEC**2+TP(K-1)**2)       CCR15050
          HPE=SIG*EPS*VFPE*(TEXIT+TP(K-1))*(TEXIT**2+TP(K-1)**2)         CCR15060
          HPW=SIG*EPS*VFPW*(TWL+TP(K-1))*(TWL**2+TP(K-1)**2)             CCR15070
          ATP=6.0*(HPP+HPS+HPE+HPW+HTC)/(DENPAR*CPPAR*DIAPAR)            CCR15080
          BTP=6.0*(HPP*TINPRM+HPS*TINSEC+HPE*TEXIT+HPW*TWL+HTC*TMP)/     CCR15090
         *    (DENPAR*CPPAR*DIAPAR)                                      CCR15100
          TP(K)=(BTP+(ATP*TP(K-1)-BTP)*EXP(-ATP*DELT))/ATP               CCR15110
          QRAD=SIG*EPS*(VFPP*(TINPRM**4-TP(K)**4)+VFPS*(TINSEC**4-TP(K)**4) CCR15120
         *     +VFPE*(TEXIT**4-TP(K)**4)+VFPW*(TWL**4-TP(K)**4))           CCR15130
          QCONV=HTC*(TP(K)-TMP)                                          CCR15140
          TIME=TIME+DELT                                                 CCR15150
          K=K+1                                                          CCR15160
          GO TO 70                                                       CCR15170
       80 CONTINUE                                                       CCR15180
C                                                                        CCR15190
C         TTP=TP(1)*0.01                                                 CCR15200
C         ZP=25.5                                                        CCR15210
C         CALL PLOT(0.0,TTP,3)                                           CCR15220
C         KK=K-1                                                         CCR15230
C         DO 189 I=2,KK                                                  CCR15240
C         ZP=DIST(I)*10.0                                                CCR15250
C         TTP=TP(I)*0.01                                                 CCR15260
C         CALL PLOT(ZP,TTP,2)                                            CCR15270
C189      CONTINUE                                                       CCR15280
      191 CONTINUE                                                       CCR15290
          RETURN                                                         CCR15300
          END                                                            CCR15310
```

UNIVERSITÉ D'OTTAWA UNIVERSITY OF OTTAWA

USERS' GUIDE FOR THE NUMERICAL MODEL FOR THE CONTROLLED MIXING COMBUSTION HISTORY FURNACE

by

Robert J. Flaxman

Prepared for

Combustion and Carbonization Research
Laboratory
CANMET

Energy Mines and Resources Canada
under
DSS Contract No. 1SU83-00105

March 1986

Users' Guide for the Numerical Model for the Controlled Mixing Combustion History Furnace.

by

Robert J. Flaxman

MICROMEDIA

25 pp

CONTENTS

Chapter page

I. INTRODUCTION 1

Main Subroutine 1
Subroutine INIT 1
Subroutine PROPS 2
Subroutine CALCU and CALCV 2
Subroutine CALCP 2
Subroutine CALCT 2
Subroutine LISOLV 3
Subroutine PRINT 3
Subroutine PROMOD 3
Subroutine CALCUP 3

II. USER'S GUIDE FOR THE FORTRAN PROGRAM 4

Introduction 4
The Flow Field Solution 4
Input Variables 5
Dependent Variable Selection 6
Iteration and Control 7
Output Data 8
Particle Velocity and Heating 9
Input Values for Particle Calculations 9
The Time Increment 10
Particle Velocity and Heating Output 10
Operating Procedure 10

Appendix page

A. GLOSSARY OF FORTRAN SYMBOLS 12

Chapter I

INTRODUCTION

The program consists of a main program and a series of subroutines. The main program defines all of the parameters involved and calls the subsequent subroutines to solve for each of the variables. The program is very systematically laid out and easy to follow; however, the reader is cautioned when using the program that some background in numerical modelling is needed before any major changes are made.

1.1 MAIN SUBROUTINE

The MAIN program contains all the control indices and variable inputs necessary to solve the problem. The main routine specifies the number of grid points, the inlet velocities, temperatures, mass fluxes, etc. It also calls the other subroutines when specified and controls all the program iteration and print statements.

1.2 SUBROUTINE INIT

The INIT subroutine has two functions; it creates the geometric grid patterns necessary for the three sets of control volumes (C, U, and V cells) and it initializes all of the dependent variables to zero or to a set of initial values. (* Note - The axi-symmetry of the tube allows a factor of 2*Pi (6.28) to be divided out; therefore, the cells are all 2-D)

1.3 SUBROUTINE PROPS

The PROPS subroutine is used to calculate the properties (density and viscosity) of the gas based on the local temperature. Further additions to the program, such as mass diffusivities or concentration-dependent densities, would be included here.

1.4 SUBROUTINE CALCU AND CALCV

The CALCU and CALCV subroutines are used to solve for the axial velocity field U(I,J) and V(I,J), respectively. The latest estimates of density, viscosity, radial velocity, axial velocity and pressure are used to establish coefficients which are used to solve for better estimates of the velocity fields. This process continues until a convergence criterion is met.

1.5 SUBROUTINE CALCP

The CALCP subroutine uses the continuity equation to solve for a pressure correction field. The most recent calculated values of axial velocity and radial velocity must be able to conserve mass; a pressure correction is applied which enables the calculated flow field to obey continuity.

1.6 SUBROUTINE CALCT

The temperature field in the flow is solved using Subroutine CALCT. This subroutine uses the most recent estimates of the dependent variables and solves the energy equation. The calculated temperatures are used to update the gas properties.

1.7 SUBROUTINE LISOLV

The matrices for each of the unknowns (U–axial velocity, V–radial velocity, PP–pressure correction, T–temperature) are solved using a Tridiagonal Matrix Algorithm to calculate new values. This is a line by line solution, in which the TDMA is used to solve each individual radial line of points as the program "sweeps" in the x–direction.

1.8 SUBROUTINE PRINT

The PRINT Subroutine is used to print out all of the dependent variable fields; it follows the same format for each set of data. The data can be printed out after convergence has been reached or at intermediate iterations before convergence.

1.9 SUBROUTINE PROMOD

The PROMOD subroutine contains all of the boundary conditions for the problem. Each of the axial velocity, radial velocity, temperature and pressure fields have specified conditions at the inlet, the outlet, the furnace wall and the furnace axis. These boundary values are specified in the PROMOD Subroutine.

1.10 SUBROUTINE CALCUP

The Subroutine CALCUP is used to calculate particle velocities and temperatures in the furnace. This subroutine is called after the velocity and the temperature field in the furnace has been solved. It uses the centre–line velocities and temperatures of the air and the furnace wall temperature to calculate the particle velocities and temperatures.

Chapter II

USER'S GUIDE FOR THE FORTRAN PROGRAM

2.1 INTRODUCTION

The program consists of two "main" routines. The first routine is used to solve the flow and temperature fields in the furnace; the second routine is used to solve the particle velocities and temperatures. The first routine is the largest and the most complex and is used to solve the governing differential equations of the flow field. The method of solution is an iterative procedure: all the dependent variables are updated with each iteration and this process continues until each of the governing equations has been satisfied within a convergence limit. The second routine uses the values of velocity and temperature calculated from the first routine. The second routine uses a step wise explicit marching scheme down the length of the furnace and calculates the particle velocity and temperature after a selected time step.

2.2 THE FLOW FIELD SOLUTION

The main routine is the one that contains all the parameters necessary for the solution of the problem. Since the program was designed for use with the CMCH drop tube furnace, many of the parameters need not be changed. The following subroutines (INIT, PROPS, CALCU, CALCV, CALCT, LISOLV, PRINT, and MODPRO) have been modified to suit this furnace and need not be altered. The last subroutine (CALCUP) is used to calculate the particle velocities and temperatures and is discussed in the next section.

The user should read through the main routine of the program noting the comments that have been inserted at different points. The glossary of terms included at the back of this manual should be used to identify the various terms. The reader will note that the main routine is separated into a series of chapters, each dealing with different steps of the solution procedure. The first chapter gives the number and the spacing of the grid points and it also initializes the control indices and monitors for the program. It is in the first chapter where the input variables will be changed. The second chapter calculates the geometric quantities and specifies all the initial and inlet conditions. The third chapter deals with the iteration loop: it calls the subroutines of the main dependent variables and calculates the intermediate output. Once the convergence criterion is met or the maximum number of iterations has been reached, the program completes the final operation and prints the output.

2.2.1 Input Variables

The input values are entered directly into the program by means of the first chapter of the main subroutine. The input variables necessary are the coal feed rate, the secondary air mass flow, the secondary flow preheat temperature and the glow bar zone temperature. These quantities are entered directly into their corresponding variable. The input variables are identified as follows:

TINPRM – primary air temperature (K)

TINSEC – secondary air temperature (K)

PRMMAS – primary air mass flow (kg/s)

SECMAS – secondary air mass flow (kg/s)

ZONE1 – zone one temperature (K)

ZONE2 – zone two temperature (K)

ZONE3 – zone three temperature (K)

ZONE4 – zone four temperature (K)

The primary mass flow arises from the stoichiometric quantity of air needed for the specified coal feed rate (10.0 g air / 1.0 g coal). The secondary mass flow arises from the desired amount of excess air.

The only input data needed for the program is the headings of the printed output tables. The PRINT subroutine uses the same format for all the output data tables and uses an input data file to read in the headings.

U VELOCITY

V VELOCITY

P PRESSURE

T TEMPERATURE

V VISCOSITY

D DENSITY

These headings are simply printed out at the top of each of respective output data tables.

2.2.2 Dependent Variable Selection

The program uses a number of "logical" parameters to determine which subroutines are to be called. The subroutines that can be selected are specified by the following terms:

INCALU – axial velocity

INCALV – radial velocity

INCALP – pressure

INCALT – temperature

INCLUP – particle velocity and temperature

INPRO – properties

By specifying "TRUE" or "FALSE", these terms will allow only the desired subroutines to be used (eg under isothermal conditions, INCALT = FALSE).

2.2.3 Iteration and Control

The maximum number of iterations used is specified by the term MAXIT. The maximum number of iterations is chosen such that a converged solution can be obtained (using a convergence criterion) without the termination of the program. The program solves the governing differential equations for each of the dependent variables, and a residual (or remainder) arises because the governing equation is not exactly satisfied until convergence is achieved. There are residuals of axial momentum, radial momentum, mass and energy. The program will continue to iterate until all the residuals are below a chosen convergence criterion; at this point, the program will stop and the converged solution is printed out. The residuals have all been non–dimensionalized and the convergence criteria was such that the sum of all the residuals of each subroutine be less than 1 %:

$$SORMAX = 0.01$$

The program uses under relaxation factors (URF) for each of the dependent variables. The URF are very necessary to obtain a converged solution; improper choice of URF can lead to oscillating or diverging solutions. It is difficult to choose a "universal" URF because they are particular to a given set of conditions. It was found that the following range of URF gave good convergence.

URFU = 0.5

URFV = 0.5

URFP = 0.2 – 0.5

URFT = 0.8 – 1.0

In particular, URFT = 0.8 gave more stable convergence with a variable glow bar temperature and UFRT = 1.0 gave more stable convergence with a uniform glow bar temperature.

The subroutine LISOLV is used to update each dependent variable at each iteration. A number of "sweeps" or passes is used at each iteration to update the dependent variable matrix. The values obtained with each pass are better guesses of the dependent variable field. The number of "sweeps" through the LISOLV subroutine by each of the dependent variable subroutines is:

NSWPU = 3 – number of sweeps for CALCU

NSWPV = 3 – number of sweeps for CALCV

NSWPP = 5 – number of sweeps for CALCP

NSWPT = 3 – number of sweeps for CALCT

2.2.4 Output Data

The calculated fields of data are printed out in tabular form. The PRINT subroutine uses a standard output form for all the output data. Intermediate sets of data can be printed also, before the solution has reached the convergence criterion. The tables are labeled by the headings stored in the input file.

2.3 PARTICLE VELOCITY AND HEATING

The particle velocities and temperatures are calculated with results from the solution of the furnace flow field. Since the particles are assumed to travel down the centre-line of the furnace, the values used from the flow field calculations are gas velocities and temperatures along the centre-line and furnace wall temperatures. The particle moves along the furnace in discrete time steps using an explicit scheme. Calculations of distance, velocity, temperature, Reynolds number, heat transfer, etc. are calculated after each time step; when the particle has reached the end of the furnace the program stops.

2.3.1 Input Values for Particle Calculations

The input values for particle velocity and heating are very few. The diameter of the particle and the emissivity were the quantities varied; however, properties such as density and heat capacity can also be changed. It was assumed that the particles were of spherical shape. The furnace was divided into four zones: primary inlet, secondary inlet, furnace wall and water-cooled probe at the exit. The inlet values were chosen as the inlet gas temperatures to the furnace and the furnace wall temperature is calculated during the solution of the gas phase. The water-cooled probe temperature was assumed equal to that of the primary inlet; however, an actual value for this temperature may be entered. The input parameters which can be changed are:

CPPAR – specific heat of particle (J/kg K)

DENPAR – density of particle (kg/m**3)

DIAPAR – diameter of particle (m)

EPS – emissivity of particle

TEXIT – temperature of water-cooled probe (K)

2.3.2 The Time Increment

The time increment was chosen such that the particle undergoes a chosen temperature increase with each step. The time step must be kept small so as not to invalidate our assumptions. The maximum time step was limited to 5 ms; larger time steps gave too large a temperature increase with each step. The time step is calculated using an approximately fixed temperature increase with each step; this was chosen as 5 K. If this gives a time step larger than the limiting value, the limiting value is used instead. These were specified in the following terms:

DELTMP – temperature increment between steps

DELT – maximum time increment between steps

2.3.3 Particle Velocity and Heating Output

The output is printed in a table; the values of the particle that are printed out are the time, velocity, distance travelled, local Reynolds number, heat transfer coefficient, heat received by radiation, heat lost by convection and particle temperature. The calculations continue until the particle exits the furnace.

2.4 OPERATING PROCEDURE

The operating procedure can now be outlined.

1. Choose the desired subroutines by means of the "logical" parameter.
2. Select the primary and secondary mass flows and the primary and secondary inlet temperatures.
3. Enter the four zone temperatures.

4. Choose the particle emissivity and particle diameter in the CALCUP subroutine.

5. Leave the general parts of the program alone, including all the CALC subroutines, INIT, PROPS, LISOLV and PRINT.

Appendix A

GLOSSARY OF FORTRAN SYMBOLS

A(J)	=	Coefficient of recurrence relation
AE(I,J)	=	Coefficient of combined convective/diffusive flux through east wall of control volume
AN(I,J)	=	Coefficient of combined convective/diffusive flux through north wall of control volume
AP(I,J)	=	Sum of coefficients of combined convective/ diffusive fluxes through all four walls of the control volume
APRM	=	Area of primary flow inlet (m**2)
AREAEW	=	Area of east/west wall of control volume
AREAN	=	Area of north wall of control volume
AREAS	=	Area of south wall of control volume
ARDEN	=	Area of east/west cell wall times density of fluid
ARDENT	=	Sum of all east/west ARDEN at a cross section
AS(I,J)	=	Coefficient of combined convective/diffusive flux through south wall of control volume
ASEC	=	Area of secondary flow inlet (m**2)
ATP	=	Coefficient of linearization for particle heating
AUP	=	Coefficient of linearization for particle motion

AW(I,J) - Coefficient of combined convective/diffusive flux through west wall of control volume

B - Constant in Sutherland equation (viscosity)

B(J) - Coefficient of recurrence formulae

BTP - Coefficient of linearization for particle heating

C - Constant used to calculate Pi (=1.0)

C(J) - Coefficient of recurrence relation

C1 - Constant term used in calculation of radiation to outside furnace wall

CALCP - Subroutine used to calculate gas pressure

CALCT - Subroutine used to calculate gas temperature

CALCU - Subroutine used to calculate gas axial velocity

CALCUP - Subroutine used to calculate particle velocity and temperature

CALCV - Subroutine used to calculate gas radial velocity

CE - Coefficient of convective flux through east wall of control volume

CMAS - Mass feed rate of coal (kg/s)

CN - Coefficient of convective flux through north wall of control volume

CONST - Ideal gas constant / atmospheric pressure (J/kg K)/(Pa)

CP - Maximum of zero and net outflow (SMP) from control volume

CPO - CP

CPP - Specific heat of air (J/kg K)

CPPAR - Specific heat of coal particle (J/kg K)

CS - Coefficient of convective flux through south wall of control volume

CST - Constant of linear interpolation in CALCUP subroutine

CW - Coeffecient of convective flux through west wall of control volume

D(J) - Coefficient of recurrence formulae

DE - Coefficient of diffusive flux through east wall of control volume

DELT - Time increment used to specify stepwise motion of particles (s)

DELTMP - Temperature increment used to limit temperature rise between time steps (K)

DEN(I,J) - Density of gas (kg/m**3)

DENA - Density of gas on axis

DENE - Density of gas at east face of a C cell

DENN - Density of gas at north face of a C cell

DENPAR - Density of coal

DENS - Density of gas at south face of a C cell

DENU - Average density of gas of a U cell

DENW - Density of gas at west face of a C cell

DENPRM - Density of primary gas at inlet

DENSEC - Density of secondary gas at inlet

DIAPAR - Diameter of particle (m)

DIST(I) - Distance travelled by particle each time step

measured from inlet plane in axial direction (m)

DN - Coefficient of diffusive flux through south wall of control volume

DS - Coefficient of diffusive flux through south wall of control volume

DST - Interpolated density of gas on the centre-line

DSTF - Density of gas based on the film temperature (average between the particle surface and the surrounding gas)

DU(I,J) - Coefficient of velocity correction term for U velocity

DUDXE - $\partial u/\partial x$ at eastern face of U cell

DUDXW - $\partial u/\partial x$ at western face of U cell

DUDX - $\partial u/\partial x$ at main grid node (I,J)

DUDY - $\partial u/\partial y$ at main grid node (I,J)

DUDYE - $\partial u/\partial y$ at mid-point of east wall of V cell

DUDYW - $\partial u/\partial y$ at mid-point of west wall of V cell

DVDX - $\partial v/\partial x$ at main grid node (I,J)

DVDXN - $\partial v/\partial x$ at mid-point of north wall of U cell

DVDXS - $\partial v/\partial x$ at mid-point of south wall of U cell

DVDY - $\partial v/\partial y$ at main grid node (I,J)

DVDYN - $\partial v/\partial y$ at mid-point of north wall of V cell

DVDYS - $\partial v/\partial y$ at mid-point of south wall of V cell

DW - Coefficient of diffusive flux through west wall of control volume

DXEP(I) - X(I+1)-X(I)

DXEPU(I) - XU(I+1)-XU(I)

DXPW(I) - X(I)-X(I-1)

DYNP(J) - Y(J+1)-Y(J)

DYNPV(J) - YV(J+1)-YV(J)

DYPS(J) - Y(J)-Y(J-1)

DYPSV(J) - YV(J)-YV(J-1)

EPS - Emissivity of coal

FLOW - Mass flow rate at a cross section based on calculated velocities and densities (kg/s)

FLOWIN - Mass flow rate entering furnace tube (kg/s)

GAMH(I,J) - Prandtl/CPP (kg K/J)

GE - Mass flux through east wall of cell

GN - Mass flux through north wall of cell

GNW - Mass flux through north wall of U cell

GP - Mass flux at location of velocity

GRAVTY - Acceleration due to gravity (9.806 kg/m s**2)

GREAT - A very large value (10**6)

GS - Mass flux through south wall of cell

GSW - Mass flux through south wall of U cell

HEDM - Heading title for the table of residual mass

HEDP - Heading title for the table of pressure

HEDT - Heading title for the table of temperature

HEDU - Heading title for the table of axial velocity

HEDV - Heading title for the table of radial velocity

HFXOLD(I) - Heat flux from heating elements to gas calculated at the previous iteration

HPE - Radiation heat transfer coefficient from

furnace exit to particle (W/m**2 K)

HPP - Radiation heat transfer coefficient from primary inlet to particle (W/m**2 K)

HPS - Radiation heat transfer coefficient from secondary inlet to particle (W/m**2 K)

HPW - Radaition heat transfer coefficient from furnace wall to particle (W/m**2 K)

HTC - Convection heat transfer coefficient from gas to particle (W/m**2 K)

HTFLX(I) - Heat flux from heating elements to gas

I - Index for independent variables and coordinates

IMON - I-index monitoring location

INCALP - Logical parameter for solution of P equation

INCALT - Logical parameter for solution of T equation

INCALU - Logical parameter for solution of U equation

INCALV - Logical parameter for solution of V equation

INIT - Subroutine used to initialize geometry and parameters

INPRO - Logical parameter for updating of gas properties

IPREF - I index of location where pressure is fixed

IT - I index of maximum dimension of dependent variables

J - Index for dependent variables and coordinates

JMON - J index of monitoring location

JPREF - J index of location where pressure is fixed

JT - J index of maximum dimension of dependent variable

KWALL - Thermal conductivity of mullite tube (W/m K)

LISOLV - Subroutine used to solve the dependent variables (Tridiagonal Matrix Algorithm)

MAXIT - Maximum number of iterations to be completed if iteration sequence is not stopped by test on value of SORCE

MODP - Part of MODPRO subroutine used to modify pressure subroutine

MODPRO - Subroutine containing boundary conditions for each of the velocity, pressure, and temperature subroutines

MODT - Part of MODPRO subroutine used to modify temperature subroutine

MODU - Part of MODPRO subroutine used to modify U (axial) velocity subroutine

MODV - Part of MODPRO subroutine used to modify V (radial) velocity subroutine

NI - Maximum value of the I index

NIM1 - NI-1

NITER - Number of iterations completed

NJ - Maximum value of the J index

NJM1 - NJ-1

NSWPP - Number of application of line iteration for P equation

NSWPT - Number of application of line iteration for

T equation

NSWPU - Number of application of line iteration for U equation

NSWPV - Number of application of line iteration for V equation

P(I,J) - Pressure P (Pa)

PATM - Atmospheric pressure (Pa)

PHI(I,J) - General representation for all dependent variables

PI - PI (3.14159..)

PP(I,J) - Pressure correction P'

PRANDL - Prandtl number

PRINT - Subroutine used to print out all the calculated values in tabular form

PRMMAS - Inlet mass flow rate of primary air

PROPS - Subroutine used to calculate air properties

QCONV - Total heat transfered from particle to surrounding gas by convection (W/m**2)

QRAD - Total heat transfered from particle to surrounding surfaces by radiation (W/m**2)

R(J) - Radius of main grid node (I,J) from symmetry axis (m)

RATIO - Ratio of total air mass to coal mass (SPRAT+1)

RCV(J) - Radius of C and U cell centre

REFL - Back flow through a given cell (kg/s)

REFLO - Back flow through a tube cross section

REFLOT - Largest back flow through all tube cross

sections

RELC - Local relative Reynolds number between particle and surrounding gas

REPRM - Reynolds number of primary flow inlet

RESEC - Reynolds number of secondary flow inlet

RESOR - Residual source for individual control volume

RESORM - Sum of residual mass sources within calculation domain

RESORT - Sum of residual sources within calculation domain for T equation

RESORU - Sum of residual sources within calculation domain for U equation

RESORV - Sum of residual sources within calculation domain for V equation

ROUT - Outside radius of mullite furnace tube

RR - Ideal gas constant (J/kg K)

RSTG - Resistance of gas (K m**2/W)

RSTR - Radiation resistance from heating elements to outside tube wall (K m**2/W)

RSTW - Resistance of furnace tube wall (K m**2/W)

RV(J) - Radius of location of V(I,J) from symmetry axis

S - Constant in Sutherland equation used to calculate dynamic viscosity

SECMAS - Inlet mass flow rate of secondary air (kg/s)

SEW(I) - 0.5*(DXEP(I)+DXPW(I))

SEWU(I) - 0.5*(DXEPU(I)+DXPWU(I))

SIG - Stefan-Boltzman constant (W/m**2 T**4)

SMP - Net outflow from control volume (kg/s)

SNS(J) - 0.5*(DYNP(J)+DYPS(J))

SNSV(J) - 0.5*(DYNPV(J)+DYPSV(I))

SORCE - Maximum of RESORM, RESORU, RESORV, RESORT

SORCE1 - Part of a source term which has been grouped for clarity

SORCE2 - See SORCE1

SORCE3 - See SORCE1

SORMAX - Maximum acceptable value of SORCE for converged solution

SORVOL - GREAT*VOL

SP(I,J) - Coefficient of linearized source treatment

SPRAT - Ratio of secondary mass flow of air to primary flow rate of air

SU(I,J) - Coefficient of linearized source treatment

T(I,J) - Temperature T (K)

TEXIT - Temperature of water-cooled probe at tube exit (K)

TGB(I) - Temperature of heating elements along furnace (K)

TIME - Time particle takes to travel DIST(I) (s)

TINPRM - Inlet temperature of primary gas (K)

TINSEC - Inlet temperature of secondary gas (K)

TMP - Interpolated temperature of gas on centre-line (K)

TMULT - Coefficient of wall shear stress expression

TP(I) - Temperature of particle after travelling

distance DIST(I) (m)

TWL - Interpolated furnace wall temperature (K)

TWLOUT - Temperature of outside wall of mullite tube (K)

U(I,J) - Component of mean velocity in axial direction U velocity (m/s)

UINC - Uniform increment of U velocity at outlet of flow domain (m/s)

UINPRM - U velocity at primary flow inlet (m/s)

UINSEC - U velocity at secondary flow inlet (m/s)

UP(I) - Velocity of particle after travelling DIST(I) (m/s)

URFP - Under relaxation factor for pressure correction

URFT - Under relaxation factor for temperature

URFU - Under relaxation factor for U velocity

URFV - Under relaxation factor for V velocity

UU - Interpolated value of gas velocity on axis (m/s)

V(I,J) - Component of mean velocity in radial direction V velocity (m/s)

VFPE - View factor from particle to furnace exit

VFPP - View factor from particle to primary inlet

VFPS - View factor from particle to secondary inlet

VFPW - View factor from particle to furnace wall

VSCP - Viscosity of gas at the particle surface (kg/m s)

VSCF - Viscosity of gas evaluated at the film temperature (see DSTF) (kg/m s)

VIS(I,J) - Viscosity (kg/m s)

VISPRM - Viscosity of primary gas at inlet (kg/m s)

VISSEC - Viscosity of secondary gas at inlet (kg/m s)

VISE - Viscosity at mid-point of east wall of cell

VISN - Viscosity at mid-point of north wall of cell

VISS - Viscosity at mid-point of south wall of cell

VISW - Viscosity at mid-point of west wall of cell

VOL - Volume of cell or control volume (m**3)

X(I) - Distance from inlet plane in axial direction (m)

XMOMIN - Momentum of gas at inlet of flow domain

XU(I) - X coordinate of storage location of U(I,J)

Y(J) - Distance from symmetry axis in radial direction (m)

YV(J) - Y coordinate of storage location of V(I,J)

ZONE1(I) - Temperature of zone one (K)

ZONE2(I) - Temperature of zone two (K)

ZONE3(I) - Temperature of zone three (K)

ZONE4(I) - Temperature of zone four (K)